Klonierung und *in vivo* Analyse von Proteinen des menschlichen inneren Kinetochors.

Dissertation

zur Erlangung des akademischen Grades
doctor rerum naturalium (Dr. rer. nat.)

vorgelegt dem Rat der Biologisch-Pharmazeutischen Fakultät
der Friedrich-Schiller- Universität Jena

von Diplombiologin
Daniela Hellwig
geboren am 15.02.1979 in Leinefelde

Gutachter

Prof. Dr. Stephan Diekmann
Fritz-Lipmann-Institut für Altersforschung
07745 Jena

Prof. Dr. Frank Grosse
Fritz-Lipmann-Institut für Altersforschung
07745 Jena

Prof. Dr. Jörg Langowski
Deutsches Krebsforschungszentrum
69120 Heidelberg

Datum der Verteidigung: 13.03.2014

Inhalt

1. Zusammenfassung

Die korrekte Trennung der Schwesterchromatiden während der Mitose ist unumgänglich für die Stabilität des Genoms und somit ein Grundpfeiler des Lebens. Um diese Herausforderung zu bewältigen, besitzt jedes Chromosom an der primären Einschnürungsstelle einen Proteinkomplex, das Kinetochor, welches die Anheftung der Mikrotubuli und die Regulation der Segregation gewährleistet.

Im Rahmen dieser Arbeit konnte gezeigt werden, dass der Kinetochorkomplex allerdings nicht nur während der Mitose essentielle Aufgaben zu erfüllen hat, sondern auch innerhalb der Interphase einer Vielzahl von Umbauprozessen durchläuft und spezifische Funktionen realisiert. Erstmals wurde eine detaillierte Analyse der dynamischen Eigenschaften, Bindungsverhältnisse, Proteingehalte und Nachbarschaften eines der inneren Kinetochorelemente, CENP-N, über den Zellzyklus hinweg durchgeführt. Diese Untersuchungen erfolgten in lebenden menschlichen Zellen mittels hochauflösender Mikroskopie und zeichnen so ein realistisches Bild von den Vorgängen am Kinetochor. Sie ermöglichen Rückschlüsse auf die Funktionen von CENP-N, welches daraufhin als Genauigkeitsfaktor für den Einbau von CENP-A postuliert wurde. Desweiteren deuten die Ergebnisse darauf hin, dass CENP-N eine Markierung des Kinetochors während der Replikation der centromerischen DNA sein könnte.

Diese Herangehensweise zum Studium der Eigenschaften wurde auf weitere Proteine des inneren Kinetochors, wie CENP-T und –W sowie den O/P/Q/R/U-Komplex, übertragen. Basierend darauf stellte sich heraus, dass das Kinetochor im Verlauf der Interphase zwei Hauptaufgaben zu erfüllen hat. Hierbei liegt der Schwerpunkt während der ersten Hälfte der Interphase auf der Erhaltung der Kinetochorstruktur selbst. Grundlage ist der korrekte Einbau von CENP-A in den centromerischen Lokus, welcher unter anderem von CENP-C und CENP-I bewerkstelligt wird. Gleichzeitig kommt er zu einem zeitweiligen Umbau der zugrunde liegenden Chromatinstruktur. Nach Abschluss dieses Vorgangs werden während der zweiten Hälfte der Interphase sukzessive alle weiteren Komponenten des CCAN neu rekrutiert und es bildet sich eine Plattform für die Anlagerung des äußeren Kinetochorproteine, welche die eigentliche Trennung der Chromatiden ermöglichen. Dieses Fundament wird verankert durch CENP-C und CENP-T. Erst nach dem Ablauf dieser Prozesse ist das centromerische Chromatin bereit für die Mitose.

2. Summary

The accurate division of sister chromatides during mitosis is essential for stability of the genome and therefore a keystone of life. To tackle this challenge each chromosome contains a protein complex at the primary constriction, called kinetochore, which facilitates the attachment of microtubules and the regulation of segregation.

This dissertation shows that the kinetochore complex executes essential tasks not only during mitosis but also undergoes several rearrangements und realizes specific functions in the course of the interphase. For the first time, the dynamic behavior, binding properties, protein content and neighborhood relationships of a kinetochore protein, CENP-N, were analyzed in detail throughout the cell cycle. These examinations were performed in living cells via high resolution microscopy, which procure a realistic picture of kinetochore-associated processes. The results provide evidence that CENP-N functions as a fidelity factor for CENP-A loading at the kinetochore. Furthermore, the findings suggest that CENP-N marks the kinetochore region during replication of centromeric chromatin.

This approach was then used to investigate characteristics of other proteins of the inner kinetochore, e.g. CENP-T and –W as well as the O/P/Q/R/U complex. Based on the obtained results the kinetochore has to achieve two main functions. During the first half of the cell cycle, the inner kinetochore is maintained in its structure. This depends on the accurate assembly of CENP-A into the centromeric locus facilitated by CENP-C and CENP-I. In parallel, a temporary rearrangement of centromeric chromatin takes place. After completion of this process, during second half of interphase other components of CCAN are successive recruited and build a platform for attachment of outer kinetochore proteins to allow proper division of chromatides. This fundament is anchored by CENP-C and CENP-T. After this event the centromeric chromatin is switched to a mitotic state.

3. Einleitung

"Der Mechanismus der indirekten Kernteilung (Karyokinese), der den Beobachter durch seine Genauigkeit und sein Ebenmaß so überrascht, zog stets die Aufmerksamkeit der Forscher auf sich. Was für Ursachen es sein sollen, welche die Tochterchromosomen sich nach den Polen der Zelle zu bewegen zwingen und welche Kräfte dabei in dem Protoplasma wirken - das sind die Fragen, die von Zeit zu Zeit das Interesse der Forscher seit den frühesten Zeiten bis auf unsere Tage an sich fesseln."

"Leitkörperchen" der Chromosomen bei einigen Angiospermen
Trankowsky 1930

3.1. Historisches

Mit dem Fortschritt in der Mikroskopietechnik sowie der Weiterentwicklung der Färbemethoden im späten 19ten Jahrhundert wurde es möglich, auch kleinste Details im Inneren von Zellen zu beobachten. Dies führte zur Entdeckung der Chromosomen und deren Verhalten während der Kernteilung durch W. Flemming im Jahr 1882. Nach dem vom griechischen abgeleiteten Wort "mitos" - Faden -, bezeichnete er den Prozess der Chromatinteilung als "Mitose" (Abbildung 1)(Flemming, 1882). Kurze Zeit später beschrieb erstmals R. Metzner färbbare Strukturen an den primären Einschnürungsstellen der Chromosomen als "Leitkörperchen", die er als Bindungsstellen der Spindelfasern während der Zellteilung deutete (Abbildung 1) (Metzner, 1894). Schon zu diesem frühen Zeitpunkt maß er seiner Entdeckung die Bedeutung als "kinetische Region" zu, welche den Weg der Chromosomen zu den Polen hin weist. In den folgenden Jahren wurden für diese Struktur verschiedenste Begriffe vorgeschlagen, bis sich um 1940 der Name "Kinetochor" (Sharp, 1934) durchsetzen konnte, wobei dieser in der heutigen Zeit den für die Bindung der Mikrotubuli in der Mitose essentiellen Proteinkomplex bezeichnet. Parallel dazu hat sich der Begriff Centromer, geprägt von Darlington 1937, für die Position am Chromosom etabliert, an welcher sich der Kinetochorkomplex bildet (Darlington, 1937).
Aufgrund der geringen Größe unterhalb der Auflösungsgrenze lichtmikroskopischer Techniken waren detailliertere Beobachtungen der Kinetochore vorerst nicht möglich. Diese gelangen Nebel und Coulon erstmals 1962 (Abbildung 1) (Nebel & Coulon, 1962). Sie beschrieben die mitotischen Kinetochore als eine dreischichtige Struktur,

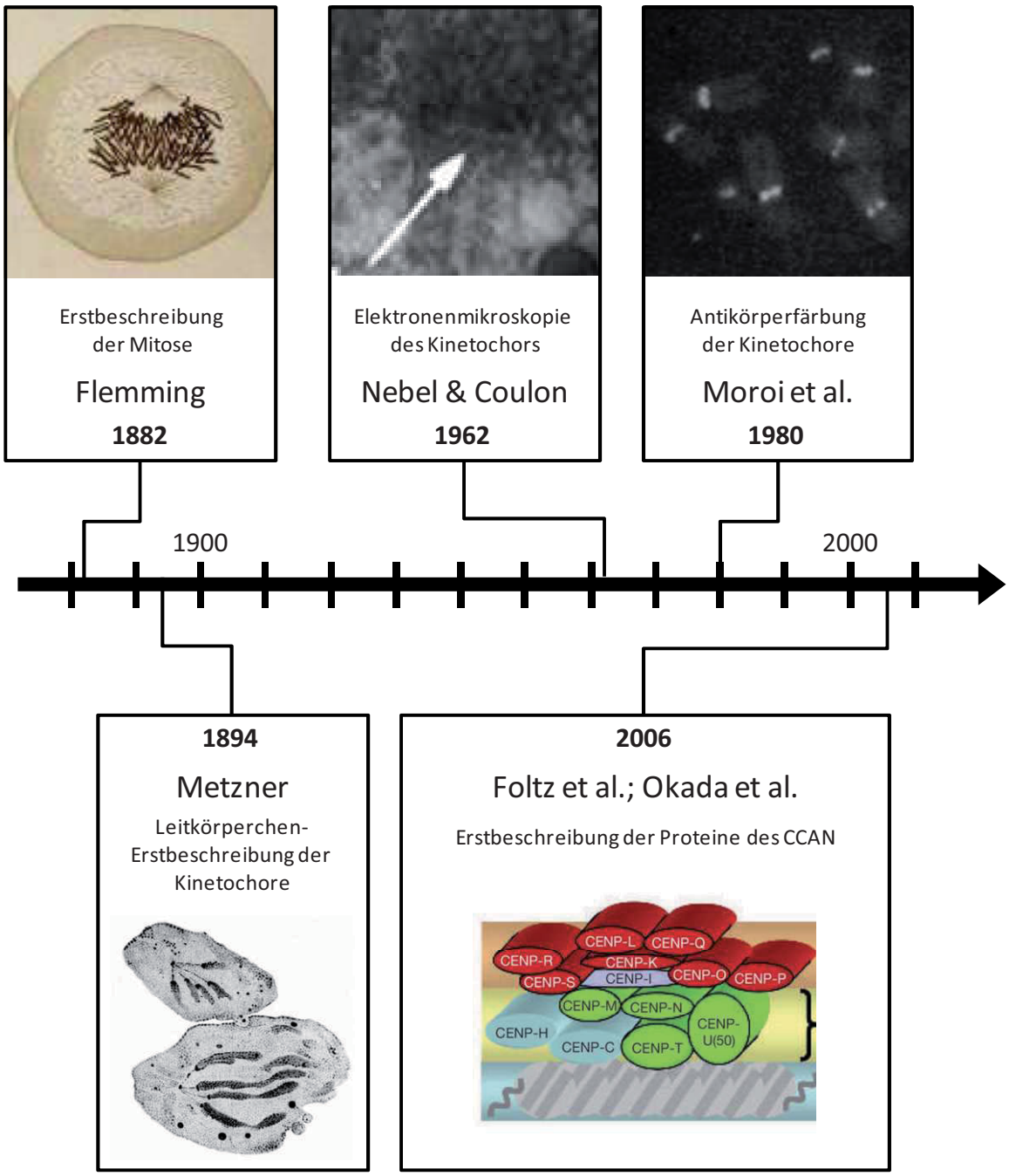

Abbildung 1: zeitliche Darstellung der Meilensteine der Kinetochorforschung (entnommen aus W. Flemming „Zellsubstanz, Kern und Kerntheilung“ 1882; R. Metzner, 1894 „Beiträge zur Granulalehre“; B.R. Nebel & E.M. Coulon“, 1962 „The fine structure of pigeon spermatocytes; Moroi et al., 1980 „Autoantibody to centromere (kinetochore) in scleroderma sera“; Foltz et al., 2006 „ The human CENP-A centromeric nucleosome-associated complex“)

an welche die Spindelfasern direkt binden. In den folgenden Jahren konnte in weiteren Untersuchungen gezeigt werden, dass die Kinetochore während der Mitose aus zwei elektronendichten Platten, dem inneren und äußeren Kinetochor, voneinander abgegrenzt durch eine elektronendünne Schicht, und der sie umschließenden fibrösen Corona, bestehen. Diese drei Schichten bilden eine etwa 300nm dicke Scheibe, welche sich bis zur

Bindung mehrerer Mikrotubuli als eine Einheit verhält (Ris & Witt, 1981; Moses et al., 1975; Brinkley & Strubblefield, 1966, Robbins & Gonatas, 1964; Krishan & Buck, 1965; Roos, 1973; Barnicot & Huxley, 1965; Counce & Meyer, 1973).
Bei der Suche nach Merkmalen, welche die Kinetochore einzigartig machen, stellte man fest, dass DNA ein essentieller Bestandteil ist (Pepper & Brinkley, 1980). Die Centromerregion menschlicher Chromosomen zeichnet sich durch α-Satelliten DNA aus (Pardue & Gall, 1970; Kurnit & Maoi, 1973; Manuelidis, 1978), welche im Menschen durch Wiederholungen von 176 Basenpaar langer Abschnitte charakterisiert ist (Musich et al., 1977). Sie gilt als ein Schlüsselelement der Kinetochorstruktur (Matsumoto et al., 1989).
Eine weiterer großer Schritt in der Kinetochorforschung war die Entdeckung, dass Patienten, welche am CREST-Syndrom (C= Calcinosis cutis, R= Raynaud-Syndrom, E= Esophageale Dysfunktion, S= Sklerodaktylie, T= Teleangiektasia) erkrankt sind, Autoantiköper bilden, die eine spezifische Anfärbung der Kinetochore erlaubt (Abbildung 1), (Moroi et al, 1980; Fritzler & Kinsella, 1980; Tan et al., 1980; Brenner, 1981). Nun war es erstmals möglich, Kinetochore nicht nur während der Mitose sondern durch den gesamten Zellzyklus hinweg nachzuweisen (Moroi et al., 1981). Mit Hilfe der Autoantikörper aus den ACA-Seren (Anticentromer-Antikörper) konnte man drei verschiedene Kinetochorproteine nachweisen. Als erstes das ca. 16kDa große CENP-A, kurz darauf CENP-B und CENP-C (Earnshaw et al., 1984; Earnshaw & Rothfield, 1985; Earnshaw et al., 1986; Ayer & Fritzler, 1984; Guldner et al., 1984; Valdivia & Brinkley, 1985; McNeilage et al., 1986; Earnshaw et al., 1987; Kingwell & Rattner, 1987).

3.2. CENP-A

3.2.1. Eigenschaften

Es zeigte sich, dass CENP-A histonähnliche Eigenschaften besitzt und im Bereich der centromerischen DNA Oktamere mit H4, H2A und H2B ausbildet (Palmer et al., 1987, 1991). CENP-A wird von einem eigenständigen Gen codiert, zeigt aber Homologien zu H3, welches es in den centromerischen Nukleosomen ersetzt. Beide Proteine sind wahrscheinlich aus einem gemeinsamen Vorläufer entstanden (Palmer et al., 1991). CENP-A-Null-Mutanten bei Mäusen sterben 3,5 bis 8,5 Tage nach der Befruchtung im Mutterleib. Allerdings sind bis zum fünften Tag schwache CENP-A Konzentrationen nachweisbar, hierbei handelt es sich um maternales CENP-A, welches in der Eizelle schon vor der Befruchtung enthalten war. Die Deletion von CENP-A führt zu Fehlverteilungen der Chromosomen in der Mitose und zur

unvollständigen Kondensierung des centromerischen Chromatins während der Interphase. Diese Defekte sind dosisabhängig und nicht in der heterozygoten Mutante zu beobachten (Howman et al., 2000; Goshima et al., 2003). Es konnte gezeigt werden, dass der Einbau des Fusionsproteins CENP-A mit GFP am Kinetochor korrekt erfolgt und keine morphologischen Schädigungen verursacht (Sullivan et al., 1994). Heterozygote CENP-A/ CENP-A-GFP Mausmutanten zeigen einen normalen Phänotyp wohingegen das komplette Ersetzen von CENP-A durch fluorenszensmarkiertes exogenes CENP-A-GFP zu einem Absterben des Fetus nach 10,5 Tagen führt (Kalitsis et al., 2003).
Bei starker Überexpression von CENP-A-GFP kommt es zu einem Einbau in die gesamte Chromosomenstruktur, welche allerdings keinen Einfluss auf das Wachstum oder den geregelten Ablauf der Mitose hat. Die Kinetochore zeigen weiterhin eine trilaminare Struktur und Mikrotubuli binden ausschließlich am Centromer. Beim Entfernen des Centromers in CENP-A-GFP stark überexprimierenden Zellen kommt es nicht zur Bildung neuer Kinetochore. Dies deutet darauf hin, dass CENP-A nicht der alleinige Marker für das Kinetochor sein kann (Van Hooser et al., 2001).
Diese Ergebnisse implizieren, dass das Hinzufügen von GFP-markiertem CENP-A in der Natur entsprechenden Konzentrationen keinen Einfluss auf den Aufbau und die Funktionalität des Kinetochors hat. Somit ermöglichen sie die Verwendung von fluoreszenzmarkiertem, exogenem Protein zur Untersuchungen der Vorgänge am Kinetochor.

3.2.2. CENP-A und Zellzyklus

Die Replikation der centromerischen DNA erfolgt diskontinuierlich in der mittleren bis späten S-Phase des Zellzyklus (O'Keefe et al., 1992; Jansen et al., 2007; Hemmerich et al., 2008). Die ursprünglich eingebauten CENP-A-Nukleosomen werden bei der Verdoppelung der genetischen Information auf die Tochterstränge aufgeteilt, wobei diese verminderte Konzentration für den reibungslosen Ablauf der folgenden Kernteilung ausreicht (Vereault et al., 2003). Um die Stabilität der centromerischen DNA zu gewährleisten, werden die nicht durch CENP-A besetzten Leerstellen während der Replikation mit H3-Nukleosomen aufgefüllt (Jansen et al, 2007). Es konnte gezeigt werden, dass das in der späten S-Phase neu synthetisierte CENP-A erst am Übergang der Telophase zur G1-Phase des daran anschließenden Zellzykus in die centromerische DNA integriert wird (Shelby et al., 2000; Jansen et al., 2007; Hemmerich et al., 2008). Dieser durch das Durchlaufen der Mitose ausgelöste Prozess führt dazu, dass in der G1-Phase jede Tochterzelle 50% der maternalen und 50% *de novo* synthetisierte CENP-A-Nukleosomen besitzt, welche die als Platzhalter

eingebauten H3 Nukleosomen verdrängen (Verreault et al., 2003; Jansen et al., 2007). Über den gesamten Zellzyklus hindurch ist CENP-A fest verankert, die beobachtbaren Konzentrationsschwankungen resultieren demnach nur aus der Aufteilung während der Verdoppelung und dem Neueinbau der Nukleosomen in das genetische Material (Hemmerich et al., 2008). Dies erklärt auch die Beobachtungen von Figueroa et al. aus dem Jahr 1998, welche bei der direkten Injektion von CENP-A Antikörpern in mitotische Zellen keinen Effekt sehen, aber eine Unterbrechung des Zellzyklus bei Zugabe der Antikörper zu Beginn der Interphase nachweisen konnten (Figueroa et al., 1998).
CENP-A wird durch den Zellzyklus hindurch modifiziert. Kurz vor dem Auflösen der Kernmembran kommt es zu einer Phosphorylierung von CENP-A an der Aminosäure Serin 7 durch die Kinasen Aurora A und anschließend durch Aurora B, wobei die Phosphorylierung durch Aurora A die nachfolgende Lokalisierung von Aurora B erst ermöglicht (Zeitlin et al., 2001; Kunitoku et al., 2003; Slattery et al., 2008).

3.2.3. CENP-A und Chromatinorganisation

Es konnte gezeigt werden, dass CENP-A direkt an die DNA bindet (Shelby et al., 1997). Der C-terminale Bereich (Aminosäuren 48-135) von CENP-A weist eine große Ähnlichkeit zu dem Histonprotein H3 auf und ist essentiell für die Lokalisierung an das Kinetochor. Sie beinhaltet die CENP-A-targeting-Domäne (CATD), welche allerdings nicht konserviert ist. Durch Einführung der CATD in das Histon H3 ($H3^{CATD}$) kommt es zur Lokalisierung an die Centromerstruktur. Allerdings kann $H3^{CATD}$ den letalen Effekt einer vollständigen Deletion von endogenem CENP-A nicht aufheben (Black et al., 2007). Im Gegensatz dazu weist der N-terminale Anteil keine Homologie zu H3 auf (Sullivan et al., 1994). Eine Besonderheit des N-Terminus von CENP-A konnte in *Arabidopsis thaliana* gezeigt werden, wobei diesem offenbar eine wichtige Aufgabe während der Meiose zukommt (Ravi et al., 2011).
CENP-A-Nukleosomen besitzen eine andere Kernstruktur als H3-Nukleosomen, innerhalb des Dimers ist die Achse zwischen den beiden CENP-A-Molekülen gegenüber H3 verschoben. Dies führt zu starken hydrophoben Interaktionen sowie einer erhöhten Stabilität und könnte Teil der epigenetischen Markierung der centromerischen DNA darstellen (Sekulic et al., 2010). Bei jeder Umwindung der DNA um ein CENP-A-Nukleosom bleiben im Gegensatz zu den H3-Nukleosomen vor und hinter dem Nukleosom 13 Basenpaar ungebunden. Dadurch wird die CENP-A-haltige centromerische DNA flexibler und ermöglich so wahrscheinlich den Aufbau des Kinetochorkomplexes in diesem Bereich (Tachiwana et al., 2011).
Neueste Studien zeigen, dass CENP-A-Nukleosomen und H3-Nukleosomen im Bereich der

centromerischen DNA in Blöcken nebeneinander existieren (Blower et al., 2002; Ribeiro et al., 2010; Sullivan et al., 2011). Bei jedem Zellzyklus wird nur ein Teil der H3-Nukleosomen durch CENP-A-haltige Nukleosomen ersetzt, wobei CENP-A nur in schon existierende Blöcke eingebaut wird. Etwa 38% der CENP-A-Blöcke werden pro Zellzyklus mit neuen CENP-A-Nukleosomen versorgt (Dunleavy et al., 2011). Die Verdopplung der centromerischen DNA zeichnet sich durch eine diskontinuierliche Replikation aus, bei der die Bereiche, welche mit CENP-A-Nukleosomen besetzt sind, zu einem anderen Zeitpunkt dupliziert werden als die H3-Nukleosomen-haltigen Abschnitte (Dunleavy et al., 2011). Desweiteren kommt es während der S-Phase zum Einbau der H3-Isotypen H3.1 und H3.3. Die beobachteten stabilen H3.1-Gehalte sowie die Absenkung der H3.3-Nukleosomen-Konzentration während der G1-Phase, dem alleinigen Zeitpunkt des CENP-A-Einbaus, deuten darauf hin, dass H3.3-Nukleosomen als Platzhalten für die fehlenden CENP-A-Nukleosomen während der Replikation fungiert (Dunleavy et al., 2011).

Mit Hilfe von Modifikationen der H3-Moleküle in den Nukleosomen wird auch die transkriptorische Aktivität aller DNA-Abschnitte reguliert. Eine doppelte Methylierung von H3 an der Aminosäure Lysin 36 (H3K36me2) ermöglicht das Ablesen der genetischen Information. Die kürzlich nachgewiesene Integration von H3K36me2 in centromerische DNA weist darauf hin, dass auch diese Bereiche transkriptorisch aktiv sein könnten (Bergmann et al., 2010).

In letzter Zeit zeigte sich, dass die CENP-A-haltigen centromerischen Nukleosomen eine zweite Konformation aufweisen können. Es konnte eine alternative Struktur in Form von Tetrameren beobachtet werden, welche aus je einem Molekül CENP-A, H4, H2A und H2B bestehen (Dimitriadis et al., 2010). Hierbei kommt es zu einem zellzyklusabhängigen Wechsel zwischen der tetramerischen und der oktamerischen Form der centromerischen Nukleosomen. Oktamere sind primär während der S-Phase während der Replikation vorhanden, wobei im restlichen Verlauf des Zellzyklus hauptsächlich Tetramere vorliegen (Bui et al., 2012). Dieser Konformationswechsel könnte der Unfähigkeit der Replikationsmaschinerie, die mit tetramischen Nukleosomen gewickelte DNA zu verdoppeln, geschuldet sein (Bui et al., 2012; Quenet et al., 2012).

3.2.4. CENP-A Einbau

Bis heute ist offen, wie CENP-A-Nukleosomen etabliert werden und welche Signale den ortspezifischen Einbau ermöglichen. In den letzten Jahren wurden hierzu umfangreiche Studien durchgeführt und verschiedene Faktoren identifiziert.

Drei Proteine, Mis18α, Mis18β und M181BP1 (Mis18-Bindeprotein 1), welche einen Komplex

bilden, wurden als CENP-A-Assemblierungsfaktoren postuliert (Du et al, 2011). Hierbei bilden Mis18α und Mis18β ein Heterodimer und interagieren mit dem eine Bindedomäne besitzenden M18BP1. Dieser Unterkomplex ermöglicht den Einbau von CENP-A und lokalisiert schwach durch die gesamte Interphase hinweg (Hayashi et al., 2004). Die Konzentration am Kinetochor steigt in der späten Anaphase stark an und sinkt in G1 wieder auf ihr Ausgangsniveau ab. RNAi-Versuche mit dem Mis18-Komplex haben gezeigt, dass es in dessen Folge zu einem verminderten CENP-A-Einbau kommt (Fujita et al., 2007; Moree et al., 2011; Dambacher et al., 2012). Allerdings deuten die Ergebnisse auch darauf hin, dass der Mis18-Komplex eine vorbereitende Funktion bei der Deacetylierung der Histone erfüllt, welche Grundvoraussetzung für den Einbau von CENP-A ist oder für den Ausbau der zu ersetzenden H3.3-Platzhalter-Moleküle verantwortlich sein könnte (Hayashi et al., 2004; Foltz et al., 2009).

HJURP („Holliday Junction Recognizing Protein“) ist ein 83kDa großes Protein, welches bereits im Cytoplasma einen Präassemblierungskomplex mit CENP-A, aber nicht mit H3, bildet, wobei jeweils 1 HJURP-Molekül mit einem CENP-A-Molekül interagiert (Foltz et al., 2009; Sanchez & Losada, 2011). Diese direkte Bindung des CENP-A-Chaperons erfolgt ohne Vermittlung durch andere Proteine, DNA oder RNA (Shuaib et al., 2010). Desweiteren führt eine erhöhte Expression von CENP-A zu einer verstärkten Expression von HJURP (Dunleavy et al., 2009). Die Bindung von HJURP an die CATD von CENP-A wird durch dessen CENP-A-Binde-Domäne (CBD) ermöglicht und verhindert mittels einer Blockade der Selbstassoziierungsdomäne die Tetramerisierung von CENP-A sowie die Bindung der H4/CENP-A-Moleküle an die H2A/H2B Moleküle (Dunleavy et al., 2009; Foltz et al., 2009). Außerdem wird durch diese Interaktion ebenfalls die Bindung an die DNA gestört, bevor CENP-A den Ort seines Einbaus erreicht hat (Hu et al., 2011). Diese Ergebnisse wurden bestätigt durch die Beobachtung, dass die Zugabe von HJURP-siRNA einen Einbau von CENP-A in die gesamten Chromosomenarme verursacht. Nach und nach kann immer weniger CENP-A an den Kinetochoren nachgewiesen werden, was zur Folge hat, dass die Zellen sich letztendlich in der Mitose sammeln (Foltz et al., 2009). Dies zeigt, dass HJURP für die Rekrutierung an das Kinetochor essentiell ist (Bernad et al., 2011). HJURP lokalisiert hauptsächlich von der späten Telophase bis in die G1-Phase an die Centromere, dem Einbauzeitpunkt von CENP-A (Dunleavy et al., 2009). An allen Positionen, an welchen HJURP nachgewiesen werden kann, ist eine vorangehende Lokalisierung des Mis18-Komplexes erfolgt (Foltz et al., 2009).

3.3. CENP-B und CENP-C

Kinetochore binden zwischen 300 und 3000 CENP-B-Moleküle, wobei die Proteinmenge von der Kinetochorgröße abhängig ist (Earnshaw et al., 1987; Shelby et al., 1996). Die Anheftung von CENP-B beruht auf der Erkennung eine spezifische Sequenz der DNA im Bereich der Centromere, der 17 Basenpaare langen CENP-B-Box (Matsumoto et al., 1998; Ohzeki et al., 2002), wobei CENP-B, im Gegensatz zu CENP-A, auch an inaktiven Centromeren nachgewiesen werden kann (Earnshaw et al., 1989, Sullivan & Schwartz 1995; Hori et al., 2012). Darauf basierend wird die centromerische DNA unterschieden, wobei alpoide DNA, welche CENP-B-Boxen enthält, als Typ 1 bezeichnet wird (Ando et al., 2002). Dieses Bindemotiv kann methyliert werden, wobei eine Hypermethylierung die Anlagerung von CENP-B verhindert (Okada et al., 2007). Die Bindung von CENP-B an die CENP-B-Box beeinflusst wiederum die Bindung von CENP-A an die centromerische DNA, wobei eine Überexpression von CENP-B eine erhöhte Einbaurate von CENP-A auslöst (Okada et al., 2007).

Das 65kDa große CENP-B besitzt eine acidische Region und kann über sein C-terminales Ende Dimere ausbilden, wodurch es zu einer Vernetzung zwischen den CENP-B-Boxen kommen kann (Yoda et al., 1998; Ohzeki et al., 2002). Dieses basal lokalisierende Protein ist nur während der G2-Phase und der Mitose fest an den Kinetochor gebunden, sonst zeigt es durch den Zellzyklus hindurch ein dynamisches Verhalten (Hemmerich et al., 2008).

Schon im Jahr 1997 konnten Earnshaw und Kollegen zeigen, dass das Y-Kinetochor kein CENP-B enthält (Earnshaw et al., 1987). Diese Ergebnisse wurden ergänzt durch die Herstellung einer CENP-B-Null-Maus, welche einen nahezu normalen Phänotyp aufweist. Die Tiere sind kleiner, gesund und besitzen eine normale Karyogenese. Sie zeigen eine verminderte Spermienproduktion, sind aber fertil. CENP-B ist somit nicht essentiell für die Funktionalität des Kinetochors (Hudson et al., 1998; Perez-Castro et al., 1998). Allerdings zeigte sich, dass das Vorhandensein von CENP-B-Boxen beim Aufbau von artifiziellen Chromosomen zu einer erhöhten Effizienz führt und legt somit nahe, dass sie einen Einfluss auf die Etablierung von Kinetochoren haben (Okada et al., 2007).

Das dritte der mit ACA-Serum nachgewiesenen Kinetochorproteine ist das 107kDa große CENP-C. Es besteht aus einer Dimerisierungsdomäne, eine zentrale Region und ein konserviertes C-Signatur-Motiv, wobei jede dieser Strukturen die korrekte Lokalisierung beeinflussen (Milks et al., 2009). Im N-terminalen Bereich des Proteins befindet sich zusätzlich eine Kern-Lokalisierung-Sequenz, welche den Transport in den Zellkern ermöglicht (Przewloka et al., 2011). Der C-Terminus von CENP-C wiederum ist essentiell für die Bindung anderer Kinetochorproteine (Milks et al., 2009).

Die zentrale Region von CENP-C enthält eine DNA- und Centromer-Bindedomäne. Basierend darauf kommt es zu einer direkten Anheftung an die alphoide DNA, welche

allerdings über RNA vermittelt wird (Sugimoto et al., 1994; Politi et al., 2002; Du et al., 2010). Innerhalb der zentralen Region sind die Aminosäurereste 426 bis 537 für die Bindung an CENP-A-Nukleosomen verantwortlich, womit es zur stöchiometrischen Bindung von zwei Molekülen CENP-C an ein CENP-A-Nukleosom kommen kann. Hierbei bildet der Histonanteil von CENP-A im C-terminalen Bereich der CATD eine Ausstülpung und ermöglich somit die Anheftung von CENP-C (Carroll et al., 2010). Durch die Dimerisierung von CENP-C werden durch ein CENP-C-Dimer je zwei CENP-A-Nukleosomen vernetzt. Neueste Studien deuten darauf hin, dass diese Vernetzung nicht nur horizontal sondern auch zwischen verschiedenen Schichten von centromerischen Nukleosomen erfolgt und somit ebenfalls eine horizontale Stabilisierung der Kinetochorstruktur bewerkstelligt werden könnte (Trazzi et al., 2009; Carroll et al., 2010; Ribeiro et al., 2010; Guse et al., 2011). Die Beobachtung, dass CENP-C ebenfalls an H3-Nukleosomen assoziieren kann, welche sich in großer Nähe zu CENP-A-Nukleosomen befinden, sowie der Nachweis einer Interaktion von 6 Aminosäuren des C-Terminus von CENP-C mit der mittleren Region von CENP-A deuten darauf hin, dass das Zusammenwirken von CENP-C und CENP-A zur Assemblierung des Kinetochors führt. Diese Bindung erfolgt allerdings nur in Anwesenheit von H3-Nukleosomen und ermöglicht somit einen starken Kontakt mit dem centromerischen Chromatin (Carroll et al., 2010, Guse et al., 2011, Hori et al., 2012).

Die Überexpression von CENP-C führt, ähnlich wie bei CENP-A, zum generalisierten Einbau in die gesamten Chromosomenarme. Hierdurch ist es aber nicht möglich funktionsfähige Kinetochore aufzubauen (Van Hooser et al., 2001). Durch die Injektion von Antikörpern gegen CENP-C während der Interphase wird die Lokalisierung des Proteins blockiert und es kommt zu Defekten während der Mitose. Nach erfolgreicher Separation der Schwesterkinetochore zeigt sich, dass die Chromatiden nicht auf die Tochterzellen verteilt werden können (Tomkiel et al., 1994). Diese Ergebnisse werden bestätigt durch RNAi-Experimente, welche ebenfalls Mitosedefekte zeigen. Hierbei wurde außerdem beobachtet, dass es durch das Fehlen von CENP-C zu einem verminderten Einbau von CENP-A kommt (Gascoigne et al., 2011). Im Mausexperiment konnte gezeigt werden, dass die Deletion von CENP-C zu Entwicklungsstörungen und einer Degeneration des Embryos nach 3,5 Tagen kommt. Diese werden wahrscheinlich durch die beobachteten Fehler während der Mitose verursacht. 2,5 Tage nach der Befruchtung, in welchen die ersten drei Zellteilungen ablaufen, konnten keine Abweichungen in der Entwicklung festgestellt werden. Das Absterben der Embryonen erfolgt früher als in der CENP-A-Null-Mutante, was darauf hinweist, dass der Wachstumsdefekt nicht allein durch die Störung im CENP-A-Einbau ausgelöst wird (Kalitsis et al., 1998). Folglich ist CENP-C essentiell für die strukturelle Integrität des Kinetochorchromatins während der Mitose, die Bindung der Mikrotubuli und den korrekten Aufbau des Kinetochors während der Interphase (Tomkiel et al., 1994, Ribeiro

et al., 2010, Hori et al., 2012).
CENP-C wird innerhalb des Zellzyklus nur von der mittleren bis späten S-Phase am Kinetochor stabilisiert, außerhalb dieses Zeitpunkt ist es dynamisch (Hemmerich et al., 2008). Neueste Untersuchungen zeigen außerdem, dass CENP-C innerhalb der Mitose für die Lokalisierung von M18BP1 mit verantwortlich ist und dieses direkt binden kann. In der Interphase ist das Verhalten von M18BP1 allerdings unabhängig von CENP-C (Moree et al., 2011; Dambacher et al., 2012).

3.4. CCAN – Konstitutives Centromer Assoziiertes Netzwerk

Nach der Entdeckung der ersten drei Kinetochorproteine kam es in den darauffolgenden Jahren zu einer Intensivierung der Forschung. Es wurden eine Reihe weiterer Kinetochorproteinen identifiziert und charakterisiert (Rattner et al., 1993; Cooke et al., 1997; He et al., 1998; Sugata et al., 1999; Nishihashi et al., 2002). Die ersten generalisierten Ansätze zeigten 2006 allerdings eine unerwartete Komplexität des inneren Kinderchors. Heute ist eine Vielzahl von Proteinen, welche am Aufbau des centromer-lokalisierten Proteinkomplexes beteiligt sind, bekannt. Dieser wird als „Konstitutives Centromer Assoziiertes Netzwerk“ – CCAN – bezeichnet (Abbildung 1) (Cheeseman & Desai, 2008; Hori et al., 2008). Es umfasst, basierend auf deren Lokalisation und biochemischen Eigenschaften, neben CENP-A, -B und -C die Proteine CENP-H und –I sowie CENP-K bis -X (Okada et al., 2006; Izuta et al., 2006; Foltz et al. 2006; Amano et al., 2009; Hori et al., 2008; Tadeu et al., 2008) (Abbildung 2). Eine Systematisierung wird durch die starke funktionale Vernetzung zwischen den Proteinen einzelner Unterkomplexen erschwert. Aufgrund ihrer erstmaligen Identifizierung mittels Immunopräzipitation werden CENP-N, -M, -T und –U als CENP-A-Nukleosomal Assoziierter Komplex (NAC) sowie CENP-H bis –L und -O bist –S als CENP-A-Nukleosomen Distal Komplex (CAD) bezeichnet, welche die Arbeitsgrundlage der hier vorgelegten Arbeit bilden (Foltz et al., 2006).

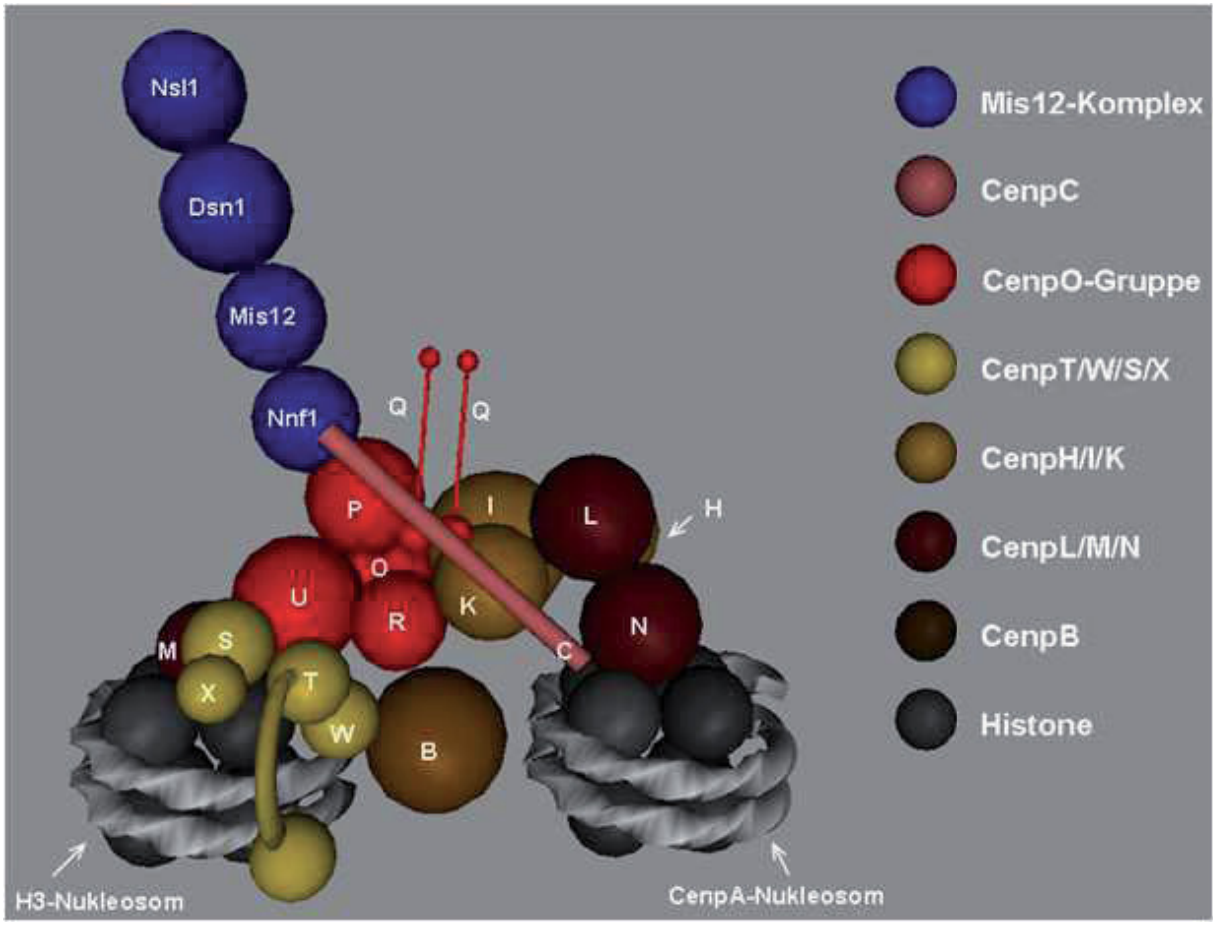

Abbildung 2: dreidimensionales Modell eines CCAN mit angelagertem hMis12-Komplex während der Interphase. Die abgebildeten Kugelvolumina entsprechen den Molekulargewichten der dargestellten Proteine des humanen Kinetochors. (entnommen aus der Dissertation von V. Döring)

3.4.1. CENP-N

Im Zuge der Entdeckung von CENP-N als Teil des NAC zeigten RNAi-Experimente, dass das Fehlen von CENP-N zu einer Verlängerung der Mitose und Fehlern in deren Ablauf führt (Abbildung 3A) (Foltz et al., 2006). Außerdem konnte beobachtet werden, dass eine Abhängigkeit der Rekrutierung von CENP-H und –O besteht, wobei es wiederum zu doppelten Einbauraten von CENP-N in CENP-O-depletierten Zellen kommt. CENP-N ist zusammen mit CENP-H erforderlich für die Anordnung der Chromosomen in der Metaphaseplatte, beide Proteine bilden zusammen mit CENP-I, -K, -L und -M eine Subkomplex und sind wahrscheinlich Teil des gleichen Prozesses (McClelland et al., 2007; Hori et al., 2008), wobei allerding die Abwesenheit von CENP-N keinen Effekt auf die Bindung der Mikrotubuli an das Kinetochor hat (McClelland et al., 2007).

CENP-N lokalisiert vor allem innerhalb der Interphase an das Kinetochor, während der Mitose kommt es zu einer Verminderung der Proteinkonzentration um 80%. Dies deutet

darauf hin, dass die beobachteten Mitosedefekte verursacht durch die Depletion von CENP-N in der Interphase begründet sind (Abbildung 3B) (McClelland et al., 2007; Hellwig et al., 2011).

Es konnte gezeigt werden, dass CENP-N *in vitro* an rekonstituierte CENP-A-Nukleosomen binden kann und *in vivo* eine enge Nachbarschaft mit CENP-A ausbildet (Carroll et al., 2009, Hellwig et al., 2011). Hierbei erkennt der N-terminale Anteil von CENP-N, wie auch HJURP, die CATD von CENP-A, wobei sich die Anheftung beider Bindungspartner zum gleichen Zeitpunkt ausschließt. Die Deletion von CENP-A führt ebenfalls zum Verlust von CENP-N *in vivo* (Abbildung 3C) (Foltz et al., 2006, Okada et al., 2006). Der C-Terminus von CENP-N beeinflusst nicht die direkte Bindung an CENP-A-Nukleosomen im *in vitro* Versuch, allerdings zeigen Deletionsmutanten eine verminderte Lokalisierung von CENP-N an das Kinetochor innerhalb von Zellen. Nur bei starker Überexpression der CENP-NΔC-Mutante, welcher der C-Terminus fehlt, kann eine Rekrutierung beobachtet werden (Carroll et al., 2009; Hellwig et al., 2011). In biochemischen Versuchen konnte weiterhin gezeigt werden, dass CENP-N direkt mit CENP-L interagiert. Die Bindung erfordert wiederum das Vorhandensein des C-terminalen Anteils von CENP-N, dessen Deletion *in vivo* eine Destabilisierung der Bindung von CENP-N an das Kinetochor in der mittleren S-Phase zur Folge hat. Diese Ergebnisse implizieren, dass der C-Terminus von CENP-N nicht zur Lokalisierung an das Kinetochor essentiell ist, aber für die eigene Stabilisierung durch andere Proteine des CCAN benötigt wird (Carroll et al., 2009; Hellwig et al., 2011).

Experimente mit siRNA gegen CENP-N zeigten eine verminderte Einbaurate von CENP-A an das centromerische Chromatin sowie eine Absenkung des CENP-C-Gehaltes. Die Reduktion von CENP-H, -K und –I an den Kinetochoren ist hierbei stärker ausgeprägt als bei RNAi-Experimenten mit CENP-A, was vermuten lässt, dass die Rekrutierungsdefekte anderer CCAN-Komponenten eine direkte Folge der Reduktion von CENP-N ist und nicht auf den mangelnden Neueinbau von CENP-A zurückzuführen ist (Carroll et al., 2009).

CENP-N besitzt ein Homolog in *Saccharomyces cerevisiae* (Abbildung 3D), Chl4, welches wichtig ist für die Etablierung neu gebildeter Kinetochore aber nicht für deren Erhaltung. Schon bestehende Kinetochore werden in Deletionsmutanten normal an die Tochterzellen vererbt, wohingegen neu eingebrachte Plasmide, an welchen die Proteinstrukturen funktionsfähiger Kinetochore noch nicht ausgebildet sind, instabil sind (Mythreye & Bloom, 2003). CENP-N in *S. cerevisiae* ist somit essentiell für die Formation von nukleaseresistenten Strukturen an neu eingebrachten Centromeren. *S. cerevisiae* Zellen, in welchen das Homolog von CENP-N deletiert wurde, ist es außerdem unmöglich, andere Komponenten des Kinetochorkomplexes, inklusive Cse4, dem Homolog von CENP-A, zu assemblieren. Dies deutet darauf hin, dass die Funktion von CENP-N beim Neueinbau von CENP-A in das centromerische Chromatin stark konserviert ist (Mythreye & Bloom, 2003).

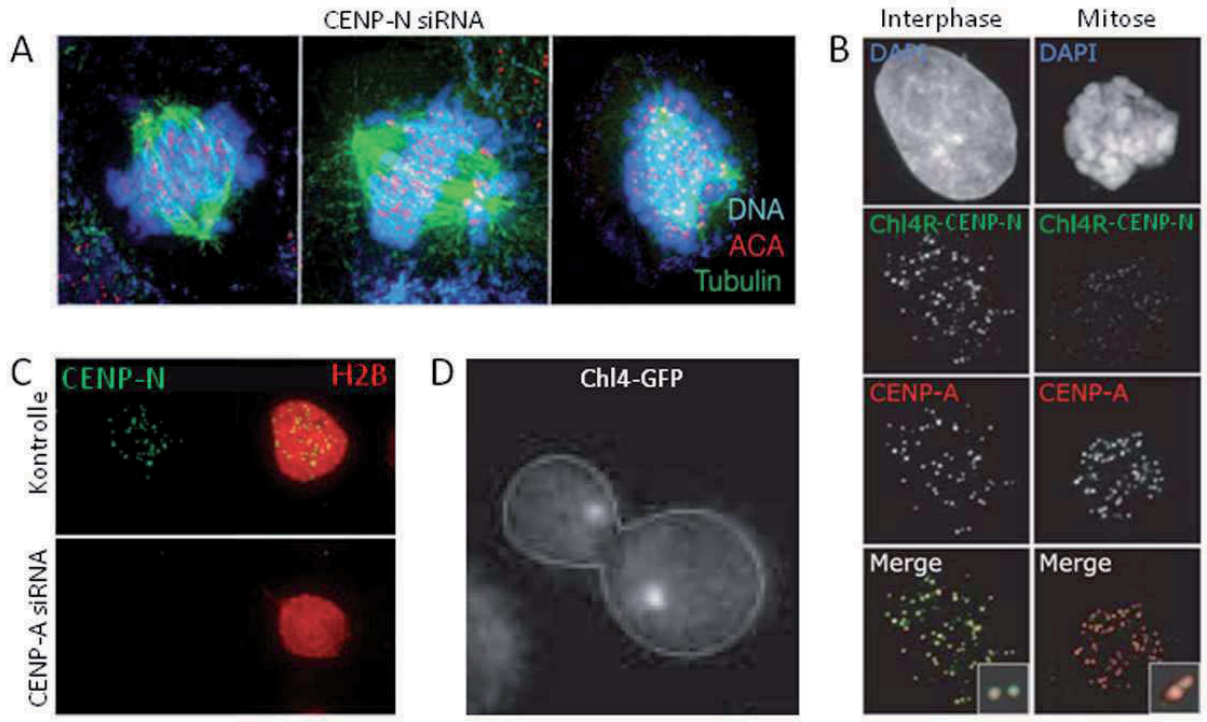

Abbildung 3: A: Mitosedefekte ausgelöst durch die Depletion von CENP-N in HeLa Zellen (entnommen aus Foltz et al., 2006); **B:** Lokalisierung von CENP-N an Kinetochoren von HeLa Zellen in Interphase und Mitose, Färbung mittels des CENP-Antikörpers Chl4R (entnommen McClelland et al., 2007); **C:** Reduktion von kinetochor-lokalisiertem CENP-N ausgelöst durch die Depletion von CENP-A in HeLa Zellen (entnommen Foltz et al., 2006); **D:** Lokalisierung von Chl4 in einer knospenden *Saccharomyces cerevisiae* Zelle (entnommen Mythreye & Bloom, 2003)

3.4.2. CENP-T/W/S/X-Komplex

CENP-T, ein weiteres Mitglied des NAC, bildet zusammen CENP-W, CENP-S und CENP-X einen essentiellen Unterkomplex des Kinetochors (Abbildung 4A und 4D) (Foltz et al., 2006, Hori et al., 2008; Amano et al., 2009; Nishino et al., 2012). Das entstehende Heterotetramer kann sich direkt an die DNA anheften und die Lokalisierung der beteiligten Komponenten bedingt sich wechselseitig (Abbildung 4C) (Hori et al., 2012). Jedes der vier Proteine besitzt eine Histonfaltungsdomäne, über welche CENP-T und CENP-W sowie CENP-S und CENP-X miteinander verbunden sind (Nishino et al., 2012). Durch die Vereinigung beider Dimere entsteht eine nukleosomenähnliche Struktur, welche die DNA im Bereich der Centromere, ähnlich wie bei CENP-A- und H3-Nukleosomen, umwinden kann (Nishino et al., 2012). Diese CENP-T/W/S/X-nukleosomalen Strukturen sind mit kanonischer H3-Nukleosomen assoziiert, wobei allerdings CENP-A-Nukleosomen in direkter Nähe vorhanden sein müssen (Hori et al., 2008; Ribeiro et al., 2010; Suzuki et al., 2011).

RNAi-Experimente mit CENP-T und CENP-W zeigen, dass der Mangel eines oder beider

Proteine nach 36 Stunden zu einem Proliferationstopp führt, welchem ein Absterben nach 96 Stunden folgt. Dieser Vorgang wird durch eine Akkumulation der Zellen in der Mitose und Mitosedefekten begleitet (Abbildung 4B) (Foltz et al., 2006; Gascoigne et al., 2011). Es ist festzustellen, dass die Depletion von CENP-S bzw. CENP-X einen ähnlichen Phänotyp verursacht, sich allerdings weniger gravierend auswirkt als die Depletion von CENP-T/W (Amano et al., 2009). Desweiteren konnte gezeigt werden, dass durch die gezielte Disruption der für die Tetramerbildung verantwortlichen Aminosäuren von CENP-S oder CENP-T die Rekrutierung der mutierten Proteine vermindert wird und es nicht zum Aufbau einer funktionellen Kinetochorsstruktur kommt (Nishino et al., 2012). Dies impliziert, dass die Fähigkeit zur Tetramerisierung des CENP-T/W/S/X-Komplexes essentiell für die Etablierung eines intakten Kinetochor ist (Hori et al., 2012).

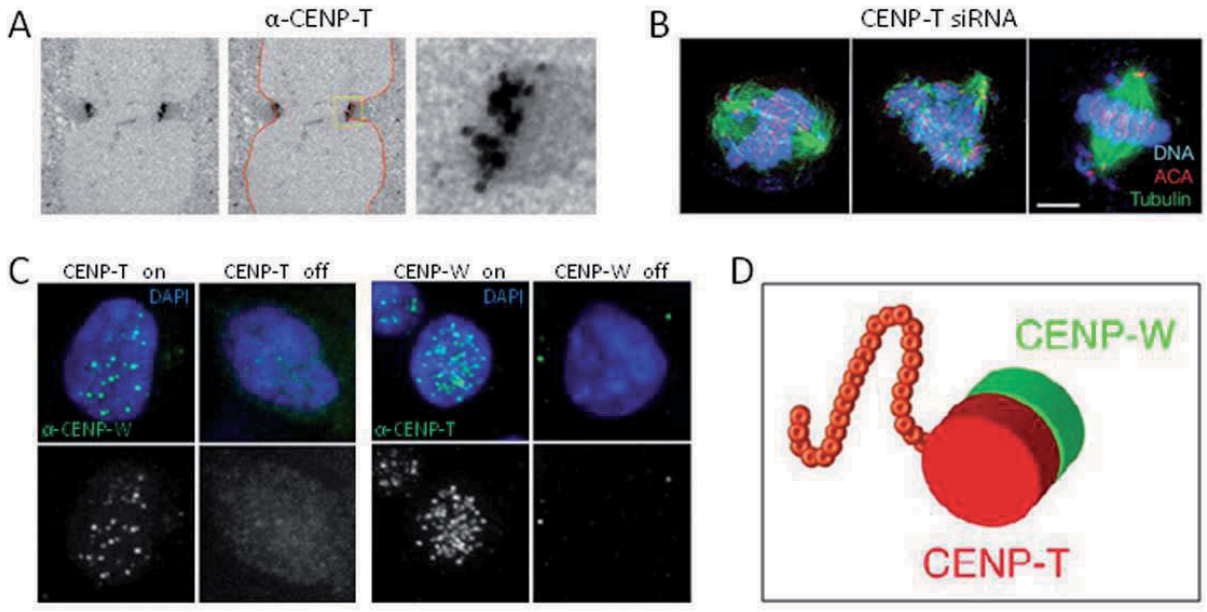

Abbildung 4: A: elektronenmikroskopische Aufnahme der Lokalisierung von CENP-T an den Kinetochor in DT40 Zellen (entnommen Suzuki et al., 2011); B: Mitosedefekte verursacht durch die Depletion von CENP-A in HeLa Zellen (entnommen Foltz et al., 2006); C: wechselseitige Abhängigkeit der Lokalisierung von CENP-T und CENP-W, die Depletion von CENP-T führt zu Störungen in der Lokalisation von CENP-W (links), das Fehlen von CENP-W verhindert die Lokalisation von CENP-T an das Kinetochor (rechts), (entnommen Hori et al., 2008); D: Modell des Subkomplexes CENP-T/ CENP-W (entnommen Suzuki et al., 2011)

Für die Funktionalität von CENP-T durch den Zellzyklus hinweg ist eine schrittweise Phosphorylierung während der G2-Phase erforderlich, welcher sich in der Anaphase eine Dephosphorylierung anschließt. Eine Blockade dieser Phosphorylierung durch Mutationen der zu modifizierenden Aminosäuren führt zum Mitosearrest. Dies deutet darauf hin, dass die

Phosphorylierung von CENP-T essentiell für den fehlerfreien Ablauf der Mitose ist (Gascoinge et al., 2011).
CENP-T zeichnet sich durch den nahezu kompletten Austausch des eingebauten Proteins im Verlauf des Zellzyklus aus. Der maximale Gehalt dieses Proteins wird während der G2-Phase erreicht und sinkt wiederum auf ein Minimum innerhalb der G1-Phase ab. Dieses Verhalten könnte darauf hindeuten, dass CENP-T eine Plattform für weitere an der Mitose beteiligten Moleküle bilden könnte (Prendergast et al., 2011).

3.4.3. CENP-O/P/Q/R/U

Die bereits im Jahr 2005 erschienene Beschreibung von CENP-U unter dem Namen CENP-50, ein Jahr bevor eine Vielzahl neuer Proteine des menschlichen inneren Kinetochors bekannt wurden, gab erste Hinweise auf eine Komplexität, welche bis zu diesem Zeitpunkt nicht vermutet wurde (Minoshima et al., 2005; Foltz et al., 2006; Okada et al., 2006). Im Laufe der Zeit wurde versucht, diese neu entdeckten Moleküle basierend auf ihren biochemischen Eigenschaft, der Lokalisierung oder Interaktionen aufgrund Deletionensanalysen einer Vielzahl von Unterkomplexen zu zuordnen (Okada et al., 2006; Foltz et al., 2006; McClelland et al., 2007; Hori et al., 2008). Hierbei kristallisierte sich heraus, dass die Proteine CENP-O, -P, -Q, -R und –U eine funktionelle Untereinheit bilden, deren Lokalisierung auf CENP-H, -I, -K, -L und –M sowie der korrekten Rekrutierung untereinander basieren (Okada et al., 2006; Foltz et al., 2006; Izuta et al., 2006; Hori et al., 2008; Amaro et al., 2010; Eskat et al., 2012).
Die Deletion von CENP-O/P/Q/U stellte sich nicht als letal heraus, allerdings kommt es zu Wachstumsstörungen in Verbindung mit Mitosedefekten, Blockierungen innerhalb der Ausbildung der Zellpolarität sowie einer Schwächung der Schwesterchromatidbindung (Minoshima et al., 2005; Okada et al., 2006; McAinsh et al., 2006; Kang et al., 2006; Hori et al., 2008). Eine Sonderstellung nimmt CENP-R ein, welches keine Wachstumsverzögerung auslöst und auch die Lokalisierung der andern Komplexelemente nicht beeinflusst. Dies suggeriert eine den andern Proteinen des Komplexes nachgeordnete Rekrutierung von CENP-R (Hori et al., 2008). Es konnte außerdem gezeigt werden, dass CENP-U direkt mit Hec1, einer Komponente des KMN-Netzwerks, interagiert und somit die Bindung der Mikrotubuli an das Kinetochor direkt ermöglicht (Minoshoma et al., 2005; McClelland et al., 2007).
Es konnten zellzklusabhängige Phosphorylierungen von CENP-U beobachtet werden, welche eine wichtige Rolle innerhalb der Reparatur von Spindelschäden spielt (Minoshima et al., 2005; Hori et al., 2008). Durch die Modifikation der Aminosäuren 62 und 63 kommt es

zur Beeinflussung der Lokalisierung von CENP-U besonders in der G2-Phase wird dessen Ubiqutinierungsgrad sowie die Degradation durch Proteasomen reguliert (Kang et al., 2006; Hori et al., 2008). Diese zellzyklusabhängige Konzentrationsschwankungen konnten auch bei den anderen Unterkomplexkomponenten, mit Ausnahme von CENP-R, nachgewiesen werden (Minoshima et al., 2005; Eskat et al., 2012).

3.5. KMN-Netzwerk

Benannt nach den beteiligten Proteinen, KNL-1, dem Mis12-Komplex (Mis12, Dsn1, Nnf1, Nsl1) und dem Ndc80-Komplex (Hec1, Nuf2, Spc24, Spc25), bildet das KMN-Netzwerk eine Verbindung zwischen den inneren Kinetochorproteinen des CCAN und den Mikrotubuli (Cheeseman et al., 2006) (Abbildung 5A). Die Bindungsfähigkeit der einzelnen Komponenten wird durch die Anwesenheit der anderen KMN-Proteine erhöht. Sie lokalisieren nur während der Mitose an der äußeren Platte des Kinetochors und übertragen den Zug der Spindelmikrotubuli während der Anaphase (Cheeseman & Desai et al., 2008). Hierbei kommt es zur direkten Anheftung der Spindelfasern an das globuläre Ende der hantelförmigen Struktur, welche durch Hec1 und Nuf2 gebildet wird, sowie an KNL-1. Diese beiden Bindungsstellen sind wiederholt angeordnet und vermitteln somit multiple Kontaktstellen zu den Mikrotubuli (DeLuca et al., 2005; Cheeseman & Desai et al., 2008) (Abbildung 5B). Neueste Untersuchungen zeigen, dass pro Kinetochor 10-30 Mikrotubuli und pro Mikrotubuli 7 Moleküle KNL-1, 9 Mis12-Komplexe und 9 Ndc80-Subkomplexe binden (Johnston et al., 2010; McEwen & Dong, 2010).

Es bestehen Anhaltpunkte auf diverse Bindungsstellen zwischen KMN-Netzwerk und dem CCAN, z.B. zwischen CENP-H, -I &-K und KNL-1, CENP-T und Hec1, CENP-C und dem Mis12-Komplex oder CENP-U und Hec1 (Cheeseman et al., 2008; Hua et al., 2010; Suzuki et al., 2011). Biochemische Experimente haben gezeigt, dass die konservierte N-terminale Region von CENP-C an das hMis12-Komplex-Protein Nnf1 bindet, wobei diese Assoziation stöchiometrisch zu sein scheint (Przewloka et al., 2011; Screpanti et al., 2011). Außerdem kommt es in Folge einer Disruption von CENP-C zur starken Verminderung der Lokalisierung des hMis12-Komplexes, welcher wiederum mit dem Mikrotubuli-bindenden Hec1-Komplex assoziiert ist (Liu et al., 2006; Kwon et al., 2007; Milks et al., 2009). Dies Beobachtungen zeigen, dass CENP-C ein Verbindungsglied zwischen centromerischen Chromatin und den Mikrotubuli-bindenden Komponenten des äußeren Kinetochors sein könnte (Hori et al., 2012).

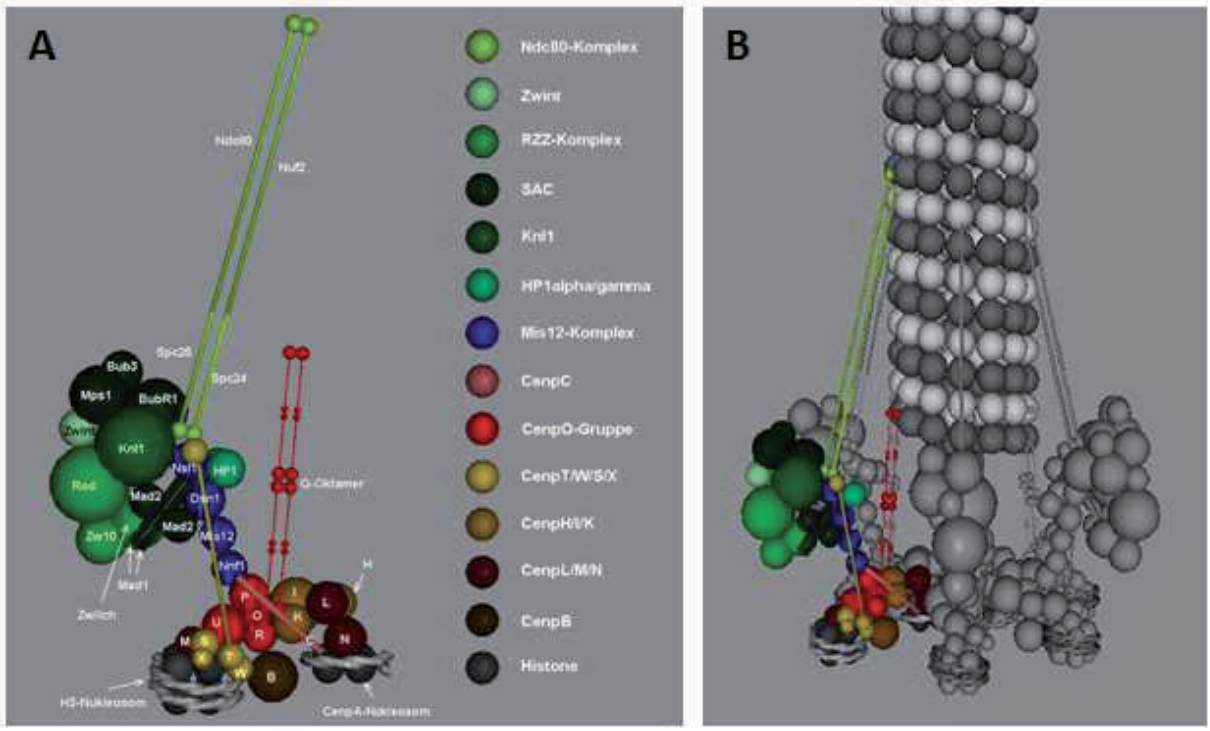

Abbildung 5: A: dreidimensionales Modell eines mitotischen Kinetochormoduls. Die Kugelvolumina entsprechen dem Molekulargewicht der humanen Proteine. B: sechs Kinetochormodule koppeln an einen Mikrotubulus an und stellen so eine stabile Verbindung her. (entnommen aus der Dissertation von V- Döring)

Eine weitere Verbindung zwischen CCAN und dem KMN-Netzwerk wird durch CENP-T vermittelt (Hori et al., 2008). Der etwa 500 Aminosäuren lange N-Terminus von CENP-T ist unstrukturiert und flexibel. Nach der Anheftung der Mikrotubuli während der Mitose kann eine Streckung dieses Bereichs beobachtet werden, welche durch den entstehenden Zug ausgelöst wird (Suzuki et al., 2011). Es konnte gezeigt werden, dass für die im *in vitro* Experiment nachgewiesene Bindung von rekombinanten CENP-T an den Hec1-Komplex ein circa 100 Aminosäuren großer Bereich des N-Terminus von CENP-T verantwortlich ist (Gascoinge et al., 2011).

Da die Rekrutierung von CENP-T und CENP-C unabhängig verläuft sowie über unterschiedliche Mechanismen realisiert wird, stellen diese beiden Proteine zwei verschiedene, parallel angeordnete Wege zur Verbindung des Centromers mit dem äußeren Kinetochor dar (Hori et al., 2008; Gascoinge et al., 2011; Hori et al., 2012).

Eine weitere Aufgabe des KMN-Netzwerks ist die Vermittlung der Regulation, welche die Anordnung der Chromosomen in der Metaphaseplatte vor der Trennung der Schwesterchromatiden ermöglicht (Cheeseman et al., 2006). Dieser sehr dynamische Prozess wird durch abwechselndes Anwachsen und Degradieren der Tubulinmoleküle am Plus-Ende der Mikrotubuli bewerkstellig, welches eine Oszillation entlang der Spindelachse bewirkt (Amaro et al., 2010). Außerdem erkennt das KMN-Netzwerk die korrekte Anbindung

der Mikrotubuli an die Kinetochore und berichtigt Fehler durch die Ablösung falsch gebundener Spindelfasern. Dieser Vorgang wird überwacht und die Trennung der Schwesterchromatiden wird wiederum vom KMN-Netzwerk so lange verzögert, bis alle Kinetochore richtig angeheftet sind (Cheeseman et al., 2006; Przewloka & Glover, 2009).
Ist die korrekte Anbindung abgeschlossen, kommt es zur Streckung und Rearrangement des CCAN sowie dem Aufbau einer Zugkraft auf die Kinetochore. In dessen Folge werden Checkpointproteine freigesetzt, entlang der Spindelfasern zu den Polen transportiert und letztendlich die Schwersterchromatide voreinander getrennt (Howell et al., 2004; Perpelescu & Fukagawa, 2011).

3.6. Aktuelles Modell des Kinetochors

Basierend auf den aktuellen Untersuchungen des Kinetochors zeichnet sich ein sehr diffiziles Bild dieses Komplexes mit einer zeitlich wohl abgestimmten Funktion ab. Hierbei fungiert CENP-A, meist im Zusammenspiel mit der α-satelliten-DNA, und anderen CCAN-Proteinen als Markierung für den kinetochorspezifischen Lokus (Hori et al., 2012). Während der G1- und S-Phase scheint die Hauptaufgabe in der Erhaltung und Verdopplung des Kinetochors zu liegen. Es kommt zum Einbau von CENP-A in das centromerische Chromatin, wobei dieser von vielen verschiedenen Komponenten beeinflusst, reguliert und überwacht wird. Zu Beginn der S-Phase werden die Nukleosomen von ihrer tetramerischen Konformation zu Oktameren umgebaut, um möglicherweise der Replikationsmaschinerie die Passage zu gewährleisten. Nach erfolgreicher Duplikation der centromerischen DNA während der S-Phase kommt es zur Rückbildung der Oktamere zu Tetrameren und somit zum Abschluss Selbsterhaltungsfunktion des Kinetochors (Bui et al., 2012).
In der S-Phase beginnt die progressive Einlagerung fast aller konstitutiven Kinetochorproteine, welche bis zum Ende der G2-Phase in den maximalen Proteingehalten kulminiert (Minoshima et al., 2005; Prendergast et al., 2011; Eskat et al., 2012). Dieser Vorgang ist eine Grundbedingung für die Erfüllung der Aufgaben des Kinetochors während der Mitose. Hierbei stellen CENP-C und CENP-T, und in dessen Folge die Etablierung der CENP-T/W/S/X-nukleosomenartigen Strukturen, Kandidaten für die Bildung eines strukturellen Kerns dar, welcher die Verbindung zwischen dem centromerischen Chromatin und dem äußeren Kinetochor bildet (Gascoinge et al., 2011; Hori et al., 2012). Zusammen sind sie in der Lage weitere innere Kinetochorproteine, die Hec1- und hMis12-Komplexe sowie KNL1 an das Kinetochor zu rekrutieren. Die Flexibilität der mittleren Region von CENP-T befähigt das innere Kinetochor zur Organisation und dem Rearrangement der Mikrotubulikopplungsstellen und könnte somit die korrekte Trennung der

Schwesterchromatide ermöglichen (Shang et al., 2010; Gascoinge et al., 2011; Hori et al., 2013)

3.7. Kinetochore verschiedener Spezies

Bis heute wurden drei verschiedene Typen von Centromeren beschrieben: Regioncentromere, Punktcentromere und Holocentromere (Pimpinelli & Goday, 1989; Pluta et al., 1996). Trotz signifikanter Unterschiede bezüglich der Sequenz, der Ausdehnung der zugrundeliegenden centromerischen DNA und der daran bindenden Kinetochorkomplexe zeigen sich generelle Ähnlichkeiten bezüglich der Anzahl und den Eigenschaften der beteiligten Proteine in allen eukaryotischen Organismen, welche hochkonserviert sind (Abbildung 6A und 6B) (Sullivan, 2001).

3.7.1. *Schizosaccharomyces pombe* - Regioncentromer

Die 35-100kb große centromerische DNA von *S. pombe* ist sehr AT-reich und wird von Heterochromatin flankiert (Pidoux & Allshire, 2005; Morris & Moazed, 2007). Jedes der 3 Chromosomen besitzt einen unkonservierten Kern, welchen bis heute keine spezielle Sequenz zugeordnet werden konnte (Clarke, 1998). Dieser Kernbereich wird beidseitig von je einem Paar invertierter, repetitiver Sequenzabschnitte umschlossen, wobei Teile der äußeren Bereiche die Formation stabiler Centromere beeinflussen (Abbildung 6A) (Steiner & Clarke, 1994; Clarke, 1998). Basierend auf der Bindung der Proteine Cnp1, welches dem humanen CENP-A entspricht, sowie Mis6 und Mis12 an den Kernbereich und an die inneren Sequenzabschnitte des Centromers wird der Aufbau komplexen Kinderchors von *Schizosaccharomyces pombe* ermöglicht (Abbildung 6B) (Goshima et al., 1999; Partridge et al., 2000; Takahashi et al., 2000; Cleveland et al., 2003). Nachdem an jedes Kinetochore vier Mikrotubuli gebunden haben, durchläuft *S. pombe* eine sogenannte „geschlossene Mitose“, das heißt, es kommt während der Mitose nicht zur Auflösung der Kernhülle (Ding et al., 1993; Knop 1999; McIntosh 1999; Gay et al., 2012)

A

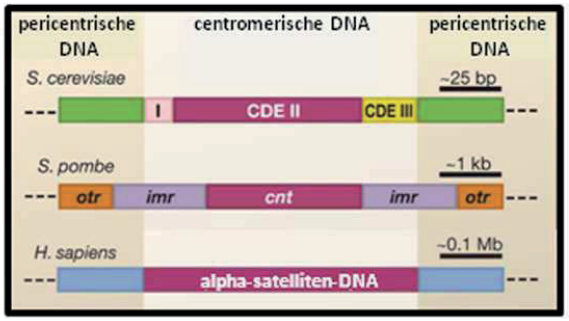

C

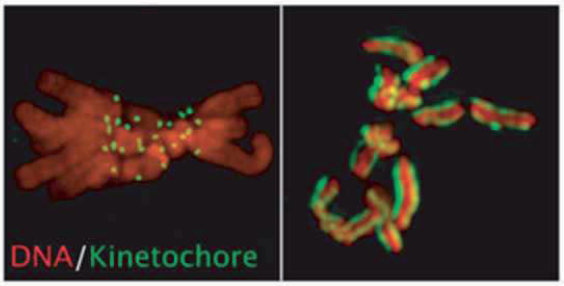

B

H. sapiens	*S. pombe*	*S. cerevisiae*
CENP-C	Cnp3	Mif2
CENP-O CENP-P CENP-Q CENP-U CENP-R	Mal2 Fta2 Fta7 Mis17	Mcm21 Ctf19 Okp1 Ame1
CENP-H CENP-I CENP-K	Fta3 Mis6 Sim4	Mcm16 Ctf3 Mcm22
CENP-T CENP-W CENP-S CENP-X	SPBC800.13/Cnp20 SPAC17G8.15 SPBC2D10.16 SPCC576.12c	Cnn1 YDR374W-A/Wip1 YOL086W-A/Mhf1 YDL160C-A/Mhf2
CENP-M CENP-N CENP-L	 Mis15 Fta1	 Chl4 Iml3 (Mcm19)
	Fta4 Cnl2 Fta5 Fta6	Nkp1 Nkp2

Abbildung 6: A: Struktur der centromerischen DNA von *Saccharomyces cerevisiae*, *Schizosaccharomyces pombe* und *Homo sapiens* (modifiziert nach Morris et al., 2007); **B**: tabellarische Darstellung der homologen Proteine des CCAN in *Homo sapiens*, *Schizosaccharomyces pombe* und *Saccharomyces cerevisiae* basierend auf Sequenzvergleichen (entnommen aus Schleiffer et la., 2012); **C**: Vergleich der Lokalisierung der Kinetochore humaner Monochromosomen (links) mit Holochromosomen eines *Caenorhabditis elegans* Embryo (rechts), (entnommen aus Oegema & Hyman, 2006)

3.7.2. *Saccharomyces cerevisiae* - Punktcentromer

Bloom und Carbon konnte 1982 erstmals centromerische DNA in *S. cerevisiae* nachweisen (Bloom & Carbon, 1982). Diese umfasst 125bp und besteht aus 3 Centromer-DNA-Elementen, CDEI, CDEII und CDEIII, wobei CDEI und CDEIII an jedem der 16 Chromosomen die gleiche Sequenz aufweisen (Abbildung 6A) (Russo & Sherman, 1989; Meraldi et al., 2006). Punktmutationen in einem dieser beiden Bereiche zerstören die Aktivität des Kinetochors (Cheeseman et al., 2006). Das nicht konservierte, AT-reiche CDEII Element interagiert mit dem CENP-A Homolog Cse4 und bildet somit die Grundlage des Punktkinetochors in *S. cerevisiae* (Stoler et al., 1995). Cse4 verfügt, ebenfalls wie CENP-A im Menschen, über ein spezielles Chaperon, welches jedoch in *S. cerevisiae* ein Heterohexamer mit $[H4\text{-}Cse4]_2$ konstituieren kann (Mizuguchi et al., 2007; Black & Cleveland 2011).

Desweiteren kommt es zur Bindung des Cbf3-Komplexes an CDEIII sowie des Proteins Cbf1 an das Element CDEI, welche durch die Interaktion miteinander die Anheftung eines einzelnen Mikrotubuli an jedes Kinetochor ermöglichen (Winey et al., 1995; Hemmerich et al., 2000; Gardner et al., 2001; Westermann et al., 2007). Basierend auf diesen DNA-

gebundenen Unterkomplexen kommt es zur Rekrutierung des Cbf19- und des Ndc80-Komplexes, welche durch die Interaktion des distalen Kinetochors mit den Spindelkomponenten als Adaptoren für das Mikrotubuli fungieren (Ortiz et al., 1999; Wigge & Kilmartin, 2001; Janke et al., 2001). Ein weiterer wichtiger Subkomplex des Kinetochors von Bäckerhefe stellt der COMA-Komplex dar, welcher teilweise den Proteinen des CCAN im Menschen entspricht (Abbildung 6B) (Ortiz et al., 1999; De Wulf et al., 2003). Der Dam1/DASH-Komplex bildet eine Ringstruktur mit 16-facher Symmetrie und ist die zentrale Komponente der Mikrotubulibindung (Cheeseman et al., 2001; Janke et al., 2001; Li et al., 2002; Cleveland et al., 2003). In *S. cerevisiae* wird die Anheftung der Mikrotubuli an die Kinetochore durch den ganzen Zellzyklus, mit Ausnahme der Replikation der centromerischen DNA während der S-Phase, aufrechterhalten (Pearson, 2004; Westermann et al., 2007; Coffmann et al., 2011).

3.7.3. *Caenorhabditis elegans* - Holocentromer

In den meisten Organismen zeichnen sich die Chromosomen durch eine primäre Einschnürung aus, an welcher sich der Kinetochorkomplex anlagert (Abbildung 6C). Im Gegensatz zu diesen monocentrischen Chromosomen besitzt *C. elegans* holocentrische Chromosomen. Die Besonderheit von holocentrischen Chromosomen besteht darin, dass die Kinetochorproteine entlang des gesamten Chromosoms binden (Abbildung 6C) (Oegema & Hyman, 2006). Die Anheftung der Mikrotubuli erfolgt auf der dem Pol zugewandten Seite des Chromosoms (Dernburg, 2001; Maddox et al., 2004; Guerra et al., 2010). Diese ungewöhnliche Strukturvariante wurde erstmals von Schrader 1935 beschrieben und als diffuses Kinetochor-Chromosom bezeichnet (Schrader, 1935). Trotz der Ausdehnung über das gesamte Chromosom existieren diskrete Bindestellen für die Mikrotubuli, wobei bisher nicht bekannt ist, ob spezifische DNA-Sequenzen zugrunde liegen (White, 1973; Melters et al., 2012). Nur eine Minderheit der Eukaryoten besitzen holocentrische Chromosomen, welche bisher in 768 Spezies nachgewiesen werden konnten, wobei diese in *Caenorhabditis elegans* am besten untersucht wurden (Melters et al., 2012). Desweiteren kommen holocentrische Chromosomen in Insekten, Pflanzen, Spinnentieren sowie anderen Arten von Fadenwürmern vor. Wahrscheinlich haben sie sich innerhalb der Evolution dreizehnmal unabhängig voneinander aus der monocentrischen Form entwickelt (Melters et al., 2012). Holocentrische Chromosomen ermöglichen eine schnelle karyotypische Evolution, da es bei Doppelstrangbrüchen oder bei Fusionen von Chromosomen nicht zum Verlust oder zur Duplizität des Kinetochors kommt. Dies erlaubt eine Veränderung des Karyotyps ohne den korrekten Ablauf der Mitose zu gefährden (Schneider et al., 2009).

Trotz der Unterschiede in der Ausdehnung ist die molekulare Komposition in *C. elegans* anderen untersuchten eukaryotischen Kinetochorkomplexen sehr ähnlich. Auch die holocentrischen Kinetochore basieren auf Homologen der CENP-A-Nukleosomen und umfassen insgesamt etwa 30 Proteine (Buchwitz et al., 1999; Sullivan, 2001; Oegema et al., 2001; Kitagawa, 2009).

3.8. Biologische Bedeutung des Kinetochors

3.8.1. Neocentromere

Auch mit der Vollendung des Humanen Genom Projekts vor über 15 Jahren ist nicht die komplette Sequenz der menschlichen Erbinformation bekannt, wobei den größten fehlenden Anteil von ~5% die centromerische DNA ausmacht (Eichler et al., 2004). Um die DNA zu segregieren, müssen die Spindelfasern unter Vermittlung des Kinetochorkomplexes an das centromerische Chromatin binden. Hierbei ist nach wie vor ungewiss, welche Rolle dabei die DNA-Sequenz spielt.
Im Normalfall besitzt jedes Chromosom ein Centromer, wobei bis heute nicht geklärt ist, wie die Aufrechterhaltung dieser 1:1 Regel gewährleistet wird (Zeiltlin, 2010). Es bestehen allerdings auch Ausnahmen, die sogenannten Neocentromere. Neocentromere sind neue primäre Einschnürungsstellen, welche fähig sind voll funktionsfähige Kinetochore auszubilden (Amor et al., 2004). Diese können neben bereits vorhandenen Centromeren existieren, wobei der schon bestehende Centromer in diesem Falle inaktiviert wird (Peretti et al., 1986; Sullivan & Schwartz, 1995)), oder aufgrund des Verlusts des bestehenden Centromers neu etabliert werden. Neu gebildete konstitutive Centromere werden meist bei Kindern festgestellt, welche Geburtsfehler und Entwicklungsstörungen zeigen. Diese Defekte stehen in Verbindung mit Chromosomenrearrangements, welche zu Fehlern im Chromosomensatz und Chromosomen mit fehlender α-satelliten-DNA führen. Die Bildung von Neocentromeren an nicht-centromerischem Chromatin wird als Rettungsmechanismus für Chromosomenfragmente, welche andernfalls verlorengehen würden, aufgefasst (Amor et al., 2004).
Neocentromere wurden vor über 70 Jahren erstmals in Mais entdeckt (Rhoades & Vilkomerson, 1942), bis heute wurde eine Vielzahl von Neocentromeren im Menschen nachgewiesen. Es konnte gezeigt werden, dass Neocentromere auch ohne α-satelliten-DNA, das heißt Sequenz-unabhängig, etabliert werden (Voullaire et al., 1993). Hierbei werden Protein- oder Chromatinstrukturen etabliert, welche über den Zellzyklus reguliert und

umgebaut werden. Die zugrundeliegenden Mechanismen sind zurzeit allerdings unbekannt. Die Bildung von Neocentromeren geschieht sehr selten, somit muss ein anderer Mechanismus als zur Erhaltung der normalen Centromerstruktur zugrunde liegen. Dies zeigt sich an der Beobachtung, dass an neu eingebrachten Plasmiden in CENP-N-defizienten *Saccharomyces cerevisiea* Zellen keine Kinetochore aufgebaut werden können, aber schon vorher existierende erhalten bleiben (Mythreye et al., 2003).

3.8.2. DNA-Reparatur

Eine weitere gezielte Lokalisierung von Kinetochorproteinen an nicht-centromerische DNA erfolgt bei der Reparatur von DNA-Doppelstrangbrüchen. Der schrittweise Ablauf dieses Vorgangs, bestehend aus der Erkennung des Schadens, der Rekrutierung der Reparaturmaschinerie und der anschließenden Behebung des Defekts, setzt den Umbau des Chromatins voraus, um Zugang zur geschädigten Struktur zu ermöglichen (Zeitlin et al., 2009). Zeitlin und Kollegen konnten 2009 zeigen, dass während der Interphase innerhalb von zwei Minuten nach Erfolgen des Strangbruches CENP-A, CENP-N und CENP-U rund um die Störungsstelle rekrutiert wird. Der schnell akkumulierende Komplex ist nicht-nukleosomaler Natur, wobei die Autoren spekulieren, dass es im weiteren Verlauf zur Ausbildung von nukleosomalen Strukturen kommen könnte. Mit einer Verzögerung von ca. dreißig Minuten ist ebenfalls CENP-T an der zu reparierenden Stelle nachweisbar. Etwa nach einer Stunde wird CENP-A abrupt vom Bruch delokalisiert (Zeitlin et al., 2009). Der gesamte Vorgang erfolgt ohne eine Verminderung der bestehenden kinetochorgebundenen Proteine. Die Lokalisierung von CENP-A an DNA-Schäden impliziert, dass die Assemblierung von CENP-A gezielt auch ohne ein vorher existierendes Template an jeder beliebigen Stelle der DNA erfolgen kann (Zeitlin 2010). Bis heute ist allerdings nicht geklärt, ob die beteiligten Kinetochorproteine bei der Reparatur von DNA-Schäden ähnliche Aufgaben erfüllen wie am Centromer.

3.8.3. Erkrankungen

Neben dem durch Bildung von Antikörpern gegen körpereigene Kinetochorproteine ausgelösten CREST-Syndrom können Fehlfunktionen dieser Strukturen die Ursache weiterer Krankheiten sein. Aneuploidie, also eine Fehlverteilung der Chromosomen auf die Tochterzellen, wird in nahezu allen Tumorarten gefunden und entsteht zu einem frühen Zeitpunkt der Tumorgenese (Tomonaga et al., 2003). Es konnte gezeigt werden, dass es

aufgrund einer Überexpression auf transkripionaler und translationaler Ebene zur Assoziation von CENP-A mit nichtcentromerischen Regionen des Chromatins kommen kann. Diese sehr häufig in Darmkrebszellen vorkommende Störung kann einher gehen mit der Dissoziation von CENP-A von den Kinetochoren, welche deren Zerstörung nach sich zieht (Tomonaga et al., 2003).

Ebenfalls ein signifikant erhöhter Gehalt an CENP-A wurde kürzlich in vielen Lungenadenokarzinomgeweben nachgewiesen. Hierbei konnte festgestellt werden, dass die Stärke der Erhöhung des Protein- und mRNA-Niveaus dieses grundlegenden Kinetochorproteins mit sinkenden Überlebensraten der Betroffenen korreliert (Wu et al., 2012).

Auch andere Proteine des Kinetochorkomplexes können eine Rolle bei der Krebsentstehung spielen. Es hat sich gezeigt, dass besonders CENP-C ein bevorzugtes Ziel von durch Viren verursachten Erkrankungen werden kann (Everett et al., 1999). Durch die Bindung des Herpes Simples Virus Protein VMW110 kann es zur Proteosomen-abhängigen Degradation von CENP-C kommen, welche in der Zerstörung der Kinetochorstruktur und der Entstehung von Pseudometaphasen währen der Mitose resultiert (Everett et al., 1999; Lomonte et al., 1999).

Das Humane Papillomavirus 18 wurde als Hochrisikoerreger für Gebärmutterhalskrebs eingestuft. Die Überexpression der freigesetzten viralen Onkogene führt zu einem Verlust von humanem p53 und pRb, in dessen Folge es zur Zerstörung der körpereigenen Tumorsuppression sowie den zellularen Mechanismen, welche die genomische Stabilität und die Zellzykluskontrolle steuern, kommt (Yaginuma et al., 2010). Allerdings kann die Entstehung von Krebs nicht nur auf den Funktionsverlust von p53 und pRb zurück zu führen sein, da zwischen der Infektion und dem Auftreten von Tumoren im Normalfall eine Zeitspanne von 10-20 Jahren liegt. Yaginuma et al. 2010 konnten zeigen, dass eines der beteiligten Onkogenprodukte ebenfalls an CENP-C bindet. Bei HPV18 kommt es allerdings nicht zur Degradation des betroffenen Kinetochorproteins. Die Autoren mutmaßen, dass die Bindung des viralen Proteins zu einer Störung der Kinetochorfunktion führt, welche wiederum die Segregation beeinflusst und damit Aneupolidie auslösen könnte.

Auf einem ganz anderen Weg kann es im Zusammenhang mit Störungen der Kinetochorproteine zu Krankheitsbildern kommen. Die Fanconi Anämie ist charakterisiert durch Entwicklungsschäden, Knochenmarksdefekte und Krebs (de Winter et al., 2009). Der involvierte Proteinkomplexes, bestehend aus 8 Eiweißen, spielt eine Rolle bei der Reparatur von DNA-Schäden (Singh et al., 2010). Kürzlich wurde festgestellt, dass CENP-S und CENP-X Teil dieser funktionellen Struktur sind. Die beiden beteiligten Kinetochorproteine bilden ein DNA-bindendes Dimer und sind unentbehrlich für die Integrität des Fanconi-Anämie-Reparaturmechanismus (Singh et al., 2010; Dornblut et al., in Revision).

3.8.4. Seneszenz

Zellulare Alterung stellt einen unumkehrbaren Wachstumsarrest verursacht durch unterschiedliche Stressfaktoren, zum Beispiel DNA-Schäden, oxidativer Stress, Telomerverkürzungen oder Onkogenaktivierung, dar (Hayflick & Moorhead, 1961; Serrano et al., 1997; Ben-Porath et al., 2005; Collado et al., 2007; Deng et al., 2008). Aufgrund der Fähigkeit von Tumorzellen zu unendlichem Wachstum ohne jemals seneszent zu werden, gilt der Alterungsprozess als Selbstverteidigungsmechanismus, um unkontrolliertes Wachstum und Tumorgeneses zu verhindern. p53 und das Retinoblastomaprotein pRb werden eine Schlüsselrolle im Zellzyklusarrest in seneszenten Zellen zugeschrieben (Maehara et al., 2010). Es konnte gezeigt werden, dass der Proteingehalt von CENP-A in Zellen, welche in Seneszenz übergegangen sind, deutlich reduziert ist. Es kommt allerdings nicht zu einer Reduktion der mRNA-Konzentration, welche signifikant stärker ausfällt als bei normalen Zellarresten. Die deutet darauf hin, dass das alterungsbedingte Absinken der CENP-A-Menge durch posttranskripionale Modifikationen erfolgt (Maehara et al., 2010). Die künstliche Reduktion von CENP-A-mRNA in primären humanen Retinoblasten induziert Alterung, wohingegen die Anwendung der gleichen Protokolle in HeLa-Zellenlinie keinen Effekt zeigte. In den HeLa-Zellen kam es durch eine natürliche Infektion mit dem Papillomavirus zu einer Inaktivierung von p53 und verursachte somit die Unsterblichkeit der Zellen. Desweiteren konnten Maehara et al. zeigen, dass die Inaktivierung von p53 in Fibroblastenzellen mit stark vermindertem CENP-A Gehalt die Fähigkeit zur Zellteilung wieder herstellten kann. Hierbei kam es zu einer Erhöhung des Anteils der Zellen mit abweichender Chromosomenanzahl. Sie schlussfolgerten daraus, dass die Reduktion von CENP-A zu Seneszenz führt und dieser Vorgang unabhängig von p53 stattfindet (Maehara et al., 2010).

Eine weitere Alterungserscheinung von Zellen konnten Duncan und Kollegen (2012) zeigen. Die verminderte Empfängniswahrscheinlichkeit älterer Frauen ist im verstärkt vorkommenden Auftreten von Aneuploidie der Eizellen durch Rekombinationsfehler begründet. In deren Folge kommt es zu ungenauen Spindelformierungen und Mikrotubuli-Kinetochor-Interaktionen sowie Defekten im Spindelassemblierungs-Checkpoint (Hassold & Hunt, 2009; Eichenlaub-Ritter et al., 2010,; Jones & Lane, 2012). Die Arbeitsgruppe stellte eine steigende Interkinetochordistanz mit direkter Korrelation zum fortschreitenden Alter der Probandinnen fest, welche auch mit dem Auftreten von nicht miteinander verbundenen Schwesterchromatiden einhergeht (Duncan et al., 2012).

Manuskript 1

Live-cell imaging reveals sustained centromere binding of CENP-T via CENP-A and CENP-B

Daniela Hellwig, Sandra Münch, Sandra Orthaus, Christian Hoischen, Peter Hemmerich, and Stephan Diekmann

Journal of Biophotonics (2008)

In dieser Arbeit wurden die dynamischen Eigenschaften sowie die molekularen Interaktionen des inneren Centromerproteins CENP-T in lebenden menschlichen Zellen untersucht. Acceptor-Bleaching-FRET Untersuchungen zeigen eine enge Nachbarschaft zwischen den N-Termini von CENP-T und CENP-A sowie zwischen CENP-T und CENP-B. Der Austausch von CENP-T am Kinetochor ist auf die S-Phase des Zellzyklus beschränkt. Diese Ergebnisse deuten darauf hin, dass CENP-T eines der grundlegenden Proteine des inneren Kinetochors ist.

Manuskript 2

Acceptor-photobleaching FRET analysis of core kinetochore and NAC proteins in living human cells

D. Hellwig, C. Hoischen, T. Ulbricht, Stephan Diekmann

European Biophysics Journal (2009)

In dieser Arbeit wurden die Nachbarschaftsverhältnisse des CENP-A-Nukleosomal Assoziierter Komplex (NAC) mittels Acceptor-Bleaching-FRET untersucht. Es zeigte sich, dass enge Nachbarschaften zwischen den inneren Kinetochorproteinen CENP-U und CENP-I, zwischen CENP-U und CENP-B sowie zwischen CENP-M und CENP-T bestehen.

Manuskript 3

Dynamics of CENP-N kinetochore binding during the cell cycle

Daniela Hellwig, Stephan Emmerth, Tobias Ulbricht, Volker Döring, Christian Hoischen, Ronny Martin, Catarina P. Samora, Andrew D. McAinsh, Christopher W. Carroll, Aaron F. Straight, Patrick Meraldi and Stephan Diekmann

Journal of Cell Science (2011)

Diese Arbeit zeigt, dass sich die N-Termini von CENP-N und CENP-A auch in der lebenden menschlichen Zelle in enger Nachbarschaft zueinander befinden. Außerdem deuten mikroskopische Messungen zu den dynamischen Eigenschaften, dem Ladeverhalten sowie den Proteingehalten *in vivo* über den Zellzyklus darauf hin, das CENP-N als einen Genauigkeitsfaktor zum Laden von CENP-A fungiert.

Manuskript 4

Premitotic Assembly of Human CENPs –T and –W Switches Centromeric Chromatin to a Mitotic State

Lisa Prendergast, Chelly van Vuuren, Agnieszka Kaczmarczyk, Volker Döring, Daniela Hellwig, Nadine Quinn; Christian Hoischen, Stephan Diekmann, Kevin F. Sullivan

PLOS Biology (2011)

Untersuchungen an CENP-T und CENP-W bezüglich der Zellzyklusregulation, Einbauzeitenpunkte und der Stabilität über Generationen hinweg zeigen, dass der CENP-T/W Unterkomplex eine Plattform zur Assemblierung weiterer Proteine des inneren und äußeren Kietochors bildet. Erst der Aufbau dieses Fundaments versetzt das centromerischen Chromatin in einen Zustand, in welchem die Mitose eingeleitet werden kann.

Manuskript 5

Step-Wise Assembly, Maturation and Dynamic Behavior of the Human CENP-P/O/R/Q/U Kinetochore Subcomplex

Anja Eskat, Wen Deng, Antje Hofmeister, Sven Rudolphi, Stephan Emmerth, Daniela Hellwig, Tobias Ulbricht, Volker Döring, James M. Bancroft, Andrew D. McAinsh, M. Christina Cordoso, Patrick Meraldi, Christian Hoischen, Heinrich Leonhardt, Stephan Diekmann

PLOS ONE (2012)

Mittels verschiedenster Floureszenztechniken *in vivo* und *in vitro* konnte gezeigt werden, dass die Proteine des CENP-P/O/R/Q/U vielfältig miteinander vernetzt sind, sich dieser Unterkomplex allerdings erst am Kinetochor bildet. Während der zweiten Hälfte des Zellzyklus kommt es zu einem Umbau innerhalb der Struktur, welche einem Reifungsmechanismus entsprechen könnte, welcher die Anheftung der Mikrotubuli innerhalb der Mitose ermöglicht.

J. Biophoton. **1**, No. 3, 245–254 (2008) / **DOI** 10.1002/jbio.200810014

Journal of BIOPHOTONICS

FULL ARTICLE

Live-cell imaging reveals sustained centromere binding of CENP-T via CENP-A and CENP-B

*Daniela Hellwig, Sandra Münch, Sandra Orthaus, Christian Hoischen, Peter Hemmerich, and Stephan Diekmann**

Leibniz-Institute for Age Research – Fritz Lipmann Institute, Dept. of Molecular Biology, Beutenbergstr. 11, D-07745 Jena, Germany

Received 18 March 2008, accepted 21 April 2008
Published online 23 May 2008

Key words: centromere, kinetochore, mitosis, live-cell imaging, NAC complex, FRAP, FCS, FRET

At the centromere, a network of proteins, the kinetochore, assembles in order to grant correct chromatin segregation. In this study the dynamics and molecular interactions of the inner kinetochore protein CENP-T were analyzed employing a variety of fluorescence microscopy techniques in living human cells. Acceptor-bleaching FRET indicates that CENP-T directly associates with CENP-A and CENP-B. CENP-T exchange into centromeres is restricted to the S-phase of the cell cycle as revealed by FRAP, suggesting a coreplicational loading mechanism, as we have recently also demonstrated for CENP-I. These properties make CENP-T one of the basic inner kinetochore proteins with most further proteins binding downstream, suggesting a fundamental role of CENP-T in kinetochore function.

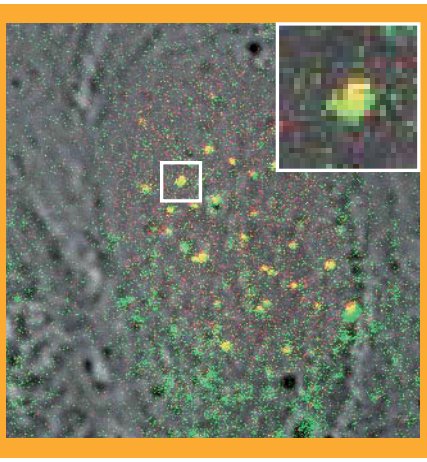

1. Introduction

The kinetochore is a multiprotein complex that assembles at centromeres and grants correct DNA segregation. The kinetochores contain a structural core composed of protein–protein interaction networks called NAC ("nucleosome-associated complex") and CAD ("CENP-A distal complex"), termed the constitutive centromere-associated network (CCAN), and further proteins and protein complexes, among them KNL-1 and the Hec 1 and hMis12 complexes (for reviews see Cheeseman and Desai, 2008; Mussachio and Salmon, 2007). The NAC proteins (CENP-C, CENP-H, CENP-U, CENP-M, CENP-T and CENP-N) were purified in association with CENP-A nucleosomes, while the CAD proteins (CENP-I, CENP-Q, CENP-R and CENP-S) could only be purified with NAC proteins [7, 17].

The exact functions of NAC and CAD proteins are uncertain, their presence at centromeres, however, is required for correct kinetochore function. Depletion of NAC and CAD proteins in human or chicken cells causes chromosome congression and mitotic defects [7, 11, 15, 17]. The NAC and CAD

* Corresponding author: e-mail: diekmann@fli-leibniz.de

proteins can be grouped into three different functional classes [9, 13, 17]. Suppression of CENP-M, CENP-N or CENP-T by siRNA caused an increase in the number of cells in mitosis, with the reduction of CENP-T resulting in the most pronounced effect [7]. Depletion of either of these three proteins disrupted recruitment of NAC proteins, in particular, reduction of CENP-T eliminated CENP-M at centromeres [7]. These data suggest a fundamental role for CENP-T in centromere assembly and function.

Little is known about the dynamic binding of the NAC and CAD proteins to the centromere site and about their binding relationships within the complexes. The inner kinetochore has a complex dynamic organization: the six inner kinetochore proteins analyzed show a cell-cycle-dependent assembly that provides, on the one hand, stability by sustained binding of some (CENP-A and CENP-I) and varying degrees of flexibility through dynamic exchange of other components (i.e. CENP-B, CENP-H, CENP-C) [8]. CENP-A replaces histone H3 in the centrometric nucleosomes and binds histone H4 as shown in vitro [3] and in vivo [18]. CENP-B binds to the complex in the direct neighborhood to CENP-A [18].

Here, we determined by cell-cycle-dependent FRAP, FRET and FCS analyses the dynamics of CENP-T binding to centromeres and its direct association with CENP-A and CENP-B.

2. Materials and experimental methods

2.1 Plasmids

Plasmid pDF197 encoding a LAP-CENP-T fusion protein was a kind gift of Dan Foltz and Iain Cheeseman and was used for amplification of full length CENP-T by PCR (Expand high fidelity^{PLUS} PCR System, Roche, Penzberg, Germany) applying forward primer 5′-GGGGACAAGTTTGTACAAAAAAGCAGGCTT-CGAAAACCTGTATTTTCAGGGCGCCACCATG-GCTGACCACAACCCTGAC-3′ and reverse primer 5′-GGGGACCACTTTGTACAAGAAAGCTGGGT-CTGGGCAGGGAAGACAGAGTT-3′. The CENP-T harboring linear PCR fragment was transferred into vector pDONR221 by BP recombination reaction (Invitrogen, Carlsbad, CA, USA). After verification by sequencing (MWG Biotech, Ebersberg, München, Germany), the CENP-T gene was cloned by LR recombination reactions into various modified pEFP-C and pEFP-N (BD Biosciences, Clontech, Palo Alto, CA, USA) based Destination vectors. As the result we obtained expression vectors carrying the genes coding for CENP-T fused to the C- as well as to the N-termini of EGFP, Cerulean, and YFP. In the construct fluorescent protein (FP)-CENP-T, the amino acid (aa) linker between the two fused proteins is SGTSLYKKAGFEN-LYFQGAT. Due to the cloning protocol, the aa sequence TQLSCTKW is added to the C-terminal end of FP-CENP-T. In the alternative construct CENP-T-FP, the aa linker sequence is TQLSCTKWLDPPVAT (with no N-terminal addition). The Cerulean sequence was a kind gift of N. Klöcker, Freiburg.

2.2 Cell culture and transfection into HEp-2 cells

HEp-2 (HeLa derivative) cells were obtained from the American Tissue Culture Collection (ATCC, Rockville, USA). The cells were cultured in Dulbecco's modified Eagle's medium DMEM (PAA Laboratories, Pasching, Austria) supplemented with 10% fetal calf serum (PAA Laboratories, Pasching, Austria) in a 9.5% CO_2 atmosphere at 37 °C and grown to subconfluency as recommended. At this stage, the medium was removed and cells were washed with magnesium- and calcium-containing PBS (Sigma-Aldrich, Taufkirchen, Germany) followed by detachment with trypsine/EDTA (PAA Laboratories, Pasching, Austria). The detached cells were dissolved in fresh DMEM and reseeded in new culture dishes. For live-cell imaging experiments, cells were seeded on 42 mm glass dishes (Saur Laborbedarf, Reutlingen, Germany) one or two days before experiments and transfected with plasmid DNA 24–48 h before observation using FuGENE HD Transfection reagent (Roche, Basel, Switzerland) according to the manufacturer's protocol.

2.3 Western blots

To control the full length protein expression of the fusion constructs, transfected HEp-2 cells were taken from culture flasks, counted in a Neubauer chamber and lyzed for 10 min at 100 °C in an appropriate volume of 2% SDS, 0.1% bromphenole blue, 35 mM dithiothreitole, 25% glycerol and 60 mM TrisHCl pH 6.8. Cell lysates with appropriate amounts of total protein were separated by SDS-PAGE and blotted onto Protran BA nitrocellulose (Schleicher and Schuell, Dassel, Germany). Proteins reacted with mouse monoclonal antibody against GFP (#sc-9996, Santa Cruz Biotechnology, Santa Cruz, USA) at a dilution of 1 : 50. Bound antibodies were detected with horse radish peroxidase-conjugated goat anti-mouse IgG antibodies (#115-035-072, Jackson Immunoresearch Laboratories, West Grove, USA) at a

dilution of 1 : 4.000 and finally with the ECL-advance system (Amersham Biosciences, Uppsala, Sweden) according to the manufacturer's instructions. The chemiluminescence was detected by Biomax light-1 Kodak film (Kodak, Stuttgart, Germany).

2.4 Fluorescence correlation spectroscopy (FCS) measurements

Fluorescence correlation spectroscopy (FCS) measurements were performed at 37 °C on a LSM 510 Meta/ConfoCor2 combi system (Carl Zeiss, Jena, Germany) using a C-Apochromat infinity-corrected 1.2 NA 40× water objective. With this setup, a spot on a previously scanned image of a cell can be selected for the FCS measurement. EGFP-tagged proteins were illuminated with the 488 nm line of a 20 mW Argon laser with a 4.3 A tube current attenuated by an acousto-optical tunable filter (AOTF) to 0.1%. The detection pinhole had a diameter of 70 μm and emission was recorded through a 505 nm long path filter. For the measurments, 15 × 10 time series of 10 s each were recorded with a time resolution of 1 μs and then superimposed for fitting to an anomalous diffusion model in three dimensions [8, 22] with triplet function [21, 23] using the software LSM-FCS software release 4.0 (Zeiss, Jena, Germany). The diffusion coefficients and anomaly parameters were extracted from fitted curves obtained from the software.

2.5 Fluorescence recovery after photobleaching (FRAP)

Fluorescence recovery after photobleaching (FRAP) experiments were carried out on a Zeiss LSM 510 Meta confocal microscope (Carl Zeiss, Jena, Germany) using a C-Apochromat infinity-corrected 1.2 NA 63× water objective and the 488 nm laser line for GFP. Five or ten images were taken before the bleach pulse and 50–200 images after bleaching of two to four centromeres of a nucleus with an image acquisition frequency of 0.5–1 frames per second at 1% laser transmission to avoid additional bleaching. During short-term FRAP experiments the pinhole was completely open to increase low fluorescence intensities and to ensure total bleaching of centromeric spots in the nucleus. In long-term FRAP experiments, the pinhole was adjusted to 2 airey units and image stacks were taken every 60 min. Quantitation of relative fluorescence intensities was done according to Chen and Huang (2001) and Schmiedeberg et al. (2004) using Excel (Microsoft, Redmond, WA, USA) and Origin software (OriginLab, Northhampton, MA, USA). Recovery halftimes in long-term FRAP experiments were determined by linear regression of the monophasic increase of fluorescence recovery.

2.6 Acceptor-bleaching-based FRET measurements (AB-FRET)

When FRET occurs, both the intensity and lifetime of the donor fluorescence decrease, while the intensity of the acceptor emission increases. All these changes can be exploited to measure the efficiency of energy transfer between the donor and the acceptor. Experiments were carried out as described by Orthaus et al., (2008).

Cerulean fluorescence was excited with the argon 458 nm laser line and detected using the Meta detector (ChS1 + ChS2: 477–499 nm). EYFP fluorescence was excited with the argon 514 nm laser line and detected in one of the confocal channels using a 530 nm long-pass filter. To minimize crosstalk between the channels, each image was collected separately in the multitrack mode, i.e. both fluorophores were exited and recorded specifically and separately. Single optical sections were selected by scanning the sample along the z-axis for optimal fluorescence signals.

Acceptor bleaching was achieved by scanning a region of interest (ROI) including one centromere of a nucleus 100 times (scans at 1.6 μs pixel time) using the 514 nm laser line at 100% intensity. Bleaching times per pixel were identical for each experiment. However, total bleaching times varied depending on the size of the bleached ROIs and the used magnification. Two to three Cerulean and EYFP fluorescence images were taken before and about 7 images were taken after the EYFP bleaching procedure to assess changes in donor and acceptor fluorescence. To minimize the effect of photobleaching of the donor during the imaging process, the image acquisition was performed at low laser intensities (1% laser intensity). To compare the time course of different experiments, Cerulean and EYFP intensities in the ROI were averaged and normalized to the highest intensity measured during the time series, respectively. The FRET efficiency E was determined by comparing the fluorescence intensity I_{DA} of the donor in presence of an acceptor with the intensity I_{DA} in the absence of an acceptor. E was calculated according to $E = 1 - (I_{DA}/I_D)$. I_{DA} was obtained by averaging the Cerulean intensities of the two prebleach images in the presence of a photochemically intact acceptor. I_D was determined by measuring the Cerulean fluorescence intensity in the first image obtained after the acceptor has been destroyed by

photobleaching. Based on the donor intensity variations in the negative control experiments of a few per cent only, we considered the presence of energy transfer when $E > 8\%$.

3. Results

CENP-T is a NAC kinetochore protein of unknown function. In order to determine its properties in living human cells, we analyzed its dynamics and neighborhood relationships by fluorescent microscopy techniques. Full-length expression of each fusion protein was verified by Western blot analysis (data not shown). Upon expression in HEp-2 cells, fluorescently tagged inner kinetochore proteins localized in vivo at centromeric regions, reflecting the distribution of endogenous centromere proteins (data not shown; [8, 18]). EGFP-tagged CENP-A was correctly incorporated into nucleosomes of centromeric heterochromatin [31] indicating that the fluorescent tag does not alter the localization of the fusion protein in comparison to the endogenous protein. CENP-B-EGFP and EGFP-CENP-C tightly bind to human centromeres [8] indicating that these tagged kinetochore proteins, as CENP-A, retained functional properties of the endogenous proteins. Also, the fluorescently tagged histone H1 showed the same distribution in the nucleus as the endogenous protein [26–27]. CENP-T was observed to localize at kinetochores in human HeLa cells in interphase and mitosis [7]. In our experiments we confirmed these findings: CENP-T showed a complete colocalization with CENP-A (Figure 1) during interphase. In mitosis, we observed CENP-T as specific dots within the chromatin in the equatorial plate (Figure 1).

3.1 Fluorescence Correlation spectroscopy (FCS)

In order to determine the dynamic behavior of CENP-T in living human Hep-2 cells, we applied FCS (Figure 2). In FCS, a low-intensity laser beam is directed into a defined measuring volume by a confocal setup. Photons emitted from fluorophores diffusing through this volume are counted over time, the photon count rate is then subjected to an autocorrelation analysis and fitting to appropriate diffusion models, from which the diffusion coefficients can be determined [8, 22]. FCS within regions of high fluorescence intensity, i.e. within the kinetochore complex, was not applicable, because such measurements are impaired by bleaching artefacts due to fluorescence saturation of the control volume. Measured autocorrelation curves could be fitted satisfactorily to a model assuming 3-dimensional obstructed (or anomalous) diffusion ([1, 25, 29] see Figure 2). Typically, in a diffusion process, the mean squared displacement (msd) of a particle is a linear function of time. Anomalous diffusion is used to

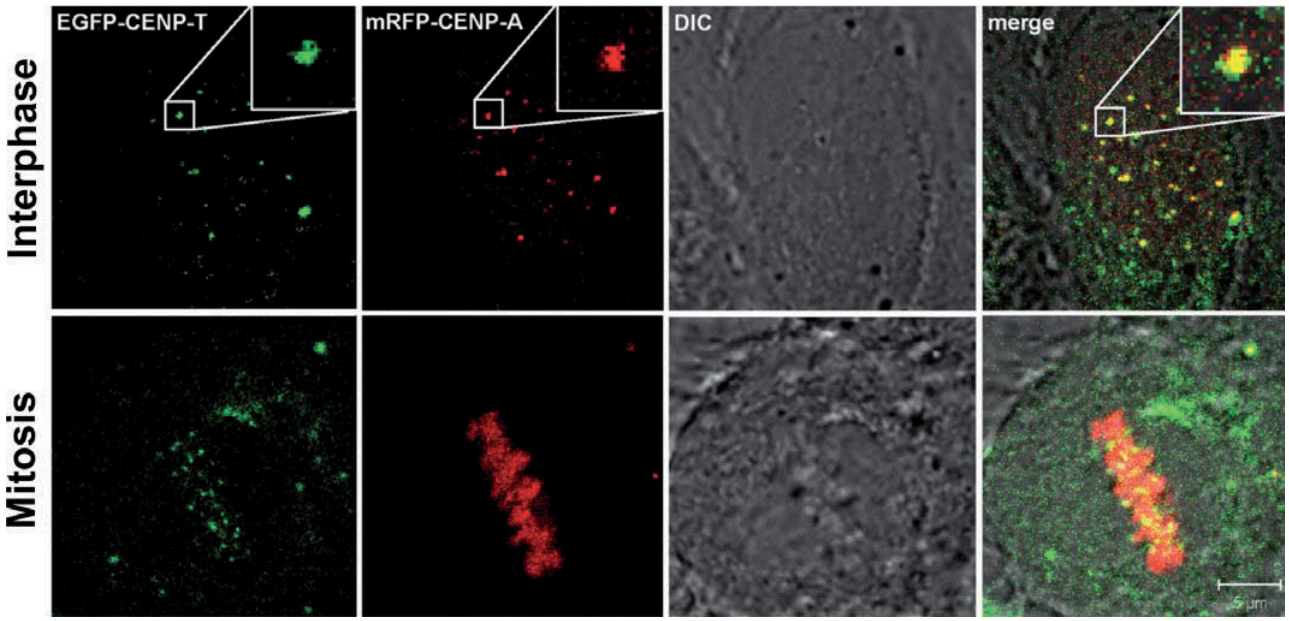

Figure 1 (online colour at: www.biophotonics-journal.org) Localization of CENP-T in living human HEp-2 cells. Cells were cotransfected with EGFP-CENP-T and mRFP-CENP-A. In interphase (upper panel), both proteins colocalize as indicated by the enlarged dot in the upper right corner of the pictures. During mitosis (lower panel), CENP-T localizes to a large extend at specific dots in the chromatin labelled with CENP-A.

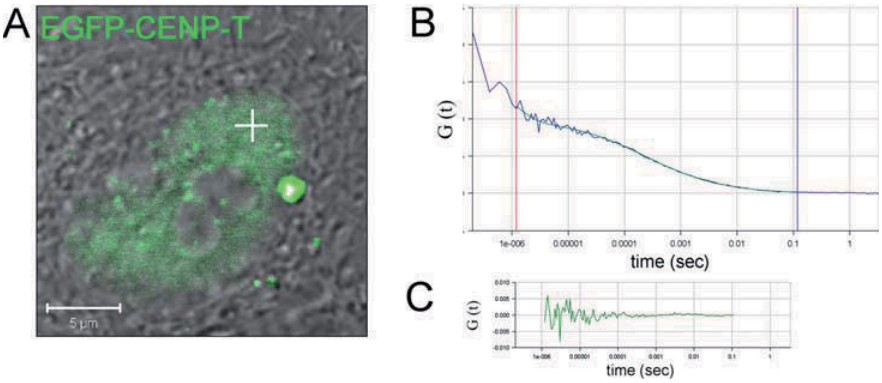

Figure 2 (online colour at: www.biophotonics-journal.org) FCS analysis of EGFP-CENP-T. A Hep-2 cell was selected that displays EGFP-CENP-T in the nucleoplasma (A). The location of the FCS measurement is indicated by a white cross. The autocorrelation of the measured fluctuation curve is shown in B (blue). Blue and red vertical lines indicate fit boundaries. The best fit according to the applied anomalous diffusion model as well as the residual plot (C) is also displayed.

describe a diffusion process with a nonlinear dependence on time. Diffusion is often described by a power law, $\mathrm{msd}(t) \sim 6Dt^{\alpha}$, with D is the diffusion coefficient and t is the elapsed time. In a typical diffusion process, $\alpha = 1$. If $\alpha > 1$, the phenomenon is called superdiffusion, which can be the result of active cellular transport processes. If $\alpha < 1$, the particle undergoes subdiffusion that might result from macromolecular crowding in the nucleo- or cytoplasm [30].

Using the obstructed diffusion model, we obtained a diffusion coefficient for nuclear nonfused EGFP of $D = 9.5 \pm 1.2\ \mu\mathrm{m}^2\ \mathrm{s}^{-1}$, in perfect agreement with published data (Wachsmuth et al., 2000). The diffusion coefficient obtained here for the fusion protein EGFP-CENP-T was $D = 0.77 \pm 0.26\ \mu\mathrm{m}^2\ \mathrm{s}^{-1}$. This reduced value can be well explained by a combination of free diffusion, unspecific collision and transient interactions with chromatin, nuclear structures or complexes. The measured D value is smaller than, but of the same order as, corresponding values of other inner kinetochore proteins, with the exception of CENP-C that moves even slower [8].

FCS also provided the anomalous diffusion parameter (α) that describes the degree of obstruction by the medium [21]. In the cell, $\alpha < 1$ and decreases continuously with increasing crowding conditions. α drops to 0.75 for proteins in solutions similarly crowed as the nucleoplasm [1]. Correspondingly, we find $\alpha = 0.73$ for nonfused EGFP in the nucleus of living cells [8]. The anomalous diffusion coefficient of EGFP-CENP-T was determined to be $\alpha = 0.57$, significantly smaller than for EGFP alone. This value for α is very similar to the corresponding value for CENP-A and within the range of α values of other inner kinetochore proteins [8]. It is too low as being only due to the increased size of the fusion protein relative to EGFP alone. The value of α alone does not allow to conclude on the mode of molecular interactions [14]. Nevertheless, our results suggest that EGFP-CENP-T, as other kinetochore proteins, might exhibit, in addition to unspecific collisions, transient binding events throughout the chromatin.

3.2 Fluorescence recovery after photobleaching (FRAP)

To address whether CENP-T dynamically exchanges or statically binds to the inner kinetochore, we applied FRAP in interphase and mitotic nuclei. Kinetochores labelled with EGFP-CENP-T were spot-bleached and fluorescence recovery in the bleached area was monitored over time by sequential imaging scans. For quantitative evaluation, bleach settings were implemented such that fluorescence in the bleached area was decreased to background levels in the first image after the bleach pulse (see Figure 3A). The microscopic images for EGFP-CENP-T revealed no recovery of fluorescence in interphase cells within 300 s (Figure 3A; quantitative values shown for 180 s, Figure 3B). We also observed no fluorescence recovery in mitotic cells (quantitative plot for 70 s, Figure 3C). The data clearly indicate that CENP-T is tightly bound to the kinetochore complex.

In order to study the long-term binding of CENP-T to the kinetochore, we followed fluorescence recovery of bleached areas over 3 h in living human cells. EGFP-CENP-T was cotransfected with PCNA-mRFP. PCNA specifically marks replication foci in S-phase, but shows only weak and diffuse fluorescence in G1 or G2 cells [28]. Mitotic cells could be well identified due to their chromosomal arrangement. In this way, we could separate cells in S-, M- and G-phases [8]. Photobleaching of S-phase cells (Figure 4A, upper panel) showed a slow recovery of $34 \pm 9\%$ after 3 h (Figure 4B) while we observed hardly any recovery ($3 \pm 9\%$)

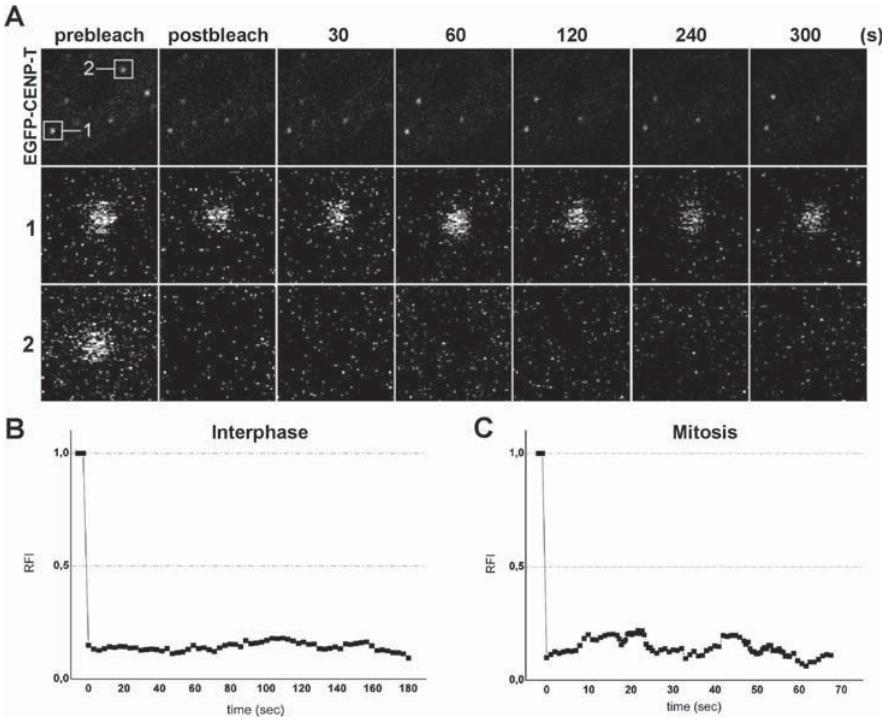

Figure 3 Short-term fluorescence recovery after photobleaching of CENP-T. EGFP-CENP-T was completely bleached by a laser pulse (488 nm, 100%) at location #2 (see upper panel, left picture). Its fluorescence recovery was measured at different time points (0, 30, 60, 120, 240 and 300 sec, see panel 2). As a control, location #1 was not bleached and showed a nearly constant fluorescence over 300 sec (see panel 1). EGFP-CENP-T showed no fluorescence recovery indicating a long residence time within the kinetochore complex of over 300 s. Quantitative fluorescence recovery in interphase during 180 s (B) and during 70 s in mitosis (C).

after 3 h in G-phases (Figure 4A, lower panel, Figure 4C). Thus, we conclude that CENP-T tighly binds to the kinetochore during the whole cell cycle and shows fluorescence recovery only during S-phase.

3.3 Fluorescence resonance energy transfer (FRET)

The cells containing the fluorescently tagged proteins were analyzed in vivo using the acceptor photobleaching method (AB-FRET). In this approach, the donor fluorescence intensity is measured (in the same sample) in the presence of an acceptor before and after destroying the acceptor by photobleaching [10]. In AB-FRET, potential energy transfer between the donor and the acceptor is eliminated by irreversibly bleaching the acceptor resulting in an increase of the donor fluorescence [2]. In our measurements, Cerulean and EYFP were used as donor and acceptor fluorophores, respectively. As described previously [18], we obtained reliable FRET data when using the ECFP analogon Cerulean [20, 24]. In transiently transfected living HEp-2 cells, the fluorescence of EYFP was destroyed by bleaching single centromeres in interphase nuclei with the unattenuated Ar 514 nm laser line. Fluorescence intensity changes in the bleached area were recorded over time in the Cerulean and EYFP channel by sequential imaging scans. FRET measurements were carried out in several independent experiments.

Many control experiments were carried out and were presented elsewhere [18]. In short, as a positive control, we had constructed the triple fusion ECFP-EYFP-CENP-A that showed strong FRET after acceptor bleaching between the neighboring fluorescence tags (with a FRET efficiency of 25%). Other control experiments allowed us to exclude photobleaching [19] or photoconversion [6, 12] of the donor Cerulean. Also, no negative influence of the bleaching procedure on cell morphology was observed (data not shown; [18]). The analysis of nonfused Cerulean and EYFP, cotransfected in living human cells, allowed us to exclude any false-positive FRET due to an unspecific association of the fluorescent tags [18]. Our control experiments indicate that if energy transfer is observed between the labelled proteins, it can only be due to a specific (direct or indirect) interaction between the proteins but not between the tags.

Here, we examined whether the N-terminus of human CENP-T is close to the N-termini of CENP-A and CENP-B at human centromeres. CENP-T showed a structured presence within the whole cell nucleus and colocalized with CENP-B at centromeres (Figure 5A, upper left picture, enlarged spots in Figure 5B). After complete bleaching of the acceptor EYFP-CENP-B at centromeric regions (Figure 5A, right pictures, enlarged spots in Figure 5B), a fluorescence intensity increase of Cerulean-CENP-T was observed (Figure 5A lower left picture, enlarged spot Figure 5B, #2). From our data, a mean FRET efficiency of $26 \pm 7\%$ was calculated indicat-

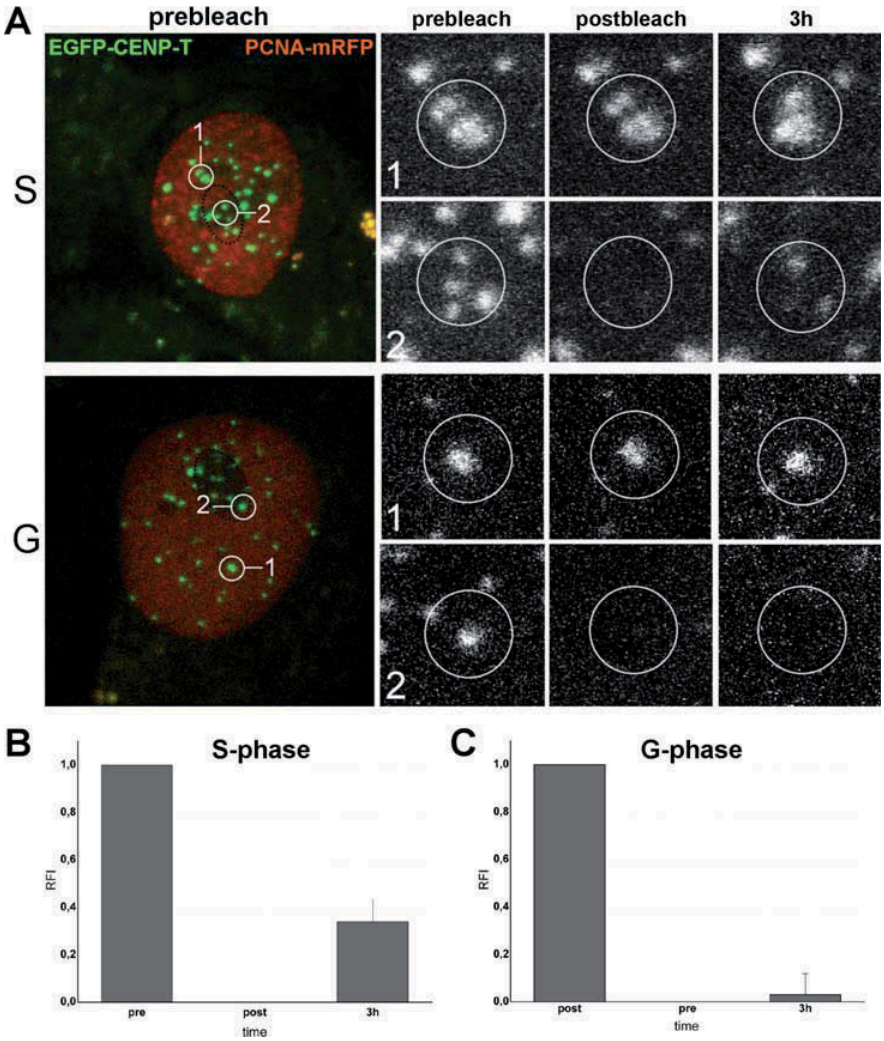

Figure 4 (online colour at: www.biophotonics-journal.org) Long-term fluorescence recovery after photobleaching of CENP-T. EGFP-CENP-T was completely bleached by a laser pulse (488 nm, 100%, marked area by black dotted line around location #2) in a S-phase cell (A, upper panel, left large picture). Its fluorescence recovery was measured in the circle #2 within the bleached area after 3 h. As a control, location #1 was not bleached and showed a nearly constant fluorescence over 3 h (see panel 1). The integrated fluorescence within a selected spot in circle #2 before and after bleaching was determined and set to 1 and 0, respectively (B). The integrated fluorescence at this spot in circle #2 after 3 h was measured and the zero-correction value after bleaching subtracted. The background level for each time point was determined at a third location within the bleached area containing no fluorescent spot and corrected for. The same procedure was carried out for cells in G-phases (A, lower panel). In G-phase, hardly any recovery was observed (3%, C). The error of these measurements is 9%.

ing an association between both proteins ($n = 8$, single kinetochores in 8 different cells). The strong bleaching of the acceptor is quantitatively displayed for a single experiment in Figure 5C for 2 time points before and 7 time points after bleaching. CENP-T is also associated with CENP-A. After complete bleaching of EYFP-CENP-A at centromeric regions (data not shown), again an increase in fluorescence was observed resulting in a FRET efficiency of $21 \pm 5\%$ ($n = 10$). Thus we conclude that the N-terminus of CENP-T is directly associated with the N-termini of CENP-A and CENP-B.

4. Discussion

At the centromere, a network of proteins assembles, forming the basis for kinetochore function. One of the inner kinetochore proteins is CENP-T, which we analyzed here by fluorescent techniques. We showed by acceptor-bleaching FRET that CENP-T, being a member of the CENP-A containing nucleosome associated (NAC) complex, directly associates with CENP-A and CENP-B in living human cells. These results have to be confirmed by fluorescence lifetime (FLIM) measurements (work in progress). Recently, we showed that CENP-A associates with CENP-B at the centromeres in living human cells [18], although these proteins do not show any interaction by yeast-two-hybrid (Y2H) analysis. Surprisingly, Y2H was also not able to detect the association between CENP-T and CENP-A or CENP-B (own unpublished data). Our dynamic data show that the kinetochore proteins have different binding and exchange behavior. During the cell cycle, we therefore expect the kinetochore to have a varying complex composition. Our FRET measurements might thus indicate a close association only at particular, longer or shorter, time periods; a potential complexity which, during interphase we did not resolve in our measurements yet.

CENP-T binds to the kinetochore with no exchange during G1 or G2 phases of the cell cycle. How-

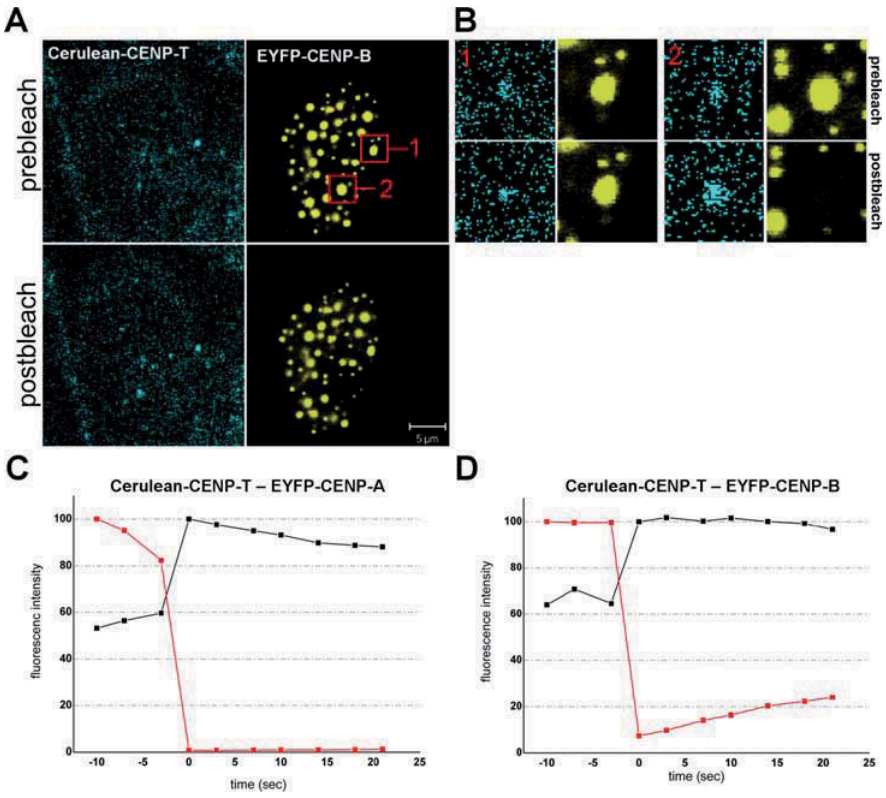

Figure 5 (online colour at: www.biophotonics-journal.org) AB-FRET of Cer-CENP-T and EYFP-CENP-B and EYFP-CENP-A. The pictures A display the prescence of Cer-CENP-T and EYFP-CENP-B in Hep-2 cells before and after the bleach laser pulse (514 nm). Two selected regions (#1, #2) were enlarged and are shown in extra pictures B. Region #1 is not bleached and retains its fluorescence while region #2 is bleached showing no EYFP-CENP-B fluorescence and an increase of Cer-CENP-T fluorescence after bleaching. C and D display the quantitative analysis of these data for single measurements for Cer-CENP-T-EYFP-CENP-A and Cer-CENP-T-EYFP-CENP-B, respectively.

ever, we observed 34 ± 9% fluorescence recovery in S-phase. Considering that genome duplication in HEp-2 cells lasts 9 to 10 h (our unpublished data) it is likely that the complete pool of centromere-bound CENP-T exchanges during S-phase. This suggests both loading and exchange of already loaded molecules involved in CENP-T assembly into centromeres. This mechanism would be clearly different from CENP-A and CENP-I incorporation that occurs via a loading-only mechanism in G1 and S-phase, respectively [8].

The dynamic properties revealed in this study identify CENP-T as one of the basic inner kinetochore proteins with further kinetochore proteins binding downstream. Indeed, depleting CENP-T by siRNA eliminated CENP-M from the kinetochore [7]. Probably, as a further consequence, also CENP-N and CENP-H would be lost since these do not bind the kinetochore in the absence of CENP-M. Elimination of CENP-T from the cell results in major mitotic defects, which are more pronounced than those caused by the depletion of CENP-N and CENP-M [7]. This supports the idea of a fundamental role of CENP-T in kinetochore function. Stable binding of CENP-T to centromeres throughout the complete cell cycle, as demonstrated here, suggests the requirement of sustained presence and function of this component in the centromere/kinetochore complex. This notion is consistent with the proposal of a unique role for CENP-T in centromere function based on the severe mitotic phenotype in CENP-T depleted cells [7].

Acknowledgement We thank N. Klöcker, D. Foltz and I. Cheeseman for the kind gift of plasmids, K. Weisshart for helpful discussions and the Deutsche Forschungs-Gemeinschaft (DFG) for support (SPP 1128).

Daniela Hellwig studied microbiology, genetics and medical microbiology in Jena. In her diploma work at the Hans-Knöll-Institute in Jena, she analyzed gene functions of the human pathogenous fungi *Candida albicans* and established a porcine intestinal epithelium assay to analyze early stages of colonization. Currently, during her PhD thesis at the Leibniz Institute for Age Research in Jena, she is determining the structure, function and dynamics of the human kinetochore protein complex.

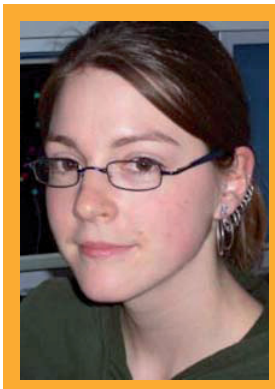

Sandra Münch studied biology at the Friedrich Schiller University in Jena. In her diploma work at the FLI in Jena, she analyzed the function of spastin (SPG4) in the human cell nucleus. She obtained her Diploma in biology in 2007. During her PhD thesis at the Leibniz Institute for Age Research in Jena, she is interested in the role of PML nuclear bodies in DNA damage response.

Sandra Orthaus studied Biology at the Friedrich Schiller University in Jena. She performed her Diploma thesis in the Department of Molecular Biology at the Institute for Molecular Biotechnology e.V., Jena. Using confocal microscopy, she analyzed functions and interspecies substitutions of the human kinetochore proteins CENP-C and CLIP170 and their yeast homologues Mif2 and Bik1 in RNAi depleted human cells. In her PhD thesis in the lab of S. Diekmann at the Leibniz Institute for Age Research (FLI) (2003–2006), she examined the architecture of the human inner kinetochore, i.e. the interaction between inner kinetochore proteins in living human cells, using fluorescence resonance energy transfer. Since October 2006 she has been working in the Genome Stability Department of Z.Q. Wang at the FLI. Currently, she is focusing on the dynamic interaction of repair proteins during the early response to DNA damage.

Christian Hoischen studied biology at the Eberhard-Karls-University Tübingen where he specialized in microbiology. His Diploma thesis was prepared at the German Research Center for Biotechnology (GBF) in Braunschweig. After studying amino acid export in corynebacteria at the Forschungszentrum Jülich in the group of Reinhard Krämer, he received his PhD at the Heinrich-Heine-University of Düsseldorf. As a postdoctoral fellow in the laboratory of Milton Sayer at the Department of Biology at the University of California, San Diego, in La Jolla, he worked on bacterial carbon metabolism. In the Molecular Biology Department at the FLI in Jena, his main research interests are the human kinetochore and the anaphase promoting complex/cyclosome.

Peter Hemmerich was educated in molecular biology, immunology and pharmacology at the Institute of Genetics at the University of Cologne. He received his PhD at the University of Constance, Germany, where he studied molecular mechanisms of systemic autoimmune diseases. He continued within this research field as a postdoctoral fellow at the Department of Molecular and Experimental Medicine at The Scripps Research Institute, La Jolla, CA, in the laboratories of Eng Tan. After returning to Germany he started to build up a research group within the Molecular Biology Department of the FLI in Jena, Germany. Peter Hemmerich's main research focus is the analysis of the structure, function and dynamics of nuclear protein complexes.

Stephan Diekmann studied physics in Hamburg and Munich. He obtained his PhD from the University Goettingen in physical chemistry. He habilitated in biology in Göttingen. He spent his postdoc years at the Max-Planck-Institute for Biophysical Chemistry with M. Eigen and at the Department of Biochemistry and Molecular Biology at Harvard University with J. Wang. After returning to Germany, he became a professor of Biophysical Chemistry at the University Jena, and, in parallel, the head of the Molecular Biology Department at the IMB in Jena (now FLI). From 1996 to 1998 he was the Scientific Director of the IMB. Since several years, his research focuses on the structure and function of the human centromere and kinetochore.

References

[1] D. S. Banks and C. Fradin, Anomalous diffusion of proteins due to molecular crowding. Biophys. J. **89**, 2960–2971 (2005).

[2] C. Berney and G. Danuser, FRET or no FRET: a quantitative comparison, Biophys. J. **84**, 3992–4010 (2003).
[3] B. E. Black, D. R. Foltz, S. Chakravarthy, K. Luger, V. L. Woods, and D. W. Cleveland, Structural determinants for generating centromeric chromatin, Nature **430**, 578–582 (2004).
[4] I. M. Cheeseman and A. Desai, Molecular architecture of the kinetochore-microtubule interface, Nature Rev. Mol. Cell. Biol. **9**, 33–46 (2008).
[5] D. Chen and S. Huang, Nucleolar components involved in ribosome biogenesis cycle between the nucleolus and nucleoplasm in interphase cells, J. Cell Biol. **153**, 169–176 (2001).
[6] T. M. Creemers, A. J. Lock, V. Subramaniam, T. M. Jovin, and S. Völker, Three photoconvertible forms of green fluorescent protein identified by spectral hole-burning, Nature Struct. Biol. **6**, 557–560 (1999).
[7] D. R. Foltz, E. T. Jansen, B. E. Black, A. O. Bailey, J. R. Yates III, and D. W. Cleveland, The human CENP-A centromeric nucleosome-associated complex, Nature Cell Biol. **8**, 458–469 (2006).
[8] P. Hemmerich, S. Weidtkamp-Peters, C. Hoischen, L. Schmiedeberg, I. Erliandri, and S. Diekmann, Dynamics of inner kinetochore assembly and maintenance in living cells, J. Cell. Biol. **180**, 1101–1114 (2008).
[9] T. Hori, M. Okada, K. Maenaka, and T. Fukagawa, CENP-O class proteins form a stable complex and are required for proper kinetochore function, Mol. Biol. Cell **19**, 843–854 (2008).
[10] A. Kenworthy, Imaging protein-protein interactions using fluorescence resonance energy transfer microscopy, Methods **24**, 289–296 (2001).
[11] S. T. Liu, J. C. Hittle, S. A. Jablonski, M. S. Campbell, K. Yoda, and T. J. Yen, Human CENP-I specifies localisation of CENP-F, MAD1 and MAD2 to kinetochores and is essential for mitosis, Nature Cell Biol. **5**, 341–345 (2003).
[12] F. Malvezzi-Campeggi, M. Jahnz, K. G. Heinze, P. Dittrich, and P. Schwille, Light-induced flickering of DsRed provides evidence for distinct and interconvertible fluorescent states, Biophys. J. **81**, 882–887 (2001).
[13] S. E. McClelland, S. Borusu, A. C. Amaro, J. R. Winter, M. Belwal, A. D. McAinsh, and P. Meraldi, The CENP-A NAC/CAD kinetochore complex controls chromosome congression and spindle bipolarity, EMBO J. **26**, 5033–5047 (2007).
[14] R. Metzler and J. Klafter, When translocation dynamics becomes anomalous, Biophys. J. **85**, 2776–2779 (2003).
[15] Y. Minoshima, T. Hori, M. Okada, H. Kimura, T. Haraguchi, Y. Hiraoka, Y.-C. Bao, T. Kawashima, T. Kitamura, and T. Fukagawa, The constitutive centromere component CENP-50 is required for recovery from spindle damage, Mol. Cell. Biol. **25**, 10315–10328 (2005).
[16] A. Musacchio and E. D. Salmon, The spindle-assembly checkpoint in space and time, Nature Rev. Mol. Cell. Biol. **8**, 379–393 (2007).
[17] M. Okada, I. M. Cheeseman, T. Hori, K. Okawa, I. X. McLeod, J. R. Yates III, A. Desai, and T. Fukagawa, The CENP-H-I complex is required for the efficient incorporation of newly synthesized CENP-A into centromeres, Nature Cell Biol. **8**, 446–457 (2006).
[18] S. Orthaus, C. Biskup, B. Hoffmann, C. Hoischen, S. Ohndorf, K. Benndorf, and S. Diekmann, Assembly of the inner kinetochore proteins CENP-A and CENP-B in living human cells, ChemBioChem **9**, 77–92 (2008).
[19] G. H. Patterson, S. M. Knobel, W. D. Sharif, S. R. Kain, and D. W. Piston, Use of the green fluorescent protein and its mutants in quantitative fluorescence microscopy, Biophys. J. **73**, 2782–2790 (1997).
[20] M. Rizzo, G. Springer, B. Granada, and D. Piston, An improved cyan fluorescent protein variant useful for FRET, Nature Biotech. **22**, 445–449 (2004).
[21] M. J. Saxton, Anomalous sub-diffusion in fluorescence photobleaching recovery: a Monte Carlo study, Biophys. J. **81**, 2226–2240 (2001).
[22] L. Schmiedeberg, K. Weisshart, S. Diekmann, G. Meyer zu Hoerste, and P. Hemmerich, High and low mobility populations of HP1 in heterochromatin of mammalian cells, Mol. Biol. Cell. **15**, 2819–2833 (2004).
[23] P. Schwille, U. Haupts, S. Maiti, and W. W. Webb, Molecular dynamics in living cells observed by fluorescence correlation spectroscopy with one- and two-photon excitation, Biophys. J. **77**, 2251–2265 (1999).
[24] M. Tramier, M. Zahid, J. C. Mevel, M. J. Masse, and M. Coppey-Moisan, Sensitivity of CFP/YFP and GFP/mCherry pairs to donor photobleaching on FRET determination by fluorescence lifetime imaging microscopy in living cells, Microsc. Res. Technol. **69**, 933–939 (2006).
[25] M. Wachsmuth, W. Waldeck, and J. Langowski, Anomalous diffusion of fluorescent probes inside living cell nuclei investigated by spatially-resolved fluorescence correlation spectroscopy, J. Mol. Biol. **298**, 677–689 (2000).
[26] M. Wachsmuth, T. Weidemann, G. Muller, U. W. Hoffmann-Rohrer, T. A. Knoch, W. Waldeck, and J. Langowski, Biophys. J. **84**, 3353–3363 (2003).
[27] T. Weidemann, M. Wachsmuth, T. A. Knoch, G. Muller, W. Waldeck, and J. Langowski, J. Mol. Biol. **334**, 229–240 (2003).
[28] S. Weidtkamp-Peters, H. P. Rahn, M. C. Cardoso, and P. Hemmerich, Histochem. Cell Biol. **125**, 91–102 (2005).
[29] M. H. Weiss, H. Hitoshi, and T. Nilsson, Anomalous Protein Diffusion in Living Cells as Seen by Fluorescence Correlation Spectroscopy. Biophys J. **84**, 4043–4052 (2003).
[30] M. Weiss, M. Elsner, F. Kartberg, and T. Nilsson, Anomalous sub-diffusion is a measure for cytoplasmic crowding in living cells. Biophys. J. **87**, 3518–3524 (2004).
[31] G. Wieland, S. Orthaus, S. Ohndorf, S. Diekmann, and P. Hemmerich, Functional complementation of human centromere protein A (CENP-A) by Cse4p from Saccharomyces cerevisiae, Mol. Cell. Biol. **24**, 6620–6630 (2004).

Eur Biophys J (2009) 38:781–791
DOI 10.1007/s00249-009-0498-x

ORIGINAL PAPER

Acceptor-photobleaching FRET analysis of core kinetochore and NAC proteins in living human cells

D. Hellwig · C. Hoischen · T. Ulbricht · Stephan Diekmann

Received: 27 February 2009 / Revised: 20 May 2009 / Accepted: 21 May 2009 / Published online: 17 June 2009

Abstract Faithful chromatin segregation is mediated and controlled by the kinetochore protein network which assembles at centromeres. In this study, the neighbourhood relations of inner kinetochore and nucleosome-associated complex (NAC) proteins were analysed in living human interphase cells by acceptor photobleaching FRET. The data indicate that CENP-U is in close vicinity to CENP-I as well as to CENP-B and that CENP-M is close to CENP-T.

Keywords Centromere · Kinetochore · Mitosis · Live-cell imaging · NAC complex · Acceptor-photobleaching FRET

Introduction

Centromeric chromatin consists of interspersed regions in which H3 histones are replaced by CENH3 (in humans: CENP-A; for reviews see Allshire and Karpen 2008; Black and Bassett 2008). This centromeric chromatin region is framed by pericentromeric heterochromatin. During interphase, centromeres form a specialised chromatin of a compact structure (interphase pre-kinetochore) distinct from the trilaminar structure of the kinetochores in mitosis after nuclear envelope break down (Roos 1973; Marshall et al. 2008). The kinetochore is a multi-protein complex which assembles at centromeres and guides correct DNA segregation. The kinetochores contain a structural core including the nucleosome-associated complex (NAC) and CENP-A distal complex (CAD) proteins, termed the constitutive centromere-associated network (CCAN), and further proteins and protein complexes, including KNL-1, Hec 1 and hMis12 complexes (for reviews, see Cheeseman and Desai 2008; Musacchio and Salmon 2007). The NAC proteins (CENP-C, -H, -U, -M, -T and -N) were purified in association with CENP-A nucleosomes, while the CAD proteins could only be purified with NAC proteins (Foltz et al. 2006; Okada et al. 2006). CENP-T and CENP-W form a DNA-binding complex which directly associates with nucleosomal DNA and with histone H3 (Hori et al. 2008a). Also proteins of the FACT (Foltz et al. 2006) and the RSF complex (Perpelescu et al. 2009) bind to CENP-A chromatin. Here we analyse the core kinetochore and NAC proteins including CENP-I.

The detailed functions of the CCAN proteins (Hori et al. 2008a) are unclear; their presence at centromeres, however, is required for correct kinetochore function. Depletion of these proteins in human or chicken cells causes chromosome congression and mitotic defects (Liu et al. 2003; Minoshima et al. 2005; Foltz et al. 2006; Okada et al. 2006). siRNA down-regulation of CENP-M, CENP-N or CENP-T caused an increase in the number of cells in mitosis (Foltz et al. 2006). The organisation of the inner kinetochore is dynamic: some inner kinetochore proteins show a cell-cycle-dependent assembly which provides both stability by sustained binding of some components (CENP-A and CENP-I) and differing degrees of flexibility through dynamic exchange of other components (i.e. CENP-B, CENP-H, CENP-C) (Hemmerich et al. 2008; Hellwig et al. 2008).

This article has been submitted as a contribution to the *Festschrift* entitled "Uncovering cellular sub-structures by light microscopy" in honour of Professor Cremer's 65th birthday.

D. Hellwig · C. Hoischen · T. Ulbricht · S. Diekmann (✉)
Department of Molecular Biology,
Leibniz-Institute for Age Research,
Fritz Lipmann Institute, Beutenbergstr. 11,
07745 Jena, Germany
e-mail: diekmann@fli-leibniz.de

The CCAN proteins can be grouped into different functional classes (Okada et al. 2006; McClelland et al. 2007; Hori et al. 2008b). The in vivo analysis of CCAN proteins, selected according to their functional classes, will be subject of future studies. Here we used another criterion for selection: since the kinetochore proteins CENP-M, -N and -U can be affinity purified with tagged CENP-A (Foltz et al. 2006), they are expected to be located in the kinetochore complex in close proximity to one another (Hori et al. 2008a). This view is supported by siRNA protein knockdown experiments (Foltz et al. 2006; Okada et al. 2006; Hori et al. 2008a). Here we therefore set out to measure the direct proximity between the inner kinetochore proteins CENP-A, -B, -C, -H, -I, -M, -T and -U in vivo by acceptor-photobleaching fluorescence resonance energy transfer (FRET) in living human cells.

Materials and experimental methods

Plasmids

Plasmids pDF149, pDF152, pDF153 and pDF197 encoding LAP-CENP-M, -N, -T and -U fusion proteins were used for amplification of full-length CENP-M, -N, -T and -U by PCR (Expand high fidelity^{PLUS} PCR System, Roche, Penzberg, Germany) applying forward primer 5′-GGGGACAAGTTTGTACAAAAAAGCAGGCTTCGAAAACCTGTATTTTCAGGGCGCCACCATGGGCATGTCGGTGTTGAGGCCCCTG-3′ and reverse primer 5′-GGGGACCACTTTGTACAAGAAAGCTGGGTCAGGTCCTCCAGGGAGGGGC-3′ for Cenp-M, forward primer 5′-GGGGACAAGTTTGTACAAAAAAGCAGGCTTCGAAAACCTGTATTTTCAGGGCGCCACCATGGATGAGACTGTTGCTGAGT-3′ and reverse primer 5′-GGGGACCACTTTGTACAAGAAAGCTGGGTTTTATCTCTAATTTTAAAATAATTCATTCTC-3′ for Cenp-N, forward primer 5′-GGGGACAAGTTTGTACAAAAAAGCAGGCTTCGAAAACCTGTATTTTCAGGGCGCCACCATGGCTGACCACAACCCTGAC-3′ and reverse primer 5′-GGGGACCACTTTGTACAAGAAAGCTGGGTCTGGGCAGGGAAGACAGAGTT-3′ for Cenp-T, and forward primer 5′-GGGGACAAGTTTGTACAAAAAAGCAGGCTTCGAAAACCTGTATTTTCAGGGCGCCACCATGGGCACTAGTATGGCCCCGCGGG-3′ and reverse primer 5′-GGGGACCACTTTGTACAAGAAAGCTGGGTTCCCTGGTCAAGGAGCTTCTCTAA-3′ for Cenp-U. CENP-M, -N, -U and -T harbouring linear PCR fragments were transferred into vector pDONR221 by BP recombination reaction (Invitrogen, Carlsbad, CA, USA). After verification by sequencing (MWG Biotech, Ebersberg, München, Germany), the genes were cloned by LR recombination reactions into various modified pEFP-C- and pEFP-N-based destination vectors (BD Biosciences, Clontech, Palo Alto, CA, USA). As a result, we obtained expression vectors carrying the genes coding for CENP-M, -N, -T and -U fused to the C termini of EGFP, Cerulean, YFP, and mCherry. In the constructed fluorescent proteins (FP)-CENP-M, -N, -T and -U, the amino acid (aa) linker between the fused proteins is SGTSLYKKAGFENLYFQGAT. Due to the cloning protocol, the aa sequence TQLSCTKW is added to the C-terminal ends of FP-CENP-M, -N, -T, and -U.

For FRET analysis with EGFP and mCherry as donor-acceptor pair, we constructed various mCherry-Cenp fusions. pEYFP-C1-Cenp-A, pEYFP-C2-CENP-B (Orthaus et al. 2008) and pEGFP-C2-Cenp-C (Hemmerich et al. 2008) were digested with AgeI and BsrGI, and for all three vectors, the 722-bp fragments were replaced with the 713-bp AgeI-BsrGI mCherry-harbouring fragment from pmCherry-H2A, resulting in pmCherry-C1-Cenp-A, pmCherry-C2-Cenp-B and pmCherry-C2-Cenp-C. pEGFP-C1-CENP-A resulted from the replacement of EYFP with EGFP in *Age*I–*Bsr*GI-digested pEYFP-C1-CENP-A (Orthaus et al. 2008). For construction of pEYFP-C2-CenpI, the 722-bp *Age*I-*Bsr*GI fragment of pEGFP-C2-Cenp-I (Hemmerich et al. 2008) was replaced with the 722-bp EYFP-carrying fragment of pEYFP-C2. A vector expressing the fusion pEGFP-mCherry served as a reference vector for positive FRET control measurements. The linker sequence between the N-terminal EGFP and mCherry is SGLRSRGDPAT.

All clones were verified by sequencing (MWG Biotech, Ebersberg, Germany). Full-length protein expression of the fusion constructs was confirmed by Western blots.

Cell culture and transfection into HEp-2 cells

HEp-2 (HeLa contaminant) cells were obtained from the American Tissue Culture Collection (ATCC, Rockville, MD, USA). The cells were cultured in Dulbecco's modified Eagle's medium DMEM (PAA Laboratories, Pasching, Austria) supplemented with 10% fetal calf serum (PAA Laboratories) in a 9.5% CO_2 atmosphere at 37°C and grown to subconfluency as recommended. At this stage, the medium was removed and cells were washed with magnesium- and calcium-containing PBS (Sigma-Aldrich, Taufkirchen, Germany) followed by detachment with trypsin/EDTA (PAA Laboratories).

The detached cells were dissolved in fresh DMEM and re-seeded in new culture dishes. For live-cell imaging experiments, cells were seeded on 42-mm glass dishes (Saur Laborbedarf, Reutlingen, Germany) 1 or 2 days before experiments and transfected with plasmid DNA 24–48 h before observation using FuGENE HD Transfection reagent (Roche, Basel, Switzerland) according to the manufacturer's protocol.

Alternatively, the DMEM-dissolved cells were counted in an improved Neubauer cell (Superior Marienfeld, Lauda-Königshofen, Germany). Aliquots of 10^6 cells were centrifuged for 10 min at 1,600 rpm. The medium was removed, and cells were suspended in 100 µl Nucleofector solution V (Amaxa, Walkersville, MD, USA) and mixed with plasmid DNA. After electroporation with the Nucleofector (Amaxa) transfected cells were seeded on 42-mm glass dishes (Saur Laborbedarf) 1 or 2 days before live-cell imaging experiments.

Western blots

To control the full-length protein expression of the fusion constructs, Western blots were carried out as described previously (Orthaus et al. 2008). In short, transfected HEp-2 cells were taken from culture flasks, counted in a Neubauer chamber and lysed for 10 min at 100°C in an appropriate volume of 2% SDS, 0.1% bromphenole blue, 35 mM dithiothreitole, 25% glycerol and 60 mM Tris–HCl pH 6.8. Cell lysates with appropriate amounts of total protein were separated by SDS-PAGE and blotted onto Protran BA nitrocellulose (Schleicher and Schuell, Dassel, Germany). Proteins reacted with mouse monoclonal antibody against EGFP (#sc-9996, Santa Cruz Biotechnology, Santa Cruz, CA, USA) at a dilution of 1:50. Bound antibodies were detected with horseradish peroxidase-conjugated goat anti-mouse IgG antibodies (#115-035-072, Jackson Immunoresearch Laboratories, West Grove, PA, USA) at a dilution of 1:4,000 and finally with the ECL-advance system (Amersham Biosciences, Uppsala, Sweden) according to the manufacturer's instructions. The chemiluminescence was detected by Biomax light-1 Kodak film (Kodak, Stuttgart, Germany).

Acceptor-photobleaching-based FRET measurements

When FRET occurs, both the intensity and lifetime of the donor fluorescence decrease while the intensity of the acceptor emission increases. All these changes can be exploited to measure the efficiency of energy transfer between the donor and the acceptor (Nagy et al. 1998; Chen et al. 2003; Jares-Erijman and Jovin 2003, 2006; Elder et al. 2009). Two FRET pairs were studied: EGFP-mCherry and Cerulean-EYFP.

Cerulean fluorescence was excited with the argon 458-nm laser line and detected using the Meta detector (ChS1 + ChS2: 477–499 nm). EYFP fluorescence was excited with the argon 514-nm laser line and detected in one of the confocal channels using a 530-nm long-pass filter. EGFP fluorescence was excited with the argon 488-nm laser line and detected using the Meta detector (ChS1 + ChS2: 505–550 nm). mCherry fluorescence was excited with the argon 561-nm laser line and detected in one of the confocal channels using a 575-nm long-pass filter. To minimise cross-talk between the channels, each image was collected separately in the multi-track mode, i.e. both fluorophores were excited and recorded specifically and separately. Single optical sections were selected by scanning the sample in the z-axis for optimal fluorescence signals.

Acceptor photobleaching was achieved by scanning a region of interest (ROI) including one centromere of a nucleus 100 times (scans at 1.6-µs pixel time) using the 514-nm (EYFP) and 561-nm (mCherry) laser line at 100% intensity. Bleaching times per pixel were identical for each experiment. However, total bleaching times differed depending on the size of the bleached ROIs and the used magnification. Three donor and acceptor fluorescence images were taken before and 7 to 12 images were taken after the acceptor-photobleaching procedure to assess changes in donor and acceptor fluorescence. To minimise the effect of photobleaching of the donor during the imaging process, the image acquisition was performed at low laser intensities. To compare the time course of different experiments, donor intensities in the ROI were averaged and normalised to the intensity measured at the first time point after photobleaching, and acceptor intensities in the ROI were averaged and normalised to the mean intensity measured at the three time points before photobleaching.

Results

The proteins closely associated with centromeric nucleosomes can be purified by CENP-A pull-down (Foltz et al. 2006; Okada et al. 2006) and thus are expected to be located in the direct neighbourhood of one another in the kinetochore complex (Hori et al. 2008a). These proteins localise to centromeres in interphase (Foltz et al. 2006). We confirmed this localisation in interphase HEp2 cells (Hellwig et al. 2008; data not shown). For FRET analyses in living human cells, these proteins were cloned in fusion with several FP (two FRET pairs: Cerulean-EYFP and EGFP-mCherry). Full-length expression of each fusion protein was verified by Western blot analysis (Hemmerich et al. 2008; Orthaus et al. 2008, 2009; data not shown).

When the fluorescent tag is fused to CENP-H via a peptide linker of 11 to 16 amino acids, CENP-H centromere localisation is prevented irrespective of whether the tag is fused to the N or the C terminus. However, a 39 amino acids long linker between CENP-H and the fluorescent protein (placed at the N terminus of CENP-H) reestablished centromere localisation (Hemmerich et al. 2008) and enabled dynamic studies. However, the long linker might place the fluorescent tag too far away from CENP-H for

FRET results to be interpreted on a molecular basis. Therefore, CENP-H was not studied by FRET.

For the other kinetochore proteins studied here, the fluorescent tag did not detectably alter the properties of the proteins in terms of their proper localisation and centromere-binding characteristics. Upon expression in HEp-2 cells, fluorescently tagged inner kinetochore proteins localised in vivo to centromeric regions, reflecting the distribution of endogenous centromere proteins (Hemmerich et al. 2008; Orthaus et al. 2008, 2009; data not shown). EGFP-tagged CENP-A was previously shown to be correctly incorporated into nucleosomes of centromeric heterochromatin (Wieland et al. 2004) indicating that the fluorescent tag did not detectably influence the localisation of the fusion protein. CENP-B-EGFP and EGFP-CENP-C tightly bound to human centromeres (Hemmerich et al. 2008) indicating that these tagged kinetochore proteins, similar to tagged CENP-A (Foltz et al. 2006), also retained functional properties of the endogenous proteins.

Human HEp-2 cells were co-transfected with two vectors containing two different genes each coding for a kinetochore protein fused to a fluorescent protein (having different colours, i.e. a FRET pair) for acceptor photobleaching FRET measurements (Wouters et al. 1998). In this approach, the donor fluorescence intensity is measured (in the same sample) in the presence of an acceptor before and after destroying the acceptor by photobleaching (Kenworthy 2001); potential energy transfer between the donor and the acceptor is eliminated by irreversibly photobleaching the acceptor, resulting in an increase in the donor fluorescence (Wouters et al. 1998; Kenworthy and Edidin 1998; Berney and Danuser 2003). As FRET pairs, we used Cerulean-EYFP and EGFP-mCherry as donor and acceptor fluorophores (Orthaus et al. 2008; Tramier et al. 2006). Fluorescence intensity changes in the bleached area were recorded over time in the donor and acceptor channels by sequential imaging scans. FRET measurements were carried out in several independent experiments.

FRET control experiments were carried out as presented previously (Orthaus et al. 2008, 2009). In short, as a positive control, after acceptor photobleaching, the triple fusion ECFP–EYFP–CENP-A showed strong FRET between the neighbouring fluorescence tags. Other control experiments excluded effects due to photobleaching (Patterson et al. 1997) or photo-conversion (Creemers et al. 1999; Malvezzi-Campeggi et al. 2001). Furthermore, no negative influence of the photobleaching procedure on cell morphology was observed (data not shown; Orthaus et al. 2008). The analysis of non-fused donor and acceptor fluorophores, co-transfected in living human cells, did not result in FRET so that we can exclude any false-positive FRET due to an unspecific association of the fluorescent tags (Orthaus et al. 2008). Thus, if energy transfer was observed between the labelled proteins, it could only be due to a specific (direct or indirect) interaction between the proteins but not between the tags.

We then analysed in living human HEp-2 cells whether the N termini of the human kinetochore proteins CENP-M, -N, -T and -U are close to the N termini of CENP-A, -B, -C, -I, -N, -T, -U and -M at human centromeres. The data were collected and treated in the following way. In each image, two centromere locations were identified (marked "1" and "2" in Fig. 1). Only at spot 2 was the acceptor bleached so that in case of FRET, the donor fluorescence intensity increased. At spot 1, the acceptor is not bleached; this location served as control. Any influence of the environment during the experiment or any influence of the acceptor photobleaching at another location in the sample on the donor might influence the donor fluorescence intensity. These 'background' FRET signals were recorded at spot 1 by measuring the time course of the donor fluorescence intensity before and after photobleaching. The donor fluorescence intensity at spot 2 was also changed due to these influences, but also due to FRET.

The donor fluorescence intensities at the bleached (spot 2) as well as the non-bleached (spot 1) locations were recorded and treated equally: at spot 2 the FRET efficiency was calculated according to $E_{\mathrm{FRET}} = 1 - (I_{\mathrm{DA}}/I_{\mathrm{D}})$ where I_{DA} and I_{D} are the donor fluorescence intensities in the presence and absence of the (intact) acceptor respectively. I_{DA} was obtained by averaging the donor intensities of the three pre-bleached images in the presence of a photochemically intact acceptor. I_{D} was determined by measuring the donor fluorescence intensity in the first image obtained after the acceptor was destroyed by photobleaching. At the unbleached spot 1, the donor fluorescence change was calculated according to $E_{\mathrm{var}} = 1 - (I_{\mathrm{DAbefore}}/I_{\mathrm{DAafter}})$ so that a corresponding value for variation efficiency, E_{var}, is obtained, which can directly be compared to the FRET efficiency E_{FRET}. The E values were grouped into intervals of 4%, and the number of cases (y-axis) was plotted versus E values (x-axis) with the x-axis values as the mid-point of the range (0–4%: mid-point 2, 4–8%: mid-point 6%, etc.) resulting in distribution diagrams of both E_{FRET} and E_{var}. E_{var} indicates the donor fluorescence intensity variation during the experiment due to background effects. FRET was interpreted to have occurred when $\mathrm{E_{FRET}}$ was clearly larger than E_{var}.

CENP-U showed a structured presence within the whole-cell nucleus and co-localised with CENP-A at centromeres (Fig. 1a, left pictures). Two centromeric locations were selected, spot 1 and spot 2 indicated in Fig. 1a and enlarged in Fig. 1b. Figure 1a and b display the fluorescence of the fusion proteins at both locations before and after photobleaching of the acceptor. Then, the acceptor mCherry fused to CENP-A was nearly completely photo-

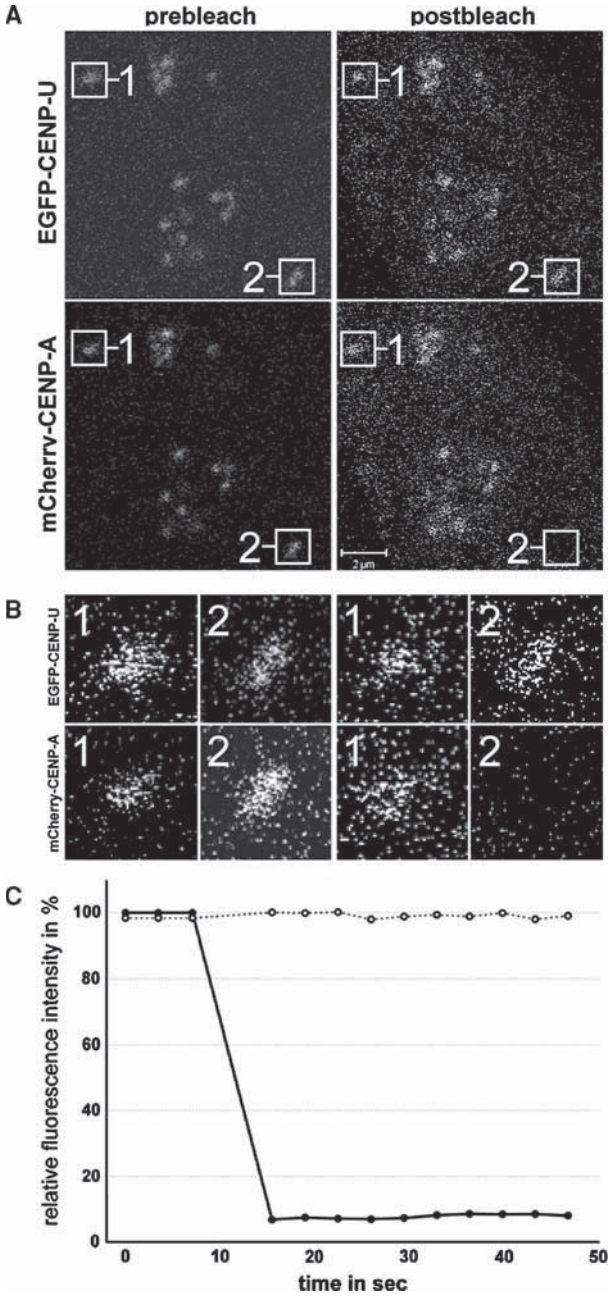

Fig. 1a–c Acceptor-bleaching FRET of the protein pair EGFP-CENP-U and mCherry-CENP-A. Human HEp-2 cells were co-transfected with both fusion proteins. A typical cell nucleus is displayed in **a** showing co-localisation at specific (centromeric) locations. Two of these locations, spots *1* and *2*, were selected for fluorescence intensity analysis before and after acceptor bleaching (see enlargement in **b**). Spot 1 served as control and showed no detectable intensity change. At spot 2, the acceptor fluorophore mCherry was bleached (compare pre-bleach and post-bleach in **a**, *lower two pictures*, and in **b**, *lower pictures*). In **c** the time course of the fluorescence intensity of the donor and the acceptor are shown. The acceptor intensities in the ROI were averaged and normalised to the mean intensity measured at the three time points before bleaching. The donor intensities in the ROI were averaged and normalised to the intensity measured at the first time point after bleaching. Bleaching of the acceptor (*closed circles*) did not result in a major fluorescence intensity change of the donor (*open circles*) indicating the absence of FRET

bleached at a centromeric region (spot 2 in Fig. 1a, lower left picture: before; lower right picture: after photobleaching; see also enlarged spots in Fig. 1b) while spot 1 served as control yielding the E_{var} values. Despite acceptor photobleaching, hardly any fluorescence intensity change in EGFP-CENP-U was observed (spot 2 in Fig. 1a upper left picture: before; upper right picture: after photobleaching; see also enlarged spots in Fig. 1b). The time course of the fluorescence intensity at spot 2 of the donor and the acceptor is shown in Fig. 1c; due to photobleaching, the acceptor fluorescence dropped to very low values of about 5% of the original and stayed low, while the donor fluorescence remained almost constant, unaffected by acceptor photobleaching. The E_{FRET} values (EGFP-CENP-U and mCherry-CENP-A in Fig. 2, grey bars) were distributed around 0% (14 kinetochores in 14 cells) and never exceeded the values of E_{var} (Fig. 2, black bars) which were measured in the same experiment at spot 1 where the acceptor was not photobleached. Thus, acceptor photobleaching had no measurable influence on the donor fluorescence intensity. EGFP-CENP-U showed no fluorescent energy transfer to mCherry-CENP-A, indicating that the N terminus of CENP-U is not in close proximity to the N terminus of CENP-A.

Correspondingly we analysed various other pairs of core kinetochore and NAC proteins including CENP-B. The 80-kDa CENP-B not only binds to the centromere but also to the pericentric heterochromatin domain distributed between sister kinetochores. It binds to a specific DNA sequence, the 17-bp CENP-B box, which is present in α-satellite repeat in human centromeres and in pericentromeric regions (Cooke et al. 1990; Ando et al. 2002). As for the co-expressed CENP-U and CENP-A, as well as for other protein pairs, the variation in donor fluorescence E_{var} at the non-bleached spot 1 was larger than the variation at the bleached spot 2, clearly indicating that no FRET occurred between the two tags at the N termini of these proteins (see Fig. 2, E_{var} black bars and E_{FRET} grey bars). For EGFP-CENP-T and mCherry-CENP-C, the variation distribution of the donor fluorescence intensities in the photobleached and the non-bleached spots overlaps well (16 kinetochores in as many cells). Also for the pairs EGFP-CENP-U with mCherry-CENP-C (13 kinetochores in 13 cells) and mCherry-CENP-M (14 kinetochores in 14 cells) as well as the pair EGFP-CENP-N with mCherry-CENP-C (12 kinetochores in 12 cells), photobleaching of the acceptor did not result in an increase in the donor fluorescence intensity, and the distributions coincided well. Among these five pairs, no FRET was observed.

The situation was different for the pair EGFP-CENP-U and mCherry-CENP-B. CENP-U colocalised with CENP-B (Fig. 3a). Again, two centromeric spots were selected (spot 1 and spot 2) and enlarged in Fig. 3b. The acceptor

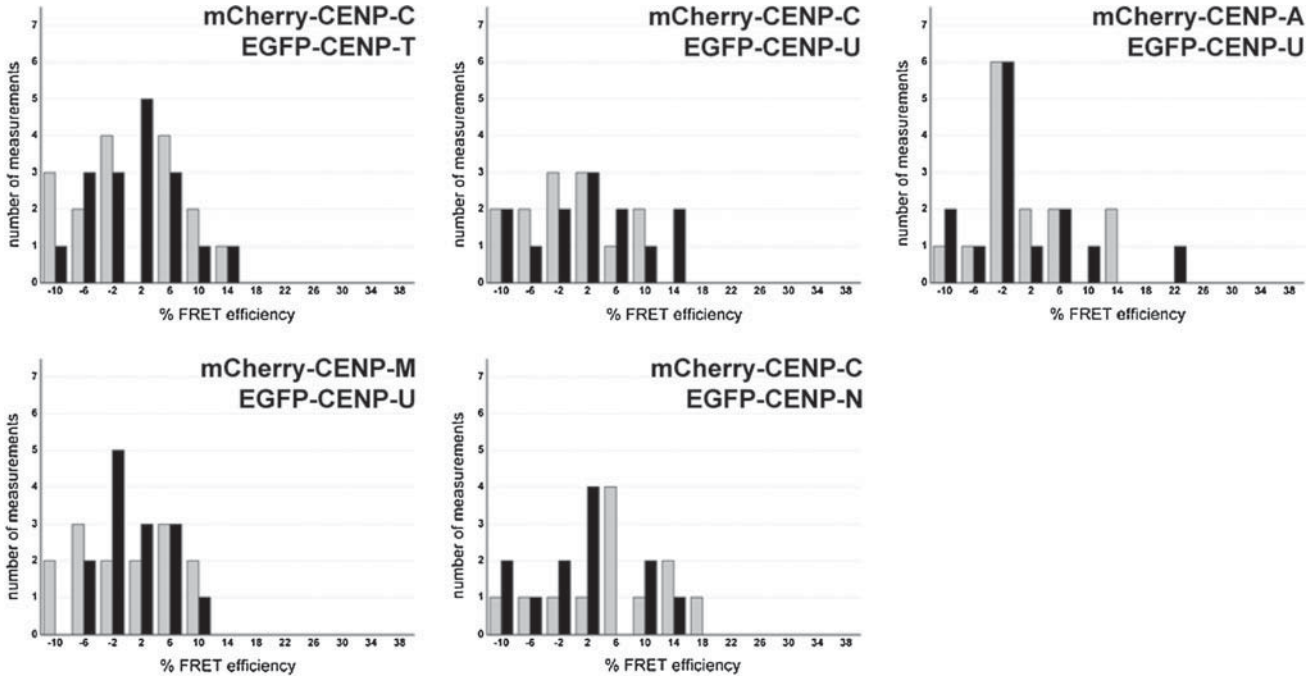

Fig. 2 Protein pairs not showing FRET. The donor fluorescence intensity variation observed during acceptor bleaching normalised to the intensity measured at the first time point after bleaching was determined for spot 1 (one example shown in Fig. 1) yielding E_{var} (*black bars*) and for spot 2 yielding E_{FRET} (*grey bars*). For the protein pairs indicated in the graphs, the number of observed single cases (grouped into E_{var} or E_{FRET} value ranges of 4%) is displayed versus the values of E_{var} or E_{FRET}. The value distributions of E_{var} and E_{FRET} coincide well, indicating the absence of FRET

mCherry was bleached at spot 2 (compare spot 2 pre-bleach and post-bleach in the bottom of Fig. 3a, b). Photobleaching had no detectable influence on the fluorescence intensity at spot 1 which served as control yielding the E_{var} values. The time course of the acceptor fluorescence intensity is plotted in Fig. 3c. Acceptor-photobleaching resulted in a nearly complete loss of fluorescence. During photobleaching, the donor fluorescence intensity increased (see Fig. 3c), indicating the presence of FRET. In 44% of the cases (18 kinetochores in 18 cells), the E_{FRET} value (Fig. 4, grey bars) was larger than the E_{var} value (Fig. 4, black bars). The max FRET efficiency values were relatively high (30%). Also for two other fusion protein pairs, Cerulean-CENP-M and EYFP-CENP-T (12 kinetochores in 12 cells) as well as Cerulean-CENP-I and EYFP-CENP-U (10 kinetochores in 10 cells), high values of E_{FRET} were observed (up to about 38%), and again, the E_{FRET} value was larger than the largest E_{var} value in about half of the cases (for Cerulean-CENP-I and EYFP-CENP-U as much as 70%), clearly indicating the presence of FRET. The single observations with $E_{FRET} > E_{var}$ however never reached 100% of all experiments; the remaining intensity changes in the donors of these pairs had values within the range of the variance E_{var} of the fluorescence intensities of the donor at the non-bleached spot. This indicates that not all but only about one-half or one-third of the protein pairs were observed in close vicinity and that quite a number of donors showed no FRET. Indeed, very high numbers of protein pairs showing FRET are not expected to be found since untagged endogenous proteins are also present in the cell, which mix with the tagged proteins so that in a number of cases the tagged donor will have an untagged protein as neighbour. This point will be explained in more detail in the section "Discussion". These data indicate that the N termini of these three protein pairs, CENP-I and CENP-U, CENP-M and CENP-T, and CENP-U and CENP-B, can be found in close proximity to one another.

In this study we used two different donor–acceptor pairs, EGFP with mCherry (Tramier et al. 2006) and Cerulean with EYFP (Orthaus et al. 2008). We studied one protein pair with both FRET pairs: we measured the proximity of CENP-M to itself by analysing EGFP-CENP-M and mCherry-CENP-M (15 kinetochores in as many cells) as well as Cerulean-CENP-M and EYFP-CENP-M (eight kinetochores). The obtained distributions of E_{FRET} and E_{var} were similar resulting in the same conclusion: in some but not many cases (about 23%) the N termini of two CENP-M proteins were measured to be close to one another (see Fig. 5a).

For a number of other protein pairs, the situation is ambiguous. In three cases, EGFP-CENP-N and mCherry-CENP-M (11 kinetochores), Cerulean-CENP-M and

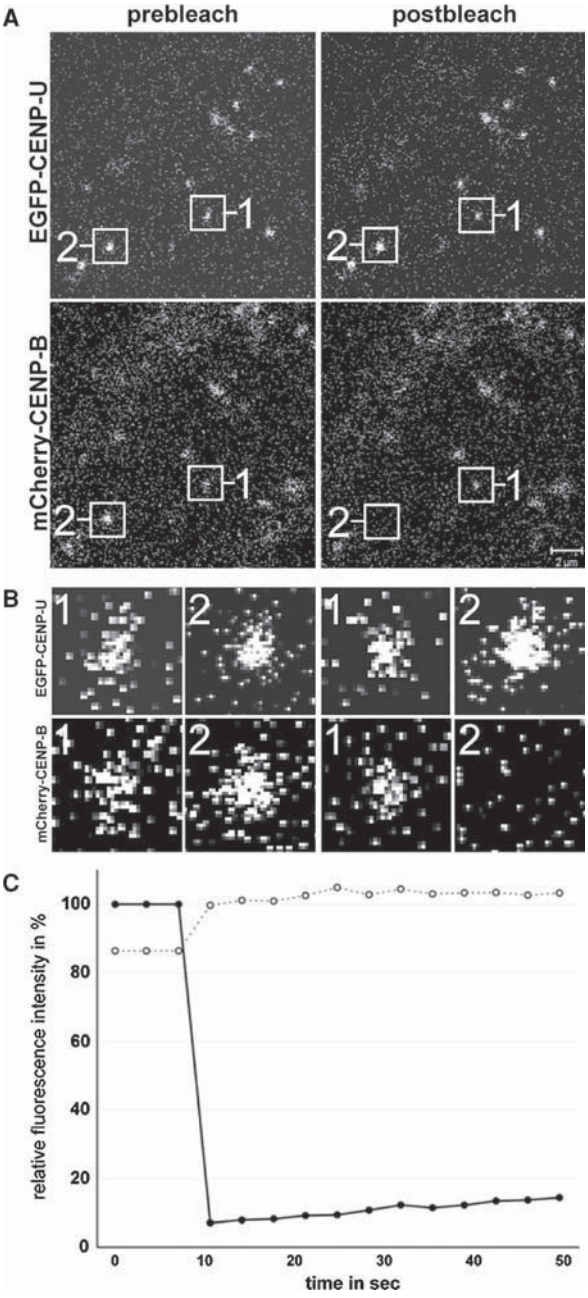

Fig. 3a–c Acceptor-bleaching FRET of the protein pair EGFP-CENP-U and mCherry-CENP-B. Human HEp-2 cells were co-transfected with both fusion proteins. A typical cell nucleus is displayed in **a** showing co-localisation at specific (centromeric) locations. Two of these locations, *spot 1* and *spot 2*, were selected for fluorescence intensity analysis before and after acceptor bleaching (see enlargement in **b**). Spot 1 served as control and showed no detectable intensity change. At spot 2, the acceptor fluorophore mCherry was bleached (compare pre-bleach and post-bleach in **a**, *lower two pictures*, and in **b**, *lower pictures*). In **c**, the time course of the fluorescence intensity of the donor and the acceptor is shown. The acceptor intensities in the ROI were averaged and normalised to the mean intensity measured at the three time points before bleaching. The donor intensities in the ROI were averaged and normalised to the intensity measured at the first time point after bleaching. Bleaching of the acceptor (*closed circles*) resulted in a fluorescence intensity increase in the donor (*open circles*) indicating the presence of FRET (with a FRET efficiency of about 14%)

EYFP-CENP-A (9 kinetochores) as well as Cerulean-CENP-T and EYFP-CENP-A (9 kinetochores), very high E_{FRET} values were measured, but only in a small number of single experiments (see Fig. 5b). Similarly, only in a small number of cases was E_{FRET} larger than the largest measured value of E_{var}. For other protein pairs: for mCherry-CENP-C and EGFP-CENP-M (13 kinetochores), mCherry-CENP-B and EGFP-CENP-M (11 kinetochores), mCherry-CENP-B and EGFP-CENP-T (14 kinetochores), mCherry-CENP-M and EGFP-CENP-M (15 kinetochores), EGFP-CENP-N and mCherry-CENP-B (18 kinetochores), EGFP-CENP-I and mCherry-CENP-M (18 kinetochores) as well as EGFP-CENP-I and mCherry-CENP-T (11 kinetochores), some but only a few E_{FRET} values were larger than the largest E_{var} value (Fig. 5a, b). In these cases, the few E_{FRET} values that were larger than E_{var} were not statistically significant. Thus in general, these protein pairs are not in close proximity to one another within the complex, and the few measured values of $E_{FRET} > E_{var}$ might be experimental errors. However, alternatively, during the cell cycle, complex structure or composition might alter so that in a few cases, the proteins are indeed close to one another allowing for FRET between the tags at their N termini. Here, the different interphase subphases G1, S-phase and G2 were not resolved (see the section "Discussion").

Discussion

At the centromere, the kinetochore proteins assemble including CENP-M, -N, -T, -U and -C. We showed here by acceptor-photobleaching FRET in living human HEp-2 interphase cells that in a high number of measured cases, the N termini of CENP-T and CENP-M, CENP-I and CENP-U, as well as CENP-B and CENP-U are in the direct neighbourhood of one another. Reduction of CENP-T eliminated CENP-M at centromeres (Foltz et al. 2006) consistent with our results. Surprisingly, yeast-two-hybrid experiments were not able to detect the association among any of these proteins studied (own unpublished data). On the other hand, for a number of proteins we did not observe single cases in which the N termini were close: CENP-U to CENP-M, -A and -C as well as CENP-C to CENP-T. Recently we showed that CENP-A is in close proximity to CENP-B at the centromeres in living human cells (Orthaus et al. 2008).

In the transfected cells, the fluorescently labelled proteins are present together with the corresponding unlabelled endogenous proteins. As a consequence, in the kinetochore complex the donor fusion proteins have acceptor-tagged as well as untagged proteins next to them. Our E_{FRET} value distributions therefore showed values of E_{FRET} similar to E_{var} for those donors without acceptors, and E_{FRET} values

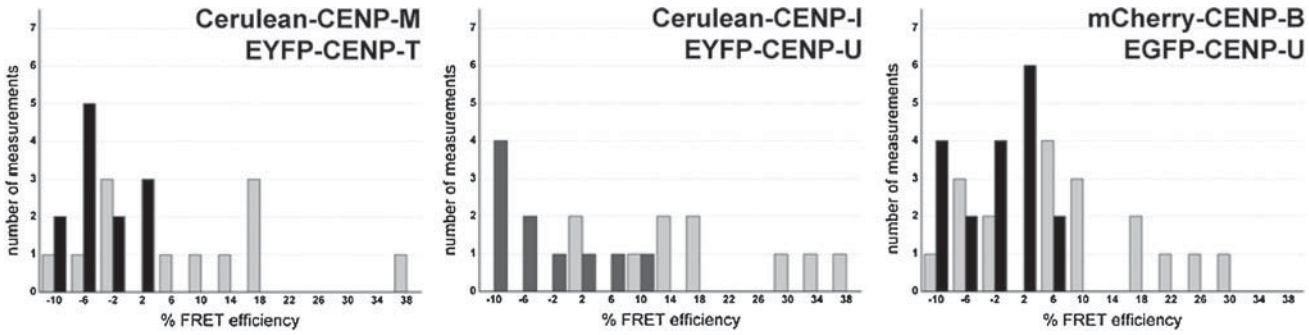

Fig. 4 Protein pairs showing FRET. The donor fluorescence intensity variation observed during acceptor bleaching normalised to the intensity measured at the first time point after bleaching was determined for spot 1 (one example shown in Fig. 3) yielding E_{var} (*black bars*) and at spot 2 yielding E_{FRET} (*grey bars*). For the protein pairs indicated in the graphs, the number of observed single cases (grouped into E_{var} or E_{FRET} value ranges of 4%) is displayed versus the values of E_{var} or E_{FRET}. Only some E_{FRET} values coincide with the distribution of E_{var} values; most E_{FRET} values exceed the E_{var} values, with E_{FRET} values of up to 38%, indicating the presence of FRET

larger than E_{var} for donors with acceptor molecules in close proximity. The number of donors in each situation is influenced by the expression levels of the tagged and the endogenous proteins, as well as by the level of incorporation of the tagged proteins into the kinetochore complex. Here we always selected cells with low expression levels of the tagged proteins, but that were high enough for high quality data, so that donor-only and acceptor-only complexes might be frequent. Observing donor molecules with high E_{FRET} values indicates that a complex was identified in which the donor fusion is in close proximity to the acceptor fusion. Our protein-exchange dynamics measurements of kinetochore proteins revealed that the inner kinetochore complex is not stable over the cell cycle but shows fast exchange of some proteins and stable incorporation of other proteins (Hemmerich et al. 2008); the kinetochore complex composition is thus flexible during the cell cycle. In our FRET results presented here, we did not distinguish different interphase cell-cycle phases. Therefore, donors with different E_{FRET} values might represent different complex compositions or complex structures differing with cell-cycle phase. We thus present the E values as measured and did not calculate mean values.

The FRET results for those protein pairs with only a few values of E_{FRET} larger than E_{var} (Fig. 5) can also be interpreted in terms of this view. These few cases with E_{FRET} larger than E_{var} are not necessarily due to experimental error but might indicate that these proteins are in direct proximity to one another only in less frequent or rare complex configurations, for example at selected time points during the cell cycle. Subphases during interphase were not resolved yet in our measurements for the following reasons: In order to distinguish G1 from S-phase and G2, we colour-labelled S-phase with PCNA fused to GFP or mRFP. Then, S-phase is identified by the particular cellular distribution of PCNA, G2 follows S-phase and G1 follows mitosis. This experimental approach works well for dynamic (e.g. FRAP) measurements when a single colour is sufficient for data acquisition (Hemmerich et al. 2008) since cells can be double-transfected with reasonable efficiency. For FRET experiments, the cells must be double-transfected to start with, thus an additional cell cycle marker (such as PCNA) would require a triple-transfection. Furthermore, the additional fluorophore might interfere with the FRET experiment. Nevertheless, cell-cycle-dependent FRET experiments are in the process of being established.

Here we observed by acceptor-bleaching FRET that in a few cases, the N terminus of CENP-T is in close proximity to that of CENP-A and CENP-B (see also Hellwig et al. 2008), as observed for several other protein pairs described here (Fig. 5). This interpretation suggests that CENP-T binds to the centromere at some distance to CENP-A but close enough that some CENP-T proteins can be detected in close vicinity to CENP-A. This interpretation fully agrees with the findings of Hori et al. (2008a) who applied different experimental approaches. Alternatively, CENP-T might bind to the centromere close to CENP-A only for a short period of time, while it binds far from CENP-A for a much longer time.

The data presented here as well as literature data are summarised in Table 1. FRET results are listed as (+) for close proximity between the two proteins and (−) when no FRET could be detected. Those cases with few positive FRET results only are listed with (?). When the acceptor-photobleaching FRET measurements were confirmed by lifetime FRET, the (+) and (−) symbols have a white centre. Literature data indicating a positive protein–protein interaction or proximity are listed with a circle while literature data indicating the absence of an interaction are represented by a square. Linker histone H1 was observed in the neighbourhood of CENP-A, -B and -C (Orthaus et al. 2009). The close vicinity of CENP-B to CENP-A and H1 was confirmed by bimolecular fluorescence complementation (BiFC; Orthaus et al. 2009). No FRET could be

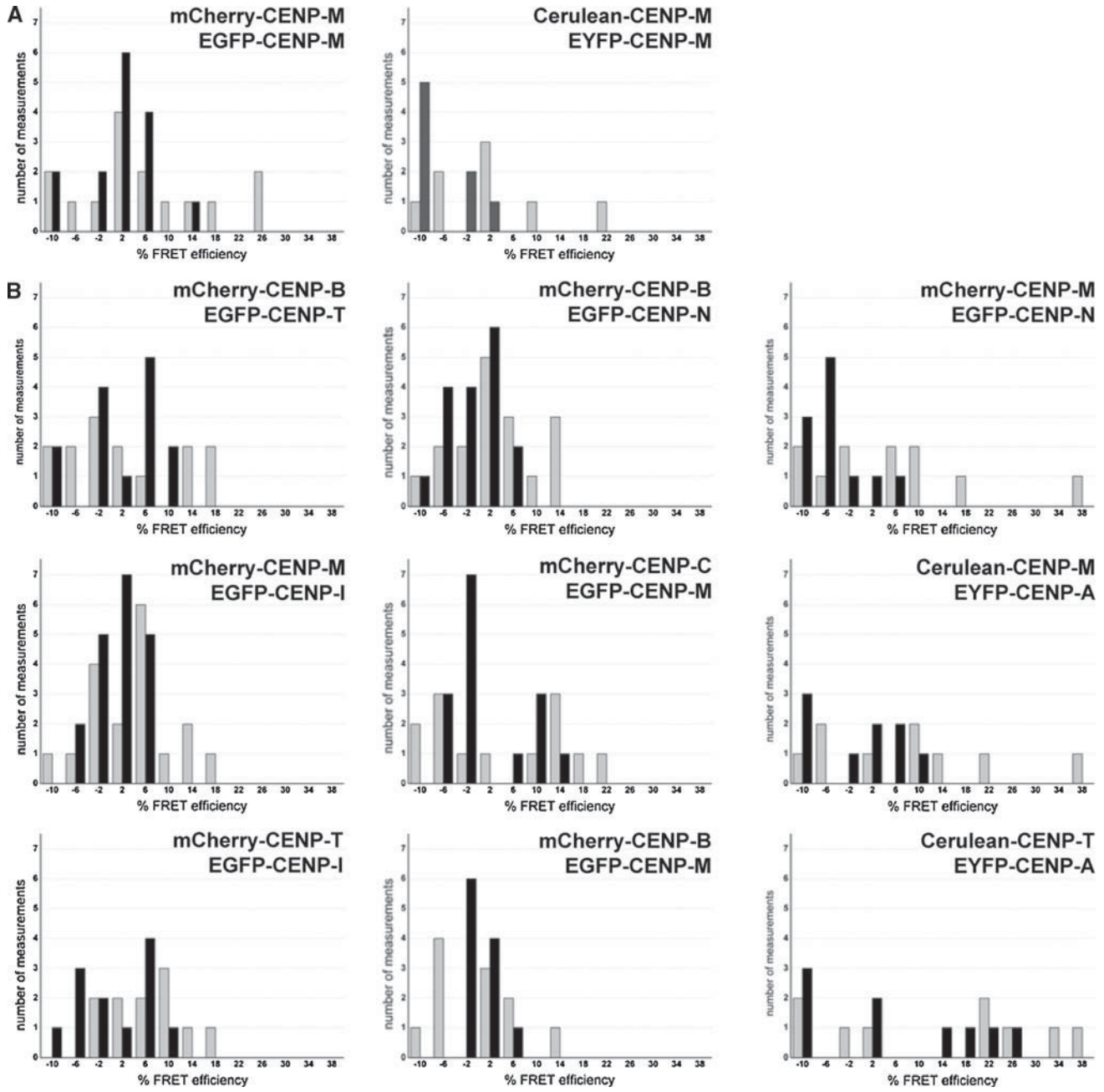

Fig. 5a, b Protein pairs rarely showing FRET. The donor fluorescence intensity variation observed during acceptor bleaching normalised to the intensity measured at the first time point after bleaching was determined for spot 1 yielding E_{var} (*black bars*) and for spot 2 yielding E_{FRET} (*grey bars*). For the protein pairs indicated in the graphs, the number of observed single cases (grouped into E_{var} or E_{FRET} value ranges of 4%) is displayed versus the values of E_{var} or E_{FRET}. Most E_{FRET} values coincide with the E_{var} values, while only some E_{FRET} values exceed them. **a** Comparison of the same protein pair using two different FRET pairs: EGFP and mCherry (*left*) or Cerulean and EYFP (*right*); **b** different protein pairs as indicated in the graphs

detected between CENP-A and the histones H2A and H3 all tagged at the N terminus (Orthaus et al. 2008). This is consistent with H2A, but not H3, being part of a CENP-A containing nucleosome. CENP-A was found to be in close vicinity to itself as well as to CENP-B (Orthaus et al. 2008) , to histone H4 (Black et al. 2007a, b; Black and Bassett 2008) and CENP-N (Carroll et al. 2009, unpublished) but not to CENP-C (Orthaus et al. 2008; Hori et al. 2008a), CENP-I (unpublished) and CENP-U (shown here). Recently, Carroll et al. (2009) showed that CENP-N is close to CENP-A and H4. We found CENP-B next to itself (unpublished; Pluta et al. 1992; Yoda et al. 1992; Kitagawa et al. 1995) and to CENP-C (unpublished; Suzuki et al. 2004) as well as CENP-C next to itself (Sugimoto et al.

Table 1 FRET results from this study as well as literature data

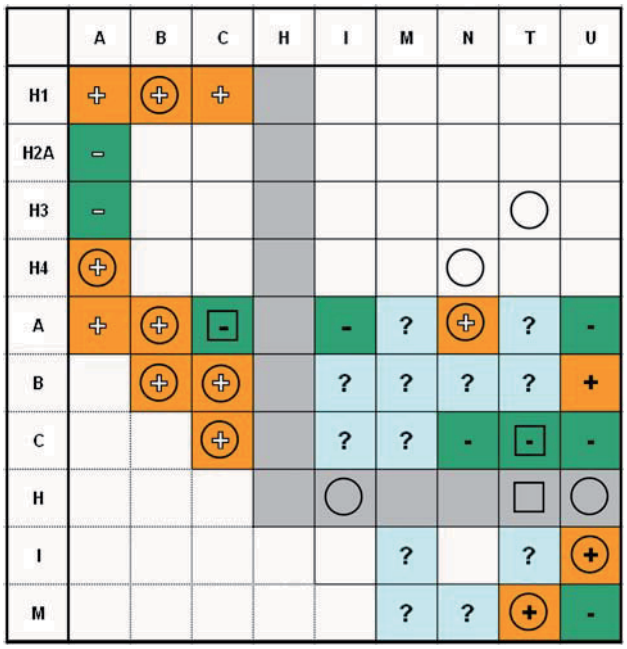

Our FRET results: *Plus signs* indicate close proximity between the two proteins. *Minus signs* indicate no FRET detected. *Question marks* indicate only a few positive FRET results. Acceptor-photobleaching FRET measurements confirmed by lifetime FRET are indicated by *symbols with white centres*. *Circles* represent literature data indicating a positive protein-protein interaction. *Squares* represent a measured absence of an interaction in the literature. CENP-H cells have a *grey background* since tagged CENP-H does not localise and was not used for FRET measurements (see "Results"). H2A might be placed next to CENP-A in centromeric nucleosomes, the N-termini however are too distal for FRET. In contrast, no FRET between H3 and CENP-A suggests that H3 is not (or hardly) present in centromeric nucleosomes

1997, unpublished). CENP-T is closely related to histone H3 but seems not to be associated with CENP-C and CENP-H (Hori et al. 2008a). Reduction of CENP-T eliminated CENP-M at centromeres potentially indicating these two kinetochore proteins being in close proximity to one another (Foltz et al. 2006). As members of the CENP-H–I complex, CENP-H and -I seem to be closely associated (Okada et al. 2006; Foltz et al. 2006; Nishihashi et al. 2002). CENP-U seems to interact with the CENP-H/CENP-I complex at the kinetochore (Minoshima et al. 2005). A yeast-two-hybrid experiment that detected interaction between CENP-M and CENP-H [mentioned as "unpublished" in Okada et al. (2006)] was not confirmed by our yeast-two-hybrid results (unpublished).

In conclusion, our in vivo measurements confirm in vitro results and yield additional data necessary to build an interaction network of core kinetochore and NAC protein components. Analysis of further protein pairs will progressively reveal the structural arrangements at centromeric chromatin.

Acknowledgments We thank N. Klöcker, D. Foltz, I. Cheeseman, M. Coppey-Moisan and N. Audugé for the kind gift of plasmids and the Deutsche Forschungs-Gemeinschaft (DFG) for support (SPP 1128).

References

Allshire RC, Karpen GH (2008) Epigentic regulation of centromeric chromatin: old dogs, new tricks? Nat Rev Gen 9:923–937

Ando S, Yang H, Nozaki N, Okazaki T, Yoda K (2002) Cenp-A, Cenp-B and Cenp-C chromatin complex that contains the I-type alpha-satellite array constitutes the prekinetochore in HeLa cells. Mol Cell Biol 22:2229–2241. doi:10.1128/MCB.22.7.2229-2241.2002

Berney C, Danuser G (2003) FRET or no FRET: a quantitative comparison. Biophys J 84:3992–4010. doi:10.1016/S0006-3495(03)75126-1

Black BE, Bassett EA (2008) The histone variant CENP-A and centromere specification. Cur Op Cell Biol 20:91–100

Black BE, Brock MA, Bedard S, Woods VL, Cleveland DW (2007a) An epigenetic mark generated by the incorporation of CENP-A into centromeric nucleosomes. Proc Natl Acad Sci USA 104:5008–5013

Black BE, Jansen LET, Maddox PS, Foltz DR, Desai AB, Shah JV, Cleveland DW (2007b) Centromere identity maintained by nucleosomes assembled with histone H3 containing the CENP-A targeting domain. Mol Cell 25:309–322

Carroll CW, Silva MCC, Godek KM, Jansen LET, Straight AF (2009) Centromere assembly requires the direct recognition of CENP-A nucleosomes by CENP-N. Nat Cell Biol (in press)

Cheeseman IM, Desai A (2008) Molecular architecture of the kinetochore-microtubule interface. Nat Rev Mol Cell Biol 9:33–46. doi:10.1038/nrm2310

Chen Y, Mills JD, Periasamy A (2003) Protein localisation in living cells and tissues using FRET and FLIM. Differentiation 71:528–541. doi:10.1111/j.1432-0436.2003.07109007.x

Cooke CA, Bernat RL, Earnshaw WC (1990) CENP-B: a major centromere protein located beneath the kinetochore. J Cell Biol 110:1475–1488. doi:10.1083/jcb.110.5.1475

Creemers TM, Lock AJ, Subramaniam V, Jovin TM, Völker S (1999) Three photoconvertible forms of green fluorescent protein identified by spectral hole-burning. Nat Struct Biol 6:557–560. doi:10.1038/10763

Elder AD, Domin A, Kaminski Schierle GS, Lindon C, Pines J, Esposito A, Kaminsiki CF (2009) A quantitative protocol for dynamic measurements of protein interactions by Förster resonance energy transfer-sensitized fluorescence emission. J R Soc Interface 6:S59–S81. doi:10.1098/rsif.2008.0381.focus

Foltz DR, Jansen ET, Black BE, Bailey AO, Yates III JR, Cleveland DW (2006) The human CENP-A centromeric nucleosome-associated complex. Nat Cell Biol 8:458–469. doi:10.1038/ncb1397

Hellwig D, Münch S, Orthaus S, Hoischen C, Hemmerich P, Diekmann S (2008) Live-cell imaging reveals sustained centromere binding of CENP-T via Cenp-A and Cenp-B. J Biophoton 1:245–254

Hemmerich P, Weidtkamp-Peters S, Hoischen C, Schmiedeberg L, Erliandri I, Diekmann S (2008) Dynamics of inner kinetochore assembly and maintenance in living cells. J Cell Biol 180:1101–1114. doi:10.1083/jcb.200710052

Hori T, Amano M, Suzuki A, Backer CB, Welburn JP, Dong Y, McEwan BF, Shang W-H, Suzuki E, Okawa K, Cheeseman IM, Fukagawa T (2008a) CCAN makes multiple contacts with centromeric DNA to provide distinct pathways to the outer kinetochore. Cell 135:1039–1052. doi:10.1016/j.cell.2008.10.019

Hori T, Okada M, Maenaka K, Fukagawa T (2008b) CENP-O class proteins form a stable complex and are required for proper kinetochore function. Mol Biol Cell 19:843–854. doi:10.1091/mbc.E07-06-0556

Jares-Erijman EA, Jovin TM (2003) FRET imaging. Nat Biotechnol 21:1387–1395. doi:10.1038/nbt896

Jares-Erijman EA, Jovin TM (2006) Imaging molecular interactions in living cells by FRET microscopy. Curr Opin Chem Biol 10:409–416. doi:10.1016/j.cbpa.2006.08.021

Kenworthy AK (2001) Imaging protein–protein interactions using fluorescence resonance energy transfer microscopy. Methods 24:289–296. doi:10.1006/meth.2001.1189

Kenworthy AK, Edidin M (1998) Distribution of a glycosylphosphatidylinositol-anchored protein at the apical surface of MDCK cells examined at a resolution of <100 A using imaging fluorescence resonance energy transfer. J Cell Biol 142:69–84. doi:10.1083/jcb.142.1.69

Kitagawa K, Masumoto H, Ikeda M, Okazaki T (1995) Analysis of protein-DNA and protein-protein interactions of centromere protein B (CENP-B) and properties of the DNA-CENP-B complex in the cell cycle. Mol Cell Biol 15:1602–1612

Liu ST, Hittle JC, Jablonski SA, Campbell MS, Yoda K, Yen TJ (2003) Human CENP-I specifies localisation of CENP-F, MAD1 and MAD2 to kinetochores and is essential for mitosis. Nat Cell Biol 5:341–345. doi:10.1038/ncb953

Malvezzi-Campeggi F, Jahnz M, Heinze KG, Dittrich P, Schwille P (2001) Light-induced flickering of DsRed provides evidence for distinct and interconvertible fluorescent states. Biophys J 81:882–887

Marshall OW, Marshall AT, Choo KHA (2008) Three-dimensional localisation of CENP-A suggests a complex higher order structure of centromeric chromatin. J Cell Biol 183:1193–1202. doi:10.1083/jcb.200804078

McClelland SE, Borusu S, Amaro AC, Winter JR, Belwal M, McAinsh AD, Meraldi P (2007) The CENP-A NAC/CAD kinetochore complex controls chromosome congression and spindle bipolarity. EMBO J 26:5033–5047. doi:10.1038/sj.emboj.7601927

Minoshima Y, Hori T, Okada M, Kimura H, Haraguchi T, Hiraoka Y, Bao Y-C, Kawashima T, Kitamura T, Fukagawa T (2005) The constitutive centromere component CENP-50 is required for recovery from spindle damage. Mol Cell Biol 25:10315–10328. doi:10.1128/MCB.25.23.10315-10328.2005

Musacchio A, Salmon ED (2007) The spindle-assembly checkpoint in space and time. Nat Rev Mol Cell Biol 8:379–393. doi:10.1038/nrm2163

Nagy P, Vamosi G, Bodnar A, Lockett SJ, Szöllösi J (1998) Intensity-based energy transfer measurements in digital imaging microscopy. Eur Biophys J 27:377–389. doi:10.1007/s002490050145

Nishihashi A, Haraguchi T, Hiraoka Y, Ikemura T, Regnier V, Dodson H, Earnshaw WC, Fukagawa T (2002) CENP-I is essential for centromere function in vertebrate cells. Dev Cell 2:463–476

Okada M, Cheeseman IM, Hori T, Okawa K, McLeod IX, Yates III JR, Desai A, Fukagawa T (2006) The CENP-H–I complex is required for the efficient incorporation of newly synthesized CENP-A into centromeres. Nat Cell Biol 8:446–457. doi:10.1038/ncb1396

Orthaus S, Biskup C, Hoffmann B, Hoischen C, Ohndorf S, Benndorf K, Diekmann S (2008) Assembly of the inner kinetochore proteins CENP-A and CENP-B in living human cells. ChemBioChem 9:77–92. doi:10.1002/cbic.200700358

Orthaus S, Klement K, Happel N, Hoischen C, Diekmann S (2009) Linker histone H1 is present in centromeric chromatin of living human cells next to inner kinetochore proteins. Nucl Acids Res. (Epub March 31) doi:10.1093/nar/gkp199

Patterson GH, Knobel SM, Sharif WD, Kain SR, Piston DW (1997) Use of the green fluorescent protein and its mutants in quantitative fluorescence microscopy. Biophys J 73:2782–2790. doi:10.1016/S0006-3495(97)78307-3

Perpelescu M, Nozaki N, Obuse C, Yang H, Yoda K (2009) Active establishment of centromeric CENP-A chromatin by RSF complex. J Cell Biol 185:397–407. doi:10.1083/jcb.200903088

Pluta AF, Saitoh N, Goldberg I, Earnshaw WC (1992) Identification of a subdomain of CENP-B that is necessary and sufficient for localisation to the human centromere. J Cell Biol 116:1081–1093. doi:10.1083/jcb.116.5.1081

Roos UP (1973) Light and electron microscopy of rat kangaroo cells in mitosis. II. Kinetochore structure and function. Chromosoma 41:195–220. doi:10.1007/BF00319696

Sugimoto K, Kuriyama K, Shibata A, Himeno M (1997) Characterization of internal DNA-binding and C-terminal dimerization domains of human centromere/kinetochore autoantigen CENP-C in vitro: role of DNA-binding and self-associating activities in kinetochore organization. Chrom Res 5:132–141

Suzuki N, Nagano M, Nozaki N, Egashira S, Okazaki T, Masumoto H (2004) CENP-B interacts with CENP-C domains containing Mif2 regions responsible for centromere localization. J Biol Chem 279:5934–5946. doi:10.1074/jbc.M306477200

Tramier M, Zahid M, Mevel JC, Masse MJ, Coppey-Moisan M (2006) Sensitivity of CFP/YFP and GFP/mCherry pairs to donor photobleaching on FRET determination by fluorescence lifetime imaging microscopy in living cells. Microsc Res Tech 69:933–939. doi:10.1002/jemt.20370

Wieland G, Orthaus S, Ohndorf S, Diekmann S, Hemmerich P (2004) Functional complementation of human centromere protein A (CENP-A) by Cse4p from *Saccharomyces cerevisiae*. Mol Cell Biol 24:6620–6630. doi:10.1128/MCB.24.15.6620-6630.2004

Wouters FS, Bastiaens PIH, Wirtz KWA, Jovin TM (1998) FRET microscopy demonstrates molecular association of non-specific lipid transfer protein (nsL-TP) with fatty acid oxidation enzymes in peroxisomes. EMBO J 17:7179–7189. doi:10.1093/emboj/17.24.7179

Yoda K, Kitagawa K, Masumoto H, Muro Y, Okazaki T (1992) A human centromere protein, CENP-B, has a DNA binding domain containing four potential alpha helices at the NH_2 terminus, which is separable from dimerising activity. J Cell Biol 119:1413–1427. doi:10.1083/jcb.119.6.1413

JCS ePress online publication date 18 November 2011

Dynamics of CENP-N kinetochore binding during the cell cycle

Daniela Hellwig[1], Stephan Emmerth[2,*], Tobias Ulbricht[1], Volker Döring[1], Christian Hoischen[1], Ronny Martin[3], Catarina P. Samora[4], Andrew D. McAinsh[4], Christopher W. Carroll[5], Aaron F. Straight[5], Patrick Meraldi[2] and Stephan Diekmann[1,‡]

[1]Molecular Biology, FLI, Beutenbergstrasse 11, 07745 Jena, Germany
[2]Institute of Biochemistry, ETH Zurich, Zurich 8093, Switzerland
[3]HKI, Beutenbergstrasse 11, 07745 Jena, Germany
[4]Centre for Mechanochemical Cell Biology, Warwick Medical School, University of Warwick, Coventry CV4 7AL, UK
[5]Deptartment of Biochemistry, Stanford University School of Medicine, Beckman Center Room 409, 279 Campus Drive, Palo Alto, CA 94503-5307, USA

*Present address: Friedrich Miescher Institute for Biomedical Research, Maulbeerstrasse 66, 4058 Basel, Switzerland
‡Author for correspondence (diekmann@fli-leibniz.de)

Accepted 4 July 2011
Journal of Cell Science 124, 1–13

doi: 10.1242/jcs.088625

Summary

Accurate chromosome segregation requires the assembly of kinetochores, multiprotein complexes that assemble on the centromere of each sister chromatid. A key step in this process involves binding of the constitutive centromere-associated network (CCAN) to CENP-A, the histone H3 variant that constitutes centromeric nucleosomes. This network is proposed to operate as a persistent structural scaffold for assembly of the outer kinetochore during mitosis. Here, we show by fluorescence resonance energy transfer (FRET) that the N-terminus of CENP-N lies in close proximity to the N-terminus of CENP-A in vivo, consistent with in vitro data showing direct binding of CENP-N to CENP-A. Furthermore, we demonstrate in living cells that CENP-N is bound to kinetochores during S phase and G2, but is largely absent from kinetochores during mitosis and G1. By measuring the dynamics of kinetochore binding, we reveal that CENP-N undergoes rapid exchange in G1 until the middle of S phase when it becomes stably associated with kinetochores. The majority of CENP-N is loaded during S phase and dissociates again during G2. We propose a model in which CENP-N functions as a fidelity factor during centromeric replication and reveal that the CCAN network is considerably more dynamic than previously appreciated.

Key words: Mitosis, Centromere, Kinetochore, CCAN complex, CENP-N, Cell cycle

Introduction

The kinetochore is a multiprotein complex that assembles at the centromeric DNA ('centromere') of each chromosome to permit proper segregation of sister chromatids during cell division. Although kinetochores are composed of over 100 different subunits, at their structural core they contain two conserved protein networks, the KMN (for KNL1/Blinkin/Spc105p, MIND/MIS12/Mtw1 and NDC80/Hec1) (De Wulf et al., 2003; Nekrasov et al., 2003; Cheeseman et al., 2004; Cheeseman et al., 2006; Obuse et al., 2004; Liu et al., 2005; Meraldi et al., 2006) and the constitutive centromere-associated network (CCAN) or CENP-A–NAC/CAD kinetochore complex (Foltz et al., 2006; Okada et al., 2006; Meraldi et al., 2006; McClelland et al., 2007; Hori et al., 2008a; Hori et al., 2008b; Amano et al., 2009) (reviewed by Santaguida and Musacchio, 2009). The KMN network is essential for kinetochore–microtubule binding (Tanaka and Desai, 2008; Cheeseman and Desai, 2008), whereas the CCAN network is associated to the centromeric nucleosomes (Carroll et al., 2009; Foltz et al., 2006). The centromeric nucleosomes, which contain the histone H3 variant CENP-A, assemble on repetitive α-satellite DNA. The structural core of the CENP-A-containing nucleosome is key to marking kinetochore position on the chromosome (Black et al., 2007a; Black et al., 2007b; Dalal et al., 2007; Sekulic and Black, 2009; Furuyama and Henikoff, 2009; Sekulic et al., 2010; Dimitriadis et al., 2010; Cho and Harrison, 2011; Zhou et al., 2011; Hu et al., 2011; Dechassa et al., 2011). Functionally, the CCAN network is required for the efficient recruitment of CENP-A into centromeric nucleosomes at the end of mitosis (Okada et al., 2006; Carroll et al., 2009; Carroll et al., 2010) and the maintenance of centromeric chromatin, but it is also involved in regulation of kinetochore fibre stability and dynamics, to control chromosome alignment and bipolar spindle assembly (Fukagawa et al., 2001; Foltz et al., 2006; Okada et al., 2006; McAinsh et al., 2006; McClelland et al., 2007; Toso et al., 2009; Amaro et al., 2010). Because several of the CCAN proteins are constitutively present at centromeres, this network has been proposed to act as a structural scaffold that is stably associated with the centromeric nucleosomes (Cheeseman and Desai, 2008). One key subunit of the CCAN is CENP-N, which binds directly to CENP-A-containing nucleosomes. It is required for the loading of all other CCAN subunits onto kinetochores (Okada et al., 2006; McClelland et al., 2007; Carroll et al., 2009). CENP-N directly binds CENP-L within the CCAN network, thus providing a possible link between the CENP-A nucleosomes and the rest of the network (Carroll et al., 2009).

In contrast to the static scaffold model, immunofluorescence experiments suggest that certain components of CCAN are not constitutively associated with the centromeres, but rather are dynamic and only associate with centromeres during certain phases of the cell cycle. In particular, it has been reported that the

kinetochore-bound levels of CENP-N decrease when cells enter mitosis, with low binding detectable during metaphase (McClelland et al., 2007). This would suggest that the CCAN network is not a constitutive scaffold, but dynamically changes during cell cycle progression.

Here, we applied a broad range of methodologies to characterise the dynamic or static nature of CENP-N in a cellular context. Using fluorescence resonance energy transfer (FRET), we demonstrate that the N-terminus of EGFP–CENP-N is in direct proximity to the N-terminus of CENP-A in vivo, consistent with a close association to CENP-A-containing nucleosomes. We further show by several independent methods that CENP-N binds to the kinetochore at the end of G1 and during S phase, and is released during G2. Detailed FRAP analysis indicates that EGFP–CENP-N exchanges fast at kinetochores in G1 and is loaded to kinetochores by fast exchange in early S phase, before binding stably with very slow loading dynamics in middle and late S phase. These dynamics result in maximal CENP-N protein levels at kinetochores in S phase, reduced levels in G2, but low values in M phase and G1. We therefore conclude that the CCAN is not constitutive, but rather has a dynamic composition at the kinetochore during the cell cycle.

Results

CENP-N binds in close proximity to CENP-A in vivo

The CCAN subunit CENP-N binds in vitro to CENP-A-containing nucleosomes via a folded region that spans the CENP-N protein (Carroll et al., 2009). However, whether CENP-A and CENP-N are closely associated in vivo is not known. To analyse the binding of cellular CENP-N to the CENP-A-containing nucleosome in centromeric chromatin, we performed a FRET-based approach, which we have previously utilised to study protein proximities and interactions in cells (Hellwig et al., 2009; Orthaus et al., 2008; Orthaus et al., 2009). We expressed a full-length human CENP-N fusion with EGFP and confirmed that the EGFP–CENP-N colocalised to kinetochores with CENP-A in human HEp-2 cells (Fig. 1A). Next, we measured the FRET efficiency between the donor fluorophore (EGFP–CENP-N) and the acceptor fluorophore (mCherry–CENP-A), a method that can only generate a positive result when the distance between donor and acceptor is less than ~10 nm (see Fig. 1). In our live cell experiments, the orientation of the fluorophore dipole moment of the acceptor relative to that of the donor is not known. Thus, we did not deduce defined distance values from our measured FRET efficiencies but interpreted the appearance of FRET as an indication that donor and acceptor chromophores are close to one another within 10 nm.

Our measurements were based on two independent, but complementary, experimental approaches: first, we measured the FRET donor fluorescence intensity with or without photo-inactivation of the acceptor (acceptor-photobleaching FRET; AB-FRET) and, second, the donor fluorescence lifetime (FLIM), which can yield more detailed information and is less error-prone. In AB-FRET, the acceptor chromophore is destroyed by photobleaching, thereby preventing FRET from the donor to the acceptor. If the donor and acceptor are in close enough proximity for energy transfer, photobleaching the acceptor results in an observable increase in donor fluorescence. In our experiments, two separate kinetochore locations were identified in each image (Fig. 1A, spots 1 and 2). In spot 2, the acceptor (mCherry–CENP-A) was photobleached, whereas spot 1 was not photobleached and served as an internal control for any non-FRET effects (Fig. 1A, and black bars in Fig. 1C). During bleaching of spot 2, the donor fluorescence intensity significantly increased (Fig. 1B, black arrow) indicating that FRET occurs between EGFP–CENP-N and mCherry–CENP-A (Hellwig et al., 2009). Careful quantification indicated that such FRET transfer occurred in 64% of the cases ($P<0.001$; Fig. 1C, grey bars), even though the FRET efficiency values were rather low. These data imply that the N-terminus of CENP-N is in close proximity to the N-terminus of CENP-A. By contrast, we detected no FRET between EGFP–CENP-N and mCherry–CENP-C (Hellwig et al., 2009) and between EYFP–CENP-C and Cerulean–CENP-A (S. Orthaus, Towards the architecture of the human kinetochore, PhD thesis, Friedrich Schiller University, Jena, Germany, 2006). These results are consistent with recent findings on the kinetochore binding of CENP-C (Przewloka et al., 2011; Screpanti et al., 2011). Additionally, we observed indications for very weak FRET between the C-terminus of CENP-C and the flexible N-terminus of CENP-A; these data however require further intensive experimentation. Recently, we observed that CENP-C binds directly and specifically to CENP-A-containing nucleosomes, requiring the extreme C-terminus of CENP-A for binding (Carroll et al., 2010).

We next confirmed our proximity results by measuring FRET in the lifetime domain (FLIM) with the same FRET pair (mCherry–CENP-A and EGFP–CENP-N) and time-correlated single photon counting (TCSPC) at kinetochore locations identified by mCherry–CENP-A. When FRET occurs in such an experiment, the donor fluorescence lifetime is decreased due to energy transfer to the acceptor. The mean donor lifetime in the absence of an acceptor was 2.49 ± 0.01 nanoseconds (69 kinetochores from 10 cells; see Fig. 1D, black bars). In the presence of the acceptor, however, the donor lifetime distribution significantly shifted to shorter values with a mean value of 2.33 ± 0.03 nanoseconds (67 kinetochores in 11 cells; see Fig. 1D, grey bars) with a mean FRET efficiency of 7% ($P<0.001$). These combined results indicate the presence of FRET between the fluorophores positioned at the N-termini of CENP-A and CENP-N, demonstrating that these entities are close to one another in vivo, consistent with previous in vitro biochemical data (Carroll et al., 2009).

CENP-N binds to kinetochores mainly in S phase and G2

Previous immunofluorescence experiments in asynchronous cell populations indicated that CENP-N levels at kinetochores decrease during mitosis (McClelland et al., 2007) suggesting that the CENP-N kinetochore binding varies during the cell cycle. To substantiate this result, we synchronised cells and quantified the levels of endogenous CENP-N at kinetochores at different phases of the cell cycle, using the CENP-N antibody (McClelland et al., 2007), from early S phase until mitosis (Fig. 2A). Cell cycle phases were identified either by PCNA (S phase), DAPI (chromosome condensation in mitosis) or CENP-F staining (G2, mitosis). After double-thymidine block release, the fluorescence intensity profile versus time shows a continuous increase at kinetochores with a clear maximum after 6 hours in the second half of S phase (Fig. 2B). Relative to this maximal value, the fluorescence intensity values after 1.5 hours (early S phase) and 9 hours (mitosis) were 19% and 27%, respectively (Fig. 2B). The low abundance of CENP-N at kinetochores during

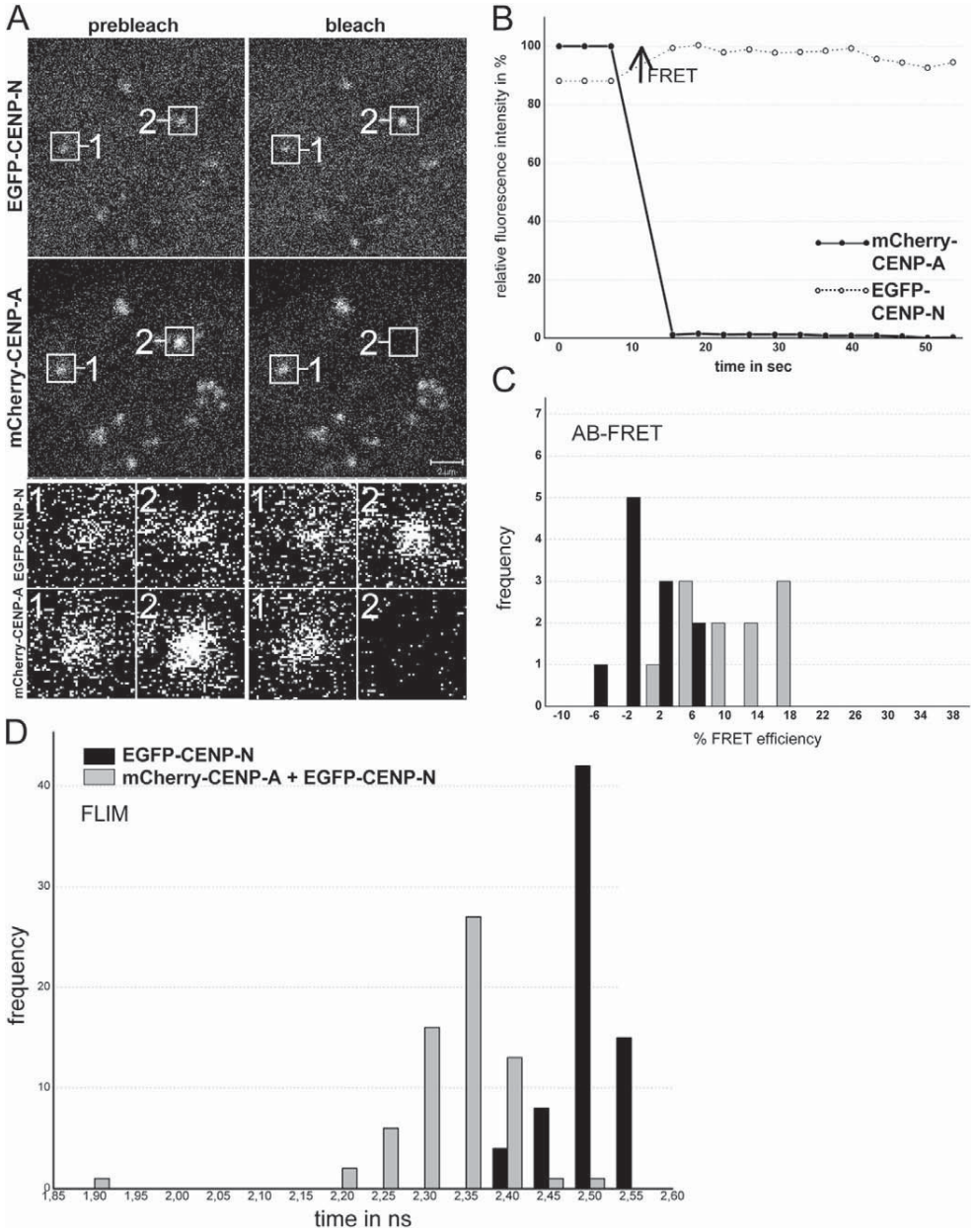

Fig. 1. FRET analysis. (**A**) AB-FRET of the protein pair EGFP–CENP-N and mCherry–CENP-A. Human HEp-2 cells were co-transfected with both fusion proteins. Typical cell nucleus, showing colocalisation at specific (centromeric) locations. Two of these locations, 1 and 2, were selected for fluorescence intensity analysis before and after acceptor bleaching (see enlargement below). Spot 1 served as control and showed no detectable intensity change. At spot 2, the acceptor fluorophore mCherry was bleached (compare prebleach and postbleach images). (**B**) Time course of the fluorescence intensity of the donor and the acceptor. The acceptor intensities in the ROI (region of interest; black circles) were averaged and normalized to the mean intensity measured at the three time points before bleaching. The donor intensities in the ROI were averaged and normalized to the intensity measured at the first time point after bleaching. Bleaching of the acceptor resulted in a fluorescence intensity increase of the donor (open circles) indicating the presence of FRET (see arrow). (**C**) Donor fluorescence intensity variation observed during acceptor bleaching was normalized to the intensity measured at the first time point after bleaching to give FRET efficiency (*E*). For spot 1 (acceptor not bleached, control, 11 kinetochores), this yielded E_{var} (black bars) and for spot 2 (acceptor bleached, 10 kinetochores) E_{FRET} (grey bars). Frequency values are the number of observed single cases (grouped into E_{var} or E_{FRET} value ranges of 4%) and are plotted against the values of E_{var} or E_{FRET}. Only some E_{FRET} values coincided with the distribution of E_{var} values, however, most E_{FRET} values exceeded the E_{var} values, indicating the presence of FRET. (**D**) Histogram of the donor fluorescence lifetimes obtained in FLIM experiments. HEp-2 cells were transfected with EGFP–CENP-N alone (donor only, black bars, control, 69 kinetochores) or co-transfected with EGFP–CENP-N and mCherry–CENP-A. In these living cells, the donor fluorescence lifetimes were measured by TCSPC. The histograms display the fitted lifetime values of all single kinetochores. The heights of the bars represent the numbers of kinetochores (frequency) whose lifetimes fall within the indicated 0.3 nanosecond range (time). When the acceptor is present (grey bars, 64 kinetochores), the donor fluorescent lifetimes were shorter than the control values for donor only (black bars), clearly indicating the presence of FRET. The weak binding to kinetochores of the CENP-NΔC mutant lacking the CENP-N C-terminus (Carroll et al., 2009) resulted in low fluorescence intensities and did not allow for FRET measurements.

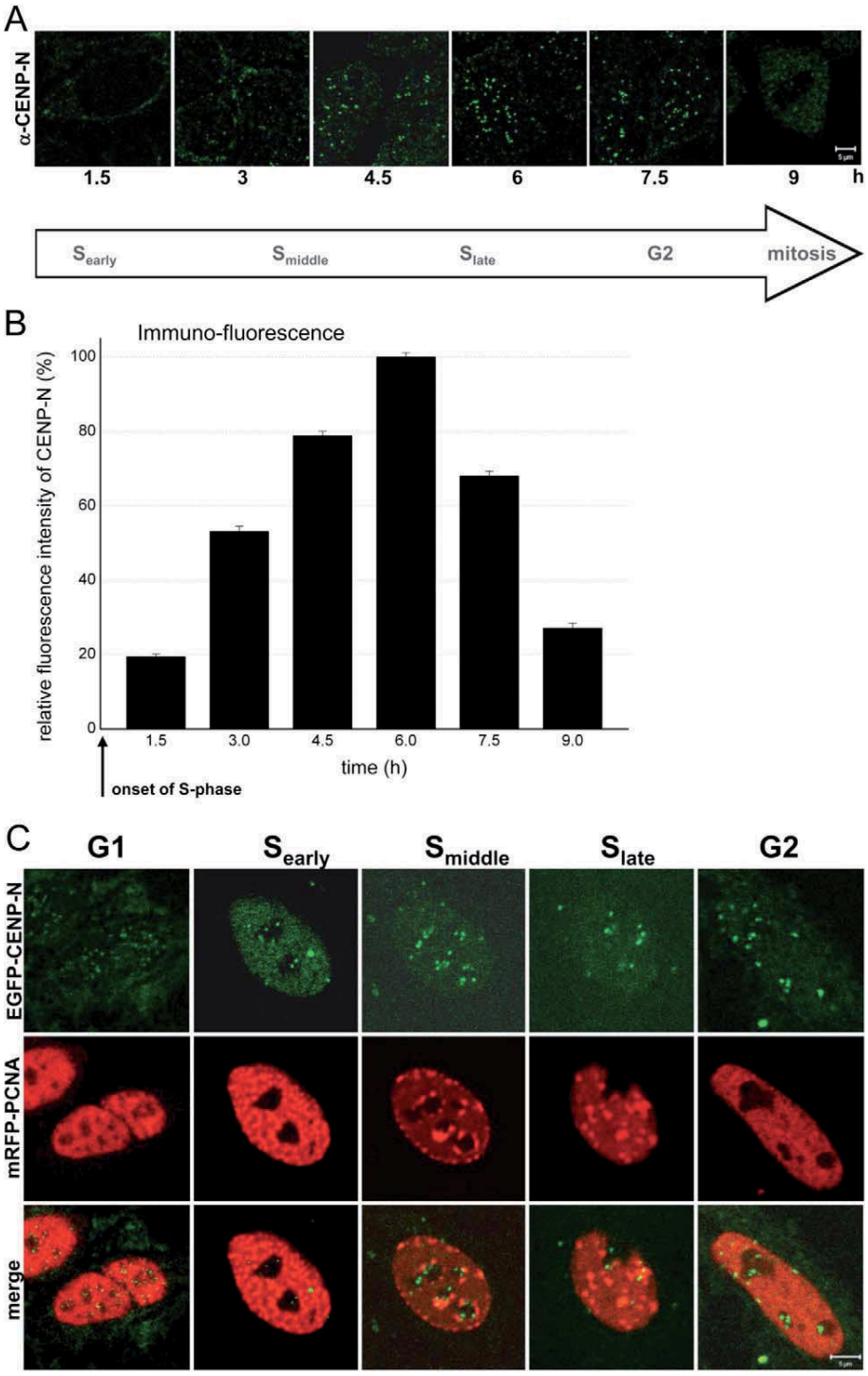

Fig. 2. Amount of endogenous immunostained and EGFP-labelled CENP-N at kinetochores in early, middle and late S phase, G2 and mitosis. (**A**) CENP-N labelled by an anti-CENP-N primary and a fluorescently labelled secondary antibody in HEp-2 nuclei fixed 1.5, 3.0, 4.5, 6.0, 7.5 and 9.0 hours after double-thymidine block release. The amount of antibody-marked endogenous CENP-N at kinetochores increased during S phase and was low in mitosis. Scale bar: 5 μm. A G1 image is not included due to the low CENP-N levels in G1. (**B**) For each kinetochore, the fluorescence intensity per area was determined and compared. The mean secondary antibody fluorescence intensity per area of 70–250 kinetochores per time point (10–20 kinetochores per cell) was determined at kinetochores within cells at different time points after double-thymidine block release. The fluorescence intensity values are plotted relative to the value at 6.0 hours (100%). Endogenous CENP-N at kinetochores increased during S phase and was depleted from kinetochores during G2. (**C**) Analysis of EGFP–CENP-N at kinetochores. Detection of EGFP–CENP-N (upper row), mRFP-PCNA as replication marker (middle row) and merge (lower row) in HEp-2 cell nuclei. The fluorescence intensity of EGFP-labelled CENP-N increased from G1 into S phase. Scale bar: 5 μm.

mitosis thus agreed with previous findings (McClelland et al., 2007).

Immunofluorescence-based quantifications, however, have the disadvantage that epitope-masking effects cannot be excluded. Therefore, for comparison, we determined whether EGFP–CENP-N is also differentially bound to kinetochores in living human cells. We analysed the localisation of EGFP–CENP-N by live-cell imaging throughout G1, early, middle and late S phase, and G2 using mRFP-PCNA localisation as a readout of the cell cycle phase (Madsen and Celis, 1985). PCNA is diffuse in G1 nuclei, coalesces into many small foci in early S phase, migrates to the inner nuclear membrane and nucleolar surface in middle S phase, grows to large foci in late S phase followed by diffuse redistribution in G2, similar to G1 localisation (Somanathan et al., 2001; Sporbert et al., 2005). Furthermore, G1 and G2 nuclei could be distinguished by determining whether mitotic

condensed chromosomes and cytokinesis, or nuclear PCNA foci preceded the cell cycle stage (Hemmerich et al., 2008). This analysis showed low levels of CENP-N bound to kinetochores during G1, and an increase in kinetochore binding during S phase (Fig. 2C). By measuring the fluorescence intensities, the cell cycle dependent levels of EGFP–CENP-N were quantified at kinetochores, in the interphase nucleus and in the whole cell. The obtained cell cycle fluctuations were very similar to those of the endogenous protein. To quantify in more detail the removal of CENP-N from the kinetochores, we measured the decrease of EGFP–CENP-N fluorescence intensity at kinetochores after S phase at particular time points in living G2 cells and observed a continuous disappearance of CENP-N during the first 3 hours after entry into G2.

Thus, CENP-N immunofluorescence and EGFP–CENP-N measurements indicated that CENP-N is recruited to kinetochores at the onset of S phase, reaches a maximal abundance during late S phase, and is continuously displaced from kinetochores during G2.

Cellular CENP-N protein levels are maximal during S phase

The S phase- and G2-specific accumulation of CENP-N at kinetochores could reflect either the general cellular abundance of CENP-N or a specific binding of CENP-N to kinetochores during S phase and G2. To distinguish between these possibilities, we determined *CENPN* mRNA and protein expression levels in the whole cell at different cell cycle phases (identified as described above). First, we measured the *CENPN* mRNA level of double-thymidine block synchronised cells over a period of 10 hours after release, well into G2 and mitosis. We observed stable *CENPN* mRNA values of 80–90% relative to β-actin (Fig. 3A), indicating that *CENPN* mRNA levels remain constant throughout the cell cycle. We next determined endogenous CENP-N protein levels in whole synchronised cells by quantitative immunofluorescence microscopy. We observed maximum fluorescence intensity in the whole cell after 6 hours in the second half of S phase (Fig. 3B). This maximum intensity was three times higher than the level during early S phase and ~1.6 times higher than the level in mitosis. These data were confirmed by an immunoblotting analysis (Fig. 3C). Three hours after double-thymidine block release we found maximal amounts of CENP-N (S phase), which decreased to $77\pm2\%$ after 7 hours (G2), $40\pm14\%$ after 9 hours (mitosis) and $36\pm10\%$ after 12 hours (G1). Finally, we also tested whether CENP-N binding to kinetochores might be influenced by the cell-cycle dependent changes in CENP-A levels. We thus quantified CENP-A levels at kinetochores by immunofluorescence and found constant CENP-A levels over S phase and G2 (Fig. 3D).

We conclude that CENP-N is present in the cell during the whole cell cycle. However, protein levels vary within a factor of three, with highest values during second half of S phase. The binding of CENP-N to kinetochores varied by a factor of five in S phase compared with mitosis–G1. This implies that during S phase, increasing cellular CENP-N protein concentrations drive CENP-N into a complex with CENP-A-containing nucleosomes. In G2, however, CENP-N is released from kinetochores. This reduction of CENP-N levels at CENP-A-containing nucleosomes in G2 is not explained by a potential reduction of CENP-A levels, but coincides with the degradation of CENP-N.

Kinetochore-binding dynamics of CENP-N

The varying presence of CENP-N at kinetochores suggests a dynamic binding behaviour. The binding of CENP-N to the kinetochores might either be stable, or transient, with fast exchange of CENP-N at the binding sites. Recently, we detected stable binding to kinetochores during the whole cell cycle for CENP-A and CENP-I, whereas hMis12 stably bound to the kinetochores only during mitosis but showed fast exchange during interphase (Hemmerich et al., 2008). To monitor the behaviour of CENP-N, we applied two independent, complementary methods, the SNAP-tag and fluorescence recovery after photobleaching (FRAP).

SNAP-tag

The SNAP-tag is a versatile protein tag that can catalyse the formation of a covalent bond to a benzyl-guanine moiety coupled to different fluorescent or non-fluorescent membrane-permeable reagents (Keppler et al., 2003). Importantly, this tag allows pulse-chase experiments at a single protein level, because no other protein in a cell will react with membrane-permeable benzyl-guanines. The tag has previously been used to show that CENP-A is loaded on centromeres exclusively in early G1 (Jansen et al., 2007). We therefore used the same technique to ask at which cell cycle stage CENP-N-SNAP is incorporated into kinetochores. First, to validate the method in our hands, we monitored the centromere assembly of CENP-A in HeLa cells (Fig. 4). Cells were transiently transfected with SNAP–CENP-A and arrested in early S phase with a double-thymidine and aphidicolin arrest. Cellular SNAP–CENP-A was quenched with BTP (a benzyl guanine not coupled to a fluorophore) for 30 minutes. Cells were released from the arrest, labelled in vivo 4 hours later with the fluorophore TMR-star, and fixed for immunofluorescence analysis 12 hours after labelling. This resulted in a mix of G2, mitotic, and early G1 cells, which could be distinguished by CENP-F staining, which labels the whole nucleus in G2 and specifically binds to kinetochores during M phase, but shows no specific localisation in early G1 cells (Liao et al., 1995). Consistent with previous data, TMR-star fluorescence on SNAP–CENP-A was only observed in G1 cells (Fig. 4A), confirming that CENP-A is specifically loaded in G1 (Jansen et al., 2007; Hemmerich et al., 2008). By contrast, when transfecting a CENP-N–SNAP construct, after double-thymidine and aphidicolin block release and applying the same protocol, we found CENP-N–SNAP present at kinetochores of G2 cells, but not of early G1 cells (Fig. 4A). This suggested that CENP-N is loaded onto kinetochores in or before G2, that it is released as cells progress through M phase, and that it is not reloaded in early G1. To extend our temporal analysis to further phases of the cell cycle, we repeated these experiments in U2OS because these cells have a longer cell cycle. Thus, again 12 hours after release and following the same experimental procedure, U2OS cells can be analysed in late-S phase. Here, TMR-star fluorescence for CENP-N–SNAP was already detected in late S phase as judged by PCNA–GFP fluorescence. Thus, CENP-N assembles at kinetochores already in late S phase or earlier (Fig. 4B). Finally, to measure the earliest time point at which CENP-N can assemble into kinetochores, CENP-N–SNAP-transfected HeLa cells were arrested in mitosis for 12 hours by a nocodazole block and quenched with BTP for 30 minutes (Fig. 4C). At 4 hours after quenching, the cells were released from nocodazole arrest. After another 5 hours, SNAP-tagged CENP-N was fluorescently labelled with TMR-star for 30 minutes and fixed for examination. TMR-star fluorescence was detected (Fig. 4C) in roughly half the cells examined,

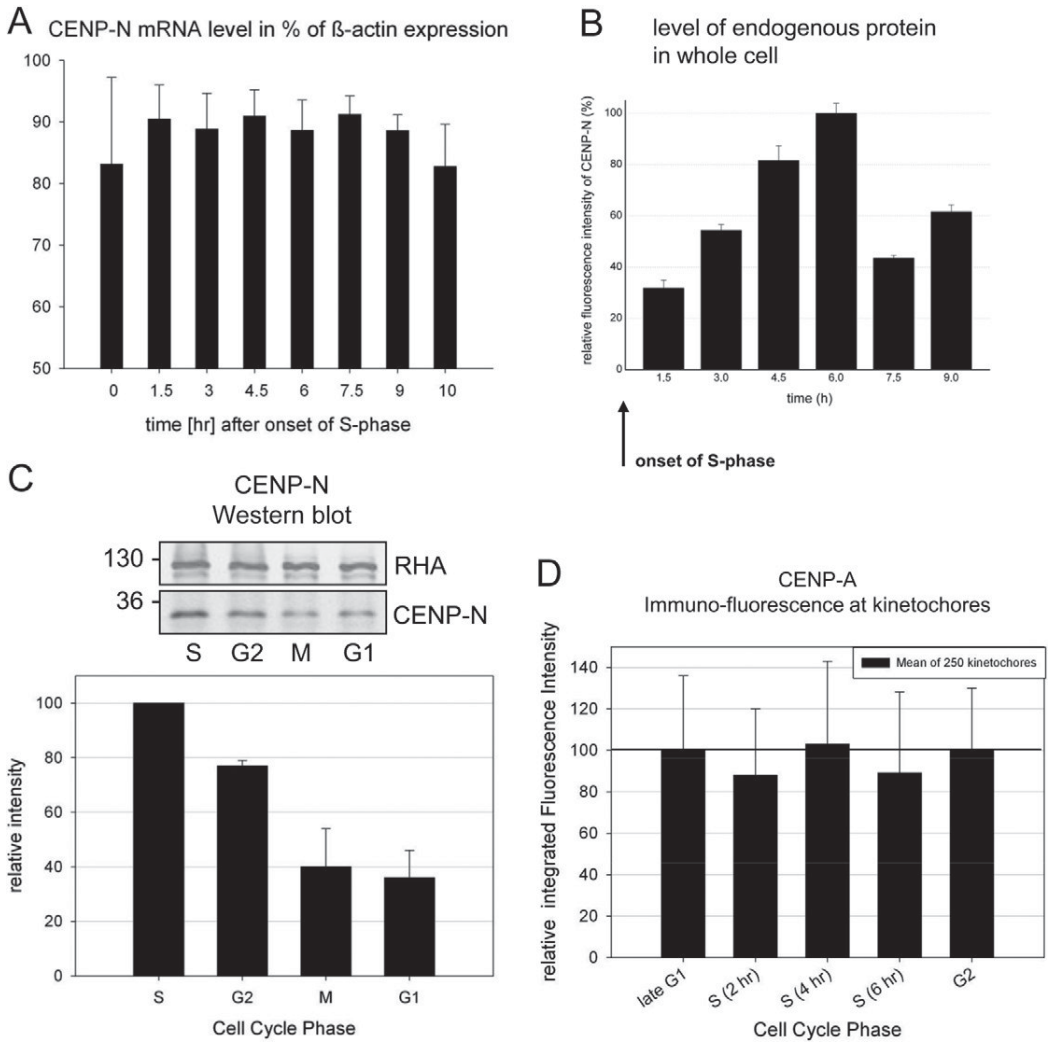

Fig. 3. ***CENPN*** **mRNA and whole cell protein levels.** (**A**) mRNA levels (mean of three independent experiments) of *CENPN* are plotted relative to the value of β-actin in the cells. Human HEp-2 cells were synchronised by a double-thymidine block and analysed after release in time intervals of 90 minutes for 11 hours. (**B**) After immunostaining of endogenous CENP-N, the whole cell fluorescence was measured and integrated at 1.5, 3.0, 4.5, 6.0, 7.5 and 9.0 hours after double-thymine block release. Whole cell fluorescence intensity values are plotted relative to the maximal value at 6.0 hours (100%). Although the mRNA levels were rather constant, the amount of CENP-N in the cell increased in S phase (with a maximum in late S phase) and decreased afterwards. (**C**) Western blot analysis of whole cell CENP-N protein levels at 3 (S phase), 7 (G2), 9 (M phase) and 12 (G1) hours after double-thymidine block release relative to the house-keeping gene product RHA. CENP-N was identified by a CENP-N-specific antibody (molecular weight marker values are shown on the left). CENP-N amounts were quantified by the ODYSSEY Infrared Imaging System and are shown in the histogram below. CENP-N levels were maximal in S phase and low in mitosis and G1. (**D**) CENP-A was antibody stained at 0 (G1–S), 2 (S), 4 (S), 6 (S) and 8 (G2) hours after HEp-2 cells double-thymidine block release and its amounts quantified by integrating the secondary antibody fluorescence intensity at kinetochores. CENP-A levels at centromeres remained constant during S phase and G2. Error bars indicate s.d.

indicating that CENP-N–SNAP can be loaded during the first 5 hours after M phase in G1. Overall, these experiments suggest a time window of middle G1 to G2 for CENP-N binding and loading to kinetochores.

FRAP

In order to refine our analysis, we carried out fluorescence recovery after photobleaching (FRAP) experiments to monitor kinetochore binding of EGFP–CENP-N in various cell cycle phases as well as measure its binding dynamics in living cells (see Fig. 5). In G1, we observed recovery of CENP-N at the kinetochores after photobleaching. In order to determine whether CENP-N is recruited to the kinetochore in G1 by a loading-only mechanism or by free exchange, the EGFP–CENP-N proteins were bleached a second time (double FRAP experiment), during recovery 60 seconds after the initial bleaching event (Hemmerich et al., 2008). This second recovery of EGFP–CENP-N had very similar kinetics of fluorescence recovery to that seen after the first bleach event (see Fig. 5B). During early S phase, we observed a partial recovery of CENP-N at the kinetochores after photobleaching (mean recovery of 50%) with half amplitude recovery times $t_{1/2}=20\pm2$ seconds (Fig. 5C). Again, the EGFP–CENP-N proteins were bleached a second time. As after the first bleach, EGFP–CENP-N showed fluorescence recovery

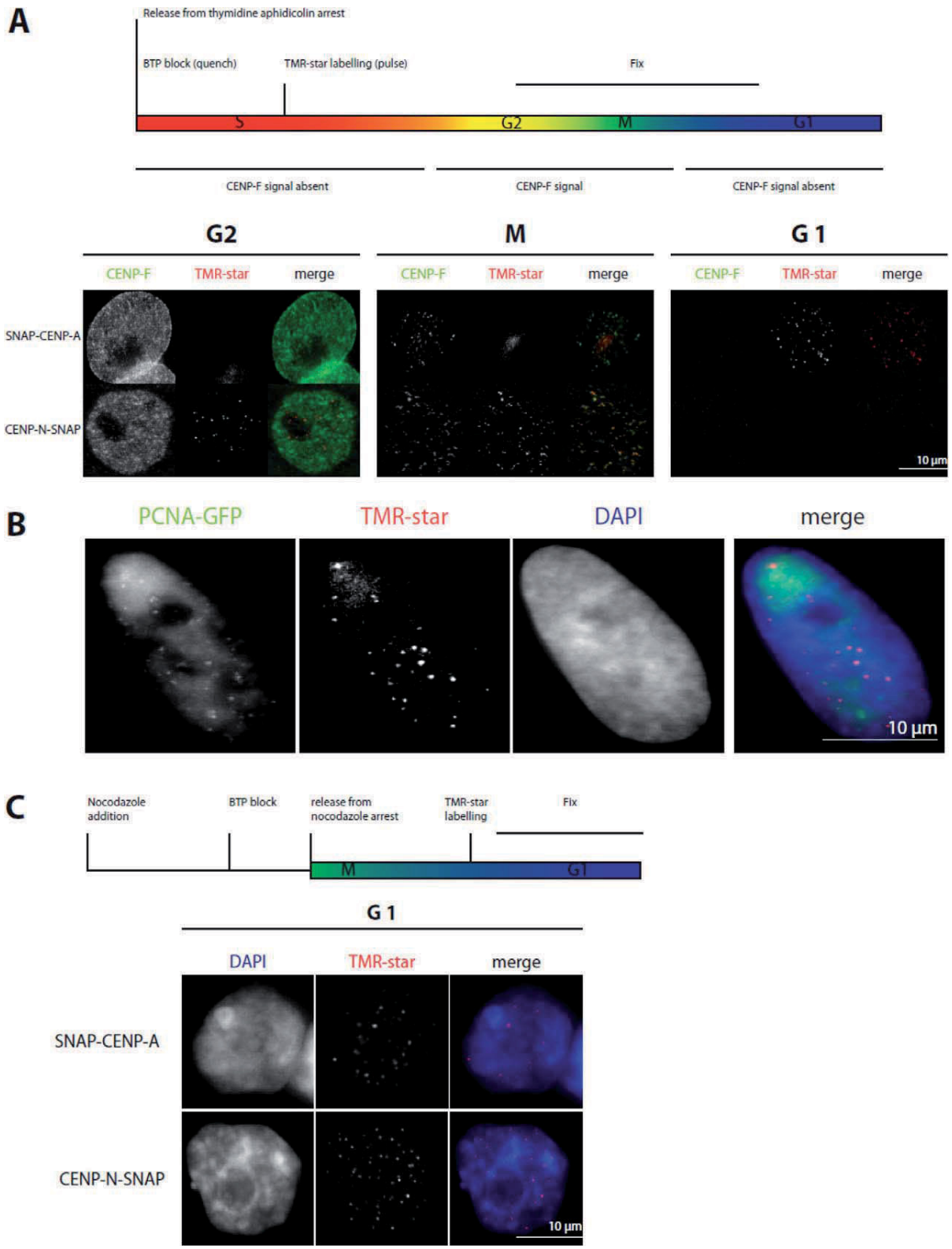

Fig. 4. CENP-N loading to kinetochores measured by the SNAP-tag technology. (**A**) Above: Scheme of the performed experiment. Below: Representative images of cells showing TMR-star fluorescence for SNAP–CENP-A only in G1 and for CENP-N–SNAP in G2 and M phase. Cell cycle phases G2 (CENP-F staining of the whole nucleus) and mitosis (specific kinetochore binding of CENP-F) are clearly identified. (**B**) The same experiment as in A was performed with U2OS cells stably expressing PCNA–GFP. CENP-N–SNAP fluorescence appeared at kinetochores in late S phase as judged from cellular PCNA distributions. (**C**) Top: Scheme of the performed experiment. Below: Representative images of cells expressing SNAP–CENP-A and CENP-N–SNAP showing fluorescence at kinetochores during G1. CENP-N was loaded to kinetochores in G1 and S phase.

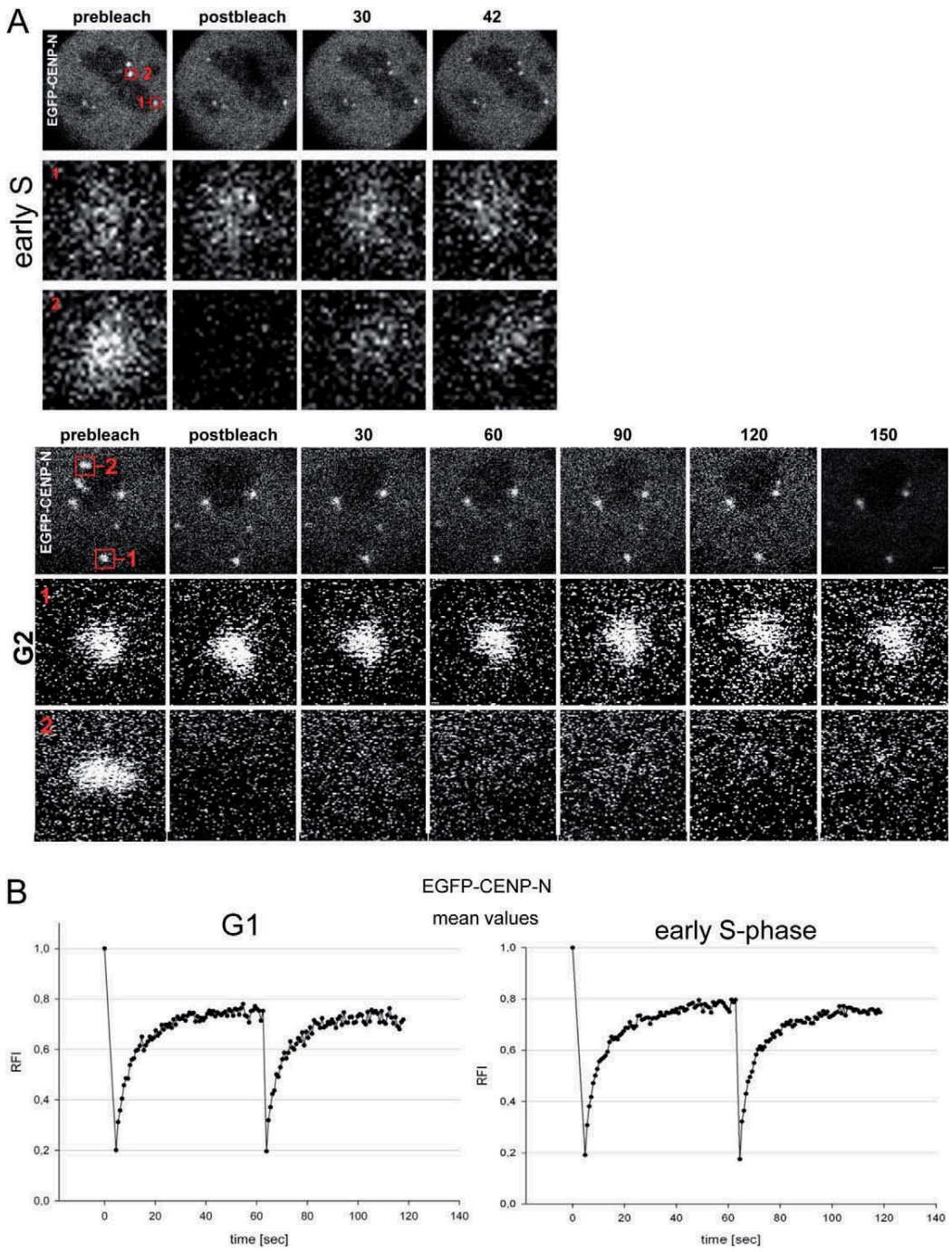

Fig. 5. EGFP–CENP-N binding dynamics to kinteochores. (**A**) EGFP–CENP-N binding to several kinetochores in HEp-2 cells in early S phase (upper three rows) and in G2 (lower three rows). In both cases, two kinetochore foci 1 and 2 were selected: spot 1 was not bleached and served as control, whereas spot 2 was photobleached. The changes in spots 1 and 2 over time are shown in the rows below at higher magnification. In early S phase, after photobleaching, fast recovery was observed in spot 2. In G2, after photobleaching, no FRAP was observed in spot 2. Quantification is presented in B and C. (**B**) Mean FRAP recovery curves of 29 kinetochores in 12 cells in late G1 (left) and 28 kinetochores in 12 cells in early S phase (right, see A). After 60 seconds during recovery, the spots were bleached a second time and again a similar recovery was measured, indicating exchange of CENP-N at the binding site. Experimental error was ± 0.10. (**C**) Mean values of 5–20 experiments were blotted for early, middle and late S phase and G2. Partial recovery of the fluorescence intensity relative to the prebleach intensity (RFI) was observed for EGFP–CENP-N in early S phase, but there was hardly any recovery during 300 seconds in middle and late S phase and during 100 seconds in G2 (see A). Experimental error was ± 0.02. (**D**) Very slow FRAP recovery ($t_{1/2}$=38 minutes) of 45% EGFP–CENP-N was observed during 4 hours in the second half of S phase. Experimental error was ± 0.06. (**E**) Diffusion of CENP-N measured by RICS. Mobility coefficient values of EGFP–CENP-N at early, middle and late S phase as well as in mitosis were measured in the cytoplasm (blue), nucleoplasm (green) and at kinetochores (red). CENP-N was strongly immobilised at kinetochores. (**F**) The CENP-N mutant EGFP–CENP-NΔC, lacking the C-terminal domain, showed fast exchange and strong recovery in middle S phase.

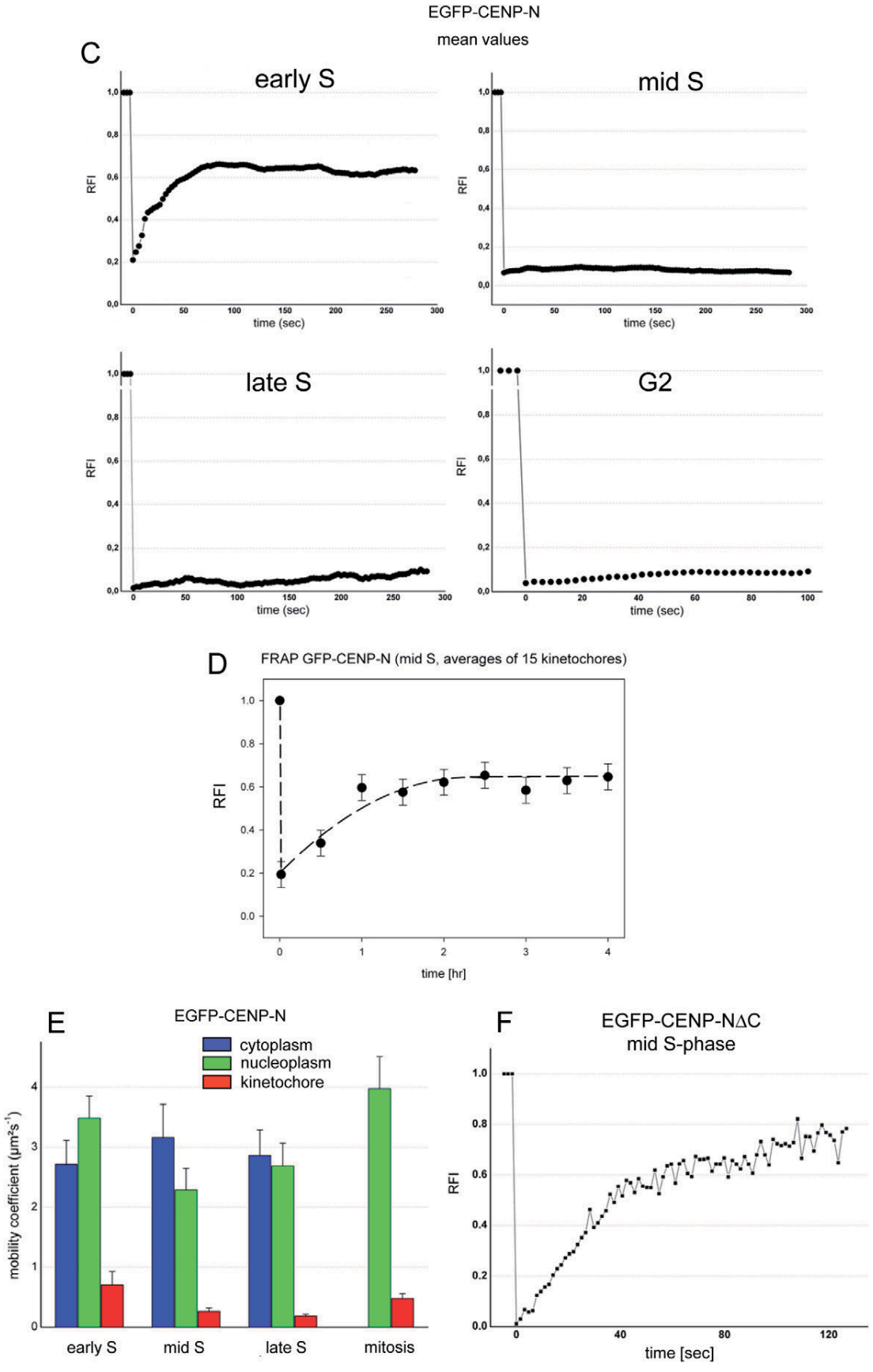

Fig. 5. See previous page for legend.

(Fig. 5A,B). This indicates that CENP-N, loaded in G1 or early S phase, is not irreversibly bound but can dissociate from the complex and rebind. In contrast to this behaviour of CENP-N, we previously observed irreversible 'loading-only' binding of CENP-A and CENP-I to the kinetochore (Hemmerich et al., 2008). In middle and late S phase, we observed a very low (0–7%) EGFP–CENP-N fluorescence recovery after photobleaching within 200 seconds (see Fig. 5C), as in G2 within 100 seconds (see Fig. 5A,C). Analysing EGFP–CENP-N fluorescence recovery over a much longer time period, now over 4 hours, in the second half of S phase, we found slow assembly of CENP-N at kinetochores with $t_{1/2}=38\pm7$ minutes and a recovery fluorescence intensity increase of $45\pm6\%$ (see Fig. 5D). These FRAP data confirm our SNAP-tag results.

RICS

To verify CENP-N binding to kinetochores and its mobility in other cellular compartments, we used raster image correlation spectroscopy (RICS) (Digman et al., 2005) to measure the diffusion of EGFP–CENP-N in the cell cytoplasm, nucleoplasm and at kinetochores (Fig. 5E). Whereas in fluorescence correlation spectroscopy (FCS) experiments the protein mobility is measured in a single confocal volume in the cell, in RICS this FCS experiment is repeated many times with the confocal volume scanning a confocal plane in the cell. In S phase, CENP-N showed a mobility coefficient of about 3 μm^2/second in the cytoplasm as well as in the nucleoplasm (Fig. 5E), which was comparable to the diffusion properties of CENP-H and CENP-I (Hemmerich et al., 2008). During mitosis, in the cellular plasma the mobility coefficient increases to about 4 μm^2/second. At kinetochores, we observed a mobility of up to one order of magnitude slower (see Fig. 5E). At kinetochores during S phase, the CENP-N mobility coefficient decreases from 0.7 ± 0.2 μm^2/second (early S phase) to 0.2 μm^2/second (late S phase) and increases again to 0.5 μm^2/second in mitosis (Fig. 5E). Low residual mobility of 0.2 μm^2/second was also observed for other CCAN proteins like CENP-T (unpublished observations). The dynamic RICS data support our FRAP results and confirm stable kinetochore attachment of CENP-N, in particular during late S phase.

CENP-NΔC mutant

Previous in vitro experiments have shown that the CENP-NΔC mutant still binds to the CENP-A nucleosomes, although binding is reduced in vivo (Carroll et al., 2009). This in vivo result was suggested to be due to additional interactions of wild-type CENP-N with CCAN subunits. We thus tested in vivo whether the C-terminal region contributes to the initial CENP-N binding in early S phase or to the stable retention in middle S phase. We analysed by FRAP the kinetochore binding of CENP-NΔC in middle S phase (when the wild-type protein shows no fast exchange). We found that CENP-NΔC exchanges fast ($t_{1/2}=23\pm2$ seconds; within experimental error this is the same time constant as wild-type CENP-N in early S phase) with a high mobile fraction (70%; see Fig. 5F). These data show that in S phase the C-terminal region mediates stable CENP-N binding to kinetochores. This is presumably due to interactions with one or more other CCAN subunit(s). The best candidate is CENP-L, which interacts with CENP-N in a C-terminal region-dependent manner in vitro (Carroll et al., 2009) as well as in mitotic *Xenopus* egg extracts (unpublished observations). The highly mobile binding of CENP-NΔC to the CENP-A-containing centromeric chromatin can explain why CENP-NΔC binding to CENP-A nucleosomes could not be detected by co-immunoprecipitation (Carroll et al., 2009). The CENP-N mutants R11A and R196A displayed reduced CENP-A nucleosome binding and inefficiently localise to kinetochores (Carroll et al., 2009). We found their kinetochore binding too low for quantitative FRAP measurements.

In conclusion, our data show that CENP-N binds to kinetochores by rapid exchange during G1 and early S phase, but is stably associated with kinetochores during the remainder of S phase and G2. During the second half of S phase, CENP-N is loaded to kinetochores more than 100 times slower than the fast exchange in early S phase. CENP-N gradually dissociates from kinetochores during G2.

Discussion

The central CENP-A targeting domain (CATD) confers nucleosomal rigidity to CENP-A-containing nucleosomes at the centromere (Black et al., 2007b; Sekulic et al., 2010), providing a unique structure distinguishing it from H3-containing nucleosomes. This structural difference is recognised by the N-terminal region of CENP-N because CENP-N binds to CENP-A-containing nucleosomes but not to H3-containing nucleosomes in vitro (Carroll et al., 2009; Sekulic and Black, 2009). Here, we show by in vivo FRET that the N-terminal region of CENP-N is indeed in close proximity to the N-terminal region of CENP-A, confirming this interaction in living human cells. Our data further show that CENP-N binds to the kinetochore in a dynamic and complex cell cycle-dependent manner as, to a large extent, CENP-N is recruited to the kinetochore during S phase and then leaves the complex in G2. These data suggest a dynamic CCAN network, as opposed to a pure structural scaffold at the kinetochores. They are also consistent with recent data on the mitotic population of the CCAN subunit CENP-I, which rapidly switches between two sister-kinetochores during metaphase, as kinetochore–microtubules change from a growing to a shrinking phase (Amaro et al., 2010). The CENP-N properties described here might be unique, but alternatively might well be shared by other CCAN proteins.

We observed two- to threefold amounts of CENP-N in the cell in S phase compared with G1 or mitosis, while CENP-N binding to kinetochores increases fivefold from G1 to late S phase. Then, CENP-N levels gradually decrease during G2 to reach low values at M phase (Fig. 6A), confirming previous initial results (McClelland et al., 2007). We postulate that CENP-N accumulation at kinetochores during S phase is driven by increasing CENP-N levels in the cell, potentially supported by post-translational modification. However, western-blot analysis showed no indications for a modification of CENP-N. When cells are arrested in mitosis by nocodazole treatment, CENP-N shows reduced electrophoretic mobility, indicating a potential phosphorylation event. This modification is, however, due to the nocodazole treatment because it is not detected when the cells are synchronised by a double-thymidine block.

Stable CENP-N kinetochore association during middle and late S phase seems to be regulated by binding of one or more CCAN protein(s), probably CENP-L, to the CENP-N C-terminal region. During S phase, one or more CCAN proteins might contribute to the changes in CENP-N dynamics by increasing their cellular levels or by post-translational modification. During G2, CENP-N dissociates from the kinetochores, potentially due to a dual mechanism involving both protein turnover and some other regulatory mechanism, to alter the dynamics of association.

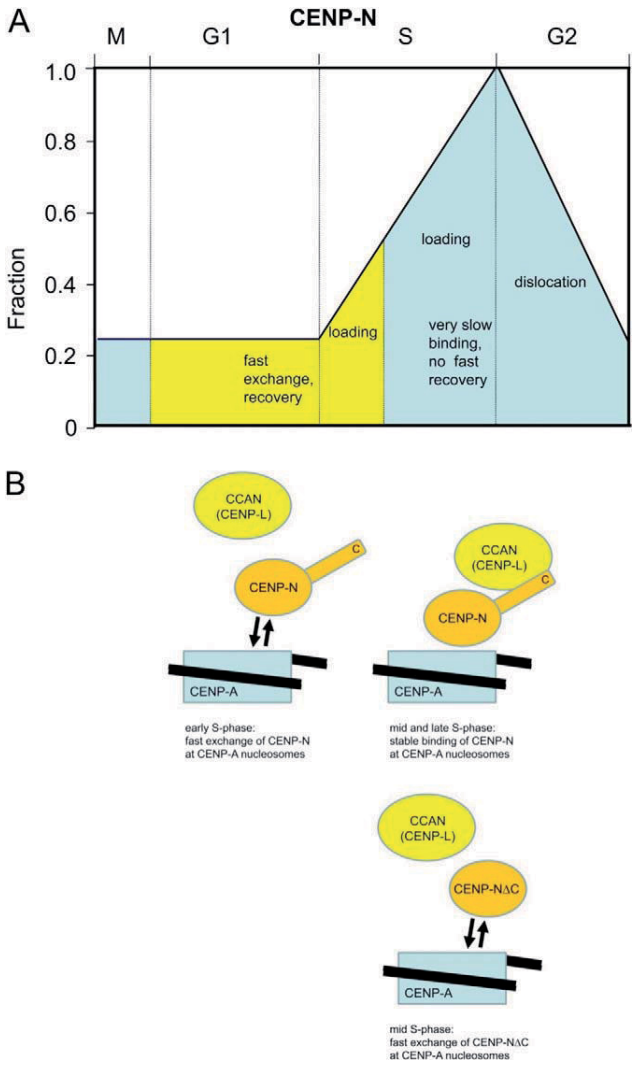

Fig. 6. Scheme of cell cycle-dependent CENP-N levels and its dynamic binding to kinetochores. (**A**) CENP-N is present at kinetochores at low levels (about 20%) during mitosis and G1. CENP-N exchanges fast at kinetochores during G1 and early S (yellow) and binds there stably during middle and late S phase with very slow loading (blue), probably due to CENP-L binding to the CENP-N C-terminus. CENP-N continuously dislocates from kinetochores during G2. (**B**) CENP-N binds to CENP-A-containing nucleosomes by fast exchange during early S phase (top left). In middle and late S phase (top right), CENP-N is stably bound due to an interaction of its C-terminus with a CCAN protein, probably CENP-L. Below: The C-terminal deletion mutant CENP-NΔC cannot be bound and fixed by CCAN (CENP-L). Accordingly, CENP-NΔC shows fast exchange also in middle S phase, with the same time constant as wild-type CENP-N in early S phase, and high recovery. A quantitative computer model is consistent with this interpretation (Bashar Ibrahim, Mathematics and Computer Science, FSU, Ernst-Abbe-Platz 1-3, 07743 Jena, Germany, personal communication; various assumptions of this model have to be verified experimentally).

CENP-N is degraded during G2 (Fig. 3C), therefore if CENP-N falls off the CENP-A-containing nucleosome it will not be replaced from the cytosolic pool, followed by degradation of released CENP-N. Reduction of CENP-N during G2 is not due to decreasing levels of CENP-A because we found constant levels of CENP-A at kinetochores during S phase and G2 (Fig. 3D). It remains unclear what initiates CENP-N synthesis at the G1–S transition and its degradation at the end of S phase.

We detected CENP-N loading to kinetochores during G1 and S phase. We observed fast exchange during G1 and early S phase but slow loading in the second half of S phase. This slow loading dynamics of CENP-N corresponds quantitatively to the slow loading of CENP-T and CENP-W during second half of S phase (Prendergast et al., 2011). Our dynamics data clearly show that the CENP-N C-terminal region contributes considerably to the CENP-N binding stability in vivo, probably by binding to CENP-L (Fig. 6B) because both proteins interact in vitro (Carroll et al., 2009) and in *Xenopus* egg extracts (unpublished observations). The observed CENP-N binding dynamics differ from those of CENP-A, CENP-B, CENP-C, CENP-H and CENP-I (Hemmerich et al., 2008), suggesting a different functional role for CENP-N. Centromeric DNA is preferentially replicated during middle and late S phase with only few centromeres being replicated during early S phase (Shelby et al., 2000; Weidtkamp-Peters et al., 2006; Wu et al., 2006). Because major parts of CENP-N are loaded to kinetochores during S phase, we speculate that CENP-N, together with its binding partner of the CCAN complex, might have a role in securing functional centromeric chromatin structure through replication. As CENP-A nucleosomes are redistributed to both sister kinetochores, CENP-N as being part of the CCAN protein complex, might ensure that CENP-A remains associated with the centromeric DNA. Depletion of CENP-N led to kinetochore assembly defects and resulted in reduced assembly of nascent CENP-A into centromeric chromatin (Foltz et al., 2006; Carroll et al., 2009). In the absence of CENP-N, replicated centromeric chromatin might be unable to correctly assemble as required for mitosis, resulting in chromosome segregation defects and potentially also in incorrect loading of CENP-A in telophase and early G1. We thus speculate that CENP-N might be a fidelity factor for the kinetochore complex during centromeric replication. The *Saccharomyces cerevisiae* orthologue of CENP-N, Chl4p (Meraldi et al., 2006), seems to have a similar role as fidelity factor: although *CHL4* is non-essential in budding yeast, *CHL4* depletion becomes essential for kinetochore assembly under conditions in which the kinetochore has been disrupted by a transient strong transcriptional activity (Mythreye and Bloom, 2003). This could suggest an evolutionary conserved role of CENP-N^{Chl4} as kinetochore fidelity factor.

Materials and Methods

Plasmids

For the expression of human CENP-A fused to the C-terminus of mCherry, the required plasmid was constructed from the vector pCerulean-C1–CENP-A (Orthaus et al., 2008). This vector was digested with AgeI-BsrGI. Into the resulting purified 4.433 bp fragment, we ligated a 713 bp AgeI-BsrGI fragment resulting from the vector pmCherry-C1 (Orthaus et al., 2009). For expressing human CENP-N fused to the C-terminus of EGFP, we used vector pH-G–CENP-N (Hellwig et al., 2009). All clones were verified by sequencing (MWG Biotech, Ebersberg, Germany). Full-length protein expression of the fusion constructs was confirmed by western blots. Under the control of the SV-40 promoter, *CENPA* was introduced at the 3′-end (yielding the fusion SNAP-tag–CENP-A) and *CENPN* at the 5′-end of the SNAP-tag gene (yielding the fusion CENP-N–SNAP-tag). Complementary DNAs were amplified from already existing constructs by PCR. Correct cloning of the obtained plasmids was verified by restriction analysis.

Cell culture, transfection, siRNA treatments and western blots

HeLa E1 and HEp-2 cells were cultured (McAinsh et al., 2006) and western blots were carried out as described recently (Orthaus et al., 2008). In order to determine cell cycle-dependent CENP-N levels, double-thymidine block synchronised HEp-2 cells were treated as above. Aliquots of equal cell numbers were taken after 3, 7, 9 and 12 hours after release and lysed. The aliquots were analysed by western

blotting. In the blot, CENP-N was identified by the CENP-N-specific antibody, and CENP-N amounts quantified by the ODYSSEY Infrared Imaging System (LiCor, Lincoln, NE) following the protocol of the manufacturer.

Immunofluorescence

For indirect immunofluorescence detection, HEp-2 cells (from the DSMZ, Braunschweig, Germany) were fixed with 3% paraformaldehyde in PBS for 15 minutes, permeabilised with 0.5% Triton X-100 in PBS for 10 minutes and blocked with 3% bovine serum albumin (BSA) in PBS. Primary antibodies were diluted as follows in PBS and 3% BSA: anti-CENP-N (McClelland et al., 2007) 1:1000; anti-CENP-A antibodies (Abcam, Cambridge, UK) 1:500. Anti-CENP-N antibodies were detected with fluorescently labelled goat anti-rabbit antibodies (Cy3 anti-rabbit, Dianova, Hamburg, Germany) at a dilution of 1:400. For live cell measurements, HEp-2 cells were co-transfected with EGFP–CENP-N and mRFP–CENP-A or mRFP–PCNA. Cell cycle phases were identified via the localisation pattern of mRFP–PCNA (Hemmerich et al., 2008), CENP-F localisation or DAPI staining identifying morphological characteristics of the cells. Fluorophores were stimulated with 561 nm argon laser line with low intensity and signals were detected via a 575 nm long path filter. 3D image stacks were acquired in 0.2 µm steps using a 63× oil NA 1.4 objective on a Zeiss LSM 510 microscope (Carl Zeiss, Jena, Germany). The 3D image stacks were quantitatively analysed using Metamorph (Molecular Devices, Sunnyvale, CA).

SNAP-tag analysis

Cells were grown in DMEM supplemented with 10% FCS and PS (100 units/ml penicillin G, 100 µg/ml strepdavidin). One day before transfecting, 100–200 µl of the cells from the confluent 10 cm dish were added to a coverslip in a six-well plate containing MEM (10% FCS and PS). For transfections, 3 µl Fugene6 (Invitrogen, Carlsbad, CA) was added to 100 µl OPTIMEM and incubated for 5 minutes. The mixture was then added dropwise to 1 µg DNA and incubated for 30 minutes. Then, it was added to one well of the six-well plate containing 2 ml of MEM (10% FCS and PS). The coverslips with the transfected cells were transferred to parafilm in a 10 cm dish and 150 µl of MEM (10% FCS and PS) containing 2 µM TMR-star was added. After 30 minutes incubation at 37℃, the coverslips were washed twice in prewarmed MEM (10% FCS and PS) and incubated in fresh media for 30 minutes at 37℃. For quenching the SNAP-tag with BTP, the same protocol was performed but the media was supplemented with 10 µM BTP instead of TMR-star.

The media in the six-well dishes was removed, 2 ml PTEMF buffer (0.2% Triton, 20 mM PIPES pH 6.8, 1 mM $MgCl_2$, 10 mM EGTA, 4% formaldehyde) was added and incubated for 10 minutes. After washing three times with 1× PBS, 2 ml blocking buffer (500 ml 1× PBS, 15 g BSA, 0.02% w/v NaN_3) was added and incubated for 30 minutes. After washing three times with 1× PBS, the coverslips were placed on parafilm and antibodies were added in the appropriate dilutions (1:2000 for anti-CENP-A and anti-CENP-N) in 200 µl blocking buffer and incubated for 1 hour. After washing three times with 1× PBS, secondary antibodies (anti-mouse or anti-rabbit Alexa Fluor 488- or Alexa Fluor 647-conjugated) were added in 1:400 dilutions in 210 µl blocking buffer and incubated for 30 minutes. The coverslips were then placed on a microscope slide containing a drop of Vectashield (Vector Laboratories, Servion, Switzerland) supplemented with DAPI and fixed with nail polish.

3D image stacks were acquired in 0.5 µm steps on a Leica DMI 6000B microinjection microscope (Leica, Wetzlar, Germany) equipped with a Leica EL6000 metal halide light source, a 63× oil NA 1.4–0.6 objective, a DAPI-EGFP-Rhod-Cy5 filter set and a Hamamatsu high resolution digital camera (ORCA-HR). All images shown are maximum intensity projections of deconvolved 3D image stacks using the software Slidebook (Intelligent Imaging Innovations, Denver, CO). Maximum intensity projections were processed using the software Adobe Photoshop.

Fluorescence recovery after photobleaching

Fluorescence recovery after photobleaching (FRAP) experiments were carried out on a Zeiss LSM 510Meta confocal microscope (Carl Zeiss, Jena, Germany) using a C-Apochromat infinity-corrected 1.2 NA 63× water objective and the 488 nm laser line for GFP. Five or ten images were taken before the bleach pulse and 50–200 images after bleaching of two to four kinetochores of a nucleus, with an image acquisition frequency of 0.5–1.0 frames per second at 1% laser transmission to avoid additional bleaching. In long-term FRAP experiments, the pinhole was adjusted to 1 airy unit and image stacks were taken every 30 minutes. Relative fluorescence intensities were quantified according to previously described methods (Chen and Huang, 2001; Schmiedeberg et al., 2004) using Microsoft Excel and Origin (OriginLab, Northampton, MA) software.

Cell cycle synchronisation

For cell cycle-dependent analysis, HEp-2 cells were reversibly arrested via double-thymidine treatment at the initiation of early S phase. In some experiments, HeLa and U2OS cells were synchronised by double-thymidine and aphidicolin block, in other cases by nocodazole treatment. The cells were seeded with a density of about 50–60%. After attachment to reaction vessel, cells were blocked with a final concentration of 5 mM thymidine for 16 hours. Cells were released and grown in fresh media for 10 hours, followed by a second cell cycle block with 5 mM thymidine. After 16 hours, cells were washed and cultured in fresh media. To investigate the cell cycle-dependent behaviour of CENP-N, every 90 minutes for 9 hours cells were harvested and used for further steps of different procedures. Cells were fixed, labelled with antibodies, and the fluorescence intensity at kinetochores measured until mitotic cells were observed.

Raster image correlation spectroscopy

Raster image correlation spectroscopy (RICS) (Digman et al., 2005) experiments were accomplished on a Zeiss LSM 710 confocal microscope (Carl Zeiss, Jena, Germany) using a C-apochromat infinity-corrected 1.2 W 40× water objective and the 488 nm laser line for EGFP–CENP-N. Time series of 50 pictures were recorded with an image acquisition frequency of 1 frame per 3.9 seconds at low laser intensity. During the measurement, the pinhole was adjusted to a diameter of 40 µm. The emission of EGFP fluorophores was detected through a 505–550 nm band path filter. For evaluation of the data, the LSM-RICS software (Zeiss, Jena, Germany) was used, yielding the diffusion coefficients of the moving fluorescent particles (Digman et al., 2005).

Acceptor photobleaching-based FRET measurements

When FRET occurs, both the intensity and lifetime of the donor fluorescence decrease whereas the intensity of the acceptor emission increases. Here, the FRET pair EGFP–mCherry was used. FRET experiments were conducted as described (Orthaus et al. 2008; Orthaus et al., 2009). If the orientation of the fluorophore dipole moment of the acceptor relative to that of the donor were known, or if at least one of them rotated freely faster than nanoseconds, a more detailed distance between donor and acceptor could be deduced from the measured FRET efficiency (E_{FRET}) values. In our live cell experiments, however, this information was not available to us. We therefore could not deduce defined distance values but interpreted the appearance of FRET as an indication that donor and acceptor chromophores are close to one another within 10 nm.

FLIM-based FRET measurements

Experiments were carried out as described (Orthaus et al., 2009). In short, the donor fluorescence lifetime was determined by time-correlated single photon counting (TCSPC) in living human HEp-2 cells. To calculate the fluorescence lifetime, the SymPhoTime software package (v4.7, Picoquant, Berlin, Germany) was used. Selected areas of the images corresponding to single kinetochores were fitted by a maximum likelihood estimation (MLE). Depending on the quality of a fit indicated by the value of χ^2, a mono- or bi-exponential fitting model including background was applied. In this way, the presence of scattered light in a few measurements could be identified and separated. However, due to low photon numbers and similar time constants, the simultaneous presence of two different donor fluorescence lifetimes for complexes with donor-only and donor-plus-acceptor in one kinetochore could not be separated by a bi-exponential fit.

RNA preparation and RT-PCR

Human HEp-2 cells were synchronised by a double-thymidine block, harvested in time intervals of 90 minutes, centrifuged and frozen in liquid nitrogen. Pellets were resuspended in 1 ml RNApure (Peqlab, Göttingen, Germany), then 200 ml chloroform was added and the mixture was vortexed. The homogenous solution was incubated at 4℃ for 5 minutes, then centrifuged at 22℃ for 15 minutes at 13,400 ***g***. The upper phase was separated, the same volume of 2-propanol and 2 µl glycogen added, the solution mixed and incubated at 4℃ for 10 minutes followed by centrifugation at 22℃ for 10 minutes at 13,400 ***g***. The supernatant was removed, 1 ml of 70% ethanol added and the solution centrifuged at 22℃ for 5 minutes at 5200 ***g***. The supernatant was removed, the pellet air dried at 22℃ and resuspended in 100 µl nuclease-free water. RNA content and purity was determined using the Nanodrop (Peqlab, Göttingen, Germany). The solution was stored at −80℃. For RNA amplification, the following primers were used: β-actin forward 5′-CATCATGAAGTGTGAACGTGGAC-3′, reverse 5′-AGCATTTGC-GGTGGACGATG-3′; CENP-N forward 5′-CAACTCTACGACACCTCTACAG-3′, reverse 5′-TGCTAAGGATTTCAATGCTTCCAG-3′. These primers amplify fragments of about 300 bp at the 3′ end of the genes. Quantitative RT-PCR was performed with a SYBR Green Kit (Eurogentec, Liege, Belgium) according to the protocols of the manufacturer. For each reaction, 100 ng template RNA was used. Data were acquired using the Applied Biosystems 7300 Real Time PCR Light Cycler (Applied Biosystems, Foster City, CA) with temperature cycles as suggested by the manufacturer, and analysed with the 7300 Real Time PCR System Sequence Detection software, version 1.2.3 (Applied Biosystems).

Acknowledgement

We thank Nikolaj Klocker (University of Freiburg, Freiburg, Germany), Daniel Foltz (University of Virginia, Charlottesville, VA)

and Iain Cheeseman (Whitehead Institute for Biomedical Research, Cambridge, MA) for the kind gift of plasmids. We acknowledge the expert technical support by S. Pfeiffer, M. Koch and S. Ohndorf.

Funding

This work was funded by the Marie Curie Cancer Care program; the Deutsche Forschungsgemeinschaft (DFG) [grant numbers SPP1128, SPP 1395/2]; the National Institutes of Health (NIH) [grant number GM074728 to A.F.S.]; and the Thueringer Aufbaubank [grant number 2007 FE 9011]. We thank the Swiss SNF for a Foerderungs-Professur [for P.M.]. Deposited in PMC for release after 12 months.

References

Amano, M., Suzuki, A., Hori, T., Backer, C., Okawa, K., Cheeseman, I. M. and Fukagawa, T. (2009). The CENP-S complex is essential for the stable assembly of outer kinetochore structure. *J. Cell Biol.* **186**, 173-182.

Amaro, A. C., Samora, C. P., Holtackers, R., Wang, E., Kingston, I. J., Alonso, M., Lampson, M., McAinsh, A. D. and Meraldi, P. (2010). Molecular control of kinetochore-mircotuble dynamics and chromosome oscillations. *Nat. Cell Biol.* **12**, 319-329.

Black, B. E., Jansen, L. E. T., Maddox, P. S., Foltz, D. R., Desai, A. B., Shah, J. V. and Cleveland, D. W. (2007a). Centromere identity maintained by nucleosomes assembled with histone H3 containing the CENP-A targeting domain. *Mol. Cell* **25**, 309-322.

Black, B. E., Brock, M. A., Bedard, S., Woods, V. L. and Cleveland, D. W. (2007b). An epigenetic mark generated by the incorporation of CENP-A into centromeric nucleosomes. *Proc. Natl. Acad. Sci. USA* **104**, 5008-5013.

Carroll, C. W., Silva, M. C. C., Godek, K. M., Jansen, L. E. T. and Straight, A. F. (2009). Centromere assembly requires the direct recognition of CENP-A nucleosomes by CENP-N. *Nat. Cell Biol.* **11**, 896-902.

Carroll, C. W., Milks, K. J. and Straight, A. F. (2010). Dual recognition of CENP-A nucleosomes is required for centromere assembly. *J. Cell Biol.* **189**, 1143-1155.

Cheeseman, I. M. and Desai, A. (2008). Molecular architecture of the kinetochore-microtubule interface. *Nat. Rev. Mol. Cell Biol.* **9**, 33-46.

Cheeseman, I. M., Niessen, S., Anderson, S., Hyndman, F., Yates, J. R., 3rd, Oegema, K. and Desai, A. (2004). A conserved protein network controls assembly of the outer kinetochore and its ability to sustain tension. *Genes Dev.* **18**, 2255-2268.

Cheeseman, I. M., Chappie, J. S., Wilson-Kubalek, E. M. and Desai, A. (2006). The conserved KMN network constitutes the core microtubule-binding site of the kinetochore. *Cell* **127**, 983-997.

Chen, D. and Huang, S. (2001). Nucleolar components involved in ribosome biogenesis cycle between the nucleolus and nucleoplasm in interphase cells. *J. Cell Biol.* **153**, 169-176.

Cho, U. S. and Harrison, S. C. (2011). Recognition of the centromere-specific histone Cse4 by the chaperone Scm3. *Proc. Natl. Acad. Sci. USA* **108**, 9367-9371.

Dalal, Y., Furuyama, T., Vermaak, D. and Henikoff, S. (2007). Structure, dynamics and evolution of centromeric nucleosomes. *Proc. Natl. Acad. Sci. USA* **104**, 15974-15981.

Dechassa, M. L., Wyns, K., Li, M., Hall, M. A., Wang, M. D. and Luger, K. (2011). Structure and Scm3-mediated assembly of budding yeast centromeric nucleosomes. *Nat. Commun.* **2**, 313.

De Wulf, P., McAinsh, A. D. and Sorger, P. K. (2003). Hierarchical assembly of the budding yeast kinetochore from multiple subcomplexes. *Genes Dev.* **17**, 2902-2921.

Digman, M. A., Brown, C. M., Sengupta, P., Wiseman, P. W., Horwitz, A. R. and Gratton, E. (2005). Measuring fast dynamics in solutions and cells with a laser scanning microscope **89**, 1317-1327.

Dimitriadis, E. K., Weber, C., Gill, R. K., Diekmann, S. and Dalal, Y. (2010). Tetrameric organization of vertebrate centromeric nucleosomes. *Proc. Natl. Acad. Sci. USA* **107**, 20317-20322.

Foltz, D. R., Jansen, L. E. T., Black, B. E., Bailey, A. O., Yates, J. R., 3rd and Cleveland, D. W. (2006). The human CENP-A centromeric complex. *Nat. Cell Biol.* **8**, 458-469.

Fukagawa, T., Mikami, Y., Nishihashi, A., Regnier, V., Haraguchi, T., Hiraoka, Y., Sugata, N., Todokoro, K., Brown, W. and Ikemura, T. (2001). CENP-H, a constitutive centromere component, is required for centromere targeting of CENP-C in vertrebrate cells. *EMBO J.* **20**, 4603-4617.

Furuyama, T. and Henikoff, S. (2009). Centromeric nucleosomes induce positive DNA supercoils. Cell **138**, 104-113.

Hellwig, D., Hoischen, C., Ulbricht, T. and Diekmann, S. (2009). Acceptor-photobleaching FRET analysis of core kinetochore and NAC proteins in living human cells. *Eur. Biophys. J.* **38**, 781-791.

Hemmerich, P., Weidtkamp-Peters, S., Hoischen, C., Schmiedeberg, L., Erliandri, I. and Diekmann, S. (2008). Dynamics of inner kinetochore assembly and maintenance in living cells. *J. Cell Biol.* **180**, 1101-1114.

Hori, T., Amano, M., Suzuki, A., Backer, C. B., Welburn, J. P., Dong, Y., McEwan, B. F., Shang, W.-H., Suzuki, E., Okawa, K. et al. (2008a). CCAN makes multiple contacts with centromeric DNA to provide distinct pathways to the outer kinetochore. *Cell* **135**, 1039-1052.

Hori, T., Okada, M., Maenaka, K. and Fukagawa, T. (2008b). CENP-O class proteins form a stable complex and are required for proper kinetochore function. *Mol. Biol. Cell* **19**, 843-854.

Hu, H., Liu, Y., Wang, M., Fang, J., Huang, H., Yang, N., Li, Y., Wang, J., Yao, X., Shi, Y., Li, G. and Xu, R. M. (2011). Structure of a CENP-A-histone H4 heterodimer in complex with chaperone HJURP. *Genes Dev.* **25**, 901-906.

Jansen, L. E. T., Black, B. E., Foltz, D. R. and Cleveland, D. W. (2007). Propagation of centromeric chromatin requires exit from mitosis. *J. Cell Biol.* **176**, 795-805.

Keppler, A., Gendreizig, S., Gronemeyer, T., Pick, H., Vogel, H. and Johansson, K. (2003). A general method for the covalent labelling of fusion proteins with small molecules in vivo. *Nat. Biotechnol.* **21**, 86-89.

Liao, H., Winkfein, R. J., Mack, G., Rattner, J. B. and Yen, T. J. (1995). CENP-F is a protein of the nuclear matrix that assembles onto kinetochores at late G2 and is rapidly degraded after mitosis. *J. Cell Biol.* **130**, 507-518.

Liu, X., McLeod, I., Anderson, S., Yates, J. R., 3rd and He, X. (2005). Molecular analysis of kinetochore architecture in fission yeast. *EMBO J.* **24**, 2919-2930.

Madsen, P. and Celis, J. E. (1985). S-phase patterns of cyclin (PCNA) antigen staining resemble topographical patterns of DNA synthesis. A role for cyclin in DNA replication? *FEBS Lett.* **193**, 5-11.

McAinsh, A. D., Meraldi, P., Draviam, V. M., Toso, A. and Sorger, P. K. (2006). The human kinetochore proteins Nnf1R and Mcm21R are required for accurate chromosome segregation. *EMBO J.* **25**, 4033-4049.

McClelland, S. E., Borusu, S., Amaro, A. C., Winter, J. R., Belwal, M., McAinsh, A. D. and Meraldi, P. (2007). The CENP-A NAC/CAD kinetochore complex controls chromosome congression and spindle bipolarity. *EMBO J.* **26**, 5033-5047.

Meraldi, P., McAinsh, A. D., Rheinbay, E. and Sorger, P. K. (2006). Phylogenetic and structural analysis of centromeric DNA and kinetochore proteins. *Genome Biol.* **7**, R23.

Mythreye, K. and Bloom, K. S. (2003). Differential kinetochore protein requirements for establishment versus propagation of centromere activity in Saccharomyces cerevisiae. *J. Cell Biol.* **160**, 833-843.

Nekrasov, V. S., Smith, M. A., Peak-Chew, S. and Kilmartin, J. V. (2003). Interactions between centromere complexes in Saccharomyces cerevisiae. *Mol. Biol. Cell* **14**, 4931-4946.

Obuse, C., Yang, H., Nozaki, N., Goto, S., Okazaki, T. and Yoda, K. (2004). Proteomics analysis of the centromere complex from HeLa interphase cells: UV-damaged DNA binding protein 1 (DDB-1) is a component of the CEN-complex, while BMI-1 is transiently co-localised with the centromeric region in interphase. *Genes Cells* **9**, 105-120.

Okada, M., Cheeseman, I. M., Hori, T., Okawa, K., McLeod, I. X., Yates, J. R., 3rd, Desai, A. and Fukagawa, T. (2006). The CENP-H-I complex is required for the efficient incorporation of newly synthesized CENP-A into centromeres. *Nat. Cell Biol.* **8**, 446-457.

Orthaus, S., Biskup, C., Hoffmann, B., Hoischen, C., Ohndorf, S., Benndorf, K. and Diekmann, S. (2008). Assembly of the inner kinetochore proteins CENP-A and CENP-B in living human cells. *Chembiochem* **9**, 77-92.

Orthaus, S., Klement, K., Happel, N., Hoischen, C. and Diekmann, S. (2009). Linker Histone H1 is present in centromeric chromatin of living human cells next to inner kinetochore proteins. *Nucleic Acids Res.* **37**, 3391-3406.

Prendergast, L., van Vuuren, C., Kaczmarczyk, A., Doering, V., Hellwig, D., Quinn, N., Hoischen, C., Diekmann, S. and Sullivan, K. F. (2011). Premitotic assembly of human CENPs -T and -W switches centromeric chromatin to a mitotic state. *PLoS Biol.* **9**, e1001082.

Przewloka, M. R., Venkei, Z., Bolanos-Garcia, V. M., Debski, J., Dadlez, M. and Glover, D. M. (2011). CENP-C is a structural platform for kinetochore assembly. *Curr. Biol.* **21**, 399-405.

Santaguida, S. and Musacchio, A. (2009). The life and miracles of kinetochores. *EMBO J.* **28**, 2511-2531.

Schmiedeberg, L., Weisshart, K., Diekmann, S., Meyer Zu Hoerste, G. and Hemmerich, P. (2004). High- and low-mobility populations of HP1 in heterochromatin of mammalian cells. *Mol. Biol. Cell* **15**, 2819-2833.

Screpanti, E., De Antoni, A., Alushin, G. M., Petrovic, A., Melis, T., Nogales, E. and Musacchio, A. (2011). Direct binding of CENP-C to the Mis12 complex joins the inner and outer kinetochore. *Curr. Biol.* **21**, 391-398.

Sekulic, N. and Black, B. E. (2009). A reader for centrometric chromatin. *Nat. Cell Biol.* **11**, 793-795.

Sekulic, N., Bassett, E. A., Rogers, D. J. and Black, B. E. (2010). The structure of $(CENP\text{-}A\text{-}H4)_2$ reveals physical features that mark centromeres. *Nature* **467**, 347-351.

Shelby, R. D., Monier, K. and Sullivan, K. F. (2000). Chromatin assembly at kinetochores is uncoupled from DNA replication. *J. Cell Biol.* **151**, 1113-1118.

Somanathan, S., Suchyna, T. M., Siegel, A. J. and Berezney, R. (2001). Targeting of PCNA to sites of DNA replication in the mammalian cell nucleus. *J. Cell Biochem.* **81**, 56-67.

Sporbert, A., Domaing, P., Leonhardt, H. and Cardoso, M. C. (2005). PCNA acts as a stationary loading platform for transiently interacting Okazaki fragment maturation proteins. *Nucleic Acids Res.* **33**, 3521-3528.

Tanaka, T. U. and Desai, A. (2008). Kinetochore-microtubule interactions: the means to the end. *Curr. Opin. Cell Biol.* **20**, 53-63.

Toso, A., Winter, J. R., Garrod, A. J., Amaro, A. C., Meraldi, P. and McAinsh, A. D. (2009). Kinetochore-generated pushing forces separate centrosomes during bipolar spindle assembly. *J. Cell Biol.* **184**, 365-372.

Weidtkamp-Peters, S., Rahn, H. P., Cardoso, M. C. and Hemmerich, P. (2006). Replication of centromeric heterochromatin in mouse fibroblasts takes place in early, middle, and late S phase. *Histochem. Cell Biol.* **125**, 91-102.

Wu, R., Singh, P. B. and Gilbert, D. M. (2006). Uncoupling global and fine-tuning replication timing determinants for mouse pericentric heterochromatin. *J. Cell Biol.* **174**, 185-194.

Zhou, Z., Feng, H., Zhou, B. R., Ghirlando, R., Hu, K., Zwolak, A., Miller Jenkins, L. M., Xiao, H., Tjandra, N., Wu, C. et al. (2011). Structural basis for recognition of centromere histone variant CenH3 by the chaperone Scm3. *Nature* **472**, 234-237.

OPEN ACCESS Freely available online

Premitotic Assembly of Human CENPs -T and -W Switches Centromeric Chromatin to a Mitotic State

Lisa Prendergast[1], Chelly van Vuuren[1], Agnieszka Kaczmarczyk[1], Volker Doering[2], Daniela Hellwig[2], Nadine Quinn[1], Christian Hoischen[2], Stephan Diekmann[2], Kevin F. Sullivan[1]*

1 Centre for Chromosome Biology, School of Natural Sciences, National University of Ireland, Galway, Galway, Ireland, **2** Leibniz Institute for Age Research, Fritz Lipmann Institute, Jena, Germany

Abstract

Centromeres are differentiated chromatin domains, present once per chromosome, that direct segregation of the genome in mitosis and meiosis by specifying assembly of the kinetochore. They are distinct genetic loci in that their identity in most organisms is determined not by the DNA sequences they are associated with, but through specific chromatin composition and context. The core nucleosomal protein CENP-A/cenH3 plays a primary role in centromere determination in all species and directs assembly of a large complex of associated proteins in vertebrates. While CENP-A itself is stably transmitted from one generation to the next, the nature of the template for centromere replication and its relationship to kinetochore function are as yet poorly understood. Here, we investigate the assembly and inheritance of a histone fold complex of the centromere, the CENP-T/W complex, which is integrated with centromeric chromatin in association with canonical histone H3 nucleosomes. We have investigated the cell cycle regulation, timing of assembly, generational persistence, and requirement for function of CENPs -T and -W in the cell cycle in human cells. The CENP-T/W complex assembles through a dynamic exchange mechanism in late S-phase and G2, is required for mitosis in each cell cycle and does not persist across cell generations, properties reciprocal to those measured for CENP-A. We propose that the CENP-A and H3-CENP-T/W nucleosome components of the centromere are specialized for centromeric and kinetochore activities, respectively. Segregation of the assembly mechanisms for the two allows the cell to switch between chromatin configurations that reciprocally support the replication of the centromere and its conversion to a mitotic state on postreplicative chromatin.

Citation: Prendergast L, van Vuuren C, Kaczmarczyk A, Doering V, Hellwig D, et al. (2011) Premitotic Assembly of Human CENPs -T and -W Switches Centromeric Chromatin to a Mitotic State. PLoS Biol 9(6): e1001082. doi:10.1371/journal.pbio.1001082

Academic Editor: Don Cleveland, University of California at San Diego, United States of America

Received November 11, 2010; **Accepted** May 4, 2011; **Published** June 14, 2011

Funding: This work was supported by SFI grant 05/RP1/B793 to KFS (http://www.sfi.ie) and DFG grants to SD (Di 258/14-1, Di 258/17-1). CvV was supported by fellowships from the HRB and the Biochemistry Society. The funders had no role in study design, data collection and analysis, decision to publish, or preparation of the manuscript.

Competing Interests: The authors have declared that no competing interests exist.

Abbreviations: CCAN, constitutive centromere associated network; FRAP, fluorescence recovery after photobleaching; GFP, green fluorescent protein

* E-mail: kevin.sullivan@nuigalway.ie

Introduction

The centromere is the genetic locus present in a single copy on each eukaryotic chromosome that provides the transmission function of the genome across mitotic and meiotic generations [1,2]. An epigenetically determined locus, it functions by directing assembly of the kinetochore in mitosis and meiosis, a dynamic protein complex that possesses microtubule binding and motor activities as well as spindle assembly checkpoint complexes [3,4]. The centromere is unique in that, in almost all species, its identity is not deterministically related to the DNA sequence that underlies it [5,6]. This has been dramatically underscored by the discovery that certain centromeres of the genus *Equus* reside on unique sequence DNA [7,8]. Rather, centromere identity seems to be specified at the chromatin level, through a distinctive population of nucleosomes made with CENP-A or cenH3, a centromere-specific histone H3 variant found in all eukaryotes [9–12].

The composition and molecular organization of CENP-A nucleosomes and their mechanistic contribution to centromere determination in several organisms has been a subject of intensive investigation and debate [13,14]. Cse4, the CENP-A of budding yeast, has been reported to form classical octameric nucleosome core complexes with histones H4, H2A, and H2B [15], tetrameric half-nucleosomes [16], and other complexes [17]. Distinctive structural organization within a CENP-A:H4 tetrameric core [18], unusual mechanical rigidity of the nucleosome [19], and a right-handed winding of DNA, opposite that of conventional nucleosomes [20] have been proposed as critical molecular features that could be involved in maintenance of centromere identity. These features are thought to function, in part, to coordinate a specific, multistep chromatin assembly pathway that initiates in anaphase/telophase in human cells and continues throughout G1 [21–26]. However, CENP-A is unlikely to be the sole determinant of centromere identity, as misincorporation of CENP-A only rarely results in ectopic centromere formation [27,28].

A large group of additional proteins assemble on centromeric chromatin in pathways that are dependent on CENP-A and feed back to influence its assembly (interphase centromere complex [ICEN] [29]; CENP-A nucleosome associated complex, CENP-A distal complex [NAC/CAD] [30]; CENP-H/I complex [31]). Collectively known as the constitutive centromere associated network (CCAN) [32], functional examination of the role of these proteins in vertebrate centromere propagation and kinetochore formation has revealed a complex network of interdependent

Author Summary

The centromere is a strange locus that derives its identity from the proteins that shape it rather than the DNA sequences it contains. It also functions in a remarkably singular way, providing a motor and command control center for the chromosome in conjunction with the kinetochore. Key to centromere identity is the chromatin that comprises it, which has a unique nucleosomal "bead on a string" including a special centromeric histone H3, called CENP-A. Found in alternating clusters of nucleosomes with "regular" histone H3, CENP-A is crucial for propagating centromere identity as well as for regulating kinetochore function. In this study, we have analysed the cell cycle dynamics of CENP-T and CENP-W, another two components of the constitutive centromere associated network. We show that, unlike CENP-A, CENP-T/W are not inherited stringently by daughter cells. Instead, these complexes - which are bound to the interstitial "regular" H3 nucleosome domains - assemble after DNA replication and are required for kinetochore formation. Thus, we propose that a stable CENP-A nucleosome population plays a role in centromere locus inheritance to daughter cells, while dynamic CENP-T/W and H3 nucleosomes provide a cycling function that triggers kinetochore assembly as cells enter mitosis in each new cell cycle.

activities [30,31,33,34]. Several members of the CCAN, including CENPs -C, -H, -I, and -N play a role in CENP-A deposition or maintanence. CENPs -C and -N interact directly with CENP-A nucleosomes and may function specifically in a CENP-A assembly pathway [31,35,36]. A role for chromatin context is revealed by the finding that CENP-B contributes to de novo centromere formation by influencing histone modifications [37]. Artificial chromatin modification with tet repressor fusion proteins can modify kinetochore function in vertebrates, revealing a role for histone H3K4 methylation in HJURP recruitment and CENP-A assembly [38,39]. The question remains, though, as to whether CENP-A nucleosomes in a proper context are sufficient to "carry the mark" for chromatin-based inheritance. A marker-based model suggests that specific molecules are stably transmitted through DNA replication, which then act as a template for the assembly of the centromere on daughter chromosomes, comparable to the semi-conservative replication of DNA [40]. Alternatively, centromere identity could depend on dynamic mechanisms in which populations of molecules regenerate the centromere in each cell cycle through a self-organization process [41]. Distinguishing the relative contribution of these types of mechanisms is critical for understanding the physical basis of chromatin-directed inheritance.

The CENP-A nucleosome is capable of multigenerational inheritance [22]. Within the CCAN/ICEN/NAC-CAD are four additional histone fold containing proteins, CENPs -T and -W, and CENPs-S and -X [30,31,42]. CENPs -T and -W are themselves tightly associated with a population of histone H3-containing nucleosomes within centromeric chromatin [32]. CENP-T was initially identified as a component of the CENP-A nucleosome associated complex (NAC), constitutively localised to the centromere during the cell cycle [30]. Reduction of levels of CENPs -T, -M, and -N disrupted the recruitment of other NAC components and also retarded progression through mitosis. FRET studies have shown that the *N* terminus of CENP-T is associated with the *N* termini of CENP-A and CENP-B [43]. Purification of complexes containing CENP-T from chicken DT40 cells identified an 11-kDa protein, CENP-W, previously identified as CUG2, as a constitutive centromere component associated with CENP-T, while a reciprocal approach in human cells also identified CENP-T as a CUG2 interactor [32,44]. The CENP-T/W complex has been shown to bind specifically to histone H3 nucleosomes and its depletion results in loss of most CCAN components, suggesting that it plays a key role in kinetochore assembly [32].

The CENP-T/W complex plays a critical role in mitosis [30,32]. As a histone fold complex, it has the potential to interact stably with DNA or nucleosomes and could, in principle, play a role in propagating centromere identity through a template-based mechanism. In order to ask whether CENPs -T or -W exhibit stable binding and transmission through mitosis, we have examined the timing and mechanisms of their assembly, their heritability at centromeres, and the requirements for their function within the HeLa cell cycle. Our results indicate that the complex is not stably associated with centromeres over multiple generations. Rather, CENPs -T and -W exhibit a pattern of assembly and function reciprocal to that of CENP-A, suggesting a differentiation of function within the centromeric chromatin fiber, with a degree of separation between centromeric and kinetochore-related activities.

Results

Cell Cycle Regulation of CENPs -T and -W

To investigate whether the CENP-T/W complex plays a templating role in propagating centromere identity, we first examined their regulation during the HeLa cell cycle. The relative abundance of CENP-T (NP_079358.3) and -W (NP_001012525.1) transcripts and protein were examined in synchronized populations of HeLa cells (Figure 1). qPCR analysis of transcripts revealed no periodicity in the expression of CENP-T or CENP-W, while CENP-A exhibited the previously reported upregulation in G2 (Figure 1A) [45]. At the protein level, CENP-T and -W exhibited cyclic behaviour, exhibiting maximal abundance in S-phase ~4-fold greater than the minimum observed in late G2 and M (Figure 1B). The relative abundance of each protein at centromeres was estimated using a tagged transgene, because of the absence of monospecific antibodies suitable for immunocytochemistry. Cell lines constitutively expressing CLIP-tagged constructs of CENP-T or -W and exhibiting normal growth kinetics were prepared (Figure S1A). In addition to normal targeting and cell proliferation, similar constructs tagged with fluorescent proteins formed heterodimeric complexes within the CCAN in human cells, assayed by FRET (A. Hofmeister and S. Diekmann, unpublished observations) and fully replaced endogenous gene products in chicken cells [32], suggesting normal protein function. Asynchronous cultures expressing CLIP-tagged proteins at steady state were labelled *in vivo* with CLIP-505, fixed and processed for immunodetection with cell cycle markers PCNA and phospho-histone H3 and with a CENP-A monoclonal antibody (Figure S1B). The abundance of CLIP-tagged CENP-W at centromeres was determined by quantitative microscopy and the population classified according to cell cycle stage (Figure 1C). CENP-W was seen to increase at centromeres in correlation with progression through S-phase, approximately doubling in concentration at centromeres in late S-phase and slightly increasing beyond this in G2 cells. CENP-T showed a similar pattern of accumulation (unpublished data). Taken together, these results show that CENPs -T and -W are constitutive centromere proteins whose abundance at centromeres correlates with the state of replication of the chromosomes.

A.

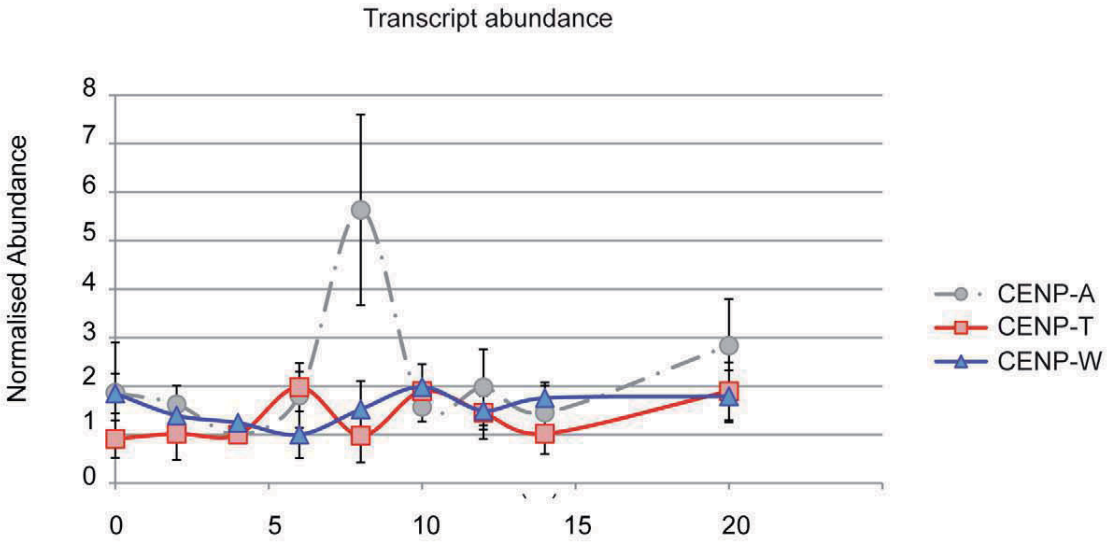
Transcript abundance
Normalised Abundance
8
7
6
5
4
3
2
1
0
0
5
10
15
20
CENP-A
CENP-T
CENP-W

B.

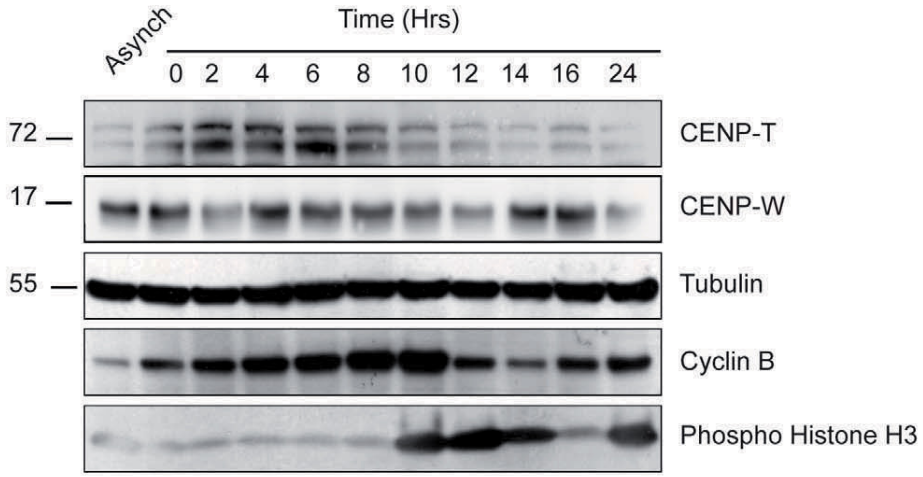
Asynch
Time (Hrs)
0 2 4 6 8 10 12 14 16 24
72
17
55
CENP-T
CENP-W
Tubulin
Cyclin B
Phospho Histone H3

C.

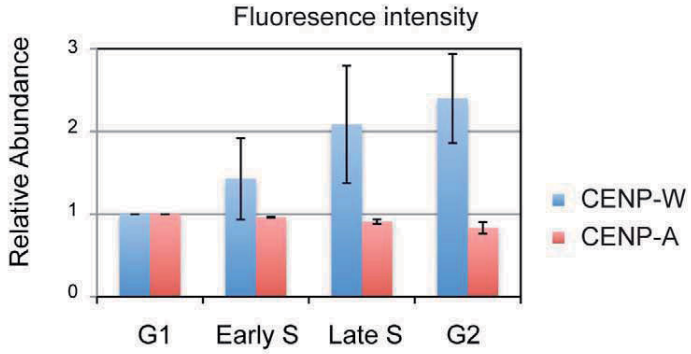
Fluoresence intensity
Relative Abundance
3
2
1
0
G1
Early S
Late S
G2
CENP-W
CENP-A

D.

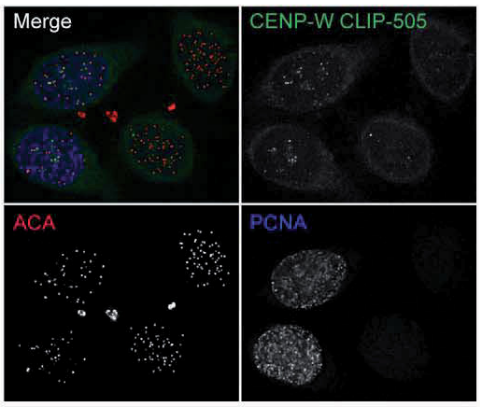
Merge
CENP-W CLIP-505
ACA
PCNA

Figure 1. Analysis of CENP-T and -W in the cell cycle. (A) HeLa cells were fractionated across the cell cycle using a double thymidine protocol. The relative abundance of CENP-T (red) and -W (blue) transcripts were measured by qPCR. CENP-A (dashed grey) is shown as a reference. No significant periodic RNA accumulation was observed. (B) Protein obtained from cell cycle fractions was examined by Western blot for CENP-T and CENP-W relative to tubulin (loading control), cyclin B, and phospho-histone H3 (Ser10). (C) The relative abundance of centromere-associated CENP-W was estimated using a cell line constitutively expressing a CLIP-tagged fusion protein. CENP-W-CLIP was labelled with CLIP-505 at steady state and fluorescence intensity quantified. Cells were counterstained for CENP-A to define centromeres and for PCNA and phospho-histone H3 to resolve the cell cycle stage of individual cells (see Figure S2). Cells were scored as S-phase (PCNA-positive), G2 and M (phospho-histone H3-positive), or G1 (negative for either PCNA or H3P). Early and late S-phase designations were made on the basis of PNCA distribution. (D) An example of cell staining showing CLIP-505-CENP-W assembly in a pair of cells in S-phase and undetected in a pair of G2 cells.
doi:10.1371/journal.pbio.1001082.g001

Expression of CENP-W Is Required for Each Mitosis

Cells depleted of CENP-A exhibit a distinct phenotypic response, maintaining normal kinetochore function for two to three cell cycles until a critical threshold of about 10% of normal levels are reached and mitosis fails [33]. This behaviour is similar to early results obtained by microinjection of antibodies to CENP-C [46], showing that cells can accommodate the loss of activity of certain CENPs by making smaller yet functional kinetochores. To determine whether depletion of CENPs -T or -W results in a similar delay in the onset of mitotic phenotype, RNAi was performed in HeLa cells using immunofluorescence and live cell microscopy to assay effects of depletion (Figure 2). Depletion of CENP-W for 48 h resulted in severe disruption of mitosis comparable to that reported by conditional depletion in chicken cells [32]. Spindles were frequently multipolar (Figure 2A) and cells exhibited an extended prometaphase with numerous misaligned chromosomes, mono-oriented chromosomes, failure of congression, and pronounced spindle rolling phenotype (Videos S1–S4). Depletion of CENP-T using pooled siRNAs yielded relatively subtle effects, resulting in characteristic fusiform spindle morphology (Figure 2A), high frequencies of misaligned chromosomes, and congression defects and mild delays in mitosis. The differences in phenotype observed for the two subunits of the complex is likely related to partial knockdown of the proteins under our experimental conditions (Figure S2). Defective mitosis was quantitatively examined by measuring the delay in anaphase onset in HeLa H2B-GFP cells 1–2 d after transfection, observing populations for 12-h windows using time-lapse microscopy (Figure 2B). By observing cells starting 24 h after initiation of transfection, the consequences of CENP-W loss on the first mitosis following depletion could be examined, revealing significant increase in the number and severity of mitotic defects in the population. HeLa H2B-GFP cells exhibit an average "pre-anaphase" time of 89 ± 38 min. Following RNAi, nearly one-third of CENP-W depleted cells showed a mitotic delay greater than 1 standard deviation above the mean and this delay was more extensive than that seen in untreated populations, with an average excess time of 154 min following CENP-W depletion (Figure 2B, inset). These defects were much more severe 48 h following transfection. These results indicate that deposition of CENP-W is required in each cell cycle for a robust mitosis. In contrast to the induced mitotic defects, depletion of CENP-T or -W did not disrupt assembly of CENP-A in cells cotransfected with siRNA and an mCherry-CENP-A plasmid (Figures S3 and S4), indicating that the mitotic defects induced by CENP-W depletion appear independently of the CENP-A loading pathway. These results suggest that, within the time frame of one cell cycle, the CENP-T/W complex plays a role primarily in kinetochore function rather than in locus maintenance.

CENPs -T and -W Are Not Stably Inherited

A different perspective on the role of the CENP-T/W complex in locus maintenance was gained by examining multigenerational stability. A pulse-chase experiment was performed using cells expressing CLIP-tagged CENPs -T or -W in conjunction with SNAP-tagged CENP-A, synchronizing cells with a double thymidine block and labelling with a fluorescent ligand at the time of release. Cells were harvested at 24-h intervals and the abundance of protein at centromeres was determined by quantitative fluorescence microscopy (Figure 2C and 2D). CENP-A showed a diminution of signal of approximately 50% per generation over two subsequent cell cycles, while CENP-T and -W CLIP signals were reduced to background within 24 h. Labelling was also performed 6 h after release, in S-phase, and cells were examined after 24 h with similar loss of the pulse population of molecules (unpublished data). CENPs -T and -W thus behave as exchangeable components of centromeric chromatin. We conclude that, unlike CENP-A, this histone H3-associated CENP-T/W histone-fold domain complex is not situated to function as a stably bound, physically heritable marker of centromere identity.

CENPs -T and -W Assemble prior to Mitosis through a Dynamic Exchange Mechanism

In order to examine the time at which the CENP-T/W complex assembles in the cell cycle, a conditional labelling strategy was employed, similar to that used to pinpoint CENP-A assembly timing in HeLa cells (Figure 3A) [22]. Cells expressing CLIP-tagged CENPs -T or -W were synchronized and reactive CLIP proteins were blocked prior to release into the cell cycle. After 6.5 h, newly synthesized CLIP-tagged proteins were labelled and cells were collected at 2-h intervals. Cells were costained for tubulin to stage cells as they progressed through mitosis and into the subsequent G1. Cells undergoing mitosis clearly exhibited newly assembled CENP-T and -W at centromeres (Figure 3B), while CENP-A assembly was not detected until telophase/G1 (Figure S5). Thus, unlike CENP-A, newly synthesised CENP-T and -W assemble in the cell cycle in which they are made, prior to the execution of mitosis.

To resolve when CENP-T and CENP-W are assembled within the proximal cell cycle, the CLIP-quench-chase-pulse experiment was repeated and the cells were counterstained with centromere (CENP-A) and cell cycle markers (PCNA and phospho-histone H3; Figure 3C). Cells were scored for CENP-T/W assembly by inspection and also classified with respect to PCNA and phospho-histone H3 staining, allowing cells to be classified as S phase (PCNA-positive), G2 and M (phospho-histone H3 morphology), or G1 (negative for either PCNA or H3P). CLIP-505 signal was detected at baseline levels in cells that were in very early stages of S-phase, identified by fine punctate PCNA staining. However, cells which had progressed further through S-phase displayed robust centromere associated CLIP-505 signal. Quantification of fluorescence intensity demonstrated an increase in centromere associated CLIP-505 signal correlated to progression through S-phase (Figure 3D).

A.

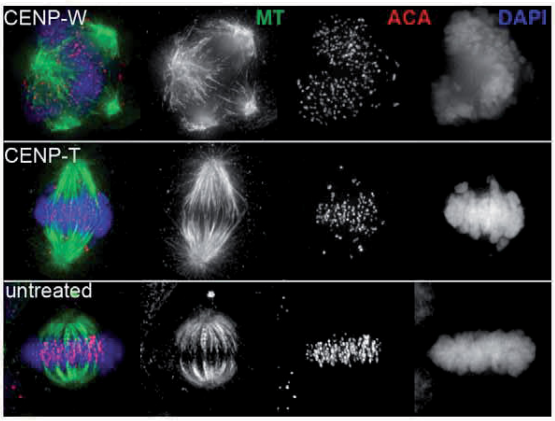
CENP-W
MT
ACA
DAPI
CENP-T
untreated

B.

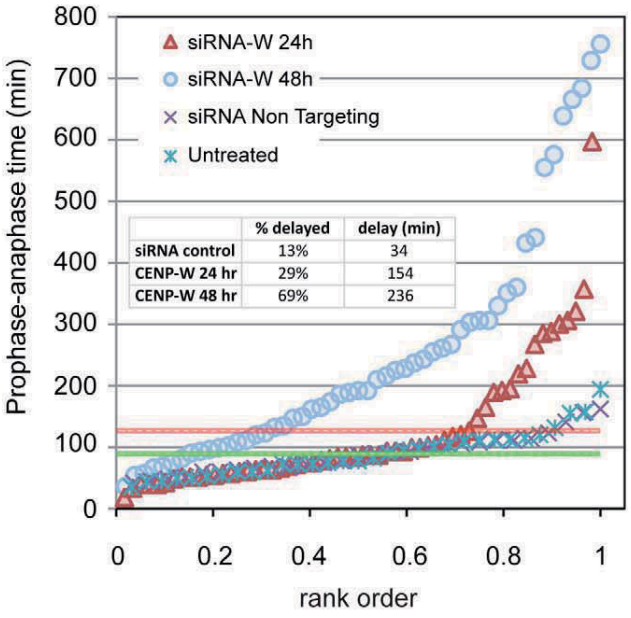
siRNA-W 24h
siRNA-W 48h
siRNA Non Targeting
Untreated
Prophase-anaphase time (min)
rank order
0
100
200
300
400
500
600
700
800
0
0.2
0.4
0.6
0.8
1
% delayed
delay (min)
siRNA control 13% 34
CENP-W 24 hr 29% 154
CENP-W 48 hr 69% 236

C.

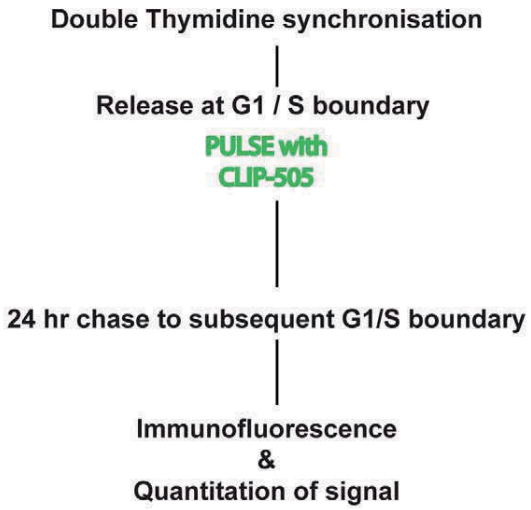
Double Thymidine synchronisation
Release at G1 / S boundary
PULSE with
CLIP-505
24 hr chase to subsequent G1/S boundary
Immunofluorescence
&
Quantitation of signal

D.

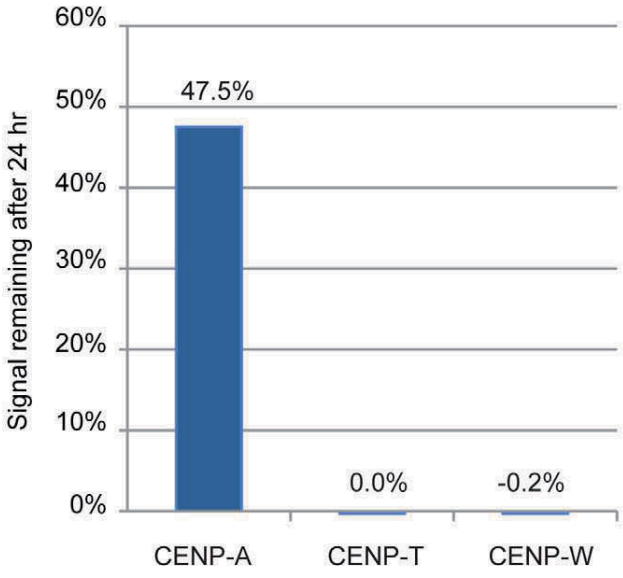
Signal remaining after 24 hr
60%
50%
40%
30%
20%
10%
0%
47.5%
0.0%
-0.2%
CENP-A
CENP-T
CENP-W

Figure 2. The CENP-T/W complex is required in each mitosis and does not exhibit persistent binding to centromeres. (A) CENPs -T and -W were depleted by RNAi in HeLa cells, resulting in defects in spindle assembly assayed by immunofluorescence for tubulin (green) and centromeres (red) with DNA stained with DAPI (blue). CENP-W depleted cells exhibit a high frequency of multipolar spindles. Depletion of CENP-T was less severe resulting in characteristic fusiform spindle structures. (B) CENP-W is required for robust mitosis in each cell cycle. Mitotic kinetics were assayed using histone H2B-GFP HeLa cells treated with CENP-W siRNA for 48 (blue circles) or 24 h (red triangles), scoring time between NEB (defined as onset of deformations in nuclear chromatin) and anaphase onset and are plotted by rank order of individual cells. Mean time for scrambled siRNA control (dark X) and untreated cells (light X) is shown as a green line, with +1 standard deviation (SD) marked with a red line. Inset graph reports the percentage of cells with NEB-anaphase times in excess of +1 SD and the average delay in anaphase onset. (C) Experimental schematic describes the pulse chase approach to assay the heritability of CLIP tagged CENPs -T and -W. (D) CENPs -T and -W do not persist at centromeres. CLIP signal intensity coincident with centromeres was quantified at the time of pulse and 24 h later. While CENP-A-SNAP signal was depleted by approximately 50%, as expected, CENP-T-CLIP and CENP-W-CLIP signal was reduced to background levels after 24 h.
doi:10.1371/journal.pbio.1001082.g002

To exclude the possibility that the observed assembly was an artefact of initiating the pulse during S-phase, a comparable pulse-labelling paradigm was employed using asynchronous cells and processed for cell cycle analysis as described above (Figure 4A). For CENP-W, approximately 50% of G1 and S-phase cells showed weak but detectable labelling, while late S-phase and nearly all premitotic H3P-positive cells (primarily G2 with some late S) showed robust assembly (Figure 4B). CENP-T exhibited a more stringent assembly pattern, with pulse labelling detected in 15% of S-phase cells and fewer than 1% of G1 cells (Figure 4B). In contrast, over 50% of the H3P-positive population showed assembly.

An independent method was employed to observe CENP-T and -W assembly dynamics in living cells using fluorescence recovery after photobleaching (FRAP). Centromere labelling with GFP fusions of CENP-T or -W was induced by transient transfection into HeLa and HEp-2 cells and mCherry-PCNA was cotransfected as a marker to allow estimation of the cell cycle stage of individual cells [47]. No fluorescence recovery was observed for either protein in G1 or early S-phase cells, whereas both CENP-T (Figure 4C) and CENP-W (Figures S3–S6) exhibited recovery in cells judged to be in late S-phase. Recovery of fluorescence in individual cells initiated after a stochastic lag time, while individual kinetochores in a given cell initiated recovery at the same time (within less than 30 min). When recovery data from multiple cells were aligned with an origin at the onset of recovery, consistent kinetics were observed for both CENP-T and CENP-W, with recovery half times of approximately 80 and 60 min, respectively. Taken together, both conditional labelling approaches indicate that the assembly of CENPs -T and -W are closely coordinated with events in the second half of S-phase. The stochastic onset of recovery observed in FRAP is suggestive of a switching mechanism that is activated late S-phase or G2 in HeLa cells.

While the precise mechanism that accommodates replicative dilution of CENP-A is not known, it most likely involves nucleosome assembly. How do CENP-T and -W interact with this assembling compartment? One possibility is that the CENP-T/W complex assembles to a fixed stoichiometry along with new histone H3 nucleosomes. CENPs -A and -I exhibit a stable binding pattern such as this, during their assembly in G1 and S-phase, respectively [47]. To test this model, double FRAP (fluorescence recovery after FRAP [FRA-FRAP]) experiments were performed for both GFP-CENP-T and -W. Centromeres in late S-phase cells were photobleached and given time to recover to approximately 50% and then bleached again (Figure 4D and 4E). Recovery persisted and reached a level of approximately 40%. The $t_{1/2}$ values were calculated for both GFP-CENP-T ($t_{1/2} = 71$ min) and GFP-CENP-W ($t_{1/2} = 41$ min), indicating GFP-CENP-W is loaded faster than GFP-CENP-T. These experiments were initiated in late S-phase and extended well into G2, and, combined with the single FRAP measurements we conclude that dynamic exchange of CENP-T and -W takes place over a broad time window preceding mitosis, beginning in S-phase. As an independent test of protein exchange at centromeres, a fluorescence loss after photoactivation (FLAP) experiment was performed using photo-activatable GFP derivatives of CENPs -T and -W. Centromeres were labelled with either protein by transient transfection along with mCherry-PCNA as marker. Cells judged to be in late S-phase on the basis of PCNA distribution were monitored and then photo-activated after disappearance of PCNA foci. Cells were imaged 3 h later in the subsequent G2 (Figure 4F). Quantitative analysis of fluorescence intensity showed an average loss of 81% ($\pm$22)% of CENP-W at centromeres during the chase period, consistent with an exchange reaction balanced with the observed assembly in FRAP. Results were comparable for CENP-T (unpublished data), demonstrating that the CENP-T/W complex assembles through a dynamic exchange mechanism that is restricted primarily to late S-phase and G2.

Discussion

Investigation of the assembly and inheritance of CENPs -T and -W reveals a dynamic pathway for assembly late in the cell cycle that is associated with rapid exchange of the proteins, such that they do not exhibit multigenerational persistence. As a group, centromere protein assembly occurs through several mechanistically distinct processes distributed throughout the cell cycle. The CENP-A assembly pathway itself is distributed from mid S-phase, when replication of CENP-A associated DNA occurs, through late G1 of the subsequent cell cycle, when RSF-dependent and MgcRacGap-dependent mechanisms stabilizes newly deposited CENP-A [21–26,47,48]. In vivo analysis of CCAN component assembly using FRAP has revealed distinct classes of protein, on the basis of the timing and mechanism, either stoichiometric or dynamic exchange, of assembly [47]. In this study, all proteins examined were stably bound in mitosis with CENPs -A and -I exhibiting stable binding throughout the cell cycle, showing assembly-coupled fluorescence recovery only during telophase/G1 and S-phase, respectively. CENPs -B, -C, and -H exhibited dynamic exchange throughout much of the cell cycle, becoming stably bound only in G2 (CENP-B) or S-phase (CENPs -C and -H). CENPs -T and -W form a novel class that is nonexchangeable during G1, exhibiting assembly-coupled dynamic exchange during S-phase and G2.

The CENP-T/W complex has been shown to interact stably with histone H3 nucleosomes [32]. Their dynamic behaviour revealed by in vivo measurements, as well as differences in their kinetics of assembly, are unexpected for stable chromatin components. The biochemically purified complex could represent a stably assembled population, perhaps comparable to that observed in G1. The onset of recovery of fluorescence in S-phase, which occurs at all centromeres simultaneously, is suggestive of an active switch rather than a passive response to DNA replication at centromeres, suggesting that a biochemically purified complex

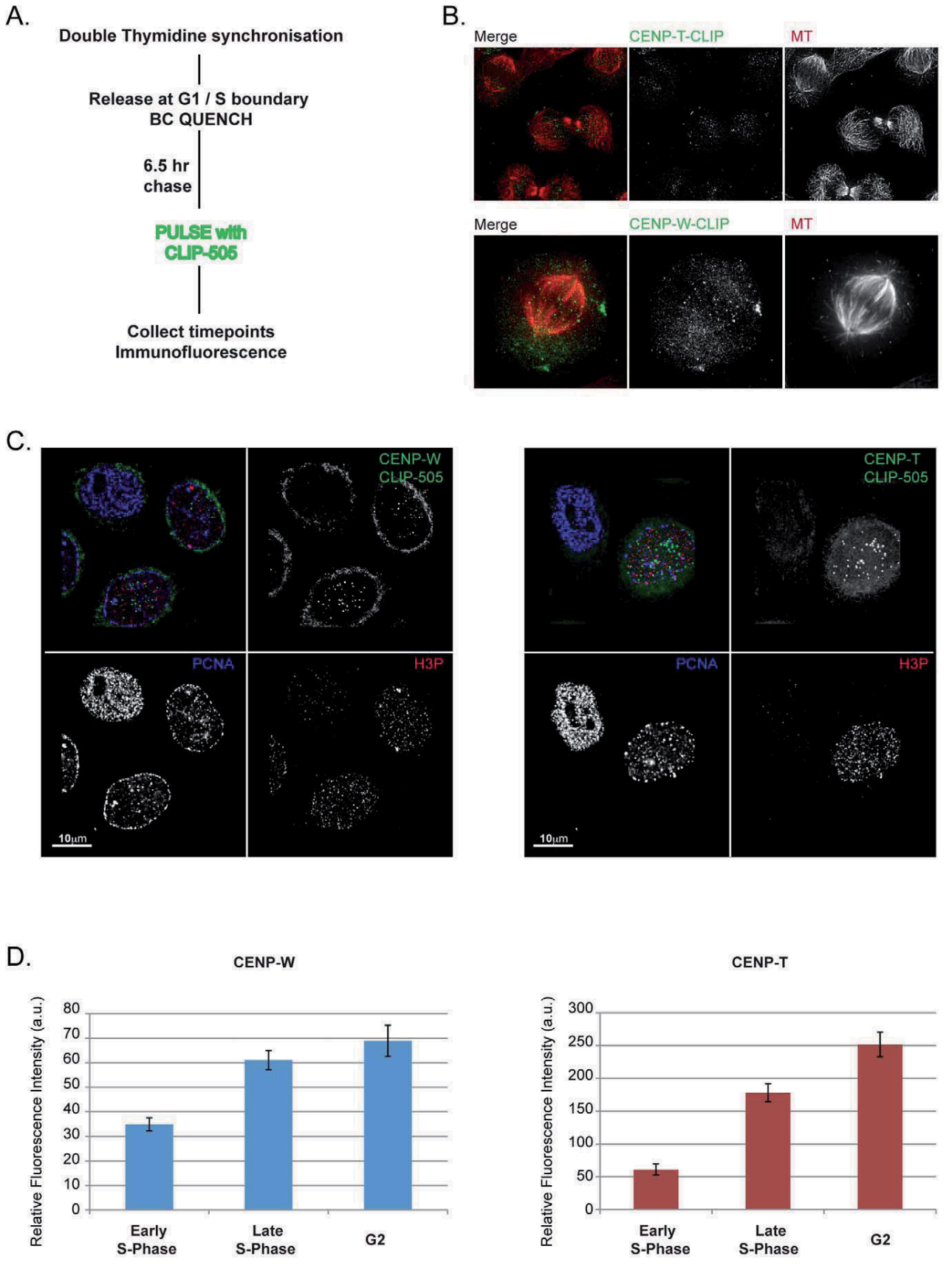
A.
Double Thymidine synchronisation
Release at G1 / S boundary
BC QUENCH
6.5 hr
chase
PULSE with
CLIP-505
Collect timepoints
Immunofluorescence
B.
Merge
CENP-T-CLIP
MT
Merge
CENP-W-CLIP
MT
C.
CENP-W
CLIP-505
PCNA
H3P
10μm
CENP-T
CLIP-505
PCNA
H3P
10μm
D.
CENP-W
Relative Fluorescence Intensity (a.u.)
80
70
60
50
40
30
20
10
0
Early
S-Phase
Late
S-Phase
G2
CENP-T
Relative Fluorescence Intensity (a.u.)
300
250
200
150
100
50
0
Early
S-Phase
Late
S-Phase
G2

Figure 3. CENPs -T and -W assemble predominantly in late S-phase and G2. (A) Schematic description of the CLIP quench-chase-pulse-chase experiment used to assay the timing of assembly of CLIP tagged CENPs -T and -W at centromeres using synchronized HeLa cells. (B) CLIP-tagged CENPs -T and -W are localized at centromeres prior to the onset of anaphase, indicating that newly synthesized CENP-T and CENP-W assemble at the centromere in the proximal cell cycle. (C) Progressive assembly of pulsed CENP-T and CENP-W in S-phase and G2. Cells were labelled with PCNA and phospho-histone H3 antibodies to document position in the cell cycle. Cells judged to be in earlier stages of S-phase have no detectable CLIP signal at centromeres, while cells later in S-phase and G2 have robust centromere-associated CLIP signal. (D) Centromere-associated CENP-T-CLIP and CENP-W-CLIP fluorescence were quantified relative to progression through the cell cycle, showing an increased signal intensity at centromeres coinciding with progression through S-phase and G2.
doi:10.1371/journal.pbio.1001082.g003

could be stabilized by dissociation from factors that may promote the exchange reactions observed in vivo. The kinetic differences observed for CENP-T and -W exchange in our FRAP studies suggest mechanistic features of their assembly reaction(s) that bear further investigation with refined in vivo analyses.

Although the precise molecular organization of the histone H3-CENP-T/W nucleosome population is not known, it is reasonable to assume that they are interspersed closely with CENP-A nucleosomes, on the basis of known protein-protein interactions [30,31] and measurement of CENP-A oligonucleosome domain size (estimated at four to six contiguous nucleosomes, M. Glynn and K.F. Sullivan, unpublished data). Analysis at the single molecule level in stretched chromatin fibers supports a very close interspersion [48]. In human cells, DNA replication in this compartment occurs in the absence of new CENP-A, resulting in replicative dilution of parental CENP-A nucleosomes [49]. It is thought that histone H3 nucleosomes assemble in their place [12,24]. We propose that CENPs -T and -W, assemble onto histone H3 nucleosomes within this compartment. The functional consequence of these assembly events would be an expansion of the histone H3/CENP-T/W compartment within postreplicative centromeric chromatin. The dynamic behaviour of protein within this compartment kinetically parallels the active establishment of the kinetochore complex, which spans the period from G2 to early mitosis in human cells [50,51]. Taken together with the known involvement of the CCAN with kinetochore formation, we suggest that assembly of the CENP-T/W complex plays a functional role in kinetochore formation following DNA replication.

The immediate requirement for CENP-W for successful execution of mitosis is consistent with the CENP-T/W complex playing an active role in kinetochore assembly in G2 and contrasts starkly with the ability of cells to accommodate loss of CENP-A over multiple generations without defect [33]. The complementary kinetics of their assembly leads to a view in which CENP-A serves a role as a placeholder, diminishing in proportion as a more direct kinetochore chromatin foundation is built up prior to mitosis. CENP-A has a distinct role as a carrier of centromere identity over multiple generations. Its replenishment cycle appears to be complete at the onset of S-phase [24–26]. We suggest that this "fully loaded" CENP-A state corresponds to replication-competent centromeric chromatin. Replication through CENP-A chromatin would initiate a switch of the centromere to a kinetochore-competent configuration, accompanied by assembly of the CENP-T/W complex onto histone H3 nucleosomes, providing an expanded platform for assembly of additional CCAN components. The lack of generational persistence of the CENP-T/W histone fold complex suggests that it is not a stably associated molecular mark for centromere identity at the chromatin level, nor does it appear to play a direct role in CENP-A assembly.

The broadly used definitions of the centromere as a genetic locus, e.g. DNA, and the kinetochore as the facultative, proteinaceous structure on the primary constriction that executes mitotic function have lost distinction with the demonstration that a chromatin protein complex carries the genetic function of the locus. The different behaviour of the CENP-A and CENP-T/W chromatin compartments suggest a degree of segregation of genetic (centromere) function and mitotic (kinetochore) function within biochemically specialized chromatin microdomains of the centromere. Investigation of the roles of individual CCAN components in the maintenance of centromere identity, establishment of kinetochore function, and the integration of these two processes may provide important paradigms for understanding epigenetic chromatin-based inheritance.

Methods

Cell Culture and Transfection

Cells were cultured as previously described [52]. siGENOME SMARTpool siRNAs (Dharmacon) M-014577-01 and M-032901-01 were used to deplete CENP-T and CENP-W respectively. siRNA was transfected into cells using DharmaFECT 1 (Dharmacon). Cells were transfected with plasmid DNA with Lipofectamine2000 reagent (Invitrogen).

Constructs

pCLIPm (NEB) was adapted for use with the Gateway system (Invitrogen) by linearising the plasmid in the MCS by restriction digest with EcoRV. Gateway adaptation reading frame cassette RFB (Invitrogen) was ligated into the plasmid to generate a pCLIPm for C-terminal CLIP tagging (GW-pCLIPm). AttB flanked PCR products were generated from cDNA for CENP-T and CENP-W and recombined with pDonr-Zeo (Invitrogen) to generate entry vectors, which were recombined with GW-pCLIPm to generate the CENP-T-CLIP and CENP-W-CLIP constructs.

Cell Lines

Cells stably expressing the CENP-A-SNAP fusion protein were a gift from L.E. Jansen. The CENP-A-SNAP cell line was transfected with the CENP-T-CLIP and CENP-W-CLIP constructs. Cells stably expressing the fusion proteins were selected by G418 (600 μg/ml; Calbiochem). The resulting monoclonal lines were expanded and examined by fluorescence microscopy after CLIP-505 labelling. CENP-T-CLIP 11 and CENP-W-CLIP 4 were used for all experiments in this paper. These lines exhibited population doubling times and cell cycle distributions indistinguishable from the parental line.

CLIP Quench and Pulse Labelling

CLIP tag activity in cells was quenched by addition of 20 μM O^6-BC (BC-block; NEB) in complete growth medium for 30 min at 37°C. SNAP or CLIP-tag proteins were pulse labelled with 2 μM CLIP-505/CLIP-Tmr Star/SNAP-Tmr Star (NEB) in complete growth medium supplemented with 1% BSA for 20 min at 37°C. After quenching or pulse labelling, cells were

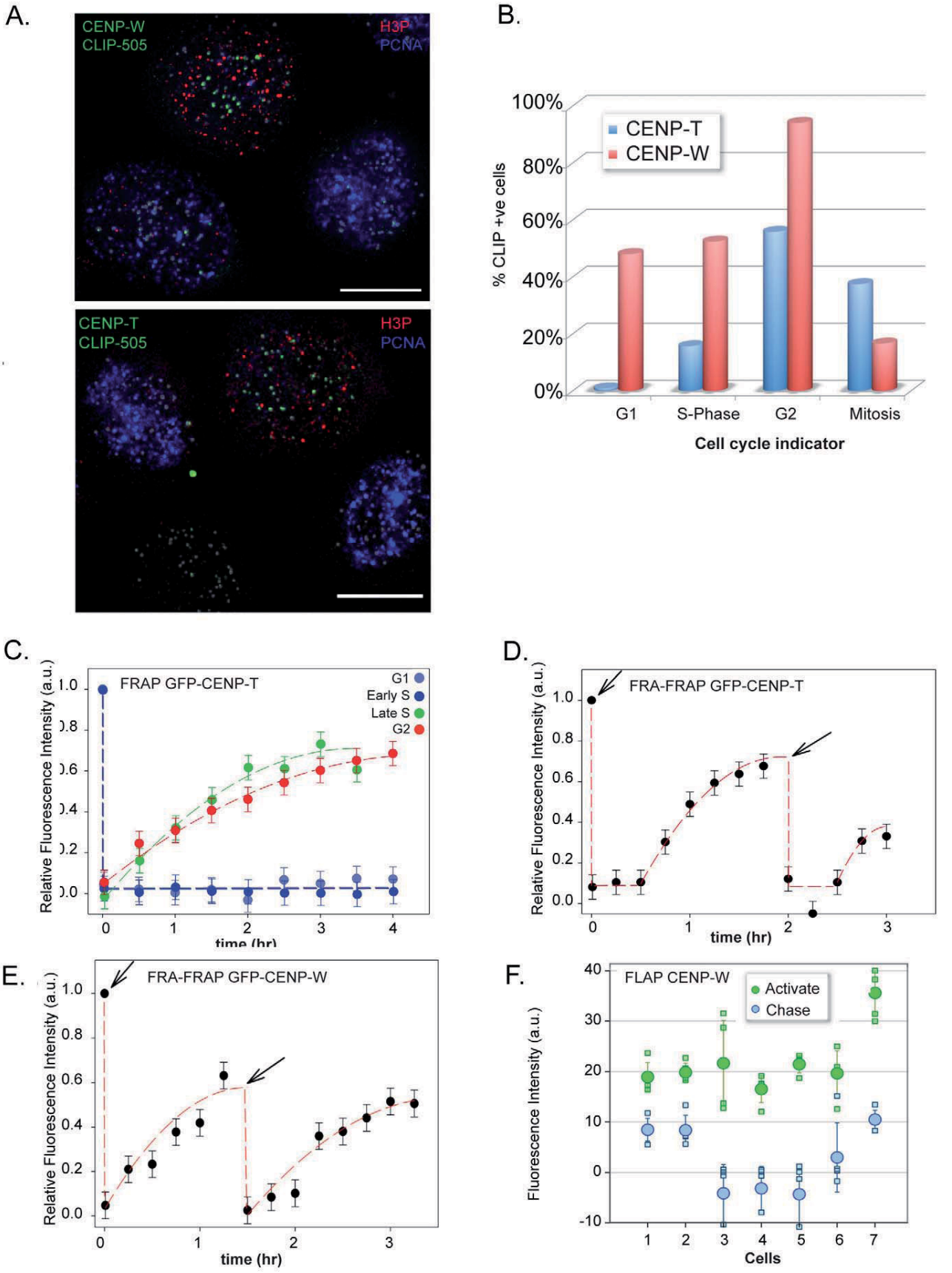
A.
CENP-W
CLIP-505
H3P
PCNA
CENP-T
CLIP-505
H3P
PCNA
B.
100%
80%
60%
40%
20%
0%
CENP-T
CENP-W
% CLIP +ve cells
G1
S-Phase
G2
Mitosis
Cell cycle indicator
C.
FRAP GFP-CENP-T
G1
Early S
Late S
G2
Relative Fluorescence Intensity (a.u.)
time (hr)
D.
FRA-FRAP GFP-CENP-T
Relative Fluorescence Intensity (a.u.)
time (hr)
E.
FRA-FRAP GFP-CENP-W
Relative Fluorescence Intensity (a.u.)
time (hr)
F.
FLAP CENP-W
Activate
Chase
Fluorescence Intensity (a.u.)
Cells

Figure 4. CENP-T and -W assembly occur through a dynamic exchange mechanism in S-phase and G2. (A) Asynchronous HeLa cells expressing CENP-T and CENP-W CLIP were used to assay timing of assembly in an unperturbed cell population. Cells were cell cycle staged by counterstaining with PCNA and phospho-histone H3. (B) Cells were classified on the basis of CLIP signal at centromeres and cell cycle stage. (C) FRAP of GFP derivatives of CENP-T only occurs during late S-phase and G2 indicating loading takes place during this period. (D) Centromere-associated GFP-CENP-T was photobleached and allowed to recover to approximately 40%. Following a second bleach event, recovery continued reaching approximately 40%, indicating an exchange-based dynamic loading process during this time period. (E) Double FRAP of GFP-CENP-W, as for CENP-T. (F) Fluorescence loss after photoactivation. Photoactivatable GFP-CENP-W was activated in G2 cells. Following a chase period of 3 h, the majority of the fluorescent signal had dissociated from the centromere.
doi:10.1371/journal.pbio.1001082.g004

washed twice with prewarmed PBS and once with complete DMEM. Following washes cells were reincubated in complete medium to allow excess labelling compound to diffuse from cells. After 30 min, cells were washed again twice in PBS followed either by reincubation in complete DMEM, or fixation.

Cell Synchronization

HeLa cells were treated with 5 mM thymidine in complete DMEM for 16 h, washed twice in PBS, once in complete DMEM, and released in complete DMEM 9 h followed by addition of thymidine to a final concentration of 5 mM for 16 h, after which cells were released again into complete DMEM.

Immunofluorescence

Cells were grown and CLIP labelled on glass coverslips followed by fixation in MeOH or 4% PFA and processed for immunofluorescence. ACA (1:500), Anti-CENP-A (a gift from K. Yoda, Nagoya University, Nagoya, Japan) was used at a dilution of 1:200, human anti-PCNA serum was used at 1:100, anti-α-tubulin (Sigma) was used at 1:500, and anti-phospho histone H3 (Abcam) was used at 1:300.

Donkey fluorescently conjugated secondary antibodies (anti-mouse-FITC (1:50) anti-mouse Cy5 (1:200), anti-rabbit TRITC (1:100), and anti-human AMCA (1:100) were obtained from Jackson Immunoresearch Laboratories. Samples were mounted in SloFADE (Invitrogen).

Microscopy

Images were captured using a DeltaVision Core system (Applied Precision) controlling an interline charge-coupled device camera (Coolsnap HQ^2; Roper) mounted on an inverted microscope (IX-71; Olympus). For each sample, images were collected at 2× binning using a 100× oil objective at 0.2 μm z sections. All images were deconvolved and maximum intensity projected using SoftWoRx (Applied Precision). For quantification, unscaled DeltaVision images were used. Centromere signal intensity was determined using ImagePro 6.3. A mask was created using CENP-A or ACA signal to define centromeres. The "centromere" mask was applied to the CLIP-505 channel and the mean fluorescence intensity measured. A background mask was created from three regions within the nucleus not containing centromeres and applied to the CLIP-505 images for measurement. Background values were then subtracted from mean signal.

Immunoblots

Whole cell extracts equivalent to 50,000 cells were separated by SDS-PAGE, transferred to PVDF membranes (Millipore), and processed for immunodetection as described previously [49]. Antibodies: anti-CENP-T (Bethyl), anti-CENP-W (C6ORF173 antibody Abcam, ab75827), anti-tubulin monoclonal (DN1A Sigma), anti-H3P Ser10 (Millipore), cyclin-B (Upstate).

Supporting Information

Figure S1 A CENP-A-SNAP cell line (gift from Lars Jansen) was stably transfected with plasmids CENP-T-pCLIPm and CENP-W-pCLIPm. Clones stably expressing CENP-T-CLIP and CENP-W-CLIP were selected and labelled using SNAP-TMR-Star to label CENP-A-SNAP and CLIP-505 to label CENP-T and CENP-W CLIP.
(EPS)

Figure S2 Quantitative reverse transcript (RT)-PCR was used to measure the levels of depletion of both CENP-T and CENP-W transcripts following a 48-h siRNA treatment. CENP-W was depleted to approximately 48% while CENP-T transcripts were reduced to approximately 36%. Corresponding Western blots shown below demonstrate comparable levels of protein depletion.
(EPS)

Figure S3 Analysis of CENP-A assembly following CENP-W depletion. (A) Experimental schematic describes the approach to assay assembly of CENP-A following depletion of CENP-W by siRNA. HeLa cells expressing H2B-GFP were cotransfected with mCherry-CENP-A and siRNA directed against CENP-W. After 48 h, cells were fixed for immunofluorescence or treated with an Aurora B inhibitor (ZM44739, JS Research Chemicals) to relieve mitotic delay associated with CENP-W depletion. Cells were examined for assembly of mCherry-CENP-A to centromeres. (B) Immunofluorescence in H2B-GFP HeLa cells using centromere marker (ACA) and tubulin following depletion of CENP-W. mCherry-CENP-A is observed at centromeres in early G1 cells displaying a tubulin staining of the midbody, while some transfected metaphase cells, indicated by presence of mCherry signal, with uncongressed chromosomes, have not assembled CENP-A at centromeres diffuse mCherry signal. (C) Cells were also treated with an Aurora B inhibitor, following 48-h CENP-W depletion. Cells judged to have entered G1 as a result of Aurora B inhibition exhibited abnormal nuclear morphology and centromeres that in most cases had failed to segregate. Transfected cells positive for mCherry-CENP-A had assembled CENP-A at centromeres.
(EPS)

Figure S4 Analysis of CENP-A assembly following CENP-T depletion. In an experiment analogous to that shown in Figure S5, immunofluorescence in H2B-GFP HeLa cells using centromere marker (ACA) and tubulin illustrates cell cycle stage in exemplary cells following depletion of CENP-T. mCherry-CENP-A is observed at centromeres in early G1 cells displaying a tubulin staining of the midbody, while some transfected metaphase cells, indicated by presence of mCherry signal, with monopolar chromosomes, have not assembled CENP-A at centromeres.
(EPS)

Figure S5 A cell line expressing SNAP-tagged CENP-A (gift of Lars Jansen) was used as a control for timed assembly in SNAP experiments. Cells were synchronized using a double thymidine arrest and quenched using BG-quench upon release for arrest. Cell were chased for 7 h to allow synthesis of "new" SNAP-CENP-A, and pulsed with a fluorescent substrate, SNAP-505. Assembly of SNAP-CENP-A to centromeres was not observed until cells had progressed through mitosis into the

subsequent G1, as previously reported. Insets detail SNAP-505 and ACA staining in interphase and mitotic cells.
(EPS)

Figure S6 FRAP of GFP derivatives of CENP-W only occurs during late S-phase and continues during G2, indicating loading takes place during this time. Experiment analogous to that shown for CENP-T in Figure 4.
(EPS)

Video S1 CENP-W knockdown induces profound mitotic delays and induces chromosome/spindle rolling in cells. HeLa-H2B-GFP cells were transfected with pooled siRNAs against CENP-W and imaged for 12 h beginning 48-h transfection at a rate of 20 frames/hour. Numerous cells are observed entering mitosis and spending extended time in a prometaphase-like state with uncongressed chromosomes. Many cells exhibit a pronounced "rolling" phenotype (see upper right quadrant) that can initiate very soon after the onset of mitosis. See Figure 2B for a quantitative interpretation of these data.
(MOV)

Video S2 4-Dimensional imaging of rolling spindles: projection. HeLa-H2B-GFP cells transfected with pooled siRNAs against CENP-W were imaged by 3-dimensional time-lapse microscopy beginning 48 h after transfection, with frames collected every 5 min. This sequence shows a projected image superimposed on a transmitted light image of cells. Two rolling cells are detailed. In one (first), the metaphase plate rotates in a continuous motion through almost 180°. In another, the metaphase plate rotates 90° with respect to the optical axis.
(MOV)

Video S3 4-Dimensional imaging of rolling spindles: reconstruction. HeLa-H2B-GFP cells transfected with pooled siRNAs against CENP-W were imaged by 3-dimensional time-lapse microscopy beginning 48 h after transfection, with frames collected every 5 min. In this sequence, the field is rocked to reveal the 3-dimensional structure of the chromosomes on the spindle. It is clear that the chromosomes are moving collectively, characteristic of whole spindle motion within the cells.
(MOV)

Video S4 Tubulin labeling confirms whole spindle motion in CENP-W depleted cells. HeLa-H2B-GFP cells were transfected with mCherry-tubulin to directly visualize spindle motion following transfection with pooled siRNAs against CENP-W. It is clear that the entire spindle is moving within cells that exhibit rolling. The spindle poles can be seen to split in some of these cells, as though the forces associated with spindle movement are able to disrupt spindle pole integrity. This may account for the multipolar spindles frequently observed in fixed specimens of CENP-W siRNA-treated cells.
(MOV)

Acknowledgments

The authors thank Lars Jansen for the generous gift of HeLa SNAP-CENP-A cells and Kinya Yoda for CENP-A monoclonal antibody. KFS is a Research Professor of Science Foundation Ireland.

Author Contributions

The author(s) have made the following declarations about their contributions: Conceived and designed the experiments: LP CvV SD KFS. Performed the experiments: LP CvV AK NQ VD DH CH KFS. Analyzed the data: LP CvV AK NQ VD DH SD KFS. Contributed reagents/materials/analysis tools: LP CvV AK NQ DH CH KFS. Wrote the paper: LP SD KFS.

References

1. Cleveland DW, Mao Y, Sullivan KF (2003) Centromeres and kinetochores: from epigenetics to mitotic checkpoint signaling. Cell 112: 407–421.
2. Przewloka MR, Glover DM (2009) The kinetochore and the centromere: a working long distance relationship. Annu Rev Genet 43: 439–465.
3. Santaguida S, Musacchio A (2009) The life and miracles of kinetochores. EMBO J 28: 2511–2531.
4. Cheeseman IM, Desai A (2008) Molecular architecture of the kinetochore-microtubule interface. Nat Rev Mol Cell Biol 9: 33–46.
5. Williams BC, Murphy TD, Goldberg ML, Karpen GH (1998) Neocentromere activity of structurally acentric mini-chromosomes in Drosophila. Nat Genet 18: 30–37.
6. Barry AE, Howman EV, Cancilla MR, Saffery R, Choo KH (1999) Sequence analysis of an 80 kb human neocentromere. Hum Mol Genet 8: 217–227.
7. Wade CM, Giulotto E, Sigurdsson S, Zoli M, Gnerre S, et al. (2009) Genome sequence, comparative analysis, and population genetics of the domestic horse. Science 326: 865–867.
8. Piras FM, Nergadze SG, Magnani E, Bertoni L, Attolini C, et al. (2010) Uncoupling of satellite DNA and centromeric function in the genus *Equus*. PLoS Genet 6: e1000845. doi:10.1371/journal.pgen.1000845.
9. Palmer DK, O'Day K, Trong HL, Charbonneau H, Margolis RL (1991) Purification of the centromere-specific protein CENP-A and demonstration that it is a distinctive histone. Proc Natl Acad Sci U S A 88: 3734–3738.
10. Sullivan KF, Hechenberger M, Masri K (1994) Human CENP-A contains a histone H3 related histone fold domain that is required for targeting to the centromere. J Cell Biol 127: 581–592.
11. Stoler S, Keith KC, Curnick KE, Fitzgerald-Hayes M (1995) A mutation in CSE4, an essential gene encoding a novel chromatin-associated protein in yeast, causes chromosome nondisjunction and cell cycle arrest at mitosis. Genes Dev 9: 573–586.
12. Allshire RC, Karpen GH (2008) Epigenetic regulation of centromeric chromatin: old dogs, new tricks? Nat Rev Genet 9: 923–937.
13. Dalal Y, Bui M (2010) Down the rabbit hole of centromere assembly and dynamics. Curr Opin Cell Biol 22: 392–402.
14. Black BE, Cleveland DW (2011) Epigenetic centromere propagation and the nature of CENP-A nucleosomes. Cell 144: 471–479.
15. Camahort R, Shivaraju M, Mattingly M, Li B, Nakanishi S, et al. (2009) Cse4 is part of an octameric nucleosome in budding yeast. Mol Cell 35: 794–805.
16. Dalal Y, Wang H, Lindsay S, Henikoff S (2007) Tetrameric structure of centromeric nucleosomes in interphase Drosophila cells. PLoS Biol 5: e218. doi:10.1371/journal.pbio.0050218.
17. Mizuguchi G, Xiao H, Wisniewski J, Smith MM, Wu C (2007) Nonhistone Scm3 and histones CenH3-H4 assemble the core of centromere-specific nucleosomes. Cell 129: 1153–1164.
18. Sekulic N, Bassett EA, Rogers DJ, Black BE (2010) The structure of (CENP-A-H4)(2) reveals physical features that mark centromeres. Nature 467: 347–351.
19. Black BE, Foltz DR, Chakravarthy S, Luger K, Woods VL, Jr., et al. (2004) Structural determinants for generating centromeric chromatin. Nature 430: 578–582.
20. Furuyama T, Henikoff S (2009) Centromeric nucleosomes induce positive DNA supercoils. Cell 138: 104–113.
21. Fujita Y, Hayashi T, Kiyomitsu T, Toyoda Y, Kokubu A, et al. (2007) Priming of centromere for CENP-A recruitment by human hMis18alpha, hMis18beta, and M18BP1. Dev Cell 12: 17–30.
22. Jansen LE, Black BE, Foltz DR, Cleveland DW (2007) Propagation of centromeric chromatin requires exit from mitosis. J Cell Biol 176: 795–805.
23. Perpelescu M, Nozaki N, Obuse C, Yang H, Yoda K (2009) Active establishment of centromeric CENP-A chromatin by RSF complex. J Cell Biol 185: 397–407.
24. Dunleavy EM, Roche D, Tagami H, Lacoste N, Ray-Gallet D, et al. (2009) HJURP is a cell-cycle-dependent maintenance and deposition factor of CENP-A at centromeres. Cell 137: 485–497.
25. Foltz DR, Jansen LE, Bailey AO, Yates JR. 3rd, Bassett EA, et al. (2009) Centromere-specific assembly of CENP-a nucleosomes is mediated by HJURP. Cell 137: 472–484.
26. Lagana A, Dorn JF, De Rop V, Ladouceur AM, Maddox AS, et al. (2010) A small GTPase molecular switch regulates epigenetic centromere maintenance by stabilizing newly incorporated CENP-A. Nat Cell Biol 12: 1186–1193.
27. Heun P, Erhardt S, Blower MD, Weiss S, Skora AD, et al. (2006) Mislocalization of the Drosophila centromere-specific histone CID promotes formation of functional ectopic kinetochores. Dev Cell 10: 303–315.
28. Van Hooser AA, Ouspenski II, Gregson HC, Starr DA, Yen TJ, et al. (2001) Specification of kinetochore-forming chromatin by the histone H3 variant CENP-A. J Cell Sci 114: 3529–3542.
29. Izuta H, Ikeno M, Suzuki N, Tomonaga T, Nozaki N, et al. (2006) Comprehensive analysis of the ICEN (Interphase Centromere Complex) components enriched in the CENP-A chromatin of human cells. Genes Cells 11: 673–684.

30. Foltz DR, Jansen LE, Black BE, Bailey AO, Yates JR, 3rd, et al. (2006) The human CENP-A centromeric nucleosome-associated complex. Nat Cell Biol 8: 458–469.
31. Okada M, Cheeseman IM, Hori T, Okawa K, McLeod IX, et al. (2006) The CENP-H-I complex is required for the efficient incorporation of newly synthesized CENP-A into centromeres. Nat Cell Biol 8: 446–457.
32. Hori T, Amano M, Suzuki A, Backer CB, Welburn JP, et al. (2008) CCAN makes multiple contacts with centromeric DNA to provide distinct pathways to the outer kinetochore. Cell 135: 1039–1052.
33. Liu ST, Rattner JB, Jablonski SA, Yen TJ (2006) Mapping the assembly pathways that specify formation of the trilaminar kinetochore plates in human cells. J Cell Biol 175: 41–53.
34. Okada M, Okawa K, Isobe T, Fukagawa T (2009) CENP-H-containing complex facilitates centromere deposition of CENP-A in cooperation with FACT and CHD1. Mol Biol Cell 20: 3986–3995.
35. Carroll CW, Milks KJ, Straight AF (2010) Dual recognition of CENP-A nucleosomes is required for centromere assembly. J Cell Biol 189: 1143–1155.
36. Carroll CW, Silva MC, Godek KM, Jansen LE, Straight AF (2009) Centromere assembly requires the direct recognition of CENP-A nucleosomes by CENP-N. Nat Cell Biol 11: 896–902.
37. Okada T, Ohzeki J, Nakano M, Yoda K, Brinkley WR, et al. (2007) CENP-B controls centromere formation depending on the chromatin context. Cell 131: 1287–1300.
38. Bergmann JH, Rodriguez MG, Martins NM, Kimura H, Kelly DA, et al. (2011) Epigenetic engineering shows H3K4me2 is required for HJURP targeting and CENP-A assembly on a synthetic human kinetochore. Embo J 30: 328–340.
39. Nakano M, Cardinale S, Noskov VN, Gassmann R, Vagnarelli P, et al. (2008) Inactivation of a human kinetochore by specific targeting of chromatin modifiers. Dev Cell 14: 507–522.
40. Meselson M, Stahl FW (1958) The replication of DNA in Escherichia coli. Proc Natl Acad Sci U S A 44: 671–682.
41. Misteli T (2001) The concept of self-organization in cellular architecture. J Cell Biol 155: 181–185.
42. Amano M, Suzuki A, Hori T, Backer C, Okawa K, et al. (2009) The CENP-S complex is essential for the stable assembly of outer kinetochore structure. J Cell Biol 186: 173–182.
43. Hellwig D, Munch S, Orthaus S, Hoischen C, Hemmerich P, et al. (2008) Live-cell imaging reveals sustained centromere binding of CENP-T via CENP-A and CENP-B. J Biophotonics 1: 245–254.
44. Kim H, Lee M, Lee S, Park B, Koh W, et al. (2009) Cancer-upregulated gene 2 (CUG2), a new component of centromere complex, is required for kinetochore function. Mol Cells 27: 697–701.
45. Shelby RD, Vafa O, Sullivan KF (1997) Assembly of CENP-A into centromeric chromatin requires a cooperative array of nucleosomal DNA contact sites. J Cell Biol 136: 501–513.
46. Tomkiel J, Cooke CA, Saitoh H, Bernat RL, Earnshaw WC (1994) CENP-C is required for maintaining proper kinetochore size and for a timely transition to anaphase. J Cell Biol 125: 531–545.
47. Hemmerich P, Weidtkamp-Peters S, Hoischen C, Schmiedeberg L, Erliandri I, et al. (2008) Dynamics of inner kinetochore assembly and maintenance in living cells. J Cell Biol 180: 1101–1114.
48. Ribeiro SA, Vagnarelli P, Dong Y, Hori T, McEwen BF, et al. (2010) A super-resolution map of the vertebrate kinetochore. Proc Natl Acad Sci U S A 107: 10484–10489.
49. Shelby RD, Monier K, Sullivan KF (2000) Chromatin assembly at kinetochores is uncoupled from DNA replication. J Cell Biol 151: 1113–1118.
50. Brenner S, Pepper D, Berns MW, Tan E, Brinkley BR (1981) Kinetochore structure, duplication, and distribution in mammalian cells: analysis by human autoantibodies from scleroderma patients. J Cell Biol 91: 95–102.
51. Bernat RL, Delannoy MR, Rothfield NF, Earnshaw WC (1991) Disruption of centromere assembly during interphase inhibits kinetochore morphogenesis and function in mitosis. Cell 66: 1229–1238.
52. Monier K, Mouradian S, Sullivan KF (2007) DNA methylation promotes Aurora-B-driven phosphorylation of histone H3 in chromosomal subdomains. J Cell Sci 120: 101–114.

OPEN ACCESS Freely available online

PLOS ONE

Step-Wise Assembly, Maturation and Dynamic Behavior of the Human CENP-P/O/R/Q/U Kinetochore Sub-Complex

Anja Eskat[1☯¤a], Wen Deng[2☯], Antje Hofmeister[1], Sven Rudolphi[1], Stephan Emmerth[3¤b], Daniela Hellwig[1¤c], Tobias Ulbricht[1], Volker Döring[1], James M. Bancroft[5], Andrew D. McAinsh[5], M. Cristina Cardoso[4], Patrick Meraldi[3], Christian Hoischen[1], Heinrich Leonhardt[2], Stephan Diekmann[1]*

1 Molecular Biology, FLI, Jena, Germany, **2** Department of Biology II, Center for Integrated Protein Science, Ludwig Maximilians University Munich, Planegg-Martinsried, Munich, Germany, **3** Institute of Biochemistry, ETH Zurich, Zurich, Switzerland, **4** Department of Biology,Technische Universität Darmstadt, Darmstadt, Germany, **5** Centre for Mechanochemical Cell Biology, Warwick Medical School, University of Warwick, Coventry, United Kingdom

Abstract

Kinetochores are multi-protein megadalton assemblies that are required for attachment of microtubules to centromeres and, in turn, the segregation of chromosomes in mitosis. Kinetochore assembly is a cell cycle regulated multi-step process. The initial step occurs during interphase and involves loading of the 15-subunit constitutive centromere associated complex (CCAN), which contains a 5-subunit (CENP-P/O/R/Q/U) sub-complex. Here we show using a fluorescent three-hybrid (F3H) assay and fluorescence resonance energy transfer (FRET) in living mammalian cells that CENP-P/O/R/Q/U subunits exist in a tightly packed arrangement that involves multifold protein-protein interactions. This sub-complex is, however, not pre-assembled in the cytoplasm, but rather assembled on kinetochores through the step-wise recruitment of CENP-O/P heterodimers and the CENP-P, -O, -R, -Q and -U single protein units. SNAP-tag experiments and immuno-staining indicate that these loading events occur during S-phase in a manner similar to the nucleosome binding components of the CCAN, CENP-T/W/N. Furthermore, CENP-P/O/R/Q/U binding to the CCAN is largely mediated through interactions with the CENP-N binding protein CENP-L as well as CENP-K. Once assembled, CENP-P/O/R/Q/U exchanges slowly with the free nucleoplasmic pool indicating a low off-rate for individual CENP-P/O/R/Q/U subunits. Surprisingly, we then find that during late S-phase, following the kinetochore-binding step, both CENP-Q and -U but not -R undergo oligomerization. We propose that CENP-P/O/R/Q/U self-assembles on kinetochores with varying stoichiometry and undergoes a pre-mitotic maturation step that could be important for kinetochores switching into the correct conformation necessary for microtubule-attachment.

Citation: Eskat A, Deng W, Hofmeister A, Rudolphi S, Emmerth S, et al. (2012) Step-Wise Assembly, Maturation and Dynamic Behavior of the Human CENP-P/O/R/Q/U Kinetochore Sub-Complex. PLoS ONE 7(9): e44717. doi:10.1371/journal.pone.0044717

Editor: Barbara Mellone, University of Connecticut, Storrs, United States of America

Received April 23, 2012; **Accepted** August 6, 2012; **Published** September 18, 2012

Funding: This work was supported by Deutsche Forschungsgemeinschaft (DFG DI 258/17-1, SPP1128, SPP1395), and Thüringer Aufbaubank (2007 FE 9011). The funders had no role in study design, data collection and analysis, decision to publish, or preparation of the manuscript.

Competing Interests: The authors have declared that no competing interests exist.

* E-mail: diekmann@fli-leibniz.de

☯ These authors contributed equally to this work.

¤a Current address: Institute of Biochemistry, ETH Zurich, Zurich, Switzerland
¤b Current address: Friedrich Miescher Institute for Biomedical Research, Basel, Switzerland
¤c Current address: HKI, Jena, Germany

Introduction

During mitosis, accurate chromosome segregation is essential for the correct transmission of the genetic material to the daughter cells. A multi-protein complex, the kinetochore, assembles at the centromere of each chromatid in order to mediate this function. Kinetochores contain an inner core that is present throughout the cell cycle [1,2], and a set of outer kinetochore proteins that stably associate with the inner core during mitosis [3,4]. The kinetochore is built from two major conserved protein networks, (1) the CCAN (constituitive centromere associated network) complex [5–13] which is associated to centromeric nucleosomes [5,14–16] that consist of repetitive α-satellite DNA containing the histone H3 variant CENP-A [17,18], and (2) the KMN network [7,19–27] which directly connects the kinetochore to microtubules [3,28,29]. Functionally, the CCAN is required for the efficient recruitment of CENP-A into centromeric nucleosomes at the end of mitosis [6,14,30,31] and the maintenance of centromeric chromatin, but is also involved in chromosome alignment, kinetochore fiber stability and bipolar spindle assembly [1,2,5,6,8,32–34]. The CCAN was suggested to establish, in interphase, an inner kinetochore structure which functions as an assembly platform for KMN network proteins in mitosis, and only the KMN proteins then connect the inner kinetochore to microtubules [3]. However, ectopical CENP-T and -C alone are able to establish a functional outer kinetochore [16,35] indicating that instead of being only a structural platform, the CCAN seems to be a regulator of the mitotic kinetochore-microtubule attachment [36].

The CCAN proteins CENP-U, -O, -P, -Q, and -R were identified as a CCAN subclass (named CENP-O class proteins)

[3,5,6,10,37]. CENP-PORQU proteins are non-essential showing, when depleted, common mitotic defects and slower proliferation rates [6,10,33,38]. Kinetochore localization of CENP-PORQU is interdependent [5,10,36]. In chicken DT40 cells, and when these genes are expressed in *E. coli*, CENP-O, -P, -U and -Q form a stable complex to which CENP-R can associate [10]. These data describe the CENP-PORQU complex as a stable unit which might function as a structural element in the CCAN. However, CENP-PORQU proteins have different protein specific functions: CENP-U [39] as well as CENP-Q [36] are able to bind to microtubules, only depletion of CENP-O seems to destabilise microtubule bundles at kinetochores influencing bipolar spindle assembly [34,39], and CENP-U interacts with Hec1, an interaction negatively regulated by Aurora-B kinase [39]. In the complex, CENP-P is closely associated with CENP-O, and CENP-U binds to CENP-Q [10,40–42]. In order to resolve these different views, we analysed protein binding, complex architecture and dynamics of the human kinetochore CENP-PORQU sub-complex by various *in vivo* techniques.

Materials and Methods

Plasmids

Plasmids pIC133, pIC190, pIC141, pIC140, and pIC235 encoding LAP-CENP-K, -Q, -P, -O, respectively -R fusion proteins were a kind gift of Dan Foltz and Iain Cheeseman. The full length cDNA clone of CENP-L, IRAUp969 EO882D, was from RZPD, Berlin, Germany). They were used for amplification of full length CENP-K, -L, -Q, -P, -O, and -R by PCR (Expand high fidelity^{PLUS} PCR System, Roche, Penzberg, Germany) applying forward primer 5′-GGGGACAAGTTTGTACAAAAA-AGCAGGCTTCGAAAACCTGTATTTTCAGGGC*GCCACCA-TGG*GCATGAATCAGGAGGATTTAGATCC -3′ and reverse primer 5′- GGGGACCACTTTGTACAAGAAAGCTGGGTC-TGATGGAAAGCTTCTAATCTTATT -3′ for CENP-K, forward primer 5′- GGGGACAAGTTTGTACAAAAAAGCAGG-CTTCGAAAACCTGTATTTTCAGGGC*GCCACC*ATGGATT-CTTACAGTGCACCAG -3′ and reverse primer 5′- GGGGAC-CACTTTGTACAAGAAAGCTGGGTCTCAATTTGAAAAAT-TGCCAGTTCTG for CENP-L, forward primer 5′- GGGGA-CAAGTTTGTACAAAAAAGCAGGCTTCGAAAACCTGTAT-TTTCAGGGCGCCACCATGGGCATGTCTGGTAAAGCAAA-TGCTTC -3′ and reverse primer 5′- GGGGACCACTTTGTA-CAAGAAAGCTGGGTAGATGCATCCAGTTTCTTATAGG -3′ for CENP-Q, forward primer 5′- GGGGACAAGTTTGTA-CAAAAAAGCAGGCTTCGAAAACCTGTATTTTCAGGGC-GCCACCATGGACGCAGAGCTGGCAGA -3′ and reverse primer 5′- GGGGACCACTTTGTACAAGAAAGCTGGGTG-TTGTTCTCCTCTGCACAAAGC -3′ for CENP-P, forward primer 5′- GGGGACAAGTTTGTACAAAAAAGCAGGCTT-CGAAAACCTGTATTTTCAGGGCGCCACCATGGAGCAG-GCGAACCCTTT -3′ and reverse primer 5′- GGGGACCAC-TTTGTACAAGAAAGCTGGGTGGAGACCAGACTCATAT-CCAAC -3′ for CENP-O, and forward primer 5′- GGGGAC-AAGTTTGTACAAAAAAGCAGGCTTCGAAAACCTGTATT-TTCAGGGCGCCACCATGGGCATGCCTGTTAAAAGATCA-CTGAA -3′ and reverse primer 5- GGGGACCACTTTGTA-CAAGAAAGCTGGGTGTTTAAAATGGCTTTAAGGAATT-CA -3′ for CENP-R. The CENP-Q, -P, -O, and -R harbouring linear PCR fragments were transferred into vector pDONR221 by BP recombination reaction (Invitrogen, Carlsbad, CA, USA). After verification by sequencing (MWG Biotech, Ebersberg, Munich, Germany), the genes were cloned by LR recombination reactions into various modified pFP-C and pFP-N (BD Biosciences, Clontech, Palo Alto, CA, USA) based Destination vectors. As the result we obtained expression vectors carrying the genes coding for CENP-Q, -P, -O, and -R fused to the C-termini as well as to the N-termini of EGFP and mCherry. In the constructed fluorescent proteins (FP)-CENP-Q, -P, -O, and -R, the amino acid (aa) linker between the fused proteins is SGTSLYKKAGFENLYFQGAT. Due to the cloning protocol, the aa sequence TQLSCTKW is added to the C-terminal ends of FP-CENP-Q, -P, -O, and -R. In the constructs where CENP-Q, -P, -O, and -R are fused to the N-termini of EGFP respectively mCherry, the (aa) linker is TQLSCTKWLDPPVAT. The cloning of CENP-U and -C [43] and CENP-N [44] have been described previously. Vector pIRES2 used for the simultaneous expression of EGFP and mRFP, was a friendly gift of J. Langowski (Heidelberg). For expression of a mRFP-EGFP fusion protein, we digested vector pmRFP-C1 with SnaBI and XmaI and ligated the resulting 1012 bps DNA fragment containing mRFP into a 7106 bp DNA obtained from a SnabI-XmaI digest of vector pH-G-C. In the resulting Gateway expression vector pH-mR-G-C, the amino acid linker between mRFP and EGFP is SGLRSRAQASNSAVDG-TAGPVAT. Full length protein expression of the fusion constructs was confirmed by Western Blots.

Live cell FRET measurements

FRET was measured by applying the acceptor photo-bleaching method using the FRET pair EGFP-mCherry. Co-transfected HEp-2 cells grown on coverslips were analyzed using a confocal laser scanning microscope (LSM 510 Meta) and a C-Apochromat 63×/1.2NA oil immersion objective (Carl Zeiss, Jena, Germany). EGFP fluorescence was excited with the Argon 488 nm laser line and analyzed using the Meta detector (ChS1+ChS2: 505–550 nm). mCherry fluorescence was excited with the 561 nm laser line (DPSS 561-10) and detected in one of the confocal channels using a 575–615 nm band-pass filter. To minimize cross talk between the channels, each image was collected separately in the multi-track-mode, i.e. both fluorophores were exited and recorded specifically and separately. Cells moderately expressing both fusion proteins with comparable expression levels were selected for analysis. Acceptor photo-bleaching was achieved by scanning a region of interest (ROI) including up to five centromeres of a nucleus 50 times (scans at 1.6 µsec pixel time) using the 561 nm laser line at 100% intensity. Bleaching times per pixel were identical for each experiment, however, total bleaching times varied depending on the size of the bleached ROIs. 4 donor and acceptor fluorescence images were taken before and up to 4 images after the acceptor photo-bleaching procedure to assess changes in donor and acceptor fluorescence. To minimize the effect of photo-bleaching of the donor during the imaging process, the image acquisition was performed at low laser intensities. To compare the time course of different experiments, donor intensities in the ROI were averaged and normalized to the intensity measured at the first time point after photo-bleaching, and acceptor intensities in the ROI were averaged and normalized to the mean intensity measured at time points 2–4 before photo-bleaching. The FRET efficiency was calculated by comparing the fluorescence intensity (I_{DA}) before bleaching (in presence of the acceptor) with the intensity (I_D) measured after bleaching (in the absence of the acceptor) according to $E = 1 - I_{DA}/I_D$. The FRET efficiencies of numerous bleached and unbleached locations were compared by a paired t-test ($\alpha = 0.05$). The difference between the means is a measure for the FRET-value, which was interpreted to have occurred when the paired t-test revealed a statistically significant difference between the two input groups with a p-value below 0.001. A p-value >0.001 was interpreted as an indication for insignificant FRET.

In two cases, the acceptor-bleaching FRET data were confirmed by additional fluorescence lifetime FLIM experiments. In FLIM experiments, the donor fluorescence lifetime was determined by time-correlated single photon counting (TCSPC) in living human HEp-2 cells. For donor fluorescence excitation, a pulsed picosecond diode laser (LDH Series, PicoQuant, Berlin, Germany) with a frequency of 20 MHz along with a dedicated driver (PDL Series, PicoQuant) was used. Via a fiber coupling unit, the excitation light was guided into a confocal laser scanning microscope (LSM 510 Meta). Laser power was adjusted to give average photon counting rates of 10^4–10^5 photons/sec (0.0001–0.001 photon counts per excitation event) or less to avoid pulse pile-up. Images of 256×256 pixels were acquired with a 63× C-Apochromat water immersion objective (NA 1.20, Carl Zeiss). Photons emitted by the sample were collected by the water immersion objective and detected by a single photon avalanche diode (PDM series, PicoQuant). The data were acquired by the PicoHarp 300 TCSPC module (PicoQuant) working in the TTTR mode (time-tagged time-resolved). To calculate the fluorescence lifetime, the SymPhoTime software package (v4.7, PicoQuant) was used. Selected areas of the images corresponding to single centromeres (resulting in the fluorescence lifetime histograms) or the sum of all centromeric regions were fitted by maximum likelihood estimation (MLE). Depending on the quality of a fit indicated by the value of χ^2, a mono- or bi-exponential fitting model including background was applied. A model was rejected when χ^2 exceeded a value of 1.5. In this way, the presence of scattered light in few measurements could be identified and separated. However, due to low photon numbers and too close time constants, the simultaneous presence of two different donor fluorescence lifetimes for complexes with donor-only and donor plus acceptor in one centromere could not be separated by a bi-exponential fit. A donor fluorescence lifetime obtained from a centromere in a cell co-expressing donor and acceptor molecules was considered to be significantly different from the control measurement, when the lifetime differed from the mean of the control values by >3 standard deviations. The FRET efficiency was calculated by comparing the donor fluorescence lifetime (τ_{DA}) in the presence of the acceptor with the respective fluorescence lifetimes (τ_D) of control measurements obtained in absence of an acceptor following $E = 1-\tau_{DA}/\tau_D$.

F3H

BHK cells containing a *lac* operator repeat array [45] were cultured in DMEM medium with 10% FCS and seeded on coverslips in 6-well plates for microscopy. After attachment, cells were co-transfected with expression vectors for the indicated fluorescent fusion proteins and a LacI-GBP fusion [46,47] using polyethylenimine (Sigma, St. Louis, USA). After about 16 hrs cells were fixed with 3.7% formaldehyde in PBS for 10 minutes, washed with PBST (PBS with 0.02% Tween), stained with DAPI and mounted in Vectashield medium (Vector Laboratories, Servison, Switzerland).

Samples were analyzed with a confocal fluorescence microscope (TCS SP5, Leica, Wetzlar, Germany) equipped with a 63×/1.4 numerical aperture Plan-Apochromat oil immersion objective as described [47]. DAPI, EGFP and mCherry were excited by 405 nm diode laser, 488 nm argon laser and 561 nm diode-pumped solid-state laser, respectively. Images were recorded with a frame size of 512×512 pixels.

Cell culture, transfection and Western Blots

HeLa, HEp-2 and U2OS cells (ATCC, Manassas, USA) were cultured and Western blots were carried out as described [44,48]. In order to determine cell cycle dependent CENP-O/Q/P levels, HEp-2 or HeLa cells were synchronised by double-thymidine block. Aliquots of equal cell numbers were taken after 2, 4, 6, 8 and 10 hrs after release and lysed. In the Western blot, CENP-O [33], CENP-P [36] and CENP-Q (Rockland, Gilbertsville, USA) are identified by specific primary antibodies which are then detected by fluorescently labelled secondary antibody (Molecular Probes, Eugene, USA). CENP-O/P/Q amounts are quantified by the ODYSSEY Infrared Imaging System (LiCor, Lincoln, USA) following the protocol of the manufacturer.

Fluorescence Cross-Correlation Spectroscopy (FCCS)

FCCS analyses [49,50] were performed at 37°C on an LSM 710 Confocor3 microscope (Carl Zeiss, Jena, Germany) using a C-Apochromat infinity-corrected 40×/1.2 NA water objective. U2OS cells were double transfected with vectors for the simultaneous expression of EGFP and mCherry fusion proteins and analysed. On cells expressing both fusion proteins at relatively low and comparable levels, we selected spots for the FCCS measurements in areas of the nucleoplasm which were free of kinetochores. For illumination of the EGFP-fusion proteins, we used the 488 nm laser line of a 25 mW Argon/2-laser (Carl Zeiss) and for simultaneous illumination of the mCherry fusion proteins a DPSS 561-10-laser (Carl Zeiss), both at moderate intensities between 0.2 and 0.5%. The detection pinhole was set to a relatively small diameter of 40 µm (corresponding to about 0.8 airy units). After passing a dichroic beam splitter for APDs (avalange photodiode detector; NTF 565), the emission of mCherry was recorded in channel 1 through a BP-IR 615–680 nm bandpath filter by an APD (Carl Zeiss), whereas the emission of EGFP was simultaneously recorded in channel 2 through a BP-IR 505–540 nm bandpath filter by a second APD. Before each measurement, we analysed possible crosstalk between the channels and used only cells without or with very little crosstalk. In addition, measurements with autocorrelation values below 1.06 for both, the mRFP channel as well as the EGFP channel, were not further analysed. For the measurements, 10×10 time series of 10 sec each were simultaneously recorded for mCherry and for EGFP. After averaging, the data were superimposed for fitting with the Fit-3Dfree-1C-1Tnw model of the ZEN-software (Carl Zeiss), a diffusion model in three dimensions with triplet function. Applying this procedure, we obtained autocorrelations of channels 1 and 2 as well as the cross-correlation of channels 1 versus channel 2. Before starting a set of experiments, the pinhole was adjusted. As negative control, U2OS cells were transfected with vector pIRES2, separately expressing EGFP and mRFP as single molecules with fluorescence intensities comparable to those in the FCCS analysis with CENP fusion proteins. As a positive control, U2OS cells were transfected with pH-mR-G-C expressing a mRFP-EGFP fusion protein, again with fluorescence intensities comparable to those in the FCCS analysis with CENP fusion proteins.

Cellular imaging

In vivo and *in situ* cellular imaging including immuno-fluorescence, SNAP-tag analysis, FRAP, RICS and cell cycle sychronisation were conducted as described in Orthaus et al. [48,51], Hellwig et al. [43,44] and McClelland et al [8]. For immuno-flourescence, primary antibodies were used at 1:250 (PCNA), 1:300 (anti-CENP-Q), 1:250 (CREST) with DAPI at 1:2000.

Results

CENP-O class proteins form a tightly packed complex

In chicken DT40 cells, the CENP-O class proteins form a tight kinetochore sub-complex [10]. Here we analysed the CENP-O class protein packaging at kinetochores in living human cells by measuring which proteins are in close proximity. We tagged all five CENP-O class proteins with fluorescent proteins, either EGFP or mCherry, at either termini, and confirmed by live cell imaging in human U2OS cells that all tagged CENP-O class proteins localise to kinetochores during interphase and mitosis, consistent with published results [5,6,10,33,36,39]. This kinetochore localisation was independent of which terminus of the CENP proteins was tagged.

Then, by FRET we measured the proximity between chromophores tagged to CENP-O class proteins. FRET between the donor fluorophore (here: EGFP) and the acceptor fluorophore (here: mCherry) can only generate a positive result when the distance between donor and acceptor is less than ~10 nm. When FRET occurs, both the intensity and lifetime of the donor fluorescence decrease while the intensity of the acceptor emission increases. We measured the FRET donor fluorescence intensity with or without photo-inactivation of the acceptor (acceptor-photo-bleaching FRET, AB-FRET) and, in order to confirm our AB-FRET results, in two cases also the donor fluorescence lifetime (FLIM). In AB-FRET, the acceptor chromophore is destroyed by photo-bleaching, thereby preventing FRET from the donor to the acceptor. Thus, when the donor is in close proximity to the acceptor (sufficient for FRET, <10 nm), photo-bleaching of the acceptor results in an observable increase in donor fluorescence. In our experiments, two separate kinetochore locations were identified in each image (marked "1" and "2"; Fig. 1A and 1D). In spot "2" the acceptor (CENP-R-mCherry (Fig. 1A), CENP-P-mCherry (Fig. 1D)) was photo-bleached, while spot "1" was not photo-bleached, serving as an internal control for any non-FRET effects. During bleaching of the acceptor (CENP-R-mCherry) in spot 2, the donor (EGFP-CENP-U) fluorescence intensity significantly increased indicating that FRET occurred between EGFP-CENP-U and CENP-R-mCherry (Fig. 1B). Careful quantification indicated that such FRET transfer occurred in 60% of the cases, yielding a FRET efficiency E_{FRET} between 6 and 18% (40 bleached spots in 18 cells, black bars in Fig. 1C). The unbleached control spots show a narrow fluorescence variation E_{var} around zero (39 bleached spots in 18 cells, grey bars in Fig. 1C). The E_{FRET} distribution is significantly different from the E_{var} control distribution ($p<0.001$). Such experiments demonstrated that the majority of pairs gave a positive FRET signal suggesting that the CENP-PORQU subunits are closely associated (see Table 1). Importantly, a number of pairs did not show FRET: We detected no FRET between EGFP-CENP-Q/CENP-P-mCherry (Fig. 1D–F). Here, after acceptor-bleaching, the donor fluorescence did not increase (Fig. 1E) and the distribution of the E_{FRET} values (black bars, Fig. 1F) superimposes with the distribution of the E_{var} control values (grey bars). Furthermore, we did not observe FRET between EGFP-CENP-P/CENP-O-mCherry and between EGFP-CENP-U/CENP-O-mCherry (see Table 1). For CENP-Q-EGFP and mCherry-CENP-P and for CENP-P-EGFP and mCherry-CENP-O, we confirmed these results by measuring FRET at kinetochores in the lifetime domain (FLIM) by time-correlated single photon counting (TCSPC) using the same fluorescent protein FRET pair EGFP-mCherry. This approach is less error prone compared to acceptor-bleaching FRET in the intensity domain, however, it is considerably more elaborate and time-consuming. We determined the CENP-Q-EGFP donor lifetime in the absence of an acceptor as $\tau = 2.45 \pm 0.10$ nsec. When the acceptor is close, the donor life time decreases due to energy transfer to the acceptor: for CENP-Q-EGFP/mCherry-CENP-P we measured $\tau = 2.08 \pm 0.04$ nsec and for CENP-P-EGFP/mCherry-CENP-O we measured $\tau = 2.16 \pm 0.05$ nsec. The FLIM results (marked by "F" in Table 1) indicate the proximity between CENP-Q and -P as well as between CENP-P and -O and confirm our acceptor-bleaching FRET data. We conclude that in human cells at kinetochores, CENP-O class proteins are in close proximity to one another. In earlier studies we had detected FRET between the CENP-U N-terminal region and the N-termini of CENP-B and CENP-I, but not to the N-termini of CENP-A and CENP-C [43].

If the orientation of the fluorophore dipole moment of the acceptor relative to that of the donor were known, or at least one of them would rotate freely faster than nanoseconds, a more detailed distance between donor and acceptor could be deduced from the measured E_{FRET} values. In our live cell experiments however, this information is not available to us. We therefore do not deduce defined distance values but interpret the appearance of FRET as an indication that donor and acceptor chromophores are close to one another within 10 nm. Our FRET data depend on which protein terminus is tagged: if the two protein termini are clearly separated in space, a fluorophore fused to one terminus might show FRET to another protein while the fluorophore fused to the other terminus might not. In a number of cases, we could not detect FRET between two fusion proteins. Measuring no FRET signal might either be due to donor and acceptor fluorophores being distal (>10 nm) or, alternatively, that donor and acceptor dipole moments are oriented relative to one another in an unfavorable way so that FRET cannot occur although donor and acceptor are close. Therefore, observing no FRET signal cannot be used for structural information.

PORQU undergoes a post-loading oligomerisation step

Recombinant CENP-Q that is expressed and purified form *E. coli* lysates, exists as a soluble homo-octameric complex [36]. We therefore asked if CENP-Q oligomerises at kinetochores in living human cells. Indeed, we observed FRET at kinetochores between the N-termini of CENP-Q and between its C-termini in interphase cells, suggesting that CENP-Q oligomerises when kinetochore-bound. In order to find out when in the cell cycle CENP-Q oligomerizes, we carried out cell cycle dependent FRET measurements between C- and N-termini of CENP-Q (see Table 1, Fig. 2). U2OS cells were synchronised by double thymidine block and released into S-phase. Subsequent cell cycle phases were identified by CENP-F and PCNA staining. We found no FRET in G1, early and mid S-phase, however, we detected a significant FRET signal in late S-phase for both, the CENP-Q N- and C-termini, and in G2 for the CENP-Q N-termini (Fig. 2). Consistent with this, quantitative immuno-flourescence demonstrates that CENP-Q protein levels increase at kinetochores during S-phase and become maximal in late S-phase (see below). We also detected a FRET proximity between two CENP-U N-termini at kinetochores in late but not in early or middle S-phase (data not shown).

PORQU proteins show multiple pair-wise interactions

Then we asked which of the CENP-O class proteins is able to interact with other protein members of this class. In the mammalian three-hybrid (F3H) assay applied here [46,47], EGFP tagged CENP-O class proteins (bait) were recruited to the *lac* operator repeat array by the GFP-binding protein fused to the Lac repressor (GBP-LacI) forming a green spot in the nucleus (Fig. 3).

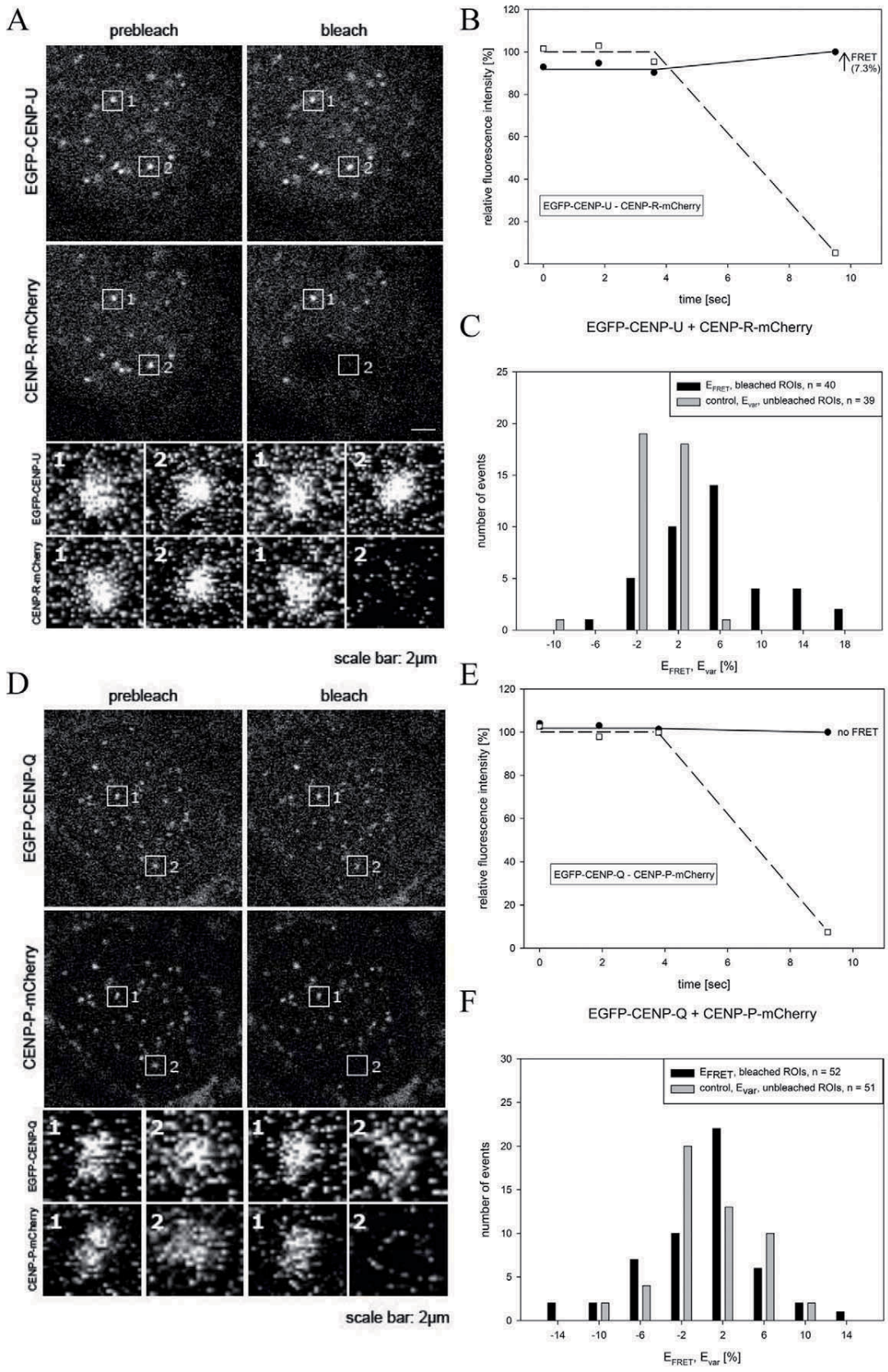
A
prebleach
bleach
EGFP-CENP-U
CENP-R-mCherry
scale bar: 2µm
B
relative fluorescence intensity [%]
time [sec]
FRET (7.3%)
EGFP-CENP-U - CENP-R-mCherry
C
EGFP-CENP-U + CENP-R-mCherry
number of events
E_FRET, bleached ROIs, n = 40
control, E_var, unbleached ROIs, n = 39
E_FRET, E_var [%]
D
prebleach
bleach
EGFP-CENP-Q
CENP-P-mCherry
scale bar: 2µm
E
relative fluorescence intensity [%]
time [sec]
no FRET
EGFP-CENP-Q - CENP-P-mCherry
F
EGFP-CENP-Q + CENP-P-mCherry
number of events
E_FRET, bleached ROIs, n = 52
control, E_var, unbleached ROIs, n = 51
E_FRET, E_var [%]

Figure 1. Acceptor-bleaching FRET of the protein pairs EGFP-CENP-U/CENP-R-mCherry (FRET signal) and EGFP-CENP-Q/CENP-P-mCherry (no FRET signal). Typical HEp-2 cell nuclei are displayed in (A) and (D) showing centromere location of all four CEN proteins. Two of these locations, spot 1 and spot 2 in each of the two graphs, were selected for fluorescence intensity analysis before and after acceptor bleaching (see enlargements below). Spot 1 served as control and showed no detectable intensity change. At spot 2, the acceptor fluorophore mCherry was bleached (compare pre-bleach and post-bleach in (A) and (D)). In (B) and (E), the time course of the fluorescence intensity of the donor and the acceptor of both FRET pairs are shown. The acceptor intensities in the ROI ("region of interest"; open squares) were averaged and normalized to the mean intensity measured at the three time points before bleaching. The donor intensities in the ROI were averaged and normalized to the intensity measured at the time point after bleaching. Bleaching of the acceptor resulted in a fluorescence intensity increase of the donor (black dots) for EGFP-CENP-U (B) indicating the presence of FRET (see arrow), but no fluorescence intensity increase for EGFP-CENP-Q (E) indicating the absence of FRET. (C) and (F): Donor fluorescence intensity variation observed during acceptor bleaching normalized to the intensity measured at the first time point after bleaching. Control: spot 1 (acceptor not bleached) yielding E_{var} (grey bars), FRET measurement: spot 2 (acceptor bleached) yielding E_{FRET} (black bars). For protein pairs indicated, number of observed single cases (grouped into E_{var} or E_{FRET} value ranges of 4%) displayed versus values of E_{var} or E_{FRET}. (C) EGFP-CENP-U (donor) and CENP-R-mCherry (acceptor): distribution of E_{FRET} (40 bleached kinetochores) is clearly distinct from the distribution of E_{var} (39 non-bleached kinetochores) indicating FRET. (F): EGFP-CENP-Q (donor) and CENP-P-mCherry (acceptor): distribution of E_{FRET} (52 bleached kinetochores) superimposes the distribution of E_{var} (51 non-bleached kinetochores) indicating no FRET.
doi:10.1371/journal.pone.0044717.g001

Co-expressed mCherry-tagged CENP-O class proteins (prey) may either interact with the EGFP-tagged protein at the *lac* operator array (visible as red spot and yellow in the overlay) or may not interact resulting in a disperse distribution. For each mCherry fusion, EGFP was used to control for unspecific interactions. In the upper two rows of Fig. 3A, the clear interaction between EGFP-CENP-O and mCherry-CENP-P as well as EGFP-CENP-P and mCherry-CENP-O are shown. The lower two rows show the corresponding results for CENP-O and CENP-Q. While EGFP-CENP-Q did not interact with and recruit mCherry-CENP-O to the *lac* spot, we found a very weak interaction in the reverse combination. Such differences for reverse combinations might be explained by sterical hindrance at the interaction site due to the attachment to GBP-LacI for one but not the other tagged terminal region. All results of this F3H interaction assay are listed in Table 2. The results of this CENP-O class protein interaction analysis indicate strong interactions between particular members of this class (Fig. 3B). CENP-O, -P and -Q each are able to strongly recruit and thus specifically bind two, while CENP-U and -R are able to recruit three of the remaining four proteins. In addition, CENP-U and CENP-R are able to bind to themselves. We detected homo-interaction of CENP-R also by a Yeast-two-Hybrid (Y2H) assay. CENP-U binding to itself is supported by our FRET data indicating close proximity between CENP-U N-termini in late S-phase (see above). Our data that CENP-P is closely associated with CENP-O, and CENP-U with CENP-Q, agree well with published results [10,41,42]; here we detected an additional weaker interaction between CENP-Q and CENP-R. However, none of the CENP-O class proteins is able to recruit all four other proteins of this class which would be expected when the

Table 1. FRET interactions between CENP-O class proteins.

EGFP fusion	mCherry fusion	p	FRET
EGFP-CENP-P	mCherry-CENP-O	<0.001	++
EGFP-CENP-P	CENP-O-mCherry	0.093	−
CENP-P-EGFP	mCherry-CENP-O	<0.001	++F
CENP-P-EGFP	CENP-O-mCherry	<0.001	++
EGFP-CENP-Q	mCherry-CENP-O	<0.001	++
EGFP-CENP-Q	CENP-O-mCherry	<0.001	++
EGFP-CENP-Q	mCherry-CENP-P	<0.001	++
EGFP-CENP-Q	CENP-P-mCherry	0.724	−
EGFP-CENP-Q	mCherry-CENP-Q	<0.001	++
CENP-Q-EGFP	CENP-Q-mCherry	<0.001	++
CENP-Q-EGFP	mCherry-CENP-P	<0.001	++F
EGFP-CENP-U	mCherry-CENP-O	<0.001	++
EGFP-CENP-U	CENP-O-mCherry	0.655	−
EGFP-CENP-U	mCherry-CENP-P	0.003	+
EGFP-CENP-U	CENP-P-mCherry	<0.001	++
EGFP-CENP-U	mCherry-CENP-Q	<0.001	++
EGFP-CENP-U	mCherry-CENP-R	<0.001	++
EGFP-CENP-U	CENP-R-mCherry	<0.001	++
CENP-U-EGFP	mCherry-CENP-P	<0.001	++
EGFP-CENP-B	CENP-Q-mCherry	<0.001	++
EGFP-CENP-O	mCherry-CENP-K	<0.001	++
CENP-O-EGFP	mCherry-CENP-K	0.004	+
EGFP-CENP-R	mCherry-CENP-K	<0.001	++
CENP-R-EGFP	mCherry-CENP-K	<0.001	++
EGFP-CENP-U	mCherry-CENP-K	<0.001	++
CENP-U-EGFP	mCherry-CENP-K	0.167	−
EGFP-CENP-U	mCherry-CENP-U	<0.001	++
CENP-N-EGFP	mCherry-CENP-K	<0.001	++

The FRET pair EGFP-mCherry is used. "F" indicates that for these fusions FRET was detected also by FLIM. ++: strong FRET, +: weak FRET, −: no FRET.
doi:10.1371/journal.pone.0044717.t001

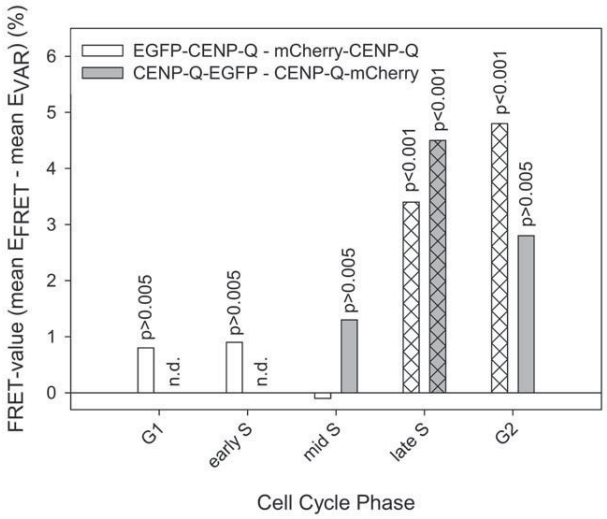

Figure 2. Cell cycle-dependent FRET between CENP-Q C- (grey bars) and N-termini (white bars). In late S-phase and G2, significant FRET is observed ($p<0.001$). In G1, early and mid S-phase, no FRET is observed ($p>0.005$).
doi:10.1371/journal.pone.0044717.g002

complex pre-forms in the nucleoplasm. Furthermore, ectopic recruitment to the *lac* operator repeat array obviously is not strong enough to enable indirect binding: e.g. CENP-L recruits CENP-R, and CENP-R recruits CENP-Q, but CENP-L is not able to attrack CENP-Q to this site. Thus, this F3H assay is, to a large extent, specific for direct interactions.

CENP-PORQU subcomplex contacts other CCAN proteins

Kinetochore localization is determined by CENP-A which is recognized by CENP-N and CENP-C [14–16]. CENP-L binds to the C-terminal region of CENP-N *in vitro* [14] and CENP-K kinetochore localisation depends on the presence of CENP-N and -C [5,8,14,52]. We therefore asked, if these kinetochore proteins, being directly or closely linked to CENP-A, are able to recruit single CENP-PORQU proteins or the whole complex to an ectopic chromatin site in human cell nuclei *in vivo*. We studied the interaction of CENP-C, -L, -K and -N with CENP-PORQU proteins by F3H; the results are listed in Table 2 and displayed in Fig. 3B. CENP-N shows binding to CENP-R and some weak binding to CENP-U, however, only for mCherry-tagged CENP-N (prey) while EGFP-tagged CENP-N (bait) does not show any interaction with CENP-PORQU proteins. CENP-L shows strong binding to CENP-R and moderate binding to CENP-U (strong in one, weak in the other version; see Table 2) and very weak binding to CENP-C (only in one orientation). Furthermore, RFP-tagged CENP-L also shows weak interactions with CENP-Q and CENP-K. Next to CENP-L, also CENP-K shows strong interactions with CENP-PORQU proteins: CENP-K strongly interacts with CENP-O and -U, moderately with CENP-R (strong in one, weak in the other version; see Table 2), and in one version weakly with CENP-Q. CENP-K also weakly binds to itself. By Y2H we detected an interaction between CENP-K and CENP-O, consistent with results of McClelland et al. [8], and an interaction between CENP-K and CENP-H, supporting data of Qui et al. [53], however no interaction had been detected by Y2H between CENP-O and either CENP-H or CENP-N [8]. We thus conclude that to some extend CENP-N, but more efficiently CENP-L and even more so CENP-K mainly recruit CENP-O, -U and -R to kinetochores but much less so CENP-Q, and not CENP-P. This finding agrees with results of Okada et al. [6] who observed in human and DT40 cells that the localization of CENP-O, -P, -Q and -H was disrupted in CENP-K and CENP-L depleted cells. Our results extend their observations by identifying the pairwise interactions responsible for the observed data: Potentially CENP-P and CENP-Q are disrupted from CENP-K and -L depleted cells due to being members of the CENP-PORQU complex and not due to specific protein-protein interactions. Similarly, the dependence of CENP-U kinetochore localization on the presence of CENP-H and -I [38] might be explained by CENP-H and -I being required for CENP-K binding which then recruits the CENP-PORQU complex. F3H yields more direct data on protein-protein interactions than depletion experiments which by their very nature also influence the presence of proteins down-stream of the depleted protein.

We observed no recruitment to the ectopic chromatin site of any CENP-PORQU protein by CENP-C. Furthermore, CENP-L and -N do not recruit all five CENP-PORQU proteins, again indicating that the CENP-PORQU complex does not pre-form in the nucleoplasm.

We confirmed these F3H results by FRET studies. We measured the close neighbourhood of CENP-K to several CENP-PORQU proteins and to CENP-N, and found proximities between the N-terminus of CENP-K with both termini of CENP-R, the N-termini of CENP-O and -U and to the C-terminus of CENP-N (see Table 1). These results place CENP-K inbetween CENP-N and the CENP-PORQU proteins.

PORQU does not preassemble in the cytoplasm

In order to analyse CENP-PORQU complex pre-assembly, in interphase we measured the mobility of the five CENP-O class proteins in the nucleoplasm of human U2OS cells by Raster Image Correlation Spectroscopy (RICS) [54] and found fast mobility between 4.7 and 5.9 ($\pm$15%) μm^2/sec. The proteins are thus more mobile than other inner kinetochore proteins [44,55]. The experimental variation of the measured mobilities, however, does not allow for a conclusion on multimerisation. We therefore performed Fluorescence Cross-Correlation Spectrometry (FCCS) studies to determine if CENP-O class proteins form hetero-dimers in the nucleoplasm. In double-transfected U2OS cells we analysed various protein pairs: EGFP-CENP-O/mCherry-CENP-P, EGFP-CENP-P/mCherry-CENP-Q, EGFP-CENP-R/mCherry-CENP-Q, EGFP-CENP-Q/mCherry-CENP-Q, CENP-O-EGFP/mCherry-CENP-Q, EGFP-CENP-U/mCherry-CENP-Q, EGFP-CENP-R/mCherry-CENP-R, EGFP-CENP-R/CENP-R-mCherry, CENP-U-EGFP/CENP-U-mCherry, CENP-U-EGFP/mCherry-CENP-U and EGFP-CENP-U/mCherry-CENP-O. For these protein pairs we found unequivocal cross-correlation only between CENP-O and CENP-P. From 12 cells, all 12 showed cross-correlation indicating that CENP-O and CENP-P move together, i.e. they are part of one and the same complex in the nucleoplasm outside kinetochores. The cross-correlation analysis (Fig. 4A) resulted in a correlation of 1.020 (Fig. 4A, insert b) indicating that 29% of the molecules are co-migrating in the nucleoplasm. As negative control, U2OS cells were analysed separately expressing EGFP and mRFP as single molecules. The cross-correlation curve (Fig. 4B) resulted in a value of 1.001 (Fig. 4B, insert b) indicating the absence of any complexation between EGFP and mRFP. As a positive control, U2OS cells were transfected with pH-mR-G-C expressing a mRFP-EGFP fusion protein. Cross-correlating the two channels against each other, we obtained a value of 1.029 indicating that about 50% of the molecules are detected as a complex (Fig. 4C). We obtained similar cross-correlation values for the fusion EGFP-mCherry, in agreement with results of Kohl et al. [56]. For such fusion proteins, 100% cross correlation should be observed. The lower value of 50% could be explained by a much slower maturation and lower stability of mRFP compared to EGFP: EGFP molecules bound to an immature mRFP are interpreted by FCCS as free molecules. Thus, cross-correlation values seem to underestimate the percentage of co-migrating molecules. Consequently, hetero-dimerisation of EGFP-CENP-O and mCherry-CENP-P probably is higher than the calculated 20–30%, we estimate 40–60%.

In 2 out of 12 analyzed cells, a weak cross-correlation ($\sim$10%) was observed for CENP-Q and CENP-R indicating that in a few cases CENP-Q and CENP-R co-migrate in the nucleoplasm outside kinetochores. The other analyzed protein pairs showed no cross-correlation demonstrating that the CENP-PORQU complex does not pre-form in the nucleoplasm outside kinetochores. CENP-R and CENP-U are able to bind to themselves at an ectopic chromatin site (see above). However, by FCCS we did not detect any cross correlation, clearly indicating that these proteins do not stably aggregate in the nucleoplasm. Recombinant CENP-Q can oligomerise to octamers [36] and, when kinetochore-bound, oligomerises in late S-phase, as detected by FRET (see above). In the nucleoplasm, however, CENP-Q does not form di- or multimers, as shown here by FCCS. This FCCS result is confirmed by the absence of a FRET signal between two tagged

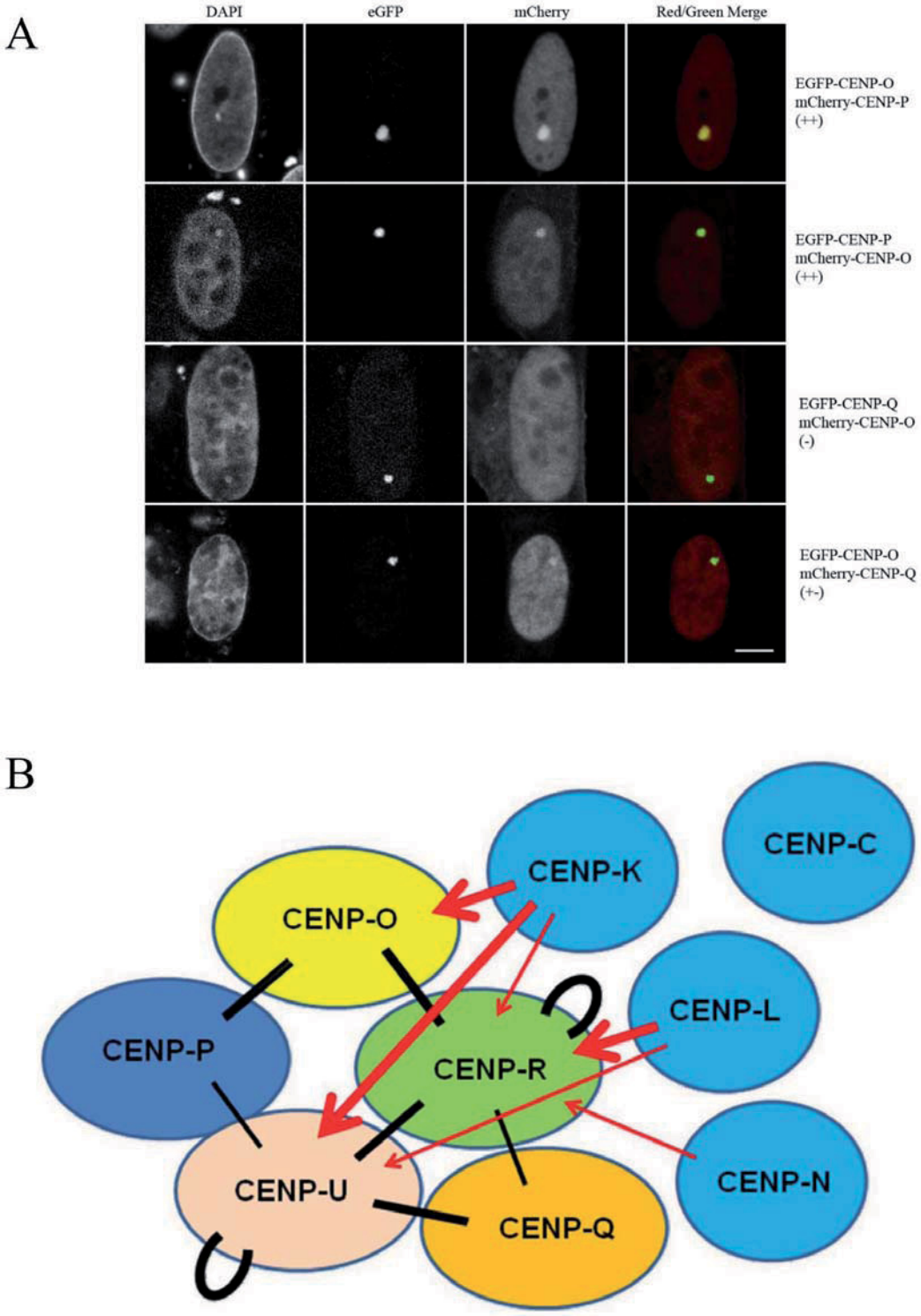

Figure 3. Centromere protein interactions analyzed by F3H assay. (A) EGFP tagged centromere proteins (bait, green) were recruited to the *lac* operator repeat array by the GFP-binding protein fused to the Lac repressor (LacI-GBP). Co-expressed mCherry tagged centromere proteins (prey, red) may either interact with the GFP-tagged protein (yellow in the overlay) or may not interact resulting in a disperse distribution. Upper two rows: interaction between EGFP-CENP-O and mCherry-CENP-P, EGFP-CENP-P and mCherry-CENP-O. Lower two rows: EGFP-CENP-Q did not interact with and recruit mCherry-CENP-O to the *lac* spot, but shows a weak interaction in the reverse combination. For all results see Table 1. Bar: 5 μm. (B): Strong F3H interactions are displayed (++: thick lines, +: thin lines). Black bars: interactions between CENP-PORQU proteins, red arrows: recruitment of CENP-PORQU proteins by CENP-K, -L, and -N. CENP-C is not able to recruit any of the CENP-PORQU proteins (data see Table 2).
doi:10.1371/journal.pone.0044717.g003

Table 2. F3H analysis of CENP-O class protein interactions.

mCherry\EGFP	CENP-O	CENP-P	CENP-Q	CENP-R	CENP-U	CENP-K	CENP-L	CENP-N	CENP-C
CENP-O	−	++	−	++	−	+	−	−	−
CENP-P	+	−	+−	+−	+	−	−	−	−
CENP-Q	+−	−	−	+	+	−	−	−	−
CENP-R	++	+−	+	++	++	+−	++	−	−
CENP-U	−	+	++	++	++	++	+−	−	−
CENP-K	++	−	+−	+	++	+−	−	−	−
CENP-L	−	−	+−	+	+	+−	−	−	+−
CENP-N	−	−	−	+	+−	−	−	−	−
CENP-C	−	−	−	−	−	−	−	−	−

GFP-tagged CENP-O class proteins, CENP-K, -L, -N and -C (rows) were bound to ectopic chromosomes sites. When RFP-tagged CENP-O class proteins, CENP-K, -L, -N and -C (lines) were recruited to these proteins, this was visible by a yellow dot. Signal intensity at the nuclear spot was used an indicator for interaction strength. ++, +: strong interaction; +−: weak interaction; −: no interaction.

doi:10.1371/journal.pone.0044717.t002

CENP-Q in the nucleoplasm outside kinetochores (data not shown).

These data show that, with the two exceptions CENP-O/-P and CENP-Q/-R, the pairwise CENP-O class protein interactions detected by F3H do not result in a homo- or hetero-dimerisation of these proteins stable enough for FCCS detection. Since these proteins do not pre-aggregate, they must enter the nucleoplasm as single proteins. CENP-O, -P, -Q and -R are small enough (molecular weights <34 kDa) for not needing a nuclear localisation domain (NLS) for entering the nucleus. Only CENP-U is larger (47.5 kDa) and indeed contains two NLS [57,58].

PORQU loads onto kinetochores in S-phase and form a stable subcomplex

We next asked when during the cell cycle the CENP-PORQU complex assembles. By applying SNAP-tag technology, we determined at which cell cycle phase CENP-O is loaded to the kinetochore. The SNAP protein tag can catalyze the formation of a covalent bond to a benzyl-guanine moiety coupled to different fluorescent or non-fluorescent membrane-permeable reagents [59]. This tag allows pulse-chase experiments at a single protein level. Consistent with previous data [60], we detected TMR-star fluorescence on SNAP-CENP-A only in G1 cells, confirming that CENP-A is specifically loaded in G1, while we observed a time window of mid G1 to G2 for CENP-N binding and loading to kinetochores [44]. Here we transfected a SNAP-CENP-O construct. After double-thymidine and aphidicolin block release and applying the same protocol, we found SNAP-CENP-O present at kinetochores of G2 cells (Fig. 5A), indicating that CENP-O is loaded onto kinetochores in or before G2. To extend our temporal analysis to further phases of the cell cycle, we repeated these experiments in U2OS cells since these cells have a longer cell cycle: 12 hrs after release and following the same experimental procedure, U2OS cells can be analysed in late-S-phase. Here, TMR-star fluorescence for SNAP-CENP-O was already detected in late S-phase as judged by PCNA-GFP fluorescence (Fig. 5B). Thus, CENP-O assembles at kinetochores already in late S-phase or earlier. Finally, to measure the earliest time point at which CENP-O can assemble into kinetochores, SNAP-CENP-O transfected HeLa cells were arrested in mitosis for 12 hrs by a nocodazole block and quenched with BTP for 30 min. 4 hrs after quenching, the cells were released from nocodazole arrest. Further 5 hrs later, SNAP-tagged CENP-O was fluorescently labelled with TMR-star for 30 min and fixed for examination. No TMR-star fluorescence was detected indicating that SNAP-CENP-O is not loaded in G1 (Fig. 5C). Overall these experiments suggest a time window of S-phase to G2 for CENP-O loading to kinetochores. Also for CENP-T and -W [61], CENP-N [44] and CENP-U [62] loading to kinetochores in S-phase was observed.

Our recent work showed that CENP-T and -W [61] as well as CENP-N [44] are loaded to human kinetochores by slow loading dynamics, mainly during the second half of S-phase. This is in contrast to CENP-A which is loaded at the end of mitosis and G1 [55,60]. We speculated that the CENP-O class proteins might also be loaded slowly, mainly in S-phase. We thus studied the dynamic binding of these EGFP-tagged CENPs by Fluorescence Recovery After Photobleaching (FRAP) in living human U2OS cells. For none of the five CENP-O class proteins, at any cell cycle phase, we could detect fluorescence recovery within 150 sec after bleaching, indicating rather stable kinetochore binding of all five proteins, consistent with observations of Minoshima et al. [38] for CENP-U. We then studied fluorescence recovery of these five proteins during the cell cycle in a longer time frame, now over 4 hours. Different cell cycle phases were identified by staining with CENP-F and by co-expressing mRFP-PCNA for identifying S-phase and its sub-phases [63,64], as recently described [44,55,65]. In G1, all five CENP-O class proteins show complete recovery; four proteins have an exchange rate ($t_{1/2}$) of about one hour while only CENP-R exchanges slower with $t_{1/2} = 2$ hrs. In S-phase and G2, CENP-O, -P and -Q show partial recovery values of 40 to 80% with a slower exchange rate compared to G1 of about 2 hrs (see Table 3 and Fig. 6; in same cases for CENP-O and -P, the recovery only allows to estimate the final recovery level (values in brackets)). These recovery amplitudes are in the same range of values as for those of CENP-T and -W (70±8%) [61] and CENP-N (45±6%, see Table 3) [44]. The slow recovery times during the second half of S-phase coincide with the slow recovery times of CENP-T and -W ($t_{1/2} = 70 \pm 10$ min) [61], but are slower than the exchange of CENP-N ($t_{1/2} = 38 \pm 7$ min) [44]. In G2, CENP-P and -Q seem to show slightly faster recovery times compared to S-phase. The FRAP dynamics of CENP-U and -R are distinct from that of CENP-O, -Q and -P. CENP-U shows 100% recovery throughout the cell cycle with the exception of late S-phase when most of CENP-U (71±2%) is immobile (the remaining 29% of CENP-U exchange with $t_{1/2} = 50 \pm 8$ min). Our FRET data indicate that CENP-U di- or multimerises in late S-phase. This CENP-U self-

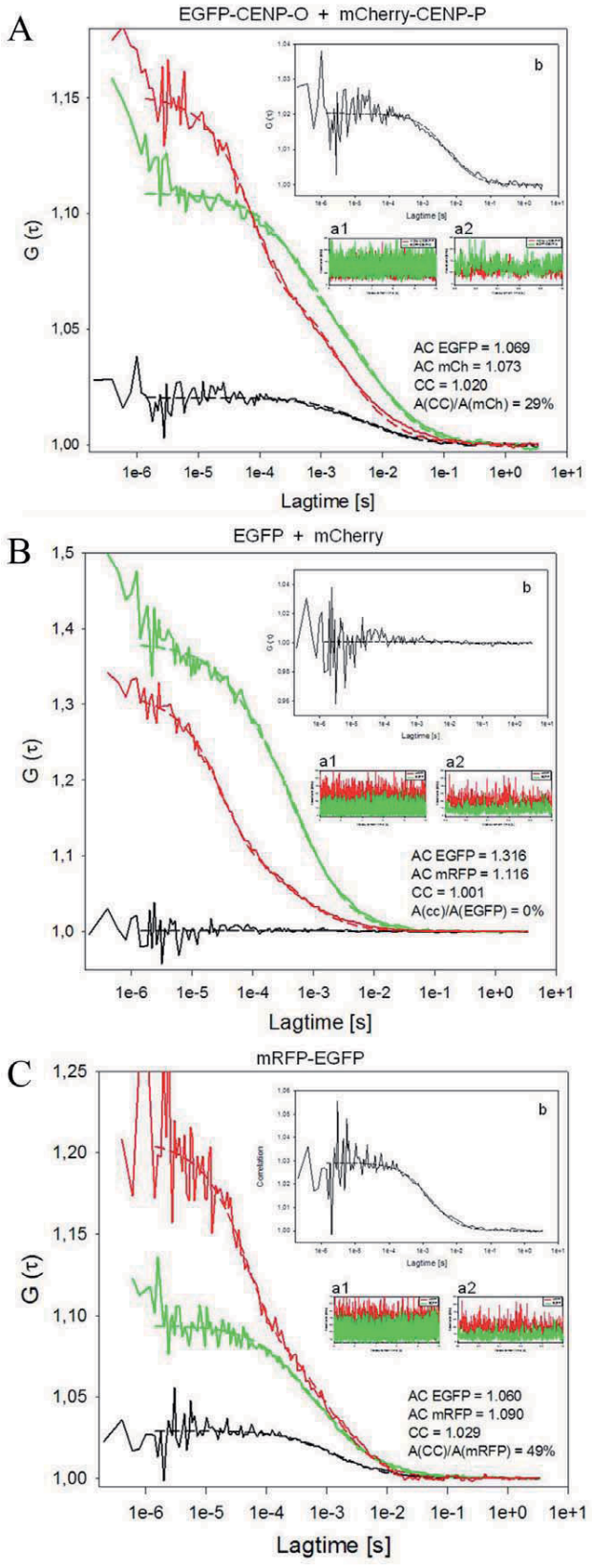

Figure 4. FCCS measurements displaying G versus lag time. Red: mCherry (A, B) or mRFP (C), green: EGFP, black: auto-correlation. Count rates are displayed over 10 sec (inserts a1) indicating the absence of photobleaching, and 1 sec (inserts a2) indicating the absence of larger protein aggregates. The cross-correlation analyses are amplified in inserts b. (A) EGFP-CENP-O and mCherry-CENP-P indicate complex formation in the nucleoplasm (amplitude of cross-correlation/amplitude of mCherry signal: 29%). The amplitude of the cross-correlation curve A(CC), relative to the diffusion-related amplitude of one of the autocorrelation curves A(AC) of EGFP or mCherry, is a measure of binding or dynamic colocalization [49,50]. According to this ratio of amplitudes A(CC)/A(AC), up to 20–30% of nucleoplasmic CENP-O and -P are hetero-dimers. Count rates were recorded simultaneously for both fluorophores. The count rate detected in a 10 sec measurement (insert a1) demonstrates the absence of photobleaching, while the count rate in a 1 sec resolution time scale (insert a2) indicates the absence of larger protein aggregates. The autocorrelations yielded 1.069 and 1.073 for EGFP-CENP-O and mCherry-CENP-P, respectively. The cross-correlation analysis (with a magnified scale of G(τ); insert b) resulted in a correlation of 1.02 indicating that 29% of the molecules are co-migrating in the nucleoplasm. (B) EGFP and mCherry expressed as single non-fused proteins (negative control) do not show any cross-correlation (A(CC)/A(EGFP) = 0%). The count rates (inserts a1 and a2) indicate the absence of photobleaching and larger proteins. The autocorrelations yielded 1.316 and 1.116 for EGFP and mRFP, respectively. The cross-correlation curve (with a magnified scale of G(τ), insert b) resulted in a value of 1.001 indicating the absence of any complexation between EGFP and mRFP. (C) mRFP-EGFP fusion protein (positive control) shows cross-correlation (A(CC)/A(mRFP) = 49%). The count rates indicate that photobleaching and the presence of larger protein aggregates can be excluded (inserts a1, a2) and that the autocorrelations of EGFP (1.06) and mRFP (1.09) were comparable to the values obtained for EGFP-CENP-O and mCherry-CENP-P. Cross-correlating the two channels against each other, we obtained a value of 1.029 indicating that about 50% of the molecules are detected as a complex (with a magnified scale of G(τ) in insert b).
doi:10.1371/journal.pone.0044717.g004

assembly could reduce CENP-U exchange at the kinetochore in late S-phase, explaining the high immobile fraction detected by FRAP. This CENP-U/-U interaction seems not be mediated by Plk1 since Plk1 binding to kinetochores occurs during late G2 [41]. Our data indicate that CENP-Q and CENP-U form di- or oligomers after kinetochore binding before the onset of mitosis, potentially denoting a conformational change.

Different from the behaviour of the other four proteins, for all cell cycle phases CENP-R shows recovery values of 100% with slow loading times of 2 to 3 hrs (Table 3). Thus, CENP-R recovery is considerably slower than that of the other four CENP-O class proteins. The observed distinct dynamical behaviour of the CENP-O class proteins indicates that the complex does not bind to the kinetochore as a pre-formed complex in the nucleoplasm and that these proteins retain distinct dynamic behaviour also when bound to the kinetochore.

Cell-cycle dependent protein abundance

The CCAN protein CENP-N shows varying abundance in the cell with a maximal protein level at kinetochores in late S-phase [8,44]. Furthermore, the presence of CENP-U at HeLa kinetochores increases during late G1 and early S-phase, remains high through late S and G2 and decreases strongly during M-phase [40]. For human CENP-O, a decrease in kinetochore presence down to about 60% from interphase to mitosis was detected by immuno-fluorescence [33]. Here we extended these CENP-O data and measured the cell cycle dependent amount of CENP-O relative to tubulin in HEp-2 cells by Western blot 2, 4, 6 (S-phase), 8 (G2), and 10 hours (M-phase) after release from a double thymidine block (Fig. 7A). The cellular amount of CENP-O remains rather stable from G1/S over the entire S-phase, is reduced already in G2 and reduces further in M-phase, consistent with findings of McAinsh et al. [33]. A corresponding Western blot

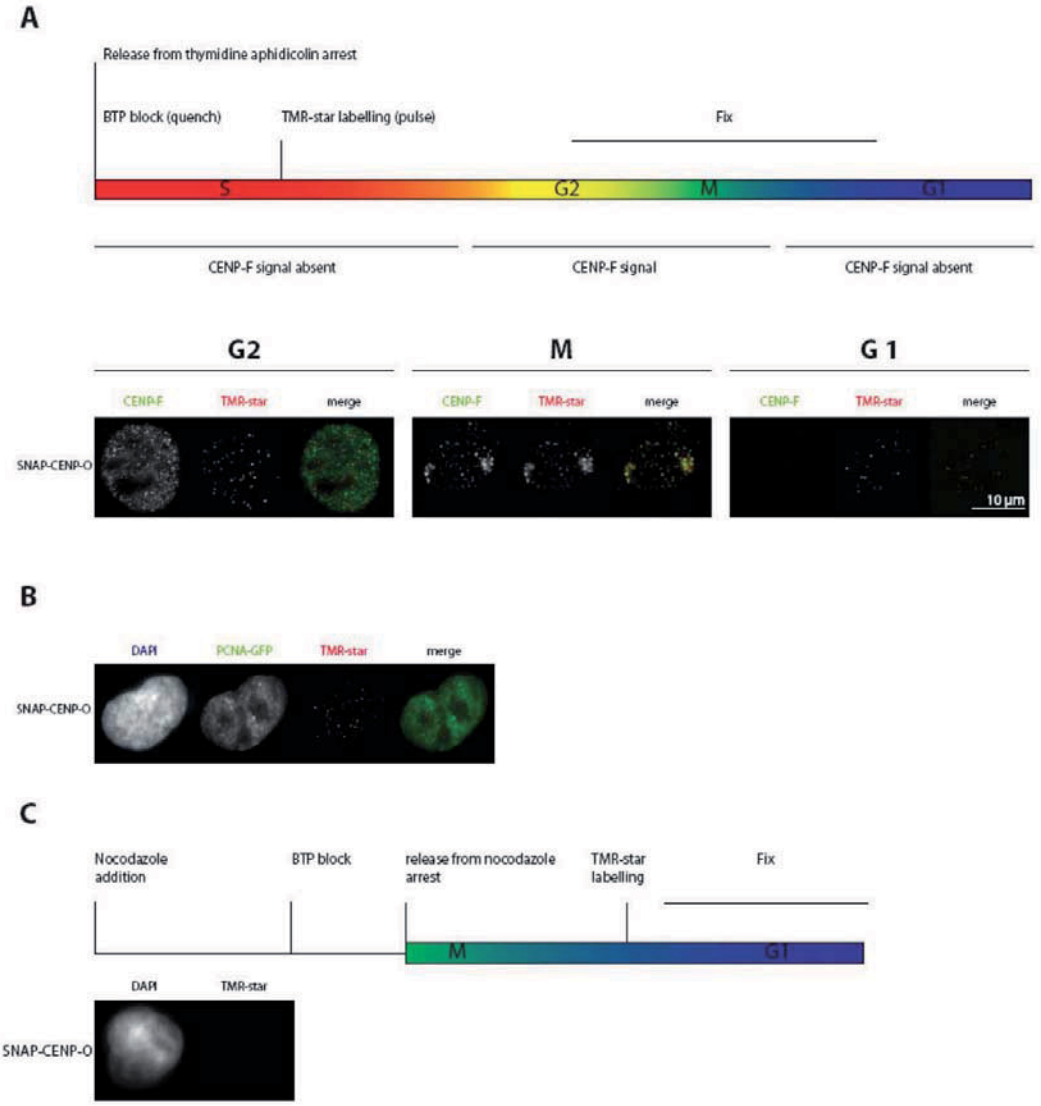

Figure 5. CENP-O loading to kinetochores measured by the SNAP-tag technology. (A) Top: schematic representation of the performed experiment. Below: representative images of cells showing TMR-star fluorescence for SNAP-CENP-O in G2, M-phase and the following G1. Cell cycle phases G2 (CENP-F staining of the whole nucleus) and mitosis (specific kinetochore binding of CENP-F) are clearly identified. (B) The same experiment as in (A) was performed with U2OS cells stably expressing PCNA-GFP. SNAP-CENP-O fluorescence appears at kinetochores in late S-phase as judged from cellular PCNA distributions. (C) Top: schematic representation of the performed experiment. Below: representative images of cells expressing SNAP-CENP-O showing no fluorescence at kinetochores during G1. CENP-O is thus loaded to kinetochores in S-phase.
doi:10.1371/journal.pone.0044717.g005

analysis was conducted for CENP-P and CENP-Q: The level of CENP-P decreases from late S-phase through G2 to M-phase (Fig. 7B, D), whereas CENP-Q displayed stable protein levels from G1/S into mitosis (Fig. 7C, D). In contrast to the constant level of CENP-Q levels in the cell, immune-fluorescence detected an increase of the amounts of CENP-Q at kinetochores during S-phase, reaching a maximum in late S-phase and strongly decreasing in G2 (Fig. 7E, F).

Discussion

The centromeric histone H3 variant CENP-A is the central marker of centromere location and inherits this location to daughter cells [55]. The kinetochore recognizes this epigenetic mark, in part, through the CCAN network of proteins. The CENP-N subunit directly binds the CENP-A CATD region of the CENP-A containing nucleosome while the CENP-C subunit binds the C-terminal tail of CENP-A [14–16]. In addition to these CENP-A binding mechanisms, CENP-T/W/S/X form a unique centromeric chromatin structure next to histone H3 containing nucleosomes that supercoils DNA [9,12,61]. If we are to fully understand the pathways and mechanisms that allow a mature kinetochore to assemble, it will be crucial to define how these chromatin-interacting complexes recruit the other 11 CCAN subunits. Of these subunits the CENP-PORQU were reported to form a stable complex when being expressed in *E. coli* [10], whereas the CENP-H, -I, -K, -L and -M (CENP-H class) are not known to associate into any stable sub-complexes [8]. Dependency experiments show that CENP-PORQU requires the CENP-H class for kinetochore binding but not *vice versa* [5,6,8,14,52]. The

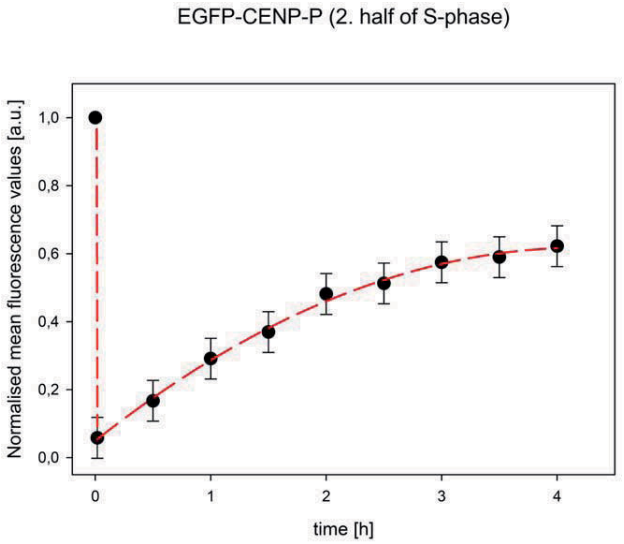

Figure 6. Fluorescence recovery after photobleaching of EGFP-CENP-P in mid S-phase. Normalised mean fluorescence values of 55 kinetochores taken in time steps of 30 min over 4 hours. Recovery levels off, indicative of an about 40% immobile fraction.
doi:10.1371/journal.pone.0044717.g006

working model thus involves the stepwise recruitment of CENP-N/CENP-TWSX≫CENP-HIKLM≫CENP-PORQU [2]. In line with this, CENP-L can bind directly to CENP-N *in vitro* [14] and may be involved in stabilising CENP-N binding to the CENP-A nucleosome [44]. We now show by F3H that CENP-N, CENP-K and CENP-L are all, to some extent, capable of recruiting CENP-O, -U and -R to an ectopic chromosomal site, whereas CENP-C is not directly involved in CENP-PORQU binding. The next step will be to identify the physical interactions that mediate this assembly reaction.

The CENP-PORQU proteins assemble at kinetochores during S-phase. For example, newly synthesized CENP-O is incorporated in S-phase and remains at the kinetochore during mitosis (although levels decrease, consistent with previous findings [33]) into the following G1 where they can exchange slowly and to near completion (however, without exchange with newly synthesized CENP-O). During the cell cycle, the CENP-PORQU proteins show different protein abundance in the cell: while CENP-Q protein levels do not change from G1/S to M-phase, the levels of CENP-O and -P decrease, CENP-P levels already during S-phase but those of CENP-O only after S-phase. The protein amount at kinetochores is maximal in late S-phase for CENP-Q, as shown here, and at late S-phase and G2 for CENP-U [40]. This variance of protein abundance in the cell and at kinetochores supports our conclusion that the CENP-PORQU complex assembles from proteins with individual behavior, and might indicate a varying stoichiometry of the CENP-PORQU proteins in the complex.

The reported stable interaction of CENP-PORQU in *E. coil* lysates [10] suggests that these proteins may form a pre-assembled complex in the nucleoplasm before loading onto kinetochores in S-phase. We show here, however, by FCCS that the CENP-PORQU subunits do not exist as a single preformed complex prior to kinetochore-binding. Instead, in the nucleoplasm, we can only detect a CENP-O/P (to an amount of about 50%), and, to a very minor extent, a CENP-Q/R heterodimer. However, by F3H we could show that each CENP-PORQU subunit can recruit two or three other proteins of this group to an ectopic chromosomal site. This confirms that these proteins specifically interact with each other in mammalian cells. One caveat of this experiment is that CCAN proteins might be specifically modified at centromere locations. These centromere specific modifications would be absent at the ectopic chromosomal site, potentially influencing protein interactions. Since pair-wise binding is weak in most cases, the strong kinetochore binding of the CENP-PORQU subunits (identified by slow FRAP recovery times) supports multi-fold CENP-PORQU interactions at the kinetochore. No single subunit of CENP-PORQU can recruit all other subunits, further supporting our finding that the complex does not pre-form in the nucleoplasm. Our FRAP experiments, consistent with previous studies [38], show that the cell cycle dependent turnover of CENP-P/O/Q is similar but distinct from the behavior of CENP-U and CENP-R. This indicates that the CENP-PORQU sub-complex does not behave as a single unit but instead is an ensemble of autonomously behaving proteins.

Our FRET measurements show that the CENP-PORQU proteins, once bound and incorporated into the inner kinetochore structure, are positioned in close proximity to one another. Previously, we reported that the amino-terminus of CENP-U was in close proximity to the amino-terminus of CENP-B and CENP-I, but not to the amino-terminus of CENP-A and CENP-C [43]. This indicates that, to some extent, CENP-PORQU is imbedded within the CCAN complex. Moreover, not all FRET connectivities should be thought of as occurring necessarily within a single CCAN inner kinetochore complex (intra-CCAN FRET). It is possible that some observed FRET proximities may reflect protein neighborhoods between two different adjacent CCAN complexes (inter-CCAN FRET). Such inter-CCAN interactions are likely, given super-resolution experiments that support models in which kinetochores are formed from multiple adjacent microtubule

Table 3. Long term FRAP results for the CENP-PORQU proteins.

Cell cycle	CENP-O		CENP-P		CENP-Q		CENP-U		CENP-R	
	rec/%	$t_{1/2}$/min	rec/%	$t_{1/2}$/min	rec/%	$t_{1/2}$/min	rec/%	$t_{1/2}$/min	rec/%	$t_{1/2}$/min
G1	100	71±15	100	77±15	90±10	57±10	100	72±15	100	125±15
early S	(45)	-	(70)	-	59±6	118±15	100	163±40	100	147±20
mid S	(40)	-	62±6	81±5	65±6	125±30	100	93±15	100	160±15
late S	75±15	131±30	49±10	103±10	75±8	136±15	29±2	50±8	100	180±20
G2	(80)	-	56±8	78±5	64±6	90±14	100	76±8	100	137±20

rec: fluorescence recovery relative to the initial fluorescence value before bleaching, $t_{1/2}$: time for half height recovery (in min). Recovery values in brackets: estimated recovery value; for these data, a $t_{1/2}$ value could not be determined.
doi:10.1371/journal.pone.0044717.t003

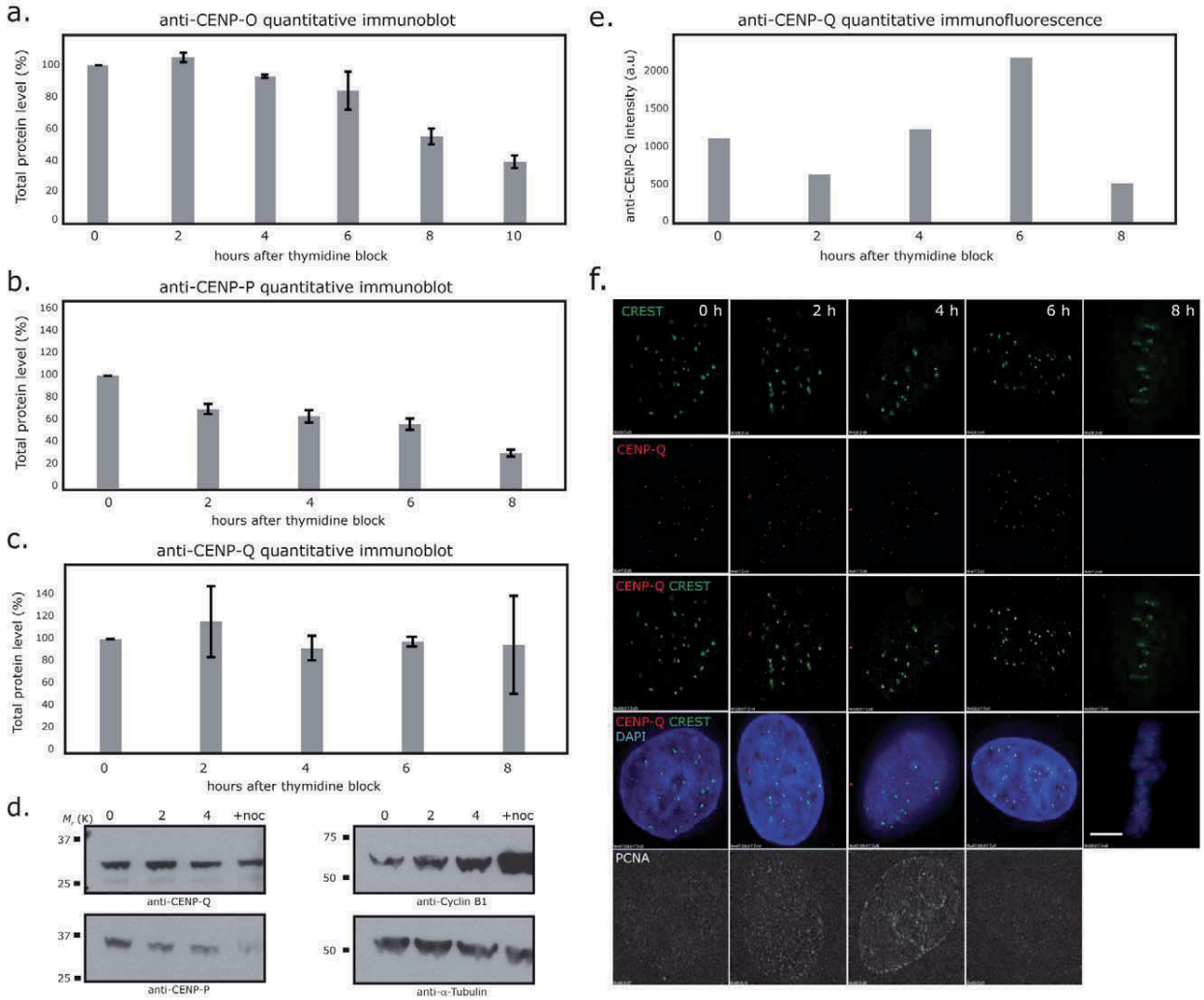

Figure 7. Levels of CENP-O/P/Q total protein during the cell cycle. (A) Quantitative immunoblot of CENP-O relative to α-Tubulin. Protein amounts are measured at G1/S (0 h), 2, 4, 6, 8 and 10 hrs after release from the double thymidine block in synchronised human HEp-2 cells. CENP-F and PCNA staining identify the time points 2, 4, and 6 hrs as S-phase, time point 8 hrs as G2 and 10 hrs as M-phase. The cellular amount of CENP-O reduces in G2 and further in M-phase. (B, C) Quantitative immuno-blots of CENP-P and CENP-Q protein levels relative to α-Tubulin at 0 (G1/S), 2 (early S), 4 (middle S), 6 (late S-phase), 8 (G2) hrs after release from double thymidine block in synchronized HeLa cells. Cycle stages were attributed from FACs analysis, PCNA staining and phase contrast microscopy (data not shown). (D) Representative immunoblots showing CENP-P, CENP-Q, Cyclin-B1 and α-Tubulin at the 0 (G1/S), 2 (early S), 4 (middle S) hrs time points and cells arrested in mitosis with nocodazole (16 hrs). (E) Quantitative four-colour immuno-flourence using anti-CENP-Q (red), CREST (green), DAPI (blue) and anti-PCNA (far red) antibodies in the same cells used in panel B. Pixel intensities of CENP-Q (signal – background) at kinetochores (n = 50 from 5 cells) are shown for each time point after release from double thymidine block (E) and representative images (F). CENP-Q loads onto kinetochores during S-phase reaching maximal binding in late S-phase (6 h). Scale bar = 5 μm.
doi:10.1371/journal.pone.0044717.g007

binding sites [66–68]. We expect that three-dimensional inner kinetochore model building will allow us to evaluate and explore these ideas.

The multifold interactions of the CENP-PORQU proteins result in stable binding of these proteins to kinetochores, suggesting a self-assembly mechanism [69]. In this regard, CENP-U and CENP-R are able to homo-dimerise at an ectopic chromosomal site (see Table 2), although we could not detect homo-dimerisation from our FCCS measurements. Nevertheless, upon kinetochore binding and before mitosis, these proteins are proximal to themselves, as detected by FRET between CENP-U/-U. Human CENP-Q, when expressed in *E. coli*, oligomerises into octameric complexes [36]. In late S-phase, after kinetochore binding and before mitosis, we detected FRET between the CENP-Q carboxy- as well as amino-terminal regions, indicating homo-di- or oligomerisation. We could not detect such homo-dimerisation at an ectopic chromosomal site, and found by FCCS that CENP-Q migrates as a monomer in the nucleoplasm, showing that the oligomerization event occurs at kinetochores. This self-association of CENP-U and -Q might hint towards the presence of more than one of these proteins (CENP-U, -Q) in one CCAN complex, indicating a varying stoichiometry in the complex. Alternatively, these proteins might make inter-CCAN interactions with themselves. Such an interaction between different CCAN complexes might induce or stabilize centromere specific chromatin structures and/or microtubule binding sites

[70]. The latter hypothesis is attractive given that both CENP-Q and CENP-U bind directly to microtubules *in vitro* [36,39]. We speculate that this self-association of CENP-Q and -U after kinetochore binding is a pre-mitotic maturation process that might switch kinetochores into the correct conformation for microtubule attachment.

Acknowledgments

We thank N. Klöcker, D. Foltz, J. Langowski and I. Cheeseman for the kind gift of plasmids and S. Pfeifer and S. Ohndorf for expert technical support.

Author Contributions

Conceived and designed the experiments: AE WD SR SE DH TU VD JMB ADM PM CH HL SD. Performed the experiments: AE WD AH SR SE DH TU VD JMB MCC CH HL. Analyzed the data: AE WD AH SR SE DH TU VD JMB ADM PM CH HL SD. Contributed reagents/materials/analysis tools: WD JMB MCC. Wrote the paper: DH ADM HL CH SD.

References

1. Perpelescu M, Fukagawa T (2011) The ABCs of CENPs. Chromosoma 120: 425–446.
2. Takeuchi K, Fukagawa T (2012) Molecular architecture of vertebrate kinetochores. Exp Cell Res 318: 1367–1374.
3. Cheeseman IM, Desai A (2008) Molecular architecture of the kinetochore-microtubule interface. Nat Rev Mol Cell Biol 9: 33–46.
4. Przewloka M, Glover DM (2009) The kinetochore and the centromere: a working long distance relationship. Annu Rev Genet 43: 439–465.
5. Foltz DR, Jansen LET, Black BE, Bailey AO, YatesIII JR, et al. (2006) The human CENP-A centromeric complex. Nat Cell Biol 8: 458–469.
6. Okada M, Cheeseman IM, Hori T, Okawa K, McLeod IX, et al. (2006) The CENP-H-I complex is required for the efficient incorporation of newly synthesized CENP-A into centromeres. Nature Cell Biol 8: 446–457.
7. Meraldi P, McAinsh AD, Rheinbay E, Sorger PK (2006) Phylogenetic and structural analysis of centromeric DNA and kinetochore proteins. Genome Biol 7: R23.
8. McClelland SE, Borusu S, Amaro AC, Winter JR, Belwal M, et al. (2007) The CENP-A NAC/CAD kinetochore complex controls chromosome congression and spindle bipolarity. EMBO J 26: 5033–5047.
9. Hori T, Amano M, Suzuki A, Backer CB, Welburn JP, et al. (2008) CCAN makes multiple contacts with centromeric DNA to provide distinct pathways to the outer kinetochore. Cell 135: 1039–1052.
10. Hori T, Okada M, Maenaka K, Fukagawa T (2008) CENP-O class proteins form a stable complex and are required for proper kinetochore function. Mol Biol Cell 19: 843–854.
11. Amano M, Suzuki A, Hori T, Backer C, Okawa K, et al. (2009) The CENP-S complex is essential for the stable assembly of outer kinetochore structure. J Cell Biol 186: 173–182.
12. Nishino T, Takeuchi K, Gascoigne KE, Suzuki A, Hori T, et al. (2012) CENP-T-W-S-X forms a unique centromeric chromatin structure with a histone-like fold. Cell 148: 487–501.
13. Santaguida S, Musacchio A (2009) The life and miracles of kinetochores. EMBO J 28: 2511–2531.
14. Carroll CW, Silva MCC, Godek KM, Jansen LET, Straight AF (2009) Centromere assembly requires the direct recognition of CENP-A nucleosomes by CENP-N. Nat Cell Biol 11: 896–902.
15. Carroll CW, Milks KJ, Straight AF (2010) Dual recognition of CENP-A nucleosomes is required for centromere assembly. J Cell Biol 189: 1143–1155.
16. Guse A, Carroll CW, Moree B, Fuller CJ, Straight AF (2011) In vitro centromere and kinetochore assembly on defined chromatin templates. Nature 477: 354–358.
17. Tachiwana H, Kagawa W, Shiga T, Osakabe A, Miya Y, et al. (2011) Crystal structure of the human centromeric nucleosome containing CENP-A. Nature 476: 232–235.
18. Bui M, Dimitriadis EK, Hoischen C, An E, Quenet D, et al. (2012) Cell cycle-dependent structural transitions in the human CENP-A nucleosome in vivo. Cell 150: 317–326.
19. De Wulf P, McAinsh AD, Sorger PK (2003) Hierarchical assembly of the budding yeast kinetochore from multiple subcomplexes. Genes Dev 17: 2902–2921.
20. Cheeseman IM, Niessen S, Anderson S, Hyndman F, Yates JR 3rd, et al. (2004) A conserved protein network controls assembly of the outer kinetochore and its ability to sustain tension. Genes Dev 18: 2255–2268.
21. Cheeseman IM, Chappie JS, Wilson-Kubalek EM, Desai A (2006) The conserved KMN network constitutes the core microtubule-binding site of the kinetochore. Cell 127: 983–997.
22. Obuse C, Yang H, Nozaki N, Goto S, Okazaki T, et al. (2004) Proteomics analysis of the centromere complex from HeLa interphase cells: UV-damaged DNA binding protein 1 (DDB-1) is a component of the CEN-complex, while BMI-1 is transiently co-localised with the centromeric region in interphase. Genes to Cells 9: 105–120.
23. Liu X, McLeod I, Anderson S, Yates JR 3rd, He X (2005) Molecular analysis of kinetochore architecture in fission yeast. EMBO J 24: 2919–2930.
24. Petrovic A, Pasqualato S, Dube P, Krenn V, Santaguida S, et al. (2010) The Mis12 complex is a protein interaction hub for outer kinetochore assembly. J Cell Biol 190: 835–852.
25. Kiyomitsu T, Iwasaki O, Obuse C, Yanagida M (2010) Inner centromere formation requires hMis14, a trident kinetochore protein that specifically recruits HP1 to human chromosomes. J Cell Biol 188: 791–807.
26. Liu D, Vleugel M, Backer CB, Hori T, Fukagawa T, et al. (2010) Regulated targeting of protein phosphatise 1 to the outer kinetochore by KNL1 opposes Aurora B kinase. J Cell Biol 188: 809–820.
27. Przewloka MR, Venkei Z, Bolanos-Garcia VM, Debski J, et al. (2011) CENP-C is a structural platform for kinetochore assembly. Curr Biol 21: 399–405.
28. Tanaka TU, Desai A (2008) Kinetochore-microtubule interactions: the means to the end. Curr Opin Cell Biol 20: 53–63.
29. Wan X, O'Quinn RP, Pierce HL, Joglekar AP, Gall WE, et al. (2009) Protein architecture of the human kinetochore microtubule attachment site. Cell 137: 672–684.
30. Moree B, Meyer CB, Fuller CJ, Straight AF (2011) CENP-C recruits M18BP1 to centromeres to promote CENP-A chromatin assembly. J Cell Biol 194: 855–871.
31. Barnhart MC, Kuich HJL, Stellfox ME, Ward JA, Bassett EA, et al. (2011) HJURP is a CENP-A chromatin assembly factor sufficient to form a functional de novo kinetochore. J Cell Biol 194: 229–243.
32. Fukagawa T, Mikami Y, Nishihashi A, Regnier V, Haraguchi T, et al. (2001) CENP-H, a constitutive centromere component, is required for centromere targeting of CENP-C in vertebrate cells. EMBO J 20: 4603–4617.
33. McAinsh AD, Meraldi P, Draviam VM, Toso A, Sorger PK (2006) The human kinetochore proteins Nnf1R and Mcm21R are required for accurate chromosome segregation. EMBO J 25: 4033–4049.
34. Toso A, Winter JR, Garrod AJ, Amaro AC, Meraldi P, et al. (2009) Kinetochore-generated pushing forces separate centrosomes during bipolar spindle assembly. J Cell Biol 184: 365–372.
35. Gascoigne KE, Takeuchi K, Suzuki A, Hori T, Fukagawa T, et al. (2011) Induced ectopic kinetochore assembly bypasses the requirement for CENP-A nucleosomes. Cell 145: 410–422.
36. Amaro AC, Samora CP, Holtackers R, Wang E, Kingston IJ, et al. (2010) Molecular control of kinetochore-microtubule dynamics and chromosome oscillations. Nature Cell Biol 12: 319–329.
37. Izuta H, Ikeno M, Suzuki N, Tomonaga T, Nozaki N, et al. (2006) Comprehensive analysis of the ICEN (Interphase Centromere Complex) components enriched in the CENP-A chromatin of human cells. Genes Cells 11: 673–684.
38. Minoshima Y, Hori T, Okada M, Kimura H, Haraguchi T, et al. (2005) The constitutive centromere component CENP-50 is required for recovery from spindle damage. Mol Cell Biol 25: 10315–10328.
39. Hua S, Wang Z, Jiang K, Huang Y, Ward T, et al. (2011) CENP-U cooperates with Hec1 to orchestrate kinetochore-microtubule attachment. J Biol Chem 286: 1627–1638.
40. Kang YH, Park JE, Yu LR, Soung NK, Yun SM, et al. (2006) Self-regulated Plk1 recruitment to kinetochores by the Plk1-PBIP1 interaction is critical for proper chromosome segregation. Mol Cell 24: 409–422.
41. Kang YH, Park C-H, Kim T-S, Soung N-K, Bang JK, et al. (2011) Mammalian Polo-like kinase 1-dependent regulation of the PBIP1-CENP-Q complex at kinetochores. J Biol Chem 286: 19744–19757.
42. Schmitzberger F, Harrison SC (2012) RWD domain: a recurring module in kinetochore architecture shown by Ctf19-Mcm21 complex structure. EMBO Rep 13: 216–222.
43. Hellwig D, Hoischen C, Ulbricht T, Diekmann S (2009) Acceptor-photobleaching FRET analysis of core kinetochore and NAC proteins in living human cells. Eur Biophys J 38: 781–791.
44. Hellwig D, Emmerth S, Ulbricht T, Doering V, Hoischen C, et al. (2011) Dynamics of CENP-N kinetochore binding during the cell cycle. J Cell Sci 124: 3871–3883.
45. Tsukamoto T, Hashiguchi N, Janicki SM, Tumbar T, Belmont AS, et al. (2000) Visualization of gene activity in living cells. Nat Cell Biol 2: 871–878.
46. Rothbauer U, Zolghadr K, Tillib S, Nowak D, Schermelleh L, et al. (2006) Targeting and tracing antigens in live cells with fluorescent nanobodies. Nat Methods 3: 887–889.
47. Zolghadr K, Mortusewicz O, Rothbauer U, Kleinhans R, Goehler H, et al. (2008) A fluorescent two-hybrid assay for direct visualization of protein interactions in living cells. Mol Cell Proteomics 7: 2279–2287.

48. Orthaus S, Biskup C, Hoffmann B, Hoischen C, Ohndorf S, et al. (2008) Assembly of the inner kinetochore proteins CENP-A and CENP-B in living human cells. Chem Bio Chem 9: 77–92.
49. Bacia K, Schwille P (2003) A dynamic view of cellular processes by *in vivo* fluorescence auto- and cross-correlation spectroscopy. Methods 29: 74–85.
50. Bacia K, Schwille P (2007) Practical guidelines for dual-color fluorescence cross-correlation spectroscopy. Nature Protocols 2.28422856.
51. Orthaus S, Klement K, Happel N, Hoischen C, Diekmann S (2009) Linker Histone H1 is present in centromeric chromatin of living human cells next to inner kinetochore proteins. Nucl Acids Res 37: 3391–3406.
52. Milks KJ, Moree B, Straight AF (2009) Dissection of CENP-C directed centromere and kinetochore assembly. Mol Biol Cell 20: 4246–4255.
53. Qui SL, Wang JN, Yu C, He DC (2009) CENP-K and CENP-H may form coiled-coils in the kinetochores. Sci China Ser C-Life Sci 52: 352–359.
54. Digman MA, Brown CM, Sengupta P, Wiseman PW, Horwitz AR, et al. (2005) Measuring fast dynamics in solutions and cells with a laser scanning microscope. Biophys J 89: 1317–1327.
55. Hemmerich P, Weidtkamp-Peters S, Hoischen C, Schmiedeberg L, Erliandri I, et al. (2008) Dynamics of inner kinetochore assembly and maintenance in living cells. J Cell Biol 180: 1101–1114.
56. Kohl T, Haustein E, Schwille P (2005) Determining protease activity *in vivo* by fluorescence cross-correlation analysis. Biophys J 89: 2770–2782.
57. Hanissian SH, Akbar U, Teng B, Janjetovic Z, Hoffmann A, et al. (2004) cDNA cloning and characterization of a novel gene encoding the MLF1-interacting protein MLF1IP. Oncogene 23: 3700–3707.
58. Suzuki H, Arakawa Y, Ito M, Saito S, Takeda N, et al. (2007) MLF1-interacting protein is mainly localized in nucleolus through N-terminal bipartite nuclear localization signal. Anticancer Res 27: 1423–1430.
59. Keppler A, Gendreizig S, Gronemeyer T, Pick H, Vogel H, et al. (2003) A general method for the covalent labelling of fusion proteins with small molecules *in vivo*. Nat Biotechnol 21: 86–89.
60. Jansen LET, Black BE, Foltz DR, Cleveland DW (2007) Propagation of centromeric chromatin requires exit from mitosis. J Cell Biol 176: 795–805.
61. Prendergast L, van Vuuren C, Kaczmarczyk A, Döring V, Hellwig D, et al. (2011) Premitotic assembly of human CENPs -T and -W switches centromeric chromatin to a mitotic state. PloS Biol 9: e1001082.
62. Lee KS, Oh DY, Kang YH, Park JE (2008) Self-regulated mechanism of Plk1 localisation to kinetochores: lessons from the Plk1-PBIP1 interaction. Cell Div 3: 4.
63. Leonhardt H, Rahn HP, Weinzierl P, Sporbert A, Cremer T, et al. (2000) Dynamics of DNA replication factories in living cells. J Cell Biol 149: 271–280.
64. Sporbert A, Domaing P, Leonhardt H, Cardoso MC (2005) PCNA acts as a stationary loading platform for transiently interacting Okazaki fragment maturation proteins. Nucleic Acids Res 33: 3521–3528.
65. Schmiedeberg L, Weisshart K, Diekmann S, Meyer zu Hoerste G, Hemmerich P (2004) High- and low-mobility populations of HP1 in heterochromatin of mammalian cells. Mol Biol Cell 15: 2819–2833.
66. Ribeiro SA, Vagnarelli P, Dong Y, Hori T, McEwen BF, et al. (2010) A super-resolution map of the vertebrate kinetochore. Proc Natl Acad Sci USA 107: 10484–10489.
67. Johnston K, Joglekar A, Hori T, Suzuki A, Fukagawa T, Salmon ED (2010) Vertebrate kinetochore protein architecture: protein copy number. J Cell Biol 189: 937–943.
68. Lawrimore J, Bloom KS, Salmon ED (2011) Point centromeres contain more than a single centromere-specific Cse4 (CENP-A) nucleosome. J Cell Biol 195: 573–582.
69. Hemmerich P, Schmiedeberg L, Diekmann S (2011) Dynamic as well as stable protein interactions contribute to genome function and maintenance. Chromosome Res 19: 131–151.
70. Dong Y, VandenBeldt KJ, Meng X, Khodjakov A, McEwen BF (2010) The outer plate in vertebrate kinetochores is a flexible network with multiple microtubule interactions. Nat Cell Biol 9: 516–522.

4. Diskussion

4.1. CENP-N

Zellzyklusabhängige Analsyetechniken und *in vivo* Messungen innerhalb lebender Zellen legten im Verlauf der letzten Jahre den Grundstein für eine Vielzahl neuer Erkenntnisse bezüglich des Aufbaus und der Funktionalität des inneren Kinetochors. Dies führte zu der Erkenntnis, dass dieser Unterkomplex nicht ausschließlich eine Gerüststruktur darstellt, welche während der Mitose lediglich als Andockstelle für die KMN-Netzwerkproteine dient (Cheeseman & Desai; 2008), sondern in der Interphase eine komplexe Funktion erfüllt. Hier ist neben CENP-T/W/S/X und CENP-O/P/Q/R/U besonders CENP-N hervorzuheben, welches im Verlauf der Mitose nur in niedriger Konzentration an das Kinetochor bindet und somit seine eigentliche Aufgabe vermutlich während der Interphase erfüllt (McClelland et al., 2007; Hellwig et al., 2011; Prendergast et al., 2011; Eskat et al., 2012).
CENP-N lokalisiert während der Mitose und der G1-Phase nur in geringen Mengen (~20%) an das Kinetochor, wobei die stabile Bindung in der Mitose, im Verlauf der G1-Phase aufgehoben ist. Mit dem Beginn der S-Phase kommt es zu einer verstärkten Rekrutierung, welche am Übergang zwischen S- und G2-Phase in einem Maximum resultiert. Während der mittleren S-Phase kommt es zu einer Stabilisierung der Bindung. Darauf folgt im Verlauf der G2-Phase bis zum Beginn der sich anschließenden Mitose eine Delokalisierung von CENP-N auf 20% des maximalen Gehaltes (McClelland et al., 2007; Hellwig et al 2011) (Abbildung 8A). Ähnliche dynamischen Eigenschaften und Bindeverhalten wie CENP-N wurden auch bei anderen Komponenten des inneren Kinetochors beobachtet und deuten auf eine Funktion auch anderer Kinetochorproteine innerhalb der S-Phase hin, welche von der Aufgabe als Gerüstbestandteil abweicht.
Die Anreicherung von CENP-N an das Kinetochor während der S-Phase geht ebenfalls mit einem erhöhten Gehalt von ungebundenem CENP-N in der gesamten Zelle einher. Hierbei ist zu bemerken, dass der fünffachen Erhöhung an den Kinetochoren lediglich eine Konzentrationserhöhung um den Faktor drei des in der Zelle insgesamt vorhandenen CENP-N gegenübersteht. Diese Diskrepanz sowie die beobachtete Immobilisierung werden nicht durch eine posttranslationale Modifikation verursacht. Im Rahmen von biochemischen Untersuchungen mittels Westernblot wurden keine Anhaltspunkte für eine Proteinmodifikation gefunden (Hellwig et al., 20011). Stattdessen wird die Bindung des inneren Kinetochors selbst verändert. *In vitro* Experimente haben gezeigt, dass eine direkte Bindung zwischen dem C-Terminus von rekombinantem CENP-N und CENP-L möglich ist (Caroll et al., 2009).

Unter Verwendung einer partiellen Deletion des C-Terminus von CENP-N konnte beobachtet werden, dass es *in-vivo* zu einer Destabilisierung der Bindung von EGFP-CENP-NΔC an das Kinetochor während der mittleren S-Phase kommt (Hellwig et al., 2011). Dies deutet darauf hin, dass die Immobilisierung von CENP-N durch die C-terminale Bindung über CENP-L in der Mitte der S-Phase ausgelöst werden könnte (Abbildung 7).

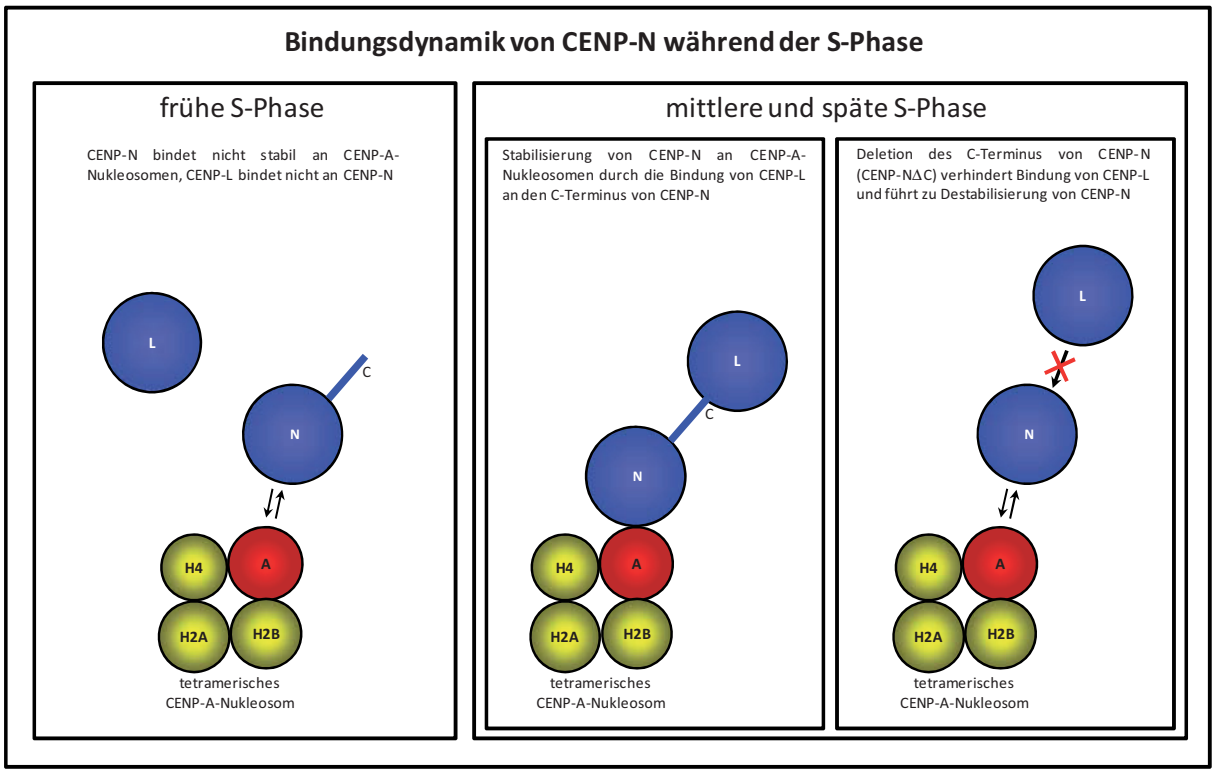

Abbildung 7: während der frühen S-Phase weist CENP-N ein dynamisches Verhalten am Kinetochor auf (links). Im Verlauf der mittleren und späten S-Phase kommt es zur Stabilisierung der Bindung mit gleichzeitigem Anstieg des Proteingehalts auf ein Maximum am Ende der S-Phase. Dieser Prozess könnte durch die Anheftung von CENP-L an den C-Terminus von CENP-N verursacht werden (Mitte). Das Fehlen des C-Terminus von CENP-N hat zur Folge, dass dieses Kinetochorprotein im Verlauf der späten S-Phase nicht mehr fest gebunden wird, welches auf die mangelnde Stabilisierung mittels CENP-L zurück zu führen sein könnte (rechts).

Desweiteren wäre es vorstellbar, dass auch durch die Veränderung der der Bindung von CENP-N zugrunde liegenden Strukturen eine erhöhte Einbaurate bzw. Stabilisierung von CENP-N ausgelöst wird. Hierbei ist besonders die Stabilisierung von CENP-C während der mittleren S-Phase zu erwähnen. CENP-C bindet, ebenfalls wie CENP-N, direkt an den CENP-A-Nukleosomen-haltigen centromerischen Lokus (Politi et al., 2002; Carroll et al., 2010). Eine Studie dieser Wechselwirkung wurde an einem rekombinant hergestellten CENP-A-Chromatinarray unter Zusatz von *Xenopus laevis* Eizellextrakt durchgeführt und zeigte, dass die Bindung von CENP-N an diese Struktur CENP-C-abhängig von statten geht.

Im Gegensatz dazu ist die Bindung von CENP-N an einzelne CENP-A-Mononukleosomen CENP-C-unabhängig (Guse et al., 2011). Dies legt nahe, dass die Rekrutierung von CENP-N an das Kinetochor in lebenden Zellen durch eine Veränderung der Bindungsbedingungen ausgelöst und durch die Stabilisierung von CENP-C beeinflusst werden könnte (Abbildung 8B).

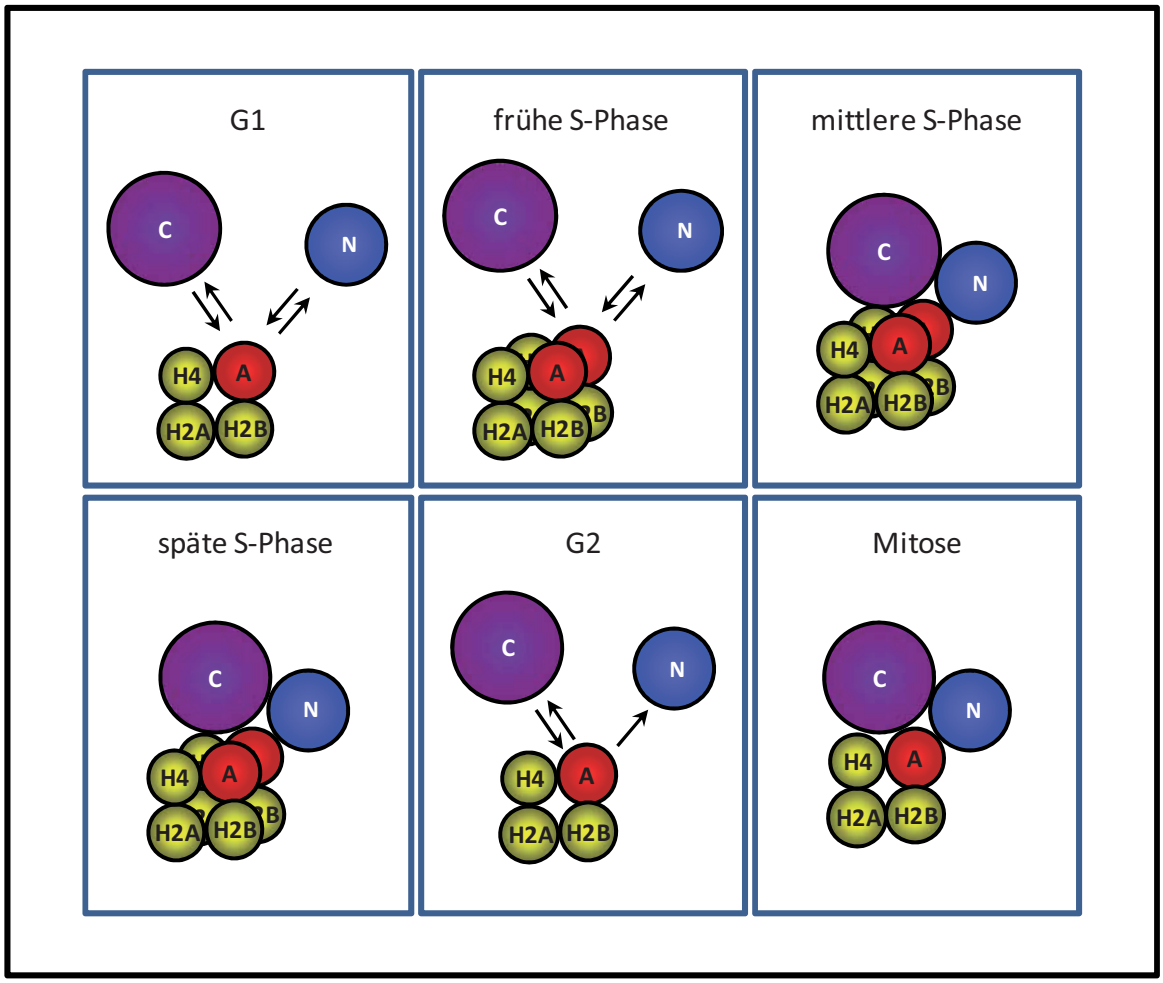

Abbildung 8: Modellhafte Darstellung des Zusammenhangs zwischen CENP-C und CENP-N über den Zellzyklus hinweg. Ein dynamische Verhalten von CENP-C könnte jeweils eine Destabilisierung bzw. Dissoziation von CENP-N nach sich ziehen (G1-, frühe S- und G2-Phase), während die feste Bindung von CENP-C den stabilen Einbau von CENP-N bedingen könnte (mittlere und späte S-Phase, Mitose).

Sowohl der Anstieg der CENP-N-Konzentration beginnend in der frühen S-Phase als auch die darauf folgende Verringerung während der G2-Phase lässt sich nicht mit einer veränderten Syntheserate erklären. Bestimmungen des Expressionslevels mittels quantitativer RT-PCR zeigen lediglich eine leichte Schwankung der CENP-N mRNA-Gehalte über den gesamten Zellzyklus hinweg (Hellwig et al., 2011). Diese Beobachtung sowie die Feststellung, dass erhöhte CENP-N-Mengen nur in Zusammenhang mit einem Zuwachs an

gebundenem Protein stattfinden, legt nahe, dass ungebundenes CENP-N einer Degradation unterworfen sein könnte.

A

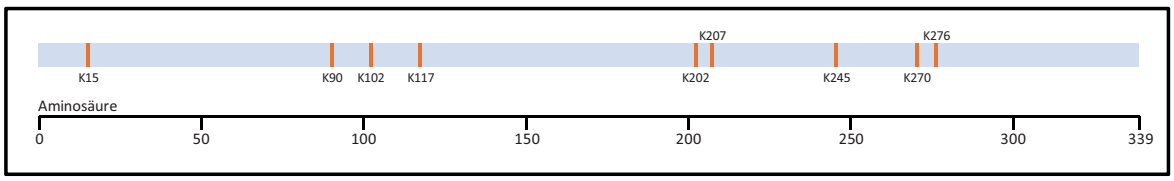

B

Protein	Anzahl poteniell ubiquitinierbarer Lysinreste
CENP-A	0
CENP-B	2
CENP-C	5
CENP-H	3
CENP-I	2
CENP-K	0
CENP-L	2
CENP-M	0
CENP-N	9

Protein	Anzahl poteniell ubiquitinierbarer Lysinreste
CENP-O	0
CENP-P	1
CENP-Q	1
CENP-R	0
CENP-S	1
CENP-T	0
CENP-U	2
CENP-W	0
CENP-X	0

Abbildung 9: **A:** graphische Darstellung der potenziellen Aminosäuren von CENP-N, an welchen eine Ubiquitinierung als Signal für die Degradation ungebundenen Proteins geschehen könnte. **B:** Liste der potientiell ubiquitinierbaren Lysinreste der CCAN-Proteine basierend auf Datenbankrecherchen

Basierend auf systemisch durchgeführten Untersuchungen des Proteoms wurden neun Aminosäuren als mögliche Ubiquitinierungsstellen postuliert (Kim et al., 2011) (Abbildung 9A). Diese Häufung von potentiell ubiquitinierbaren Aminosäureresten stellt eine Ausnahme innerhalb der CCAN-Proteine dar. Einzig CENP-C und CENP-H weisen fünf bzw. drei mögliche Ubiquitinierungsstellen auf, alle anderen Proteine des inneren Kinetochors besitzen lediglich zwei oder weniger ubiquitinierbare Lysinreste (Abbildung 9B). Somit wäre eine kontrollierte Degradation von CENP-N durchaus vorstellbar.

Neueste Untersuchungen haben gezeigt, dass zwischen zwei Zellteilungen die gesamte Chromatinstruktur im centromerischen Bereich einer umfassenden Konformationsänderung unterworfen ist (Bui et al., 2012). Im Gegensatz zu H3-Nukleosomen zeigen CENP-A-haltige Nukleosomen eine ausgeprägte innere Dynamik. Nach Abschluss der Mitose sowie im Verlauf der G1-Phase liegen die CENP-A-Nukleosomen als Tetramere vor, wobei diese aus jeweils einem Molekül H2A, H2B, H4 und CENP-A bestehen. Am Übergang zwischen G1 und S-Phase kann eine Mischung aus Tetrameren und Oktameren beobachtet werden, wobei es im Rahmen der Oktamerbildung zu einer Verdopplung der tetramerischen Struktur kommt. Hierbei konnte gezeigt werden, dass die Duplikation von einem Höhenzuwachs um den Faktor zwei begleitet wird. Die im Verlauf der S-Phase ausschließlich als Oktamere vorliegenden CENP-A-Nukleosomen werden in der G2-Phase wieder zu Tetrameren reduziert, welche während der Mitose unverändert in dieser Form erhalten bleiben

(Dimitriadis et al., 2010; Bui et al., 2012) (Abbildung 13). Des Weiteren konnte eine Acetylierung der Aminosäure 124 von CENP-A in der G1-Phase gezeigt werden. Diese Modifikation von K124 ist in der S- und G2-Phase sowie in der Mitose nicht nachweisbar (Bui et al., 2012). Die Remodelierung der Nukleosomen und die Deacetylierung von K124 von CENP-A gehen ebenfalls mit Veränderungen der Lokalisierung und Dynamik der CENP-A-Chaperons HJURP einher. HJURP bindet innerhalb der G2-Phase des Zellzyklus an die Kinetochorstruktur und wird während des Übergangs zwischen G1- und S-Phase wiederum delokalisiert (Dunleavy et al., 2011; Bui et al., 2012). Dies könnte darauf hindeuten, dass HJURP nur an das Kinetochor binden kann, wenn die CENP-A-Nukleosomen in ihrer tetramerischen Konformation vorliegen bzw. CENP-A am Lysinrest 124 acetyliert ist (Bui et al., 2012).

Andere Studien zeigen, dass eine der Funktionen von HJURP die Rekrutierung der CENP-A-H4-Dimere an das Kinetochor ist, wobei es zur Ausbildung eines Präassemblierungskomplexes bereits im Zytoplasma der Zelle kommt (Foltz et al., 2009; Sanchez & Losada, 2011; Zhou et al., 2011). Hierbei bindet HJURP mit Hilfe seiner CENP-A-Bindedomäne (CBD) die CENP-A-Targeting-Domäne (CATD) von CENP-A und verhindert dadurch die unspezifische Bindung von CENP-A an nicht-centromerische DNA (Foltz et al., 2009; Hu et al., 2011). *In vitro* Studien haben gezeigt, dass CENP-N ebenfalls an die CATD von CENP-A bindet (Carroll et al., 2009). Im Rahmen von FRET-Messungen konnte in lebenden Zellen die enge Nachbarschaftzwischen CENP-N und CENP-A bestätigt werden (Hellwig et al., 2011). Dies könnte darauf hindeuten, dass HJURP, ausgelöst durch die Modifizierung von CENP-A, im Bereich des Centromers CENP-A nicht mehr binden kann und somit die Bindestelle für CENP-N frei gibt. Hierauf folgt das Besetzen der CATD durch CENP-N und könnte somit den steigenden Gehalt von CENP-N am Kinetochor während der S-Phase erklären. Auf einen möglichen Zusammenhang zwischen CENP-N und HJURP deuten auch die gemessene Anzahl entsprechender Proteine in *S. cerevisiae* hin. Es konnte festgestellt werden, dass durchschnittlich 1,6 ± 0,3 Moleküle Chl4 (Homolog von CENP-N) und 1,3 ± 0,3 Moleküle Scm3 (Homolog von HJURP) an jedes Kinetochor binden (Lawrimore et al., 2011). Bei dieser Untersuchung fällt auf, dass jede andere Komponente des CCAN in *S. cerevisiae* in deutlich größeren Mengen vorhanden ist. Die Autoren konnten auch zeigen, dass die Proteinmengen in anderen Organismen im gleichen Verhältnis zueinander stehen, wobei hingegen die absoluten Zahlen variieren (Lawrimore et al., 2011).

HJURP besitzt innerhalb der CBD ein nach seiner Aminosäuresequenz benanntes TLTY-Motiv (Aminosäuren 54 bis 61), welches essentiell für die Bindung an CENP-A ist (Shuiab et al., 2010). Ein direkter Aminosäuresequenzvergleich zwischen CENP-N und HJURP zeigt keine Homologie im Bereich der CBD innerhalb von CENP-N. Durch die Einteilung der Aminosäuren der CBD von HJURP sowie aller Aminosäuren von CENP-N nach ihren

biochemischen Eigenschaften zeigt sich eine Ähnlichkeit des TLTY-Motivs mit den Aminosäuren 249 - 256 von CENP-N (Abbildung 10A). Dies könnte darauf hindeuten, dass CENP-N über ähnliche chemische Bindungsverhältnisse an die CATD von CENP-A lokalisiert.

In *S. cerevisiae* konnte gezeigt werden, dass das Homolog von CENP-N, Chl4, nicht essentiell für die Aufrechterhaltung von bereits bestehenden Kinetochoren ist. Im Gegensatz dazu scheint es bei der Neuetablierung von stabilen Kinetochoren unabdingbar zu sein. In Folge dieser Beobachtungen wurde CENP-N als Genauigkeitsfaktor postuliert, welcher den korrekten Einbau von CENP-A unterstützt (Mythreye & Bloom, 2003). Da im Menschen der Verlust von CENP-N starke Auswirkungen auf die Mitose hat, indem es zu einem verminderten Einbau von CENP-A während der G1-Phase kommt, könnte die Funktion als Genauigkeitsfaktor evolutionär konserviert sein.

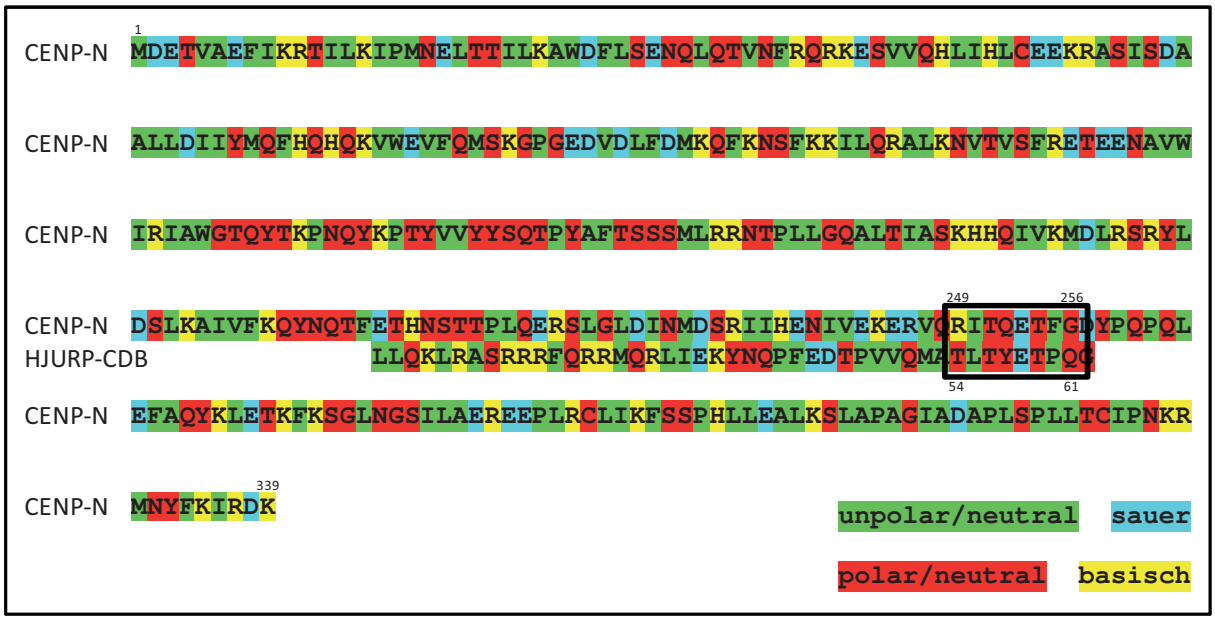

Abbildung 10: Die Proteinsequenzen von CENP-N und der CENP-A-Bindedomäne (CDB) von HJURP wurden nach den biochemischen Eigenschaften der Aminosäurereste in unpolar/neutral (grün), polar/neutral (rot), sauer (blau) und basisch (gelb) eingeteilt. Hierdurch fällt auf, dass es im Bereich der Aminosäuren 249-256 von CENP-N und 54-61 der CBD von HJURP, welche das TLTY-Motiv enthält, zu einer Übereinstimmung kommt.

Es liegt allerdings nahe, dass CENP-N in der mittleren bis späten S-Phase als dem Zeitpunkt mit der höchsten Konzentration gebundenen Proteins im Verlauf des Zellzyklus seine zentrale Funktion erfüllt. Dies führte zu den Annahmen, dass CENP-N eventuell in die Stabilisierung der CENP-A-Nukleosomen während der S-Phase involviert ist (Dorn & Maddox, 2011) oder dass es bei der Reetablierung des Kinetochors nach der Replikation eine Rolle spielt und somit neben CENP-C essentiell für die Konstitution eines funktionellen Kinetochors sein könnte (Quenet & Dalal, 2012).

4.2. CENP-T

Sowohl CENP-T als auch CENP-W sind essentielle Bestandteile der Kinetochorstruktur und haben die Fähigkeit, sich an DNA anzuheften. Die Assoziation von CENP-T erfolgt im Bereich der H3-Nukleosomen exklusiv an centromerischer DNA, allerdings nur, wenn CENP-A ebenfalls vorhanden ist (Hori et al., 2008; Gascoigne & Cheeseman, 2012).
Die Kristallstruktur von CENP-T und CENP-W zeigt, dass beide Proteine ein Heterodimer bilden, welches in seiner Struktur homolog zu den H2A/H2B- bzw. H3/H4-Dimeren ist. Sie zeichnen sich jeweils durch eine Histonfaltungsdomäne aus, welche die Dimerisierung ermöglicht (Nishino et al., 2012). Neueste Untersuchungen deuten darauf hin, dass CENP-T und CENP-W gemeinsam mit einem Dimer bestehend aus CENP-S und CENP-X, welche ebenfalls über ihre Histonfaltungsdomänen verbunden sind, eine neue tetramerische Nukleosomenspezies bilden könnten. Diese sind in der Lage, DNA zu binden und zu wickeln, wobei im Gegensatz zu kanonischen Nukleosomen nur jeweils 100 Basenpaare pro Umwindung verwendet werden (Foltz & Stukenberg, 2012; Nishino et al., 2012) (Abbildung 12 & 13).
CENP-T und CENP-W zeigen eine ungewöhnliche Dynamik innerhalb des Zellzyklus. Während der Mitose und der G1-Phase binden beide Proteine nur in geringen Mengen fest an das Kinetochor. Im weiteren Verlauf des Zellzyklus werden immer größere Mengen von CENP-T und CENP-W rekrutiert, bis in der G2-Phase ein Maximum erreicht ist. Darauf hin sinkt der Gehalt an gebundenem Protein wieder ab (Prendergast et al., 2011). Diese dynamischen Beobachtungen legen allerdings nahe, dass die postulierte Plattformbildung von CENP-T nicht direkt in der Mitose ihre Funktion zu erfüllen hat. Die Destabilisierung sowie das Erreichen des Maximums bereits in der G2-Phase mit anschließende Absinken des Proteingehalts in der Mitose deuten darauf hin, dass die etablierte Plattform ein Fundament darstellt, welches sich in der G2-Phase etabliert (Hori et al., 2007; Joglekar et al., 2006; Cheeseman & Desai, 2008; Dorn & Maddox, 2011 Gascoigne et al., 2011; Prendergast et al., 2011) (Abbildung 13). Zusammen mit CENP-C und CENP-N könnte CENP-T demzufolge die strukturelle Grundlage für die in der Mitose zu verrichtende mechanische Arbeit vorbereiten. Es wäre vorstellbar, dass es zur Ausbildung eines Ankers kommt, welche das Fundament für die Rekrutierung des äußeren Kinetochors legt. Die basalen Kinetochorproteine verlieren gegen Ende der Interphase ihre Bedeutung und werden daraufhin delokalisiert (Hellwig et al., 2010; Prendergast et al., 2011; Hori et al., 2013).
Die Depletion von CENP-T oder CENP-W führen zu starken Störungen der Mitose. Im

Gegensatz zu den beobachteten Mitosedefekten ausgelöst durch CENP-C oder CENP-N kommt es allerdings nicht zu einer Interferenz mit dem Ladeverhalten von CENP-A (Foltz et al., 2009; Carroll et al., 2009; Gascoigne et al., 2011; Prendergast et al., 2011). Somit liegt es nahe, dass die durch den Mangel des CENP-T/W Komplex ausgelösten Beeinträchtigungen unabhängig von der korrekten Assemblierung der CENP-A-Nukleosomen ist.

CENP-T und –W zeichnen sich durch einen sehr starken Austausch des gebundenen Proteinbestands zwischen zwei Zellteilungen aus. Es konnte gezeigt werden, dass im Rahmen einer Verdopplung nahezu alle Moleküle dieser beiden Kinetochorkomponenten neu eingebaut werden. Im Gegensatz dazu wird CENP-A pro Zellzyklus nur zu 50% *de novo* rekrutiert (Vereault et al., 2003; Prendergast et al., 2011). Dessen Einbau erfolgt ab dem Ende der Mitose bis in die G1-Phase, wobei die Synthese von CENP-A im vorrangegangen Zellzyklus von statten geht (Shelby et al., 2000; Hemmerich et al., 2008; Jansen et al.2007; Bernad et al., 2011). Die beiden Komponenten des CENP-T/W-Komplexes zeigen auch in diesem Punkt ein anderes Verhalten als CENP-A. Es wurde beobachtet, dass CENP-T und CENP-W in ein und demselben Zellzyklus synthetisiert und in den inneren Kinetochor integriert werden. Dies verweist auf einen von CENP-A mechanistisch unabhängigen Rekrutierungswegs dieses Histonfaltungskomplexes (Abbildung 11).

Während der N-Term von CENP-T eine globuläre Struktur bildet, kommt es zu einer Ausstülpung des C-Terminus in Richtung der Chromosomenaußenseite. Diese flexible Verlängerung ermöglicht es CENP-T während der Mitose mit dem KMN-Bestandteil Hec1 zu interagieren (Suzuki et al., 2011; Gascoigne et al., 2011) (Abbildung 12). Um dies zu bewirken, kommt es zu einer Phosphorylierung dieser Region von CENP-T im Verlauf der G2-Phase durch die Cyclin-abhängige Kinase (CDK). Diese Modifikation steigt im weiteren Verlauf der Mitose nach und nach an, bis sie während der Anaphase wieder abfällt (Gascoigne et al., 2011).

Untersuchungen in *S. cerevisiae* haben gezeigt, dass das Homolog zu CENP-T, Cnn1, innerhalb der Interphase in gleichen Mengen an den Kinetochor lokalisiert (Gascoigne & Cheeseman, 2012; Bock et al., 2012). Diese Beobachtung scheint die evolutionär konservierte Funktion von CENP-T zu bestätigen, da der Punktkinetochor von *S. cerevisiae* über den ganzen Zellzyklus hinweg an die Mikrotubuli gebunden ist. Somit ist es auch nötig, dass über die gesamte Zeit die fundamentgebende Aufgabe durch Cnn1 erfüllt wird. Im Gegensatz zum Menschen kommt es in *S. cerevisiae* allerdings innerhalb der Mitose zu einer Erhöhung der Cnn1-Gehalte, welche auf eine Remodulierung der Architektur des Kinetochors während der Meta-Anaphasetransition hinweist (Schleiffer et al., 2012). Desweiteren konnte gezeigt werden, dass ebenfalls in der Phosphorylierung Unterschiede zu Säugern bestehen. Cnn1 liegt bereits in der G1-Phase zu einem gewissen Anteil als

phosphoryliertes Protein vor. Der Grad der Modifikation steigt mit dem Eintritt in die S-Phase an und wird bis zur Metaphase auf einem hohen Niveau gehalten. Dies suggeriert die Erzeugung eines Phosphorylierungschwellenwertes, welcher zum Eintritt in die Anaphase benötigt wird. Während der Anaphase kommt es zur Dephosphorylierung von Cnn1, welcher wiederrum einen negativen Schwellenwert erzeugt und die Delokalisierung der überschüssigen Cnn1-Kopien am Ende der Anaphase auslöst (Bock et al., 2012). Ebenso wie CENP-T weist Cnn1 in *S. cerevisiae* eine zellzyklusabhängige Bindung zu Ndc80, dem Homolog von Hec1, auf. Diese ist besonders stark in der Anaphase ausgeprägt und gibt somit einen weiteren Hinweis darauf, dass die Fähigkeit von CENP-T/Cnn1 seinen Bindungspartner Hec1/Ndc80 zu verankern, um mit der mitotischen Spindel zu interagieren, eine konservierte Eigenschaft zu seien scheint (Schleiffer et al., 2012; Bock et al., 2012; Gascoigne & Cheeseman, 2012).

4.3. CCAN

Die Feststellung, dass alle am Aufbau des inneren Kinetochors beteiligte Proteine ein ähnliches Expressionsmuster aufweisen, legt nahe, dass die Bestandteile des CCAN einer co-regulierte Transkription unterliegen. Diese stehen unter dem Einfluss verschiedener Transkriptionsfaktoren sowie Mikro-RNA's (Reinhold et al., 2011).
Innerhalb des inneren Kinetochors kommt es zu einer Vielzahl an Bindungen zwischen den verschiedenen Proteinen (Abbildung 12). Da die einzelnen Komponenten zu unterschiedlichen Zeitpunkten des Zellzykus in verschieden großen Mengen vorliegen, kommt es zu einem steten Umbau der Kinetochorkomposition und -struktur (Hellwig et al., 2008; Dunleavy et al., 2009; Eskat et al., 2012) (Abbildung 11). Es konnte gezeigt werden, dass sogar die CENP-A-Nukleosomen selbst, und somit auch die generelle Struktur des centromerischen Chromatins, über den Zellzyklus hinweg einer Konformationsänderung unterliegen (Bui et al., 2012). Dies legt nahe, dass auch die Bindung anderer Proteine variabel sein könnte. Hierbei ist festzustellen, dass die beobachteten Nachbarschaften von CENP-M zu CENP-T, CENP-I zu CENP-U sowie CENP-B zu CENP-U in großer Häufigkeit auftreten und

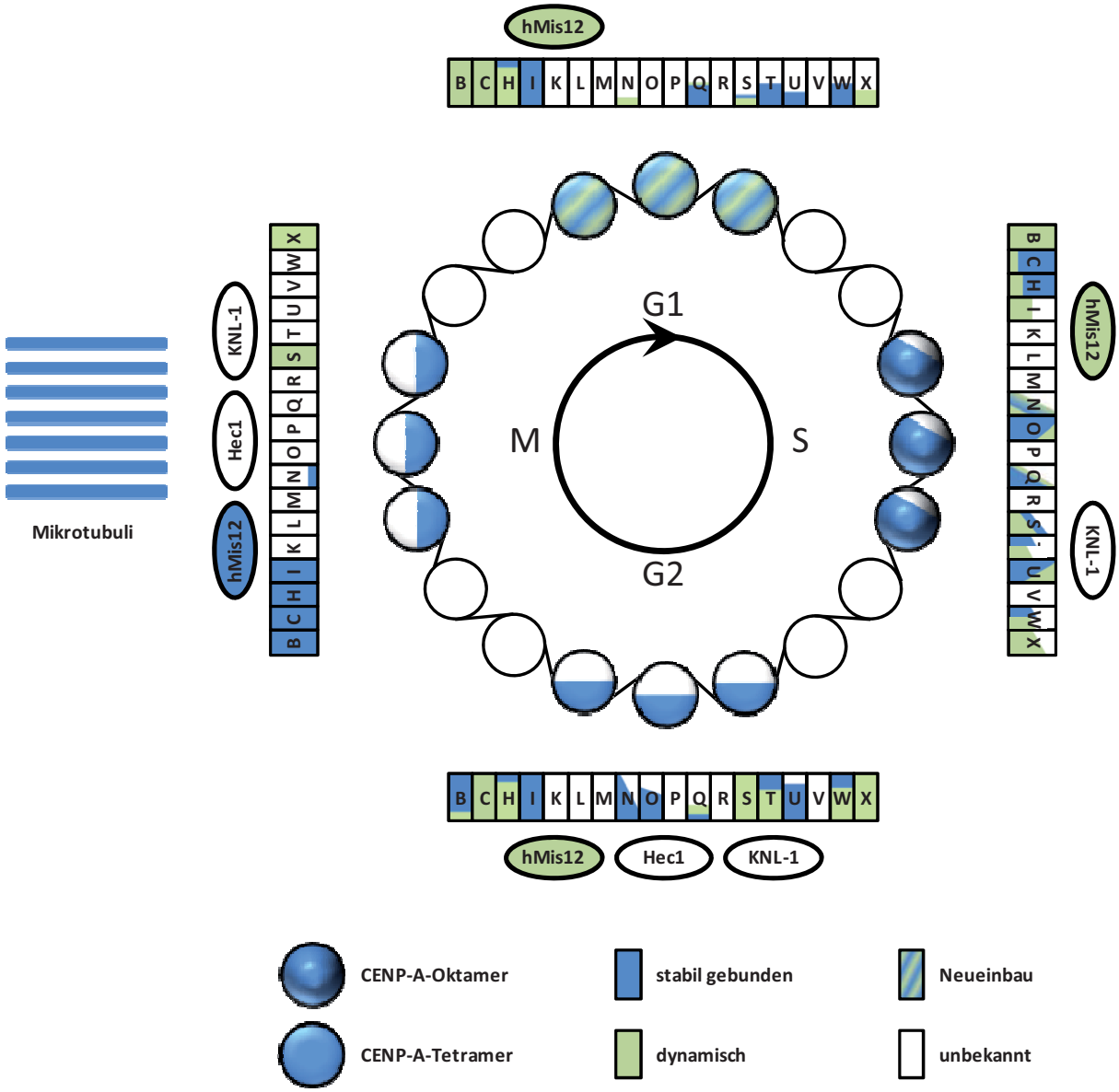

Abbildung 11: Modell der Proteingehalte, der Dynamik und des Ladeverhaltens der Proteine des inneren Kinetochors sowie ausgewählten Proteinen des äußeren Kinetochors über den Zellzyklus hinweg. (Modifiziert nach Dorn & Maddox, 2011)

somit eine über den Zellzyklus etablierte Bindung darstellen könnten (Hellwig et al., 2009). Eine Reihe weiterer Elemente des inneren Kinetochors zeigt nur in seltenen Fällen eine geringe Entfernung zueinander und könnte suggerieren, dass es sich hierbei basierend auf der variierenden Zusammensetzung um wandelbare Nachbarschaften handelt, welche nur in Teilen des Zellzyklus bestehen. Es wäre auch möglich, dass sich diese Proteine in unterschiedlichen CCAN-Komplexen befinden und ausschließlich bei bestimmten Konformationen der zu Grunde liegenden Chromatinstruktur eng beieinander liegen (Hellwig et al., 2009).

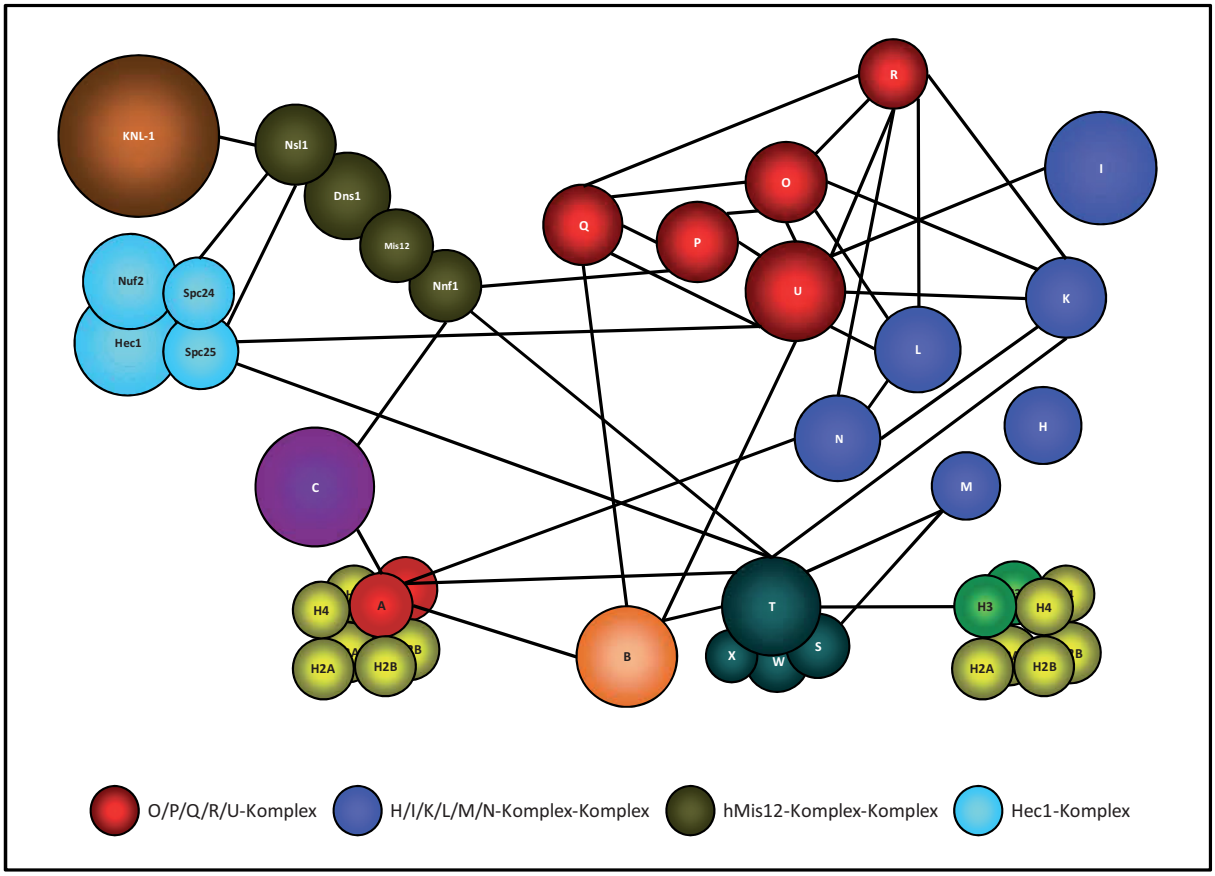

Abbildung 12: schematische Darstellung der Interaktionen bzw. Nachbarschaften der inneren und ausgewählten äußeren Kinetochorproteine. Es wurden nur Zusammenhänge dargestellt, welche über Förster-Resonanz-Energie-Transfer sowie biochemische Analysen gezeigt werden konnten. Ergebnisse aus Hefe-2-Hybrid-Studien und RNAi-Untersuchungen wurden aufgrund hoher Falschpositivraten sowie schwieriger Wertbarkeit außer Acht gelassen.

Es konnte gezeigt werden, das die Proteine des CENP-P, -O, -Q, -R und -U in die Struktur des inneren Kinetochors eingebettet sind (Eskat et al., 2012). Sie bilden einen funktionalen Unterkompex, der sich basierend auf CENP-H, -I, -K, -L und –M etabliert und an welche wiederum direkt oder indirekt mittels KMN-Proteinen die Spindelmikrotubuli binden können (Minoshima et al., 2005; McAinsh et al., 2006; McClelland et al., 2007; Hua et al., 2011; Amaro et al., 2010; Eskat et al., 2012) (Abbildung 12). Dies wird ebenfalls untermauert durch die Beobachtung, dass die separate Deletion von CENP-O, -P, -Q oder –U den gleichen phänotypischen Wachstumsdefekt auslöst wie kombinierte Deletionen mehrerer Komponenten. Diese nicht additiven Effekte deuten auf einen gemeinsamen funktionellen Pfad hin, erstrecken sich allerdings nicht auf CENP-R, womit dieses Protein eine Sonderstellung im Komplex einnimmt (Hori et al., 2008). Desweiteren zeigte sich, dass sich dieser vielfach miteinander verwebte Komplex (Abbildung 12) entweder mit einer variierenden Stöchiometrie, inklusive partieller Di- bzw. Oligomerisierung mancher

Komponenten, aufbaut oder dass Nachbarschaften zwischen verschiedenen CCAN-Komplexen ausgebildet werden können. Korrelierende Messungen der Diffusionsgeschwindigkeiten dieser CCAN-Komponenten deuten darauf hin, dass es nicht zur Ausbildung eines größeren Präassemblierungskomplexes kommt. Es konnten allerdings bereits im Nukleoplasma vorgeformte Heterodimere von CENP-O und CENP-P sowie von CENP-Q und CENP-R beobachtet werden (Amaro et al., 2010; Eskat et al., 2012).

Weiterhin konnte gezeigt werden, dass jedes am P/O/Q/R/U-Subkomplex beteiligte Protein eine individuelle Dynamik aufweist sowie zu unterschiedlichen Zeitpunkten verschieden stark an das Kinetochor rekrutiert wird (Abbildung 11). Während CENP-P, -O, -Q und U zu variablen Anteilen mobil bzw. stabil an das Kinetochor gebunden sind, kann CENP-R über den gesamten Zellzyklus hinweg zu 100% austauschen. Diese die Sonderstellung von CENP-R verhärtende Feststellung sowie die Beobachtung, dass die Deletion dieses Proteins keine Auswirkungen auf die Rekrutierung der andern Elemente des Komplexes hat, suggeriert, dass CENP-R oberhalb von CENP-O/P/Q/U am Kinetochor lokalisiert (Hori et al., 2008) Es ist außerdem auffällig, dass CENP-U immer zu gleichen Mengen lokalisiert, wobei CENP-O und CENP-P innerhalb der späten S-Phase bzw. in der G2-Phase vom Kinetochor verschwindet (Kang et al., 2006; Eskat et al., 2012). Dies legt die Vermutung nahe, dass der P/O/Q/R/U-Subkomplex aus Proteinen mit jeweils einzigartigen Eigenschaften zu bestehen scheint und deutet darauf hin, dass diese unterschiedliche Funkionen zu erfüllen haben.

Sowohl die Fähigkeit der Einzelproteine andere Teile des Komplexes an das Kinetochor zu rekrutieren als auch die Möglichkeit zur Heterooligomerisierung einiger Elemente des O/P/Q/R/U-Subkomplexes deuten auf einen Selbstassemblierungsprozess hin. CENP-U und CENP-Q zeigen außerdem während der späten S-Phase im Bereich des Kinetochors Nachbarschaftsverhältnisse zu sich selbst (Eskat et al., 2012). Dies bestätigt die Annahme, dass sich die stöchiometrischen Verhältnisse im Verlauf des Zellzyklus ändern oder dass in gewissen Zeitspannen verschiedene CCAN-Komplexe eine größere Nähe aufweisen. Desweiteren könnte diese Selbstassoziierung von CENP-U und CENP-Q sowie der gesamte Aufbau des O/P/Q/R/U-Komplexes in der S-Phase ein wichtiger Schritt im Rahmen der Reifungsprozess des Kinetochors sein (Eskat et al., 2012).

Auch eine Funktion der Proteine im Rahmen der Reparatur bzw. Regeneration von Spindelschäden wurde postuliert. Hierbei ist zu erwähnen, dass es zu einer Phosphorylierung von CENP-U durch die Proteinkinase Plk1 kommt, welche wiederum in der G2-Phase einen Schutz vor Abbau und der Zerstörung der Bindung der Mikrotubuli an den Kinetochor sowie der Verbindung zwischen den Schwesterchromatiden durch Proteasomen bieten könnte (Hori et al., 2008). Es wurde angenommen, dass diese Phosphorylierung den gebundenen Mikrotubuli die Möglichkeit bietet, sich im Falle der Falschanheftung wieder abzulösen und neu zu binden ohne abgebaut zu werden (Hua et al., 2011). Dies zeigt die

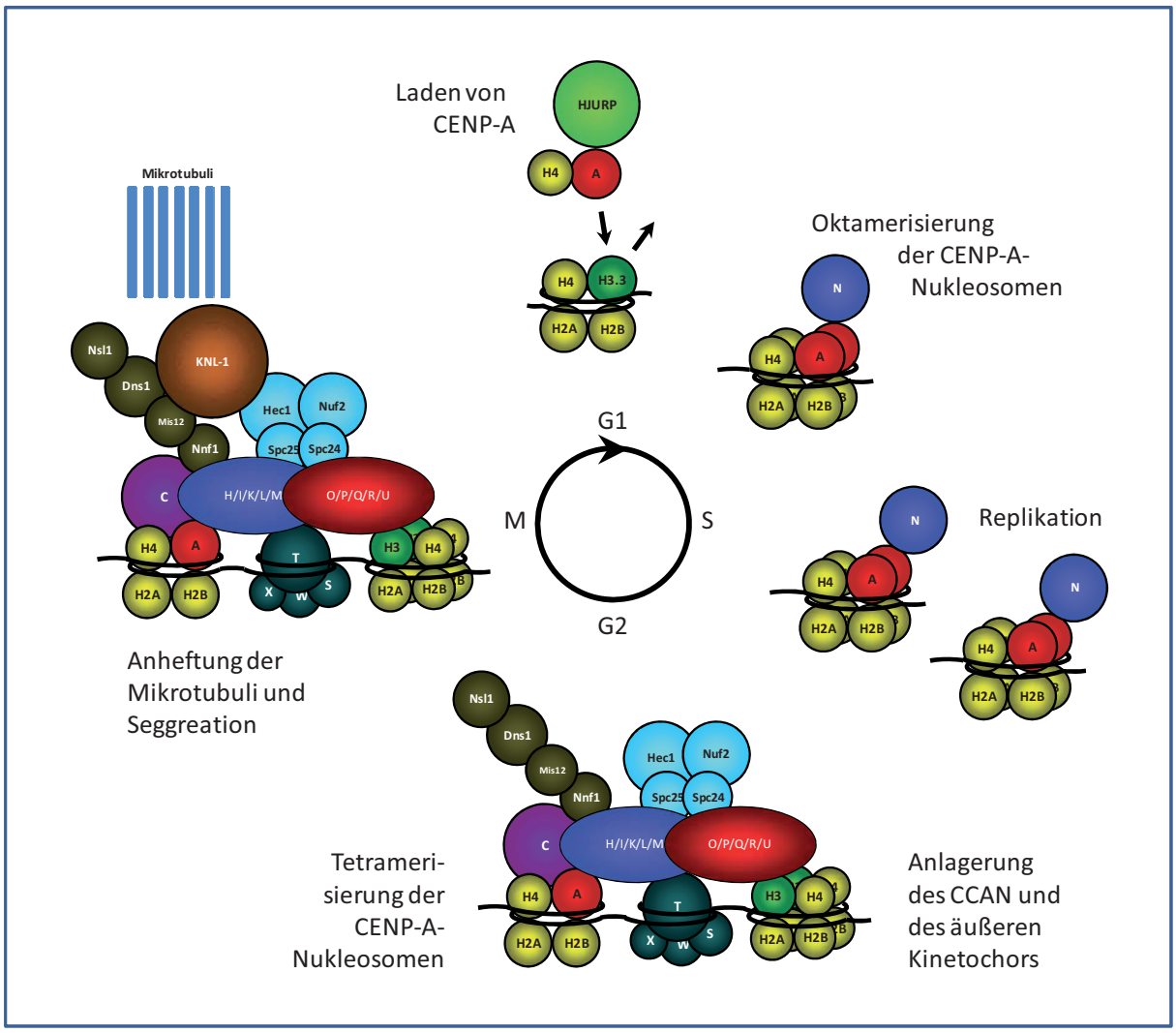

Abbildung 13: vereinfachte Darstellung der Abläufe am Kinetochor im Verlauf des Zellzyklus. Es zeigt sich eine funktionelle Teilung über die Zeit, welche in der ersten Hälfte des Zellzyklus mit der Etablierung und Aufrechterhaltung des an das centromerische Chromatin gebundenen Kinetochorkomplexes sowie der Verdopplung des genetischen Materials einhergeht. Gegen Ende der S-Phase beginnt die Rekrutierung der CENP-T/W/S/X-haltigen Nukleosomen und anderer CCAN-Proteine, welche ein Fundament für das äußere Kinetochor und letztendlich der Mikrotubuli während der Mitose bilden.

Wichtigkeit der korrekten Rekrutierung des O/P/Q/R/U-Komplexes und legt nahe, dass ein Umbau in die erforderliche Konformation vor der Mitose die Bindung der Mikrotubuli erst ermöglicht (Eskat et al., 2012).

5. Ausblick

Die im Lauf der letzten Jahre erlangten Erkenntnisse, woran die hier beschriebenen Arbeiten einen Anteil gehabt haben, zeichnen ein völlig neues und deutlich komplexeres Bild des Kinetochorkomplexes. Hierbei sind vor allem die Ergebnisse über CENP-N hervorzuheben, welche exemplarisch für eine umfassende Analyse stehen. Darauf aufbauende Untersuchungen in der Arbeitsgruppe Molekularbiologie am Fritz-Lippmann-Institut für Altersforschung an anderen Kinetochorproteinen haben sich daran orientiert und somit zur Gewinnung neuer Erkenntnisse beigetragen.

Da heute die Grundelemente des inneren Kinetochors bekannt sind, ist es möglich, übergeordnete Fragen zu stellen. Wie werden die Übergänge zwischen G1 und S-Phase bzw. zwischen der späten S- und G2-Phase gesteuert? Hierzu sind Untersuchung der Modifikationen der beteiligten Proteine und deren auslösenden Regulatoren (z.B. Kinasen) notwendig.

Prinzipiell ist festzuhalten, dass die bis heute erlangten Einsichten auf die Mitose übertragen werden müssen. Da diese Phase des Zellzyklus allerdings hochdynamisch und von nur kurzer Dauer ist, wird diese Aufgabe sich schwierig gestalten. Basierend auf den schon etablierten Methoden und Erfahrungen müssen neue Wege eingeschlagen werden. Ein vielversprechender Ansatzpunkt ist die Verwendung von photoaktivierbaren (z.B. PA-GFP) bzw. photokonvertierbaren (Kaede) Fluorophorvarianten, welche die Möglichkeit eröffnen, über die Anregung mit einem Laserpuls, gezielt spezifische Proteinpopulationen zu markieren und deren weiteres Verhalten in der lebenden Zelle zu verfolgen. Dies hat den großen Vorteil gegenüber den bisherig genutzten FRAP-Verfahren, das unter Ausnutzung der unterschiedlichen Emissionsspektren von Kaede schon vor der Mitose geladene Proteine von neu hinzugekommenen unterschieden werden können sowie deren differentielle Dynamiken erfassbar wären. Durch Verwendung von photoaktivierbarem GFP ist es möglich, nur die an ein einzelnes Kinetochor gebundenen Proteine über einen langen Zeitraum hinweg zu beobachten und somit die Problematik des stark ausgeprägten unspezifischen Fluoreszenzhintergrundes während der Mitose zu umgehen.

Diese Vielzahl an noch ausstehenden Untersuchungen zeigen deutlich, dass auch nach 130 Jahren wissenschaftlicher Tätigkeit rund um den Kinetochor nach wie vor unzählige Fragen offen sind und er auch weiterhin ein interessantes und vielversprechendes Forschungsfeld bleiben wird.

Literatur

Allshire, R. C. and G. H. Karpen. "Epigenetic Regulation of Centromeric Chromatin: Old Dogs, New Tricks?" *Nat Rev Genet* 9, no. 12 (2008): 923-37.

Amano, M., A. Suzuki, T. Hori, C. Backer, K. Okawa, I. M. Cheeseman and T. Fukagawa. "The Cenp-S Complex Is Essential for the Stable Assembly of Outer Kinetochore Structure." *J Cell Biol* 186, no. 2 (2009): 173-82.

Amaro, A. C., C. P. Samora, R. Holtackers, E. Wang, I. J. Kingston, M. Alonso, M. Lampson, A. D. McAinsh and P. Meraldi. "Molecular Control of Kinetochore-Microtubule Dynamics and Chromosome Oscillations." *Nat Cell Biol* 12, no. 4 (2010): 319-29.

Amor, D. J., K. Bentley, J. Ryan, J. Perry, L. Wong, H. Slater and K. H. Choo. "Human Centromere Repositioning "in Progress"." *Proc Natl Acad Sci U S A* 101, no. 17 (2004): 6542-7.

Ando, S., H. Yang, N. Nozaki, T. Okazaki and K. Yoda. "Cenp-a, -B, and -C Chromatin Complex That Contains the I-Type Alpha-Satellite Array Constitutes the Prekinetochore in Hela Cells." *Mol Cell Biol* 22, no. 7 (2002): 2229-41.

Ayer, L. M. and M. J. Fritzler. "Anticentromere Antibodies Bind to Trout Testis Histone 1 and a Low Molecular Weight Protein from Rabbit Thymus." *Mol Immunol* 21, no. 9 (1984): 761-70.

Bacia, K. and P. Schwille. "A Dynamic View of Cellular Processes by in Vivo Fluorescence Auto- and Cross-Correlation Spectroscopy." *Methods* 29, no. 1 (2003): 74-85.

Banks, D. S. and C. Fradin. "Anomalous Diffusion of Proteins Due to Molecular Crowding." *Biophys J* 89, no. 5 (2005): 2960-71.

Barnhart, M. C., P. H. Kuich, M. E. Stellfox, J. A. Ward, E. A. Bassett, B. E. Black and D. R. Foltz. "Hjurp Is a Cenp-a Chromatin Assembly Factor Sufficient to Form a Functional De Novo Kinetochore." *J Cell Biol* 194, no. 2 (2011): 229-43.

Barnicot, N. A. and H. E. Huxley. "Electron Microscope Observations on Mitotic Chromosomes." *Q J Microsc Sci* 106, no. 3 (1965): 197-214.

Barry, A. E., E. V. Howman, M. R. Cancilla, R. Saffery and K. H. Choo. "Sequence Analysis of an 80 Kb Human Neocentromere." *Hum Mol Genet* 8, no. 2 (1999): 217-27.

Ben-Porath, I. and R. A. Weinberg. "The Signals and Pathways Activating Cellular Senescence." *Int J Biochem Cell Biol* 37, no. 5 (2005): 961-76.

Bergmann, J. H., M. G. Rodriguez, N. M. Martins, H. Kimura, D. A. Kelly, H. Masumoto, V. Larionov, L. E. Jansen and W. C. Earnshaw. "Epigenetic Engineering Shows H3k4me2 Is Required for Hjurp Targeting and Cenp-a Assembly on a Synthetic Human Kinetochore." *EMBO J* 30, no. 2 (2011): 328-40.

Bernad, R., P. Sanchez, T. Rivera, M. Rodriguez-Corsino, E. Boyarchuk, I. Vassias, D. Ray-Gallet, A. Arnaoutov, M. Dasso, G. Almouzni and A. Losada. "Xenopus Hjurp and Condensin Ii Are Required for Cenp-a Assembly." *J Cell Biol* 192, no. 4 (2011): 569-82.

Bernat, R. L., M. R. Delannoy, N. F. Rothfield and W. C. Earnshaw. "Disruption of Centromere Assembly During Interphase Inhibits Kinetochore Morphogenesis and Function in Mitosis." *Cell* 66, no. 6 (1991): 1229-38.

Berney, C. and G. Danuser. "Fret or No Fret: A Quantitative Comparison." *Biophys J* 84, no. 6 (2003): 3992-4010.

Black, B. E. and E. A. Bassett. "The Histone Variant Cenp-a and Centromere Specification." *Curr Opin Cell Biol* 20, no. 1 (2008): 91-100.

Black, B. E., M. A. Brock, S. Bedard, V. L. Woods, Jr. and D. W. Cleveland. "An Epigenetic Mark Generated by the Incorporation of Cenp-a into Centromeric Nucleosomes." *Proc Natl Acad Sci U S A* 104, no. 12 (2007): 5008-13.

Black, B. E. and D. W. Cleveland. "Epigenetic Centromere Propagation and the Nature of Cenp-a Nucleosomes." *Cell* 144, no. 4 (2011): 471-9.

Black, B. E., D. R. Foltz, S. Chakravarthy, K. Luger, V. L. Woods, Jr. and D. W. Cleveland. "Structural Determinants for Generating Centromeric Chromatin." *Nature* 430, no. 6999 (2004): 578-82.

Black, B. E., L. E. Jansen, P. S. Maddox, D. R. Foltz, A. B. Desai, J. V. Shah and D. W. Cleveland. "Centromere Identity Maintained by Nucleosomes Assembled with Histone H3 Containing the Cenp-a Targeting Domain." *Mol Cell* 25, no. 2 (2007): 309-22.

Bloom, K. S. and J. Carbon. "Yeast Centromere DNA Is in a Unique and Highly Ordered Structure in Chromosomes and Small Circular Minichromosomes." *Cell* 29, no. 2 (1982): 305-17.

Blower, M. D., B. A. Sullivan and G. H. Karpen. "Conserved Organization of Centromeric Chromatin in Flies and Humans." *Dev Cell* 2, no. 3 (2002): 319-30.

Bock, L. J., C. Pagliuca, N. Kobayashi, R. A. Grove, Y. Oku, K. Shrestha, C. Alfieri, C. Golfieri, A. Oldani, M. Dal Maschio, R. Bermejo, T. R. Hazbun, T. U. Tanaka and P. De Wulf. "Cnn1 Inhibits the Interactions between the Kmn Complexes of the Yeast Kinetochore." *Nat Cell Biol* 14, no. 6 (2012): 614-24.

Brenner, S., D. Pepper, M. W. Berns, E. Tan and B. R. Brinkley. "Kinetochore Structure, Duplication, and Distribution in Mammalian Cells: Analysis by Human Autoantibodies from Scleroderma Patients." *J Cell Biol* 91, no. 1 (1981): 95-102.

Brinkley, B. R. and E. Stubblefield. "The Fine Structure of the Kinetochore of a Mammalian Cell in Vitro." *Chromosoma* 19, no. 1 (1966): 28-43.

Buchwitz, B. J., K. Ahmad, L. L. Moore, M. B. Roth and S. Henikoff. "A Histone-H3-Like Protein in C. Elegans." *Nature* 401, no. 6753 (1999): 547-8.

Bui, M., E. K. Dimitriadis, C. Hoischen, E. An, D. Quenet, S. Giebe, A. Nita-Lazar, S. Diekmann and Y. Dalal. "Cell-Cycle-Dependent Structural Transitions in the Human Cenp-a Nucleosome in Vivo." *Cell* 150, no. 2 (2012): 317-26.

Camahort, R., M. Shivaraju, M. Mattingly, B. Li, S. Nakanishi, D. Zhu, A. Shilatifard, J. L. Workman and J. L. Gerton. "Cse4 Is Part of an Octameric Nucleosome in Budding Yeast." *Mol Cell* 35, no. 6 (2009): 794-805.

Carroll, C. W., K. J. Milks and A. F. Straight. "Dual Recognition of Cenp-a Nucleosomes Is Required for Centromere Assembly." *J Cell Biol* 189, no. 7 (2010): 1143-55.

Carroll, C. W., M. C. Silva, K. M. Godek, L. E. Jansen and A. F. Straight. "Centromere Assembly Requires the Direct Recognition of Cenp-a Nucleosomes by Cenp-N." *Nat Cell Biol* 11, no. 7 (2009): 896-902.

Cheeseman, I. M., C. Brew, M. Wolyniak, A. Desai, S. Anderson, N. Muster, J. R. Yates, T. C. Huffaker, D. G. Drubin and G. Barnes. "Implication of a Novel Multiprotein Dam1p Complex in Outer Kinetochore Function." *J Cell Biol* 155, no. 7 (2001): 1137-45.

Cheeseman, I. M., J. S. Chappie, E. M. Wilson-Kubalek and A. Desai. "The Conserved Kmn Network Constitutes the Core Microtubule-Binding Site of the Kinetochore." *Cell* 127, no. 5 (2006): 983-97.

Cheeseman, I. M. and A. Desai. "Molecular Architecture of the Kinetochore-Microtubule Interface." *Nat Rev Mol Cell Biol* 9, no. 1 (2008): 33-46.

Cheeseman, I. M., T. Hori, T. Fukagawa and A. Desai. "Knl1 and the Cenp-H/I/K Complex Coordinately Direct Kinetochore Assembly in Vertebrates." *Mol Biol Cell* 19, no. 2 (2008): 587-94.

Cheeseman, I. M., S. Niessen, S. Anderson, F. Hyndman, J. R. Yates, 3rd, K. Oegema and A. Desai. "A Conserved Protein Network Controls Assembly of the Outer Kinetochore and Its Ability to Sustain Tension." *Genes Dev* 18, no. 18 (2004): 2255-68.

Chen, D. and S. Huang. "Nucleolar Components Involved in Ribosome Biogenesis Cycle between the Nucleolus and Nucleoplasm in Interphase Cells." *J Cell Biol* 153, no. 1 (2001): 169-76.

Chen, Y., J. D. Mills and A. Periasamy. "Protein Localization in Living Cells and Tissues Using Fret and Flim." *Differentiation* 71, no. 9-10 (2003): 528-41.

Cho, U. S. and S. C. Harrison. "Recognition of the Centromere-Specific Histone Cse4 by the Chaperone Scm3." *Proc Natl Acad Sci U S A* 108, no. 23 (2011): 9367-71.

Clarke, L. "Centromeres: Proteins, Protein Complexes, and Repeated Domains at Centromeres of Simple Eukaryotes." *Curr Opin Genet Dev* 8, no. 2 (1998): 212-8.

Cleveland, D. W., Y. Mao and K. F. Sullivan. "Centromeres and Kinetochores: From Epigenetics to Mitotic Checkpoint Signaling." *Cell* 112, no. 4 (2003): 407-21.

Coffman, V. C., P. Wu, M. R. Parthun and J. Q. Wu. "Cenp-a Exceeds Microtubule Attachment Sites in Centromere Clusters of Both Budding and Fission Yeast." *J Cell Biol* 195, no. 4 (2011): 563-72.

Collado, M., M. A. Blasco and M. Serrano. "Cellular Senescence in Cancer and Aging." *Cell* 130, no. 2 (2007): 223-33.

Cooke, C. A., R. L. Bernat and W. C. Earnshaw. "Cenp-B: A Major Human Centromere Protein Located beneath the Kinetochore." *J Cell Biol* 110, no. 5 (1990): 1475-88.

Cooke, C. A., B. Schaar, T. J. Yen and W. C. Earnshaw. "Localization of Cenp-E in the Fibrous Corona and Outer Plate of Mammalian Kinetochores from Prometaphase through Anaphase." *Chromosoma* 106, no. 7 (1997): 446-55.

Counce, S. J. and G. F. Meyer. "Differentiation of the Synaptonemal Complex and the Kinetochore in Locusta Spermatocytes Studied by Whole Mount Electron Microscopy." *Chromosoma* 44, no. 2 (1973): 231-53.

Creemers, T. M., A. J. Lock, V. Subramaniam, T. M. Jovin and S. Volker. "Three Photoconvertible Forms of Green Fluorescent Protein Identified by Spectral Hole-Burning." *Nat Struct Biol* 6, no. 6 (1999): 557-60.

Dalal, Y. and M. Bui. "Down the Rabbit Hole of Centromere Assembly and Dynamics." *Curr Opin Cell Biol* 22, no. 3 (2010): 392-402.
Dalal, Y., T. Furuyama, D. Vermaak and S. Henikoff. "Structure, Dynamics, and Evolution of Centromeric Nucleosomes." *Proc Natl Acad Sci U S A* 104, no. 41 (2007): 15974-81.
Dalal, Y., H. Wang, S. Lindsay and S. Henikoff. "Tetrameric Structure of Centromeric Nucleosomes in Interphase Drosophila Cells." *PLoS Biol* 5, no. 8 (2007): e218.
Dambacher, S., W. Deng, M. Hahn, D. Sadic, J. Frohlich, A. Nuber, C. Hoischen, S. Diekmann, H. Leonhardt and G. Schotta. "Cenp-C Facilitates the Recruitment of M18bp1 to Centromeric Chromatin." *Nucleus* 3, no. 1 (2012): 101-10.
Darlington, C.D. "Recent Advances in Cytology." *J.And A Churchill Limited.*, (1937).
de Winter, J. P. and H. Joenje. "The Genetic and Molecular Basis of Fanconi Anemia." *Mutat Res* 668, no. 1-2 (2009): 11-9.
De Wulf, P., A. D. McAinsh and P. K. Sorger. "Hierarchical Assembly of the Budding Yeast Kinetochore from Multiple Subcomplexes." *Genes Dev* 17, no. 23 (2003): 2902-21.
Dechassa, M. L., K. Wyns, M. Li, M. A. Hall, M. D. Wang and K. Luger. "Structure and Scm3-Mediated Assembly of Budding Yeast Centromeric Nucleosomes." *Nat Commun* 2, (2011): 313.
DeLuca, J. G., Y. Dong, P. Hergert, J. Strauss, J. M. Hickey, E. D. Salmon and B. F. McEwen. "Hec1 and Nuf2 Are Core Components of the Kinetochore Outer Plate Essential for Organizing Microtubule Attachment Sites." *Mol Biol Cell* 16, no. 2 (2005): 519-31.
Deng, Y., S. S. Chan and S. Chang. "Telomere Dysfunction and Tumour Suppression: The Senescence Connection." *Nat Rev Cancer* 8, no. 6 (2008): 450-8.
Dernburg, A. F. "Here, There, and Everywhere: Kinetochore Function on Holocentric Chromosomes." *J Cell Biol* 153, no. 6 (2001): F33-8.
Digman, M. A., C. M. Brown, P. Sengupta, P. W. Wiseman, A. R. Horwitz and E. Gratton. "Measuring Fast Dynamics in Solutions and Cells with a Laser Scanning Microscope." *Biophys J* 89, no. 2 (2005): 1317-27.
Dimitriadis, E. K., C. Weber, R. K. Gill, S. Diekmann and Y. Dalal. "Tetrameric Organization of Vertebrate Centromeric Nucleosomes." *Proc Natl Acad Sci U S A* 107, no. 47 (2010): 20317-22.
Ding, R., K. L. McDonald and J. R. McIntosh. "Three-Dimensional Reconstruction and Analysis of Mitotic Spindles from the Yeast, Schizosaccharomyces Pombe." *J Cell Biol* 120, no. 1 (1993): 141-51.
Dong, Y., K. J. Vanden Beldt, X. Meng, A. Khodjakov and B. F. McEwen. "The Outer Plate in Vertebrate Kinetochores Is a Flexible Network with Multiple Microtubule Interactions." *Nat Cell Biol* 9, no. 5 (2007): 516-22.
Dorn, J. F. and P. S. Maddox. "Kinetochore Dynamics: How Protein Dynamics Affect Chromosome Segregation." *Curr Opin Cell Biol* 24, no. 1 (2012): 57-63.
Du, Y., C. N. Topp and R. K. Dawe. "DNA Binding of Centromere Protein C (Cenpc) Is Stabilized by Single-Stranded Rna." *PLoS Genet* 6, no. 2 (2010): e1000835.
Duncan, F. E., J. E. Hornick, M. A. Lampson, R. M. Schultz, L. D. Shea and T. K. Woodruff. "Chromosome Cohesion Decreases in Human Eggs with Advanced Maternal Age." *Aging Cell* 11, no. 6 (2012): 1121-4.
Dunleavy, E. M., G. Almouzni and G. H. Karpen. "H3.3 Is Deposited at Centromeres in S Phase as a Placeholder for Newly Assembled Cenp-a in G(1) Phase." *Nucleus* 2, no. 2 (2011): 146-57.
Dunleavy, E. M., D. Roche, H. Tagami, N. Lacoste, D. Ray-Gallet, Y. Nakamura, Y. Daigo, Y. Nakatani and G. Almouzni-Pettinotti. "Hjurp Is a Cell-Cycle-Dependent Maintenance and Deposition Factor of Cenp-a at Centromeres." *Cell* 137, no. 3 (2009): 485-97.
Earnshaw, W., B. Bordwell, C. Marino and N. Rothfield. "Three Human Chromosomal Autoantigens Are Recognized by Sera from Patients with Anti-Centromere Antibodies." *J Clin Invest* 77, no. 2 (1986): 426-30.
Earnshaw, W. C., N. Halligan, C. Cooke and N. Rothfield. "The Kinetochore Is Part of the Metaphase Chromosome Scaffold." *J Cell Biol* 98, no. 1 (1984): 352-7.
Earnshaw, W. C., P. S. Machlin, B. J. Bordwell, N. F. Rothfield and D. W. Cleveland. "Analysis of Anticentromere Autoantibodies Using Cloned Autoantigen Cenp-B." *Proc Natl Acad Sci U S A* 84, no. 14 (1987): 4979-83.
Earnshaw, W. C., H. Ratrie, 3rd and G. Stetten. "Visualization of Centromere Proteins Cenp-B and Cenp-C on a Stable Dicentric Chromosome in Cytological Spreads." *Chromosoma* 98, no. 1 (1989): 1-12.
Earnshaw, W. C. and N. Rothfield. "Identification of a Family of Human Centromere Proteins Using Autoimmune Sera from Patients with Scleroderma." *Chromosoma* 91, no. 3-4 (1985): 313-21.

Earnshaw, W. C., K. F. Sullivan, P. S. Machlin, C. A. Cooke, D. A. Kaiser, T. D. Pollard, N. F. Rothfield and D. W. Cleveland. "Molecular Cloning of Cdna for Cenp-B, the Major Human Centromere Autoantigen." *J Cell Biol* 104, no. 4 (1987): 817-29.

Eichenlaub-Ritter, U., N. Staubach and T. Trapphoff. "Chromosomal and Cytoplasmic Context Determines Predisposition to Maternal Age-Related Aneuploidy: Brief Overview and Update on Mcak in Mammalian Oocytes." *Biochem Soc Trans* 38, no. 6 (2010): 1681-6.

Eichler, E. E., R. A. Clark and X. She. "An Assessment of the Sequence Gaps: Unfinished Business in a Finished Human Genome." *Nat Rev Genet* 5, no. 5 (2004): 345-54.

Elder, A.D.; Domin, A.; Kaminski Schierle, G.S.; Lindon, C.; Pines, J.; Esposito, A.; Kaminski, C.F. "A Quantitative Protocol for Dynamic Measurements of Protein Interactions by Förster Resonance Energy Transfer-Sensitized Fluorescence Emission." *J R Soc Interface* 6, (2009): 59-81.

Eskat, A., W. Deng, A. Hofmeister, S. Rudolphi, S. Emmerth, D. Hellwig, T. Ulbricht, V. Doring, J. M. Bancroft, A. D. McAinsh, M. C. Cardoso, P. Meraldi, C. Hoischen, H. Leonhardt and S. Diekmann. "Step-Wise Assembly, Maturation and Dynamic Behavior of the Human Cenp-P/O/R/Q/U Kinetochore Sub-Complex." *PLoS One* 7, no. 9 (2012): e44717.

Everett, R. D., W. C. Earnshaw, J. Findlay and P. Lomonte. "Specific Destruction of Kinetochore Protein Cenp-C and Disruption of Cell Division by Herpes Simplex Virus Immediate-Early Protein Vmw110." *EMBO J* 18, no. 6 (1999): 1526-38.

Figueroa, J., R. Saffrich, W. Ansorge and M. M. Valdivia. "Microinjection of Antibodies to Centromere Protein Cenp-a Arrests Cells in Interphase but Does Not Prevent Mitosis." *Chromosoma* 107, no. 6-7 (1998): 397-405.

Flemming, W. "Zellsubstanz, Kern Und Zelltheilung." *Verlag von F.C.W. Vogel*, (1882).

Foltz, D. R., L. E. Jansen, A. O. Bailey, J. R. Yates, 3rd, E. A. Bassett, S. Wood, B. E. Black and D. W. Cleveland. "Centromere-Specific Assembly of Cenp-a Nucleosomes Is Mediated by Hjurp." *Cell* 137, no. 3 (2009): 472-84.

Foltz, D. R., L. E. Jansen, B. E. Black, A. O. Bailey, J. R. Yates, 3rd and D. W. Cleveland. "The Human Cenp-a Centromeric Nucleosome-Associated Complex." *Nat Cell Biol* 8, no. 5 (2006): 458-69.

Foltz, D. R. and P. T. Stukenberg. "A New Histone at the Centromere?" *Cell* 148, no. 3 (2012): 394-6.

Fritzler, M. J. and T. D. Kinsella. "The Crest Syndrome: A Distinct Serologic Entity with Anticentromere Antibodies." *Am J Med* 69, no. 4 (1980): 520-6.

Fujita, Y., T. Hayashi, T. Kiyomitsu, Y. Toyoda, A. Kokubu, C. Obuse and M. Yanagida. "Priming of Centromere for Cenp-a Recruitment by Human Hmis18alpha, Hmis18beta, and M18bp1." *Dev Cell* 12, no. 1 (2007): 17-30.

Fukagawa, T., Y. Mikami, A. Nishihashi, V. Regnier, T. Haraguchi, Y. Hiraoka, N. Sugata, K. Todokoro, W. Brown and T. Ikemura. "Cenp-H, a Constitutive Centromere Component, Is Required for Centromere Targeting of Cenp-C in Vertebrate Cells." *EMBO J* 20, no. 16 (2001): 4603-17.

Furuyama, T. and S. Henikoff. "Centromeric Nucleosomes Induce Positive DNA Supercoils." *Cell* 138, no. 1 (2009): 104-13.

Gardner, R. D., A. Poddar, C. Yellman, P. A. Tavormina, M. C. Monteagudo and D. J. Burke. "The Spindle Checkpoint of the Yeast Saccharomyces Cerevisiae Requires Kinetochore Function and Maps to the Cbf3 Domain." *Genetics* 157, no. 4 (2001): 1493-502.

Gascoigne, K. E. and I. M. Cheeseman. "Kinetochore Assembly: If You Build It, They Will Come." *Curr Opin Cell Biol* 23, no. 1 (2011): 102-8.

Gascoigne, K. E. and I. M. Cheeseman. "T Time for Point Centromeres." *Nat Cell Biol* 14, no. 6 (2012): 559-61.

Gascoigne, K. E., K. Takeuchi, A. Suzuki, T. Hori, T. Fukagawa and I. M. Cheeseman. "Induced Ectopic Kinetochore Assembly Bypasses the Requirement for Cenp-a Nucleosomes." *Cell* 145, no. 3 (2011): 410-22.

Gay, G., T. Courtheoux, C. Reyes, S. Tournier and Y. Gachet. "A Stochastic Model of Kinetochore-Microtubule Attachment Accurately Describes Fission Yeast Chromosome Segregation." *J Cell Biol* 196, no. 6 (2012): 757-74.

Gonatas, N. K., H. M. Zimmerman and S. Levine. "Ultrastructure of Inflammation with Edema in the Rat Brain." *Am J Pathol* 42, (1963): 455-69.

Goshima, G., T. Kiyomitsu, K. Yoda and M. Yanagida. "Human Centromere Chromatin Protein Hmis12, Essential for Equal Segregation, Is Independent of Cenp-a Loading Pathway." *J Cell Biol* 160, no. 1 (2003): 25-39.

Goshima, G., S. Saitoh and M. Yanagida. "Proper Metaphase Spindle Length Is Determined by Centromere Proteins Mis12 and Mis6 Required for Faithful Chromosome Segregation." *Genes Dev* 13, no. 13 (1999): 1664-77.

Guerra, M., G. Cabral, M. Cuacos, M. Gonzalez-Garcia, M. Gonzalez-Sanchez, J. Vega and M. J. Puertas. "Neocentrics and Holokinetics (Holocentrics): Chromosomes out of the Centromeric Rules." *Cytogenet Genome Res* 129, no. 1-3 (2010): 82-96.

Guldner, H. H., H. J. Lakomek and F. A. Bautz. "Human Anti-Centromere Sera Recognise a 19.5 Kd Non-Histone Chromosomal Protein from Hela Cells." *Clin Exp Immunol* 58, no. 1 (1984): 13-20.

Guse, A., C. W. Carroll, B. Moree, C. J. Fuller and A. F. Straight. "In Vitro Centromere and Kinetochore Assembly on Defined Chromatin Templates." *Nature* 477, no. 7364 (2011): 354-8.

Hanissian, S. H., U. Akbar, B. Teng, Z. Janjetovic, A. Hoffmann, J. K. Hitzler, N. Iscove, K. Hamre, X. Du, Y. Tong, S. Mukatira, J. H. Robertson and S. W. Morris. "Cdna Cloning and Characterization of a Novel Gene Encoding the Mlf1-Interacting Protein Mlf1ip." *Oncogene* 23, no. 20 (2004): 3700-7.

Hassold, T. and P. Hunt. "Maternal Age and Chromosomally Abnormal Pregnancies: What We Know and What We Wish We Knew." *Curr Opin Pediatr* 21, no. 6 (2009): 703-8.

Hayashi, T., Y. Fujita, O. Iwasaki, Y. Adachi, K. Takahashi and M. Yanagida. "Mis16 and Mis18 Are Required for Cenp-a Loading and Histone Deacetylation at Centromeres." *Cell* 118, no. 6 (2004): 715-29.

Hayflick, L. and P. S. Moorhead. "The Serial Cultivation of Human Diploid Cell Strains." *Exp Cell Res* 25, (1961): 585-621.

He, D., C. Zeng, K. Woods, L. Zhong, D. Turner, R. K. Busch, B. R. Brinkley and H. Busch. "Cenp-G: A New Centromeric Protein That Is Associated with the Alpha-1 Satellite DNA Subfamily." *Chromosoma* 107, no. 3 (1998): 189-97.

Hellwig, D., S. Emmerth, T. Ulbricht, V. Doring, C. Hoischen, R. Martin, C. P. Samora, A. D. McAinsh, C. W. Carroll, A. F. Straight, P. Meraldi and S. Diekmann. "Dynamics of Cenp-N Kinetochore Binding During the Cell Cycle." *J Cell Sci* 124, no. Pt 22 (2011): 3871-83.

Hellwig, D., C. Hoischen, T. Ulbricht and S. Diekmann. "Acceptor-Photobleaching Fret Analysis of Core Kinetochore and Nac Proteins in Living Human Cells." *Eur Biophys J* 38, no. 6 (2009): 781-91.

Hellwig, D., S. Munch, S. Orthaus, C. Hoischen, P. Hemmerich and S. Diekmann. "Live-Cell Imaging Reveals Sustained Centromere Binding of Cenp-T Via Cenp-a and Cenp-B." *J Biophotonics* 1, no. 3 (2008): 245-54.

Hemmerich, P., L. Schmiedeberg and S. Diekmann. "Dynamic as Well as Stable Protein Interactions Contribute to Genome Function and Maintenance." *Chromosome Res* 19, no. 1 (2011): 131-51.

Hemmerich, P., T. Stoyan, G. Wieland, M. Koch, J. Lechner and S. Diekmann. "Interaction of Yeast Kinetochore Proteins with Centromere-Protein/Transcription Factor Cbf1." *Proc Natl Acad Sci U S A* 97, no. 23 (2000): 12583-8.

Hemmerich, P., S. Weidtkamp-Peters, C. Hoischen, L. Schmiedeberg, I. Erliandri and S. Diekmann. "Dynamics of Inner Kinetochore Assembly and Maintenance in Living Cells." *J Cell Biol* 180, no. 6 (2008): 1101-14.

Heun, P., S. Erhardt, M. D. Blower, S. Weiss, A. D. Skora and G. H. Karpen. "Mislocalization of the Drosophila Centromere-Specific Histone Cid Promotes Formation of Functional Ectopic Kinetochores." *Dev Cell* 10, no. 3 (2006): 303-15.

Hori, T., M. Amano, A. Suzuki, C. B. Backer, J. P. Welburn, Y. Dong, B. F. McEwen, W. H. Shang, E. Suzuki, K. Okawa, I. M. Cheeseman and T. Fukagawa. "Ccan Makes Multiple Contacts with Centromeric DNA to Provide Distinct Pathways to the Outer Kinetochore." *Cell* 135, no. 6 (2008): 1039-52.

Hori, T. and T. Fukagawa. "Establishment of the Vertebrate Kinetochores." *Chromosome Res* 20, no. 5 (2012): 547-61.

Hori, T., M. Okada, K. Maenaka and T. Fukagawa. "Cenp-O Class Proteins Form a Stable Complex and Are Required for Proper Kinetochore Function." *Mol Biol Cell* 19, no. 3 (2008): 843-54.

Hori, T., W. H. Shang, K. Takeuchi and T. Fukagawa. "The Ccan Recruits Cenp-a to the Centromere and Forms the Structural Core for Kinetochore Assembly." *J Cell Biol* 200, no. 1 (2013): 45-60.

Howell, B. J., B. Moree, E. M. Farrar, S. Stewart, G. Fang and E. D. Salmon. "Spindle Checkpoint Protein Dynamics at Kinetochores in Living Cells." *Curr Biol* 14, no. 11 (2004): 953-64.

Howman, E. V., K. J. Fowler, A. J. Newson, S. Redward, A. C. MacDonald, P. Kalitsis and K. H. Choo. "Early Disruption of Centromeric Chromatin Organization in Centromere Protein a (Cenpa) Null Mice." *Proc Natl Acad Sci U S A* 97, no. 3 (2000): 1148-53.

Hu, H., Y. Liu, M. Wang, J. Fang, H. Huang, N. Yang, Y. Li, J. Wang, X. Yao, Y. Shi, G. Li and R. M. Xu. "Structure of a Cenp-a-Histone H4 Heterodimer in Complex with Chaperone Hjurp." *Genes Dev* 25, no. 9 (2011): 901-6.

Hua, S., Z. Wang, K. Jiang, Y. Huang, T. Ward, L. Zhao, Z. Dou and X. Yao. "Cenp-U Cooperates with Hec1 to Orchestrate Kinetochore-Microtubule Attachment." *J Biol Chem* 286, no. 2 (2011): 1627-38.

Hudson, D. F., K. J. Fowler, E. Earle, R. Saffery, P. Kalitsis, H. Trowell, J. Hill, N. G. Wreford, D. M. de Kretser, M. R. Cancilla, E. Howman, L. Hii, S. M. Cutts, D. V. Irvine and K. H. Choo. "Centromere Protein B Null Mice Are Mitotically and Meiotically Normal but Have Lower Body and Testis Weights." *J Cell Biol* 141, no. 2 (1998): 309-19.

Izuta, H., M. Ikeno, N. Suzuki, T. Tomonaga, N. Nozaki, C. Obuse, Y. Kisu, N. Goshima, F. Nomura, N. Nomura and K. Yoda. "Comprehensive Analysis of the Icen (Interphase Centromere Complex) Components Enriched in the Cenp-a Chromatin of Human Cells." *Genes Cells* 11, no. 6 (2006): 673-84.

Janke, C., J. Ortiz, J. Lechner, A. Shevchenko, A. Shevchenko, M. M. Magiera, C. Schramm and E. Schiebel. "The Budding Yeast Proteins Spc24p and Spc25p Interact with Ndc80p and Nuf2p at the Kinetochore and Are Important for Kinetochore Clustering and Checkpoint Control." *EMBO J* 20, no. 4 (2001): 777-91.

Jansen, L. E., B. E. Black, D. R. Foltz and D. W. Cleveland. "Propagation of Centromeric Chromatin Requires Exit from Mitosis." *J Cell Biol* 176, no. 6 (2007): 795-805.

Jares-Erijman, E. A. and T. M. Jovin. "Fret Imaging." *Nat Biotechnol* 21, no. 11 (2003): 1387-95.

Jares-Erijman, E. A. and T. M. Jovin. "Imaging Molecular Interactions in Living Cells by Fret Microscopy." *Curr Opin Chem Biol* 10, no. 5 (2006): 409-16.

Johnston, K., A. Joglekar, T. Hori, A. Suzuki, T. Fukagawa and E. D. Salmon. "Vertebrate Kinetochore Protein Architecture: Protein Copy Number." *J Cell Biol* 189, no. 6 (2010): 937-43.

Jones, K. T. and S. I. Lane. "Chromosomal, Metabolic, Environmental, and Hormonal Origins of Aneuploidy in Mammalian Oocytes." *Exp Cell Res* 318, no. 12 (2012): 1394-9.

Kalitsis, P., K. J. Fowler, E. Earle, B. Griffiths, E. Howman, A. J. Newson and K. H. Choo. "Partially Functional Cenpa-Gfp Fusion Protein Causes Increased Chromosome Missegregation and Apoptosis During Mouse Embryogenesis." *Chromosome Res* 11, no. 4 (2003): 345-57.

Kalitsis, P., K. J. Fowler, E. Earle, J. Hill and K. H. Choo. "Targeted Disruption of Mouse Centromere Protein C Gene Leads to Mitotic Disarray and Early Embryo Death." *Proc Natl Acad Sci U S A* 95, no. 3 (1998): 1136-41.

Kalitsis, P., A. C. MacDonald, A. J. Newson, D. F. Hudson and K. H. Choo. "Gene Structure and Sequence Analysis of Mouse Centromere Proteins a and C." *Genomics* 47, no. 1 (1998): 108-14.

Kang, Y. H., C. H. Park, T. S. Kim, N. K. Soung, J. K. Bang, B. Y. Kim, J. E. Park and K. S. Lee. "Mammalian Polo-Like Kinase 1-Dependent Regulation of the Pbip1-Cenp-Q Complex at Kinetochores." *J Biol Chem* 286, no. 22 (2011): 19744-57.

Kang, Y. H., J. E. Park, L. R. Yu, N. K. Soung, S. M. Yun, J. K. Bang, Y. S. Seong, H. Yu, S. Garfield, T. D. Veenstra and K. S. Lee. "Self-Regulated Plk1 Recruitment to Kinetochores by the Plk1-Pbip1 Interaction Is Critical for Proper Chromosome Segregation." *Mol Cell* 24, no. 3 (2006): 409-22.

Kenworthy, A. K. "Imaging Protein-Protein Interactions Using Fluorescence Resonance Energy Transfer Microscopy." *Methods* 24, no. 3 (2001): 289-96.

Keppler, A., S. Gendreizig, T. Gronemeyer, H. Pick, H. Vogel and K. Johnsson. "A General Method for the Covalent Labeling of Fusion Proteins with Small Molecules in Vivo." *Nat Biotechnol* 21, no. 1 (2003): 86-9.

Kim, H., M. Lee, S. Lee, B. Park, W. Koh, D. J. Lee, D. S. Lim and S. Lee. "Cancer-Upregulated Gene 2 (Cug2), a New Component of Centromere Complex, Is Required for Kinetochore Function." *Mol Cells* 27, no. 6 (2009): 697-701.

Kim, W., E. J. Bennett, E. L. Huttlin, A. Guo, J. Li, A. Possemato, M. E. Sowa, R. Rad, J. Rush, M. J. Comb, J. W. Harper and S. P. Gygi. "Systematic and Quantitative Assessment of the Ubiquitin-Modified Proteome." *Mol Cell* 44, no. 2 (2011): 325-40.

Kingwell, B. and J. B. Rattner. "Mammalian Kinetochore/Centromere Composition: A 50 Kda Antigen Is Present in the Mammalian Kinetochore/Centromere." *Chromosoma* 95, no. 6 (1987): 403-7.

Kitagawa, K., H. Masumoto, M. Ikeda and T. Okazaki. "Analysis of Protein-DNA and Protein-Protein Interactions of Centromere Protein B (Cenp-B) and Properties of the DNA-Cenp-B Complex in the Cell Cycle." *Mol Cell Biol* 15, no. 3 (1995): 1602-12.

Kitagawa, R. "Key Players in Chromosome Segregation in Caenorhabditis Elegans." *Front Biosci* 14, (2009): 1529-57.

Kiyomitsu, T., O. Iwasaki, C. Obuse and M. Yanagida. "Inner Centromere Formation Requires Hmis14, a Trident Kinetochore Protein That Specifically Recruits Hp1 to Human Chromosomes." *J Cell Biol* 188, no. 6 (2010): 791-807.

Knop, M., G. Pereira and E. Schiebel. "Microtubule Organization by the Budding Yeast Spindle Pole Body." *Biol Cell* 91, no. 4-5 (1999): 291-304.

Kohl, T., E. Haustein and P. Schwille. "Determining Protease Activity in Vivo by Fluorescence Cross-Correlation Analysis." *Biophys J* 89, no. 4 (2005): 2770-82.

Krishan, A. and R. C. Buck. "Structure of the Mitotic Spindle in L Strain Fibroblasts." *J Cell Biol* 24, (1965): 433-44.

Kunitoku, N., T. Sasayama, T. Marumoto, D. Zhang, S. Honda, O. Kobayashi, K. Hatakeyama, Y. Ushio, H. Saya and T. Hirota. "Cenp-a Phosphorylation by Aurora-a in Prophase Is Required for Enrichment of Aurora-B at Inner Centromeres and for Kinetochore Function." *Dev Cell* 5, no. 6 (2003): 853-64.

Kurnit, D. M. and J. J. Maio. "Subnuclear Redistribution of DNA Species in Confluent and Growing Mammalian Cells." *Chromosoma* 42, no. 1 (1973): 23-36.

Kwon, M. S., T. Hori, M. Okada and T. Fukagawa. "Cenp-C Is Involved in Chromosome Segregation, Mitotic Checkpoint Function, and Kinetochore Assembly." *Mol Biol Cell* 18, no. 6 (2007): 2155-68.

Lagana, A., J. F. Dorn, V. De Rop, A. M. Ladouceur, A. S. Maddox and P. S. Maddox. "A Small Gtpase Molecular Switch Regulates Epigenetic Centromere Maintenance by Stabilizing Newly Incorporated Cenp-A." *Nat Cell Biol* 12, no. 12 (2010): 1186-93.

Lawrimore, J., K. S. Bloom and E. D. Salmon. "Point Centromeres Contain More Than a Single Centromere-Specific Cse4 (Cenp-a) Nucleosome." *J Cell Biol* 195, no. 4 (2011): 573-82.

Lee, K. S., D. Y. Oh, Y. H. Kang and J. E. Park. "Self-Regulated Mechanism of Plk1 Localization to Kinetochores: Lessons from the Plk1-Pbip1 Interaction." *Cell Div* 3, (2008): 4.

Leonhardt, H., H. P. Rahn, P. Weinzierl, A. Sporbert, T. Cremer, D. Zink and M. C. Cardoso. "Dynamics of DNA Replication Factories in Living Cells." *J Cell Biol* 149, no. 2 (2000): 271-80.

Li, Y. C., C. Lee, W. S. Chang, S. Y. Li and C. C. Lin. "Isolation and Identification of a Novel Satellite DNA Family Highly Conserved in Several Cervidae Species." *Chromosoma* 111, no. 3 (2002): 176-83.

Liao, H., R. J. Winkfein, G. Mack, J. B. Rattner and T. J. Yen. "Cenp-F Is a Protein of the Nuclear Matrix That Assembles onto Kinetochores at Late G2 and Is Rapidly Degraded after Mitosis." *J Cell Biol* 130, no. 3 (1995): 507-18.

Liu, D., M. Vleugel, C. B. Backer, T. Hori, T. Fukagawa, I. M. Cheeseman and M. A. Lampson. "Regulated Targeting of Protein Phosphatase 1 to the Outer Kinetochore by Knl1 Opposes Aurora B Kinase." *J Cell Biol* 188, no. 6 (2010): 809-20.

Liu, S. T., J. C. Hittle, S. A. Jablonski, M. S. Campbell, K. Yoda and T. J. Yen. "Human Cenp-I Specifies Localization of Cenp-F, Mad1 and Mad2 to Kinetochores and Is Essential for Mitosis." *Nat Cell Biol* 5, no. 4 (2003): 341-5.

Liu, S. T., J. B. Rattner, S. A. Jablonski and T. J. Yen. "Mapping the Assembly Pathways That Specify Formation of the Trilaminar Kinetochore Plates in Human Cells." *J Cell Biol* 175, no. 1 (2006): 41-53.

Liu, X., I. McLeod, S. Anderson, J. R. Yates, 3rd and X. He. "Molecular Analysis of Kinetochore Architecture in Fission Yeast." *EMBO J* 24, no. 16 (2005): 2919-30.

Lomonte, P. and R. D. Everett. "Herpes Simplex Virus Type 1 Immediate-Early Protein Vmw110 Inhibits Progression of Cells through Mitosis and from G(1) into S Phase of the Cell Cycle." *J Virol* 73, no. 11 (1999): 9456-67.

Maddox, P. S., K. Oegema, A. Desai and I. M. Cheeseman. ""Holo"Er Than Thou: Chromosome Segregation and Kinetochore Function in C. Elegans." *Chromosome Res* 12, no. 6 (2004): 641-53.

Madsen, P. and J. E. Celis. "S-Phase Patterns of Cyclin (Pcna) Antigen Staining Resemble Topographical Patterns of DNA Synthesis. A Role for Cyclin in DNA Replication?" *FEBS Lett* 193, no. 1 (1985): 5-11.

Maehara, K., K. Takahashi and S. Saitoh. "Cenp-a Reduction Induces a P53-Dependent Cellular Senescence Response to Protect Cells from Executing Defective Mitoses." *Mol Cell Biol* 30, no. 9 (2010): 2090-104.

Malvezzi-Campeggi, F., M. Jahnz, K. G. Heinze, P. Dittrich and P. Schwille. "Light-Induced Flickering of Dsred Provides Evidence for Distinct and Interconvertible Fluorescent States." *Biophys J* 81, no. 3 (2001): 1776-85.

Manuelidis, L. "Chromosomal Localization of Complex and Simple Repeated Human Dnas." *Chromosoma* 66, no. 1 (1978): 23-32.

Marshall, O. J., A. T. Marshall and K. H. Choo. "Three-Dimensional Localization of Cenp-a Suggests a Complex Higher Order Structure of Centromeric Chromatin." *J Cell Biol* 183, no. 7 (2008): 1193-202.

Masumoto, H., H. Masukata, Y. Muro, N. Nozaki and T. Okazaki. "A Human Centromere Antigen (Cenp-B) Interacts with a Short Specific Sequence in Alphoid DNA, a Human Centromeric Satellite." *J Cell Biol* 109, no. 5 (1989): 1963-73.

McAinsh, A. D., P. Meraldi, V. M. Draviam, A. Toso and P. K. Sorger. "The Human Kinetochore Proteins Nnf1r and Mcm21r Are Required for Accurate Chromosome Segregation." *EMBO J* 25, no. 17 (2006): 4033-49.

McClelland, S. E., S. Borusu, A. C. Amaro, J. R. Winter, M. Belwal, A. D. McAinsh and P. Meraldi. "The Cenp-a Nac/Cad Kinetochore Complex Controls Chromosome Congression and Spindle Bipolarity." *EMBO J* 26, no. 24 (2007): 5033-47.

McEwen, B. F. and Y. Dong. "Contrasting Models for Kinetochore Microtubule Attachment in Mammalian Cells." *Cell Mol Life Sci* 67, no. 13 (2010): 2163-72.

McIntosh, J. R. and E. T. O'Toole. "Life Cycles of Yeast Spindle Pole Bodies: Getting Microtubules into a Closed Nucleus." *Biol Cell* 91, no. 4-5 (1999): 305-12.

McNeilage, L. J., S. Whittingham, N. McHugh and A. J. Barnett. "A Highly Conserved 72,000 Dalton Centromeric Antigen Reactive with Autoantibodies from Patients with Progressive Systemic Sclerosis." *J Immunol* 137, no. 8 (1986): 2541-7.

Melters, D. P., L. V. Paliulis, I. F. Korf and S. W. Chan. "Holocentric Chromosomes: Convergent Evolution, Meiotic Adaptations, and Genomic Analysis." *Chromosome Res* 20, no. 5 (2012): 579-93.

Meraldi, P., A. D. McAinsh, E. Rheinbay and P. K. Sorger. "Phylogenetic and Structural Analysis of Centromeric DNA and Kinetochore Proteins." *Genome Biol* 7, no. 3 (2006): R23.

Meselson, M. and F. W. Stahl. "The Replication of DNA in Escherichia Coli." *Proc Natl Acad Sci U S A* 44, no. 7 (1958): 671-82.

Metzler, R. and J. Klafter. "When Translocation Dynamics Becomes Anomalous." *Biophys J* 85, no. 4 (2003): 2776-9.

Metzner, R. "Beiträge Zur Granulalehre. I.: Kern Und Kerntheilung." *Arch Anat Physiol*, (1894): 309–348.

Milks, K. J., B. Moree and A. F. Straight. "Dissection of Cenp-C-Directed Centromere and Kinetochore Assembly." *Mol Biol Cell* 20, no. 19 (2009): 4246-55.

Minoshima, Y., T. Hori, M. Okada, H. Kimura, T. Haraguchi, Y. Hiraoka, Y. C. Bao, T. Kawashima, T. Kitamura and T. Fukagawa. "The Constitutive Centromere Component Cenp-50 Is Required for Recovery from Spindle Damage." *Mol Cell Biol* 25, no. 23 (2005): 10315-28.

Misteli, T. "The Concept of Self-Organization in Cellular Architecture." *J Cell Biol* 155, no. 2 (2001): 181-5.

Mizuguchi, G., H. Xiao, J. Wisniewski, M. M. Smith and C. Wu. "Nonhistone Scm3 and Histones Cenh3-H4 Assemble the Core of Centromere-Specific Nucleosomes." *Cell* 129, no. 6 (2007): 1153-64.

Monier, K., S. Mouradian and K. F. Sullivan. "DNA Methylation Promotes Aurora-B-Driven Phosphorylation of Histone H3 in Chromosomal Subdomains." *J Cell Sci* 120, no. Pt 1 (2007): 101-14.

Moree, B., C. B. Meyer, C. J. Fuller and A. F. Straight. "Cenp-C Recruits M18bp1 to Centromeres to Promote Cenp-a Chromatin Assembly." *J Cell Biol* 194, no. 6 (2011): 855-71.

Moroi, Y., A. L. Hartman, P. K. Nakane and E. M. Tan. "Distribution of Kinetochore (Centromere) Antigen in Mammalian Cell Nuclei." *J Cell Biol* 90, no. 1 (1981): 254-9.

Moroi, Y., C. Peebles, M. J. Fritzler, J. Steigerwald and E. M. Tan. "Autoantibody to Centromere (Kinetochore) in Scleroderma Sera." *Proc Natl Acad Sci U S A* 77, no. 3 (1980): 1627-31.

Morris, C. A. and D. Moazed. "Centromere Assembly and Propagation." *Cell* 128, no. 4 (2007): 647-50.

Moses, M. J., S. J. Counce and D. F. Paulson. "Synaptonemal Complex Complement of Man in Spreads of Spermatocytes, with Details of the Sex Chromosome Pair." *Science* 187, no. 4174 (1975): 363-5.

Musacchio, A. and E. D. Salmon. "The Spindle-Assembly Checkpoint in Space and Time." *Nat Rev Mol Cell Biol* 8, no. 5 (2007): 379-93.

Musich, P. R., J. J. Maio and F. L. Brown. "Subunit Structure of Chromatin and the Organization of Eukaryotic Highly Repetitive DNA: Indications of a Phase Relation between Restriction Sites and Chromatin Subunits in African Green Monkey and Calf Nuclei." *J Mol Biol* 117, no. 3 (1977): 657-77.

Mythreye, K. and K. S. Bloom. "Differential Kinetochore Protein Requirements for Establishment Versus Propagation of Centromere Activity in Saccharomyces Cerevisiae." *J Cell Biol* 160, no. 6 (2003): 833-43.
Nagy, P., G. Vamosi, A. Bodnar, S. J. Lockett and J. Szollosi. "Intensity-Based Energy Transfer Measurements in Digital Imaging Microscopy." *Eur Biophys J* 27, no. 4 (1998): 377-89.
Nakano, M., S. Cardinale, V. N. Noskov, R. Gassmann, P. Vagnarelli, S. Kandels-Lewis, V. Larionov, W. C. Earnshaw and H. Masumoto. "Inactivation of a Human Kinetochore by Specific Targeting of Chromatin Modifiers." *Dev Cell* 14, no. 4 (2008): 507-22.
Nebel, B. R. and E. M. Coulon. "The Fine Structure of Chromosomes in Pigeon Spermatocytes." *Chromosoma* 13, (1962): 272-91.
Nekrasov, V. S., M. A. Smith, S. Peak-Chew and J. V. Kilmartin. "Interactions between Centromere Complexes in Saccharomyces Cerevisiae." *Mol Biol Cell* 14, no. 12 (2003): 4931-46.
Nishihashi, A., T. Haraguchi, Y. Hiraoka, T. Ikemura, V. Regnier, H. Dodson, W. C. Earnshaw and T. Fukagawa. "Cenp-I Is Essential for Centromere Function in Vertebrate Cells." *Dev Cell* 2, no. 4 (2002): 463-76.
Nishino, T., K. Takeuchi, K. E. Gascoigne, A. Suzuki, T. Hori, T. Oyama, K. Morikawa, I. M. Cheeseman and T. Fukagawa. "Cenp-T-W-S-X Forms a Unique Centromeric Chromatin Structure with a Histone-Like Fold." *Cell* 148, no. 3 (2012): 487-501.
O'Keefe, R. T., S. C. Henderson and D. L. Spector. "Dynamic Organization of DNA Replication in Mammalian Cell Nuclei: Spatially and Temporally Defined Replication of Chromosome-Specific Alpha-Satellite DNA Sequences." *J Cell Biol* 116, no. 5 (1992): 1095-110.
Obuse, C., H. Yang, N. Nozaki, S. Goto, T. Okazaki and K. Yoda. "Proteomics Analysis of the Centromere Complex from Hela Interphase Cells: Uv-Damaged DNA Binding Protein 1 (Ddb-1) Is a Component of the Cen-Complex, While Bmi-1 Is Transiently Co-Localized with the Centromeric Region in Interphase." *Genes Cells* 9, no. 2 (2004): 105-20.
Oegema, K., A. Desai, S. Rybina, M. Kirkham and A. A. Hyman. "Functional Analysis of Kinetochore Assembly in Caenorhabditis Elegans." *J Cell Biol* 153, no. 6 (2001): 1209-26.
Oegema, K. and A. A. Hyman. "Cell Division." *WormBook*, (2006): 1-40.
Ohzeki, J., M. Nakano, T. Okada and H. Masumoto. "Cenp-B Box Is Required for De Novo Centromere Chromatin Assembly on Human Alphoid DNA." *J Cell Biol* 159, no. 5 (2002): 765-75.
Okada, M., I. M. Cheeseman, T. Hori, K. Okawa, I. X. McLeod, J. R. Yates, 3rd, A. Desai and T. Fukagawa. "The Cenp-H-I Complex Is Required for the Efficient Incorporation of Newly Synthesized Cenp-a into Centromeres." *Nat Cell Biol* 8, no. 5 (2006): 446-57.
Okada, M., K. Okawa, T. Isobe and T. Fukagawa. "Cenp-H-Containing Complex Facilitates Centromere Deposition of Cenp-a in Cooperation with Fact and Chd1." *Mol Biol Cell* 20, no. 18 (2009): 3986-95.
Okada, T., J. Ohzeki, M. Nakano, K. Yoda, W. R. Brinkley, V. Larionov and H. Masumoto. "Cenp-B Controls Centromere Formation Depending on the Chromatin Context." *Cell* 131, no. 7 (2007): 1287-300.
Orthaus, S., C. Biskup, B. Hoffmann, C. Hoischen, S. Ohndorf, K. Benndorf and S. Diekmann. "Assembly of the Inner Kinetochore Proteins Cenp-a and Cenp-B in Living Human Cells." *Chembiochem* 9, no. 1 (2008): 77-92.
Orthaus, S., K. Klement, N. Happel, C. Hoischen and S. Diekmann. "Linker Histone H1 Is Present in Centromeric Chromatin of Living Human Cells Next to Inner Kinetochore Proteins." *Nucleic Acids Res* 37, no. 10 (2009): 3391-406.
Ortiz, J., O. Stemmann, S. Rank and J. Lechner. "A Putative Protein Complex Consisting of Ctf19, Mcm21, and Okp1 Represents a Missing Link in the Budding Yeast Kinetochore." *Genes Dev* 13, no. 9 (1999): 1140-55.
Palmer, D. K., K. O'Day, H. L. Trong, H. Charbonneau and R. L. Margolis. "Purification of the Centromere-Specific Protein Cenp-a and Demonstration That It Is a Distinctive Histone." *Proc Natl Acad Sci U S A* 88, no. 9 (1991): 3734-8.
Palmer, D. K., K. O'Day, M. H. Wener, B. S. Andrews and R. L. Margolis. "A 17-Kd Centromere Protein (Cenp-a) Copurifies with Nucleosome Core Particles and with Histones." *J Cell Biol* 104, no. 4 (1987): 805-15.
Pardue, M. L. and J. G. Gall. "Chromosomal Localization of Mouse Satellite DNA." *Science* 168, no. 3937 (1970): 1356-8.
Partridge, J. F., B. Borgstrom and R. C. Allshire. "Distinct Protein Interaction Domains and Protein Spreading in a Complex Centromere." *Genes Dev* 14, no. 7 (2000): 783-91.
Patterson, G. H., S. M. Knobel, W. D. Sharif, S. R. Kain and D. W. Piston. "Use of the Green Fluorescent Protein and Its Mutants in Quantitative Fluorescence Microscopy." *Biophys J* 73, no. 5 (1997): 2782-90.

Pearson, C. G., E. Yeh, M. Gardner, D. Odde, E. D. Salmon and K. Bloom. "Stable Kinetochore-Microtubule Attachment Constrains Centromere Positioning in Metaphase." *Curr Biol* 14, no. 21 (2004): 1962-7.

Pepper, D. A. and B. R. Brinkley. "Tubulin Nucleation and Assembly in Mitotic Cells: Evidence for Nucleic Acids in Kinetochores and Centrosomes." *Cell Motil* 1, no. 1 (1980): 1-15.

Peretti, D., P. Maraschio, S. Lambiase, F. Lo Curto and O. Zuffardi. "Indirect Immunofluorescence of Inactive Centromeres as Indicator of Centromeric Function." *Hum Genet* 73, no. 1 (1986): 12-6.

Perez-Castro, A. V., F. L. Shamanski, J. J. Meneses, T. L. Lovato, K. G. Vogel, R. K. Moyzis and R. Pedersen. "Centromeric Protein B Null Mice Are Viable with No Apparent Abnormalities." *Dev Biol* 201, no. 2 (1998): 135-43.

Perpelescu, M. and T. Fukagawa. "The Abcs of Cenps." *Chromosoma* 120, no. 5 (2011): 425-46.

Perpelescu, M., N. Nozaki, C. Obuse, H. Yang and K. Yoda. "Active Establishment of Centromeric Cenp-a Chromatin by Rsf Complex." *J Cell Biol* 185, no. 3 (2009): 397-407.

Petrovic, A., S. Pasqualato, P. Dube, V. Krenn, S. Santaguida, D. Cittaro, S. Monzani, L. Massimiliano, J. Keller, A. Tarricone, A. Maiolica, H. Stark and A. Musacchio. "The Mis12 Complex Is a Protein Interaction Hub for Outer Kinetochore Assembly." *J Cell Biol* 190, no. 5 (2010): 835-52.

Pidoux, A. L. and R. C. Allshire. "The Role of Heterochromatin in Centromere Function." *Philos Trans R Soc Lond B Biol Sci* 360, no. 1455 (2005): 569-79.

Pimpinelli, S. and C. Goday. "Unusual Kinetochores and Chromatin Diminution in Parascaris." *Trends Genet* 5, no. 9 (1989): 310-5.

Piras, F. M., S. G. Nergadze, E. Magnani, L. Bertoni, C. Attolini, L. Khoriauli, E. Raimondi and E. Giulotto. "Uncoupling of Satellite DNA and Centromeric Function in the Genus Equus." *PLoS Genet* 6, no. 2 (2010): e1000845.

Pluta, A. F. and W. C. Earnshaw. "Specific Interaction between Human Kinetochore Protein Cenp-C and a Nucleolar Transcriptional Regulator." *J Biol Chem* 271, no. 31 (1996): 18767-74.

Pluta, A. F., N. Saitoh, I. Goldberg and W. C. Earnshaw. "Identification of a Subdomain of Cenp-B That Is Necessary and Sufficient for Localization to the Human Centromere." *J Cell Biol* 116, no. 5 (1992): 1081-93.

Politi, V., G. Perini, S. Trazzi, A. Pliss, I. Raska, W. C. Earnshaw and G. Della Valle. "Cenp-C Binds the Alpha-Satellite DNA in Vivo at Specific Centromere Domains." *J Cell Sci* 115, no. Pt 11 (2002): 2317-27.

Prendergast, L., C. van Vuuren, A. Kaczmarczyk, V. Doering, D. Hellwig, N. Quinn, C. Hoischen, S. Diekmann and K. F. Sullivan. "Premitotic Assembly of Human Cenps -T and -W Switches Centromeric Chromatin to a Mitotic State." *PLoS Biol* 9, no. 6 (2011): e1001082.

Przewloka, M. R. and D. M. Glover. "The Kinetochore and the Centromere: A Working Long Distance Relationship." *Annu Rev Genet* 43, (2009): 439-65.

Przewloka, M. R., Z. Venkei, V. M. Bolanos-Garcia, J. Debski, M. Dadlez and D. M. Glover. "Cenp-C Is a Structural Platform for Kinetochore Assembly." *Curr Biol* 21, no. 5 (2011): 399-405.

Qiu, S., J. Wang, C. Yu and D. He. "Cenp-K and Cenp-H May Form Coiled-Coils in the Kinetochores." *Sci China C Life Sci* 52, no. 4 (2009): 352-9.

Quenet, D. and Y. Dalal. "The Cenp-a Nucleosome: A Dynamic Structure and Role at the Centromere." *Chromosome Res* 20, no. 5 (2012): 465-79.

Rattner, J. B., A. Rao, M. J. Fritzler, D. W. Valencia and T. J. Yen. "Cenp-F Is A .Ca 400 Kda Kinetochore Protein That Exhibits a Cell-Cycle Dependent Localization." *Cell Motil Cytoskeleton* 26, no. 3 (1993): 214-26.

Ravi, M., F. Shibata, J. S. Ramahi, K. Nagaki, C. Chen, M. Murata and S. W. Chan. "Meiosis-Specific Loading of the Centromere-Specific Histone Cenh3 in Arabidopsis Thaliana." *PLoS Genet* 7, no. 6 (2011): e1002121.

Reinhold, W. C., I. Erliandri, H. Liu, G. Zoppoli, Y. Pommier and V. Larionov. "Identification of a Predominant Co-Regulation among Kinetochore Genes, Prospective Regulatory Elements, and Association with Genomic Instability." *PLoS One* 6, no. 10 (2011): e25991.

Rhoades, M. M. and H. Vilkomerson. "On the Anaphase Movement of Chromosomes." *Proc Natl Acad Sci U S A* 28, no. 10 (1942): 433-6.

Ribeiro, S. A., P. Vagnarelli, Y. Dong, T. Hori, B. F. McEwen, T. Fukagawa, C. Flors and W. C. Earnshaw. "A Super-Resolution Map of the Vertebrate Kinetochore." *Proc Natl Acad Sci U S A* 107, no. 23 (2010): 10484-9.

Ris, H. and P. L. Witt. "Structure of the Mammalian Kinetochore." *Chromosoma* 82, no. 2 (1981): 153-70.

Rizzo, M. A., G. H. Springer, B. Granada and D. W. Piston. "An Improved Cyan Fluorescent Protein Variant Useful for Fret." *Nat Biotechnol* 22, no. 4 (2004): 445-9.

Robbins, E. and N. K. Gonatas. "The Ultrastructure of a Mammalian Cell During the Mitotic Cycle." *J Cell Biol* 21, (1964): 429-63.
Roos, U. P. "Light and Electron Microscopy of Rat Kangaroo Cells in Mitosis. Ii. Kinetochore Structure and Function." *Chromosoma* 41, no. 2 (1973): 195-220.
Rothbauer, U., K. Zolghadr, S. Tillib, D. Nowak, L. Schermelleh, A. Gahl, N. Backmann, K. Conrath, S. Muyldermans, M. C. Cardoso and H. Leonhardt. "Targeting and Tracing Antigens in Live Cells with Fluorescent Nanobodies." *Nat Methods* 3, no. 11 (2006): 887-9.
Russo, P. and F. Sherman. "Transcription Terminates near the Poly(a) Site in the Cyc1 Gene of the Yeast Saccharomyces Cerevisiae." *Proc Natl Acad Sci U S A* 86, no. 21 (1989): 8348-52.
Sanchez, P. and A. Losada. "New Clues to Understand How Cenp-a Maintains Centromere Identity." *Cell Div* 6, no. 1 (2011): 11.
Santaguida, S. and A. Musacchio. "The Life and Miracles of Kinetochores." *EMBO J* 28, no. 17 (2009): 2511-31.
Saxton, M. J. "Anomalous Subdiffusion in Fluorescence Photobleaching Recovery: A Monte Carlo Study." *Biophys J* 81, no. 4 (2001): 2226-40.
Schleiffer, A., M. Maier, G. Litos, F. Lampert, P. Hornung, K. Mechtler and S. Westermann. "Cenp-T Proteins Are Conserved Centromere Receptors of the Ndc80 Complex." *Nat Cell Biol* 14, no. 6 (2012): 604-13.
Schmiedeberg, L., K. Weisshart, S. Diekmann, G. Meyer Zu Hoerste and P. Hemmerich. "High- and Low-Mobility Populations of Hp1 in Heterochromatin of Mammalian Cells." *Mol Biol Cell* 15, no. 6 (2004): 2819-33.
Schmitzberger, F. and S. C. Harrison. "Rwd Domain: A Recurring Module in Kinetochore Architecture Shown by a Ctf19-Mcm21 Complex Structure." *EMBO Rep* 13, no. 3 (2012): 216-22.
Schneider, M. C., A. A. Zacaro, R. Pinto-da-Rocha, D. M. Candido and D. M. Cella. "Complex Meiotic Configuration of the Holocentric Chromosomes: The Intriguing Case of the Scorpion Tityus Bahiensis." *Chromosome Res* 17, no. 7 (2009): 883-98.
Schrader, F. "Notes an the Mitotic Behavior of Long Chromosomes." *Cytologia* 6, (1935): 422–430.
Schwille, P., U. Haupts, S. Maiti and W. W. Webb. "Molecular Dynamics in Living Cells Observed by Fluorescence Correlation Spectroscopy with One- and Two-Photon Excitation." *Biophys J* 77, no. 4 (1999): 2251-65.
Screpanti, E., A. De Antoni, G. M. Alushin, A. Petrovic, T. Melis, E. Nogales and A. Musacchio. "Direct Binding of Cenp-C to the Mis12 Complex Joins the Inner and Outer Kinetochore." *Curr Biol* 21, no. 5 (2011): 391-8.
Sekulic, N., E. A. Bassett, D. J. Rogers and B. E. Black. "The Structure of (Cenp-a-H4)(2) Reveals Physical Features That Mark Centromeres." *Nature* 467, no. 7313 (2010): 347-51.
Sekulic, N. and B. E. Black. "A Reader for Centromeric Chromatin." *Nat Cell Biol* 11, no. 7 (2009): 793-5.
Serrano, M., A. W. Lin, M. E. McCurrach, D. Beach and S. W. Lowe. "Oncogenic Ras Provokes Premature Cell Senescence Associated with Accumulation of P53 and P16ink4a." *Cell* 88, no. 5 (1997): 593-602.
Shang, W. H., T. Hori, A. Toyoda, J. Kato, K. Popendorf, Y. Sakakibara, A. Fujiyama and T. Fukagawa. "Chickens Possess Centromeres with Both Extended Tandem Repeats and Short Non-Tandem-Repetitive Sequences." *Genome Res* 20, no. 9 (2010): 1219-28.
Sharp, L. "Introduction to Cytology." *McGraw-Hill Book Co. Inc. New York & London*, (1934).
Shelby, R. D., K. M. Hahn and K. F. Sullivan. "Dynamic Elastic Behavior of Alpha-Satellite DNA Domains Visualized in Situ in Living Human Cells." *J Cell Biol* 135, no. 3 (1996): 545-57.
Shelby, R. D., K. Monier and K. F. Sullivan. "Chromatin Assembly at Kinetochores Is Uncoupled from DNA Replication." *J Cell Biol* 151, no. 5 (2000): 1113-8.
Shelby, R. D., O. Vafa and K. F. Sullivan. "Assembly of Cenp-a into Centromeric Chromatin Requires a Cooperative Array of Nucleosomal DNA Contact Sites." *J Cell Biol* 136, no. 3 (1997): 501-13.
Shuaib, M., K. Ouararhni, S. Dimitrov and A. Hamiche. "Hjurp Binds Cenp-a Via a Highly Conserved N-Terminal Domain and Mediates Its Deposition at Centromeres." *Proc Natl Acad Sci U S A* 107, no. 4 (2010): 1349-54.
Singh, T. R., D. Saro, A. M. Ali, X. F. Zheng, C. H. Du, M. W. Killen, A. Sachpatzidis, K. Wahengbam, A. J. Pierce, Y. Xiong, P. Sung and A. R. Meetei. "Mhf1-Mhf2, a Histone-Fold-Containing Protein Complex, Participates in the Fanconi Anemia Pathway Via Fancm." *Mol Cell* 37, no. 6 (2010): 879-86.
Slattery, S. D., R. V. Moore, B. R. Brinkley and R. M. Hall. "Aurora-C and Aurora-B Share Phosphorylation and Regulation of Cenp-a and Borealin During Mitosis." *Cell Cycle* 7, no. 6 (2008): 787-95.

Somanathan, S., T. M. Suchyna, A. J. Siegel and R. Berezney. "Targeting of Pcna to Sites of DNA Replication in the Mammalian Cell Nucleus." *J Cell Biochem* 81, no. 1 (2001): 56-67.
Sporbert, A., P. Domaing, H. Leonhardt and M. C. Cardoso. "Pcna Acts as a Stationary Loading Platform for Transiently Interacting Okazaki Fragment Maturation Proteins." *Nucleic Acids Res* 33, no. 11 (2005): 3521-8.
Steiner, N. C. and L. Clarke. "A Novel Epigenetic Effect Can Alter Centromere Function in Fission Yeast." *Cell* 79, no. 5 (1994): 865-74.
Stoler, S., K. C. Keith, K. E. Curnick and M. Fitzgerald-Hayes. "A Mutation in Cse4, an Essential Gene Encoding a Novel Chromatin-Associated Protein in Yeast, Causes Chromosome Nondisjunction and Cell Cycle Arrest at Mitosis." *Genes Dev* 9, no. 5 (1995): 573-86.
Sugata, N., E. Munekata and K. Todokoro. "Characterization of a Novel Kinetochore Protein, Cenp-H." *J Biol Chem* 274, no. 39 (1999): 27343-6.
Sugimoto, K., K. Kuriyama, A. Shibata and M. Himeno. "Characterization of Internal DNA-Binding and C-Terminal Dimerization Domains of Human Centromere/Kinetochore Autoantigen Cenp-C in Vitro: Role of DNA-Binding and Self-Associating Activities in Kinetochore Organization." *Chromosome Res* 5, no. 2 (1997): 132-41.
Sugimoto, K., H. Yata, Y. Muro and M. Himeno. "Human Centromere Protein C (Cenp-C) Is a DNA-Binding Protein Which Possesses a Novel DNA-Binding Motif." *J Biochem* 116, no. 4 (1994): 877-81.
Sullivan, B. A. and S. Schwartz. "Identification of Centromeric Antigens in Dicentric Robertsonian Translocations: Cenp-C and Cenp-E Are Necessary Components of Functional Centromeres." *Hum Mol Genet* 4, no. 12 (1995): 2189-97.
Sullivan, K. F. "A Solid Foundation: Functional Specialization of Centromeric Chromatin." *Curr Opin Genet Dev* 11, no. 2 (2001): 182-8.
Sullivan, K. F., M. Hechenberger and K. Masri. "Human Cenp-a Contains a Histone H3 Related Histone Fold Domain That Is Required for Targeting to the Centromere." *J Cell Biol* 127, no. 3 (1994): 581-92.
Sullivan, L. L., C. D. Boivin, B. Mravinac, I. Y. Song and B. A. Sullivan. "Genomic Size of Cenp-a Domain Is Proportional to Total Alpha Satellite Array Size at Human Centromeres and Expands in Cancer Cells." *Chromosome Res* 19, no. 4 (2011): 457-70.
Suzuki, A., T. Hori, T. Nishino, J. Usukura, A. Miyagi, K. Morikawa and T. Fukagawa. "Spindle Microtubules Generate Tension-Dependent Changes in the Distribution of Inner Kinetochore Proteins." *J Cell Biol* 193, no. 1 (2011): 125-40.
Suzuki, H., Y. Arakawa, M. Ito, S. Saito, N. Takeda, H. Yamada and J. Horiguchi-Yamada. "Mlf1-Interacting Protein Is Mainly Localized in Nucleolus through N-Terminal Bipartite Nuclear Localization Signal." *Anticancer Res* 27, no. 3B (2007): 1423-30.
Suzuki, N., M. Nakano, N. Nozaki, S. Egashira, T. Okazaki and H. Masumoto. "Cenp-B Interacts with Cenp-C Domains Containing Mif2 Regions Responsible for Centromere Localization." *J Biol Chem* 279, no. 7 (2004): 5934-46.
Tachiwana, H., W. Kagawa, T. Shiga, A. Osakabe, Y. Miya, K. Saito, Y. Hayashi-Takanaka, T. Oda, M. Sato, S. Y. Park, H. Kimura and H. Kurumizaka. "Crystal Structure of the Human Centromeric Nucleosome Containing Cenp-A." *Nature* 476, no. 7359 (2011): 232-5.
Tadeu, A. M., S. Ribeiro, J. Johnston, I. Goldberg, D. Gerloff and W. C. Earnshaw. "Cenp-V Is Required for Centromere Organization, Chromosome Alignment and Cytokinesis." *EMBO J* 27, no. 19 (2008): 2510-22.
Takahashi, K., E. S. Chen and M. Yanagida. "Requirement of Mis6 Centromere Connector for Localizing a Cenp-a-Like Protein in Fission Yeast." *Science* 288, no. 5474 (2000): 2215-9.
Takeuchi, K. and T. Fukagawa. "Molecular Architecture of Vertebrate Kinetochores." *Exp Cell Res* 318, no. 12 (2012): 1367-74.
Tan, E. M., G. P. Rodnan, I. Garcia, Y. Moroi, M. J. Fritzler and C. Peebles. "Diversity of Antinuclear Antibodies in Progressive Systemic Sclerosis. Anti-Centromere Antibody and Its Relationship to Crest Syndrome." *Arthritis Rheum* 23, no. 6 (1980): 617-25.
Tanaka, T. U. and A. Desai. "Kinetochore-Microtubule Interactions: The Means to the End." *Curr Opin Cell Biol* 20, no. 1 (2008): 53-63.
Tomkiel, J., C. A. Cooke, H. Saitoh, R. L. Bernat and W. C. Earnshaw. "Cenp-C Is Required for Maintaining Proper Kinetochore Size and for a Timely Transition to Anaphase." *J Cell Biol* 125, no. 3 (1994): 531-45.
Tomonaga, T., K. Matsushita, S. Yamaguchi, T. Oohashi, H. Shimada, T. Ochiai, K. Yoda and F. Nomura. "Overexpression and Mistargeting of Centromere Protein-a in Human Primary Colorectal Cancer." *Cancer Res* 63, no. 13 (2003): 3511-6.

Toso, A., J. R. Winter, A. J. Garrod, A. C. Amaro, P. Meraldi and A. D. McAinsh. "Kinetochore-Generated Pushing Forces Separate Centrosomes During Bipolar Spindle Assembly." *J Cell Biol* 184, no. 3 (2009): 365-72.

Tramier, M., M. Zahid, J. C. Mevel, M. J. Masse and M. Coppey-Moisan. "Sensitivity of Cfp/Yfp and Gfp/Mcherry Pairs to Donor Photobleaching on Fret Determination by Fluorescence Lifetime Imaging Microscopy in Living Cells." *Microsc Res Tech* 69, no. 11 (2006): 933-9.

Trankowsky, D.A. „Leitkörperchen“ Der Chromosomen Bei Einigen Angiospermen." *Cell & Tissue Research* 10, (1930): 736-743.

Trazzi, S., G. Perini, R. Bernardoni, M. Zoli, J. C. Reese, A. Musacchio and G. Della Valle. "The C-Terminal Domain of Cenp-C Displays Multiple and Critical Functions for Mammalian Centromere Formation." *PLoS One* 4, no. 6 (2009): e5832.

Tsukamoto, T., N. Hashiguchi, S. M. Janicki, T. Tumbar, A. S. Belmont and D. L. Spector. "Visualization of Gene Activity in Living Cells." *Nat Cell Biol* 2, no. 12 (2000): 871-8.

Valdivia, M. M. and B. R. Brinkley. "Fractionation and Initial Characterization of the Kinetochore from Mammalian Metaphase Chromosomes." *J Cell Biol* 101, no. 3 (1985): 1124-34.

Van Hooser, A. A., Ouspenski, II, H. C. Gregson, D. A. Starr, T. J. Yen, M. L. Goldberg, K. Yokomori, W. C. Earnshaw, K. F. Sullivan and B. R. Brinkley. "Specification of Kinetochore-Forming Chromatin by the Histone H3 Variant Cenp-A." *J Cell Sci* 114, no. Pt 19 (2001): 3529-42.

Verreault, A. "Histone Deposition at the Replication Fork: A Matter of Urgency." *Mol Cell* 11, no. 2 (2003): 283-4.

Voullaire, L. E., H. R. Slater, V. Petrovic and K. H. Choo. "A Functional Marker Centromere with No Detectable Alpha-Satellite, Satellite Iii, or Cenp-B Protein: Activation of a Latent Centromere?" *Am J Hum Genet* 52, no. 6 (1993): 1153-63.

Wachsmuth, M., W. Waldeck and J. Langowski. "Anomalous Diffusion of Fluorescent Probes inside Living Cell Nuclei Investigated by Spatially-Resolved Fluorescence Correlation Spectroscopy." *J Mol Biol* 298, no. 4 (2000): 677-89.

Wachsmuth, M., T. Weidemann, G. Muller, U. W. Hoffmann-Rohrer, T. A. Knoch, W. Waldeck and J. Langowski. "Analyzing Intracellular Binding and Diffusion with Continuous Fluorescence Photobleaching." *Biophys J* 84, no. 5 (2003): 3353-63.

Wade, C. M., E. Giulotto, S. Sigurdsson, M. Zoli, S. Gnerre, F. Imsland, T. L. Lear, D. L. Adelson, E. Bailey, R. R. Bellone, H. Blocker, O. Distl, R. C. Edgar, M. Garber, T. Leeb, E. Mauceli, J. N. MacLeod, M. C. Penedo, J. M. Raison, T. Sharpe, J. Vogel, L. Andersson, D. F. Antczak, T. Biagi, M. M. Binns, B. P. Chowdhary, S. J. Coleman, G. Della Valle, S. Fryc, G. Guerin, T. Hasegawa, E. W. Hill, J. Jurka, A. Kiialainen, G. Lindgren, J. Liu, E. Magnani, J. R. Mickelson, J. Murray, S. G. Nergadze, R. Onofrio, S. Pedroni, M. F. Piras, T. Raudsepp, M. Rocchi, K. H. Roed, O. A. Ryder, S. Searle, L. Skow, J. E. Swinburne, A. C. Syvanen, T. Tozaki, S. J. Valberg, M. Vaudin, J. R. White, M. C. Zody, Platform Broad Institute Genome Sequencing, Team Broad Institute Whole Genome Assembly, E. S. Lander and K. Lindblad-Toh. "Genome Sequence, Comparative Analysis, and Population Genetics of the Domestic Horse." *Science* 326, no. 5954 (2009): 865-7.

Wan, X., R. P. O'Quinn, H. L. Pierce, A. P. Joglekar, W. E. Gall, J. G. DeLuca, C. W. Carroll, S. T. Liu, T. J. Yen, B. F. McEwen, P. T. Stukenberg, A. Desai and E. D. Salmon. "Protein Architecture of the Human Kinetochore Microtubule Attachment Site." *Cell* 137, no. 4 (2009): 672-84.

Weidemann, T., M. Wachsmuth, T. A. Knoch, G. Muller, W. Waldeck and J. Langowski. "Counting Nucleosomes in Living Cells with a Combination of Fluorescence Correlation Spectroscopy and Confocal Imaging." *J Mol Biol* 334, no. 2 (2003): 229-40.

Weidtkamp-Peters, S., H. P. Rahn, M. C. Cardoso and P. Hemmerich. "Replication of Centromeric Heterochromatin in Mouse Fibroblasts Takes Place in Early, Middle, and Late S Phase." *Histochem Cell Biol* 125, no. 1-2 (2006): 91-102.

Weiss, M., M. Elsner, F. Kartberg and T. Nilsson. "Anomalous Subdiffusion Is a Measure for Cytoplasmic Crowding in Living Cells." *Biophys J* 87, no. 5 (2004): 3518-24.

Weiss, M., H. Hashimoto and T. Nilsson. "Anomalous Protein Diffusion in Living Cells as Seen by Fluorescence Correlation Spectroscopy." *Biophys J* 84, no. 6 (2003): 4043-52.

Westermann, S., D. G. Drubin and G. Barnes. "Structures and Functions of Yeast Kinetochore Complexes." *Annu Rev Biochem* 76, (2007): 563-91.

White, M.J.D. "Animal Cytology and Evolution." *Cambridge University Press*, (1973).

Wieland, G., S. Orthaus, S. Ohndorf, S. Diekmann and P. Hemmerich. "Functional Complementation of Human Centromere Protein a (Cenp-a) by Cse4p from Saccharomyces Cerevisiae." *Mol Cell Biol* 24, no. 15 (2004): 6620-30.

Wigge, P. A. and J. V. Kilmartin. "The Ndc80p Complex from Saccharomyces Cerevisiae Contains Conserved Centromere Components and Has a Function in Chromosome Segregation." *J Cell Biol* 152, no. 2 (2001): 349-60.

Williams, B. C., T. D. Murphy, M. L. Goldberg and G. H. Karpen. "Neocentromere Activity of Structurally Acentric Mini-Chromosomes in Drosophila." *Nat Genet* 18, no. 1 (1998): 30-7.

Winey, M., C. L. Mamay, E. T. O'Toole, D. N. Mastronarde, T. H. Giddings, Jr., K. L. McDonald and J. R. McIntosh. "Three-Dimensional Ultrastructural Analysis of the Saccharomyces Cerevisiae Mitotic Spindle." *J Cell Biol* 129, no. 6 (1995): 1601-15.

Wouters, F. S., P. I. Bastiaens, K. W. Wirtz and T. M. Jovin. "Fret Microscopy Demonstrates Molecular Association of Non-Specific Lipid Transfer Protein (Nsl-Tp) with Fatty Acid Oxidation Enzymes in Peroxisomes." *EMBO J* 17, no. 24 (1998): 7179-89.

Wu, Q., Y. M. Qian, X. L. Zhao, S. M. Wang, X. J. Feng, X. F. Chen and S. H. Zhang. "Expression and Prognostic Significance of Centromere Protein a in Human Lung Adenocarcinoma." *Lung Cancer* 77, no. 2 (2012): 407-14.

Wu, R., P. B. Singh and D. M. Gilbert. "Uncoupling Global and Fine-Tuning Replication Timing Determinants for Mouse Pericentric Heterochromatin." *J Cell Biol* 174, no. 2 (2006): 185-94.

Yaginuma, Y., K. Yoda and K. Ogawa. "Characterization of Physical Binding between Human Papillomavirus 18 Protein E7 and Centromere Protein C." *Oncology* 79, no. 3-4 (2010): 219-28.

Yoda, K., S. Ando, A. Okuda, A. Kikuchi and T. Okazaki. "In Vitro Assembly of the Cenp-B/Alpha-Satellite DNA/Core Histone Complex: Cenp-B Causes Nucleosome Positioning." *Genes Cells* 3, no. 8 (1998): 533-48.

Yoda, K., K. Kitagawa, H. Masumoto, Y. Muro and T. Okazaki. "A Human Centromere Protein, Cenp-B, Has a DNA Binding Domain Containing Four Potential Alpha Helices at the Nh2 Terminus, Which Is Separable from Dimerizing Activity." *J Cell Biol* 119, no. 6 (1992): 1413-27.

Zeitlin, S. G. "Centromeres: The Wild West of the Post-Genomic Age." *Epigenetics* 5, no. 1 (2010): 34-40.

Zeitlin, S. G., N. M. Baker, B. R. Chapados, E. Soutoglou, J. Y. Wang, M. W. Berns and D. W. Cleveland. "Double-Strand DNA Breaks Recruit the Centromeric Histone Cenp-A." *Proc Natl Acad Sci U S A* 106, no. 37 (2009): 15762-7.

Zeitlin, S. G., C. M. Barber, C. D. Allis and K. F. Sullivan. "Differential Regulation of Cenp-a and Histone H3 Phosphorylation in G2/M." *J Cell Sci* 114, no. Pt 4 (2001): 653-61.

Zhou, Z., H. Feng, B. R. Zhou, R. Ghirlando, K. Hu, A. Zwolak, L. M. Miller Jenkins, H. Xiao, N. Tjandra, C. Wu and Y. Bai. "Structural Basis for Recognition of Centromere Histone Variant Cenh3 by the Chaperone Scm3." *Nature* 472, no. 7342 (2011): 234-7.

Zolghadr, K., O. Mortusewicz, U. Rothbauer, R. Kleinhans, H. Goehler, E. E. Wanker, M. C. Cardoso and H. Leonhardt. "A Fluorescent Two-Hybrid Assay for Direct Visualization of Protein Interactions in Living Cells." *Mol Cell Proteomics* 7, no. 11 (2008): 2279-87.

Angaben zum Eigenanteil

Manuskript 1: Live-cell imaging reveals sustained centromere binding of CENP-T via CENP-A and CENP-B

Das Manuskript wurde entworfen und geschrieben von Stephan Diekmann und mir selbst als Erstsautor. Sandra Münch führte die Experimente zu 3.1 Fluorescence Correlation spectroscopy (FCS) sowie deren Auswertung und die Erstellung der angeschlossenen Abbildung durch. Christian Hoischen übernahm die Planung der Klonierungen der verwendeten Fluoreszenzplamide. Die folgenden Punkte sowie die damit verbundenen Abbildungen wurden von mir selbst bearbeitet bzw. erstellt.

3. Results: Localisation studies

3.2. Fluorescence recovery after photobleaching (FRAP)

3.3. Fluroescence resonance enegry transfer (FRET)

Manuskript 2: Acceptor-photobleaching FRET analysis of core kinetochore and NAC proteins in living human cells

Das Manuskript wurde entworfen und geschrieben von Stephan Diekmann und mir selbst als Erstsautor. Christian Hoischen übernahm die Planung der Klonierungen der verwendeten Fluoreszensplamide. Tobias Ulbricht übernahm Teile der Arbeiten im Rahmen der Zellkultur. Alle Experimente sowie die damit verbundenen Abbildungen wurden von mir selbst bearbeitet bzw. erstellt.

Manuskript 3: Dynamics of CENP-N kienetochore binding during the cell cycle

Das Manuskript wurde entworfen und geschrieben von Stephan Diekmann, Andrew D. McAinsh, Aaron F. Straight, Patrick Meraldi und mir selbst als Erstsautor. Christian Hoischen übernahm die Planung der Klonierungen der verwendeten Fluoreszenzplamide. Ronny Martin führte die Präparation der RNA, die RT-PCR-Experimente und deren Auswertung durch. Tobias Ulbricht führte die quantitativen Immunofluoreszenzen mittels Western-Blot durch und erstellte die dazugehörige Abbildung. Volker Döring erstellte die Langzeit-Frap-

Messungen sowie die Doppel-FRAP-Messungen sowie die angeschlossenen Figuren. Stephan Emmerth führte die SNAP-Tag-Versuche im Labor von Patrick Meraldi an der ETH Zürich durch. Die folgenden Punkte sowie die damit verbundenen Abbildungen wurden von mir selbst bearbeitet bzw. erstellt.

CENP-N binds n close proximity to CENP-A in vivo (FRET, FLIM)

CENP-N binds to kinetochore mainly in S phase and G2

Cellular CENP-N protein levels are maximal during S phase (immunofluorescence experiments via microscopy of whole cells

Kinetochore-binding dynamics of CENP-N (FRAP, RICS, CENP-NΔC mutant)

Manuskript 4: Premitotic Assembly of Human CENPs –T and –W Switches Centromeric Chromatin to a Mitotic State

Ich war beteiligt an den grundlegenden Klonierungsarbeiten der verwendeten Plasmide dieser Arbeit. Desweiteren habe ich die Lokalisierungsstudien und die zellzyklusabhängige Kurz- und Langzeit-FRAP-Experimente von CENP-T durchgeführt und ausgewertet.

Manuskript 5: Step-Wise Assembly, Maturation and Dynamic Behavior of Human CENP-P/O/R/Q/U Kinetochore Sub-Complex

Ich habe die Klonierungsarbeiten für die Fluoreszenzemikroskopie (FRAP, FRET, FLIM, FCCS) und F3H-Studien verwendeten Plasmide dieser Arbeit kloniert. Außerdem wurden erste Lokalisierungs- und Kurzzeit-FRAP-Messungen zu CENP-P, -O, -R, -Q und –U von mir durchgeführt.

Jena, Februar 2013

_____

Prof. Stephan Diekmann

Eigenständigkeitserklärung

Hiermit erkläre ich, dass ich die vorliegende Arbeit selbst verfasst habe und keine anderen als die angegebenen Hilfsmittel verwendet habe. Alle Stellen, die anderen Werken im Wortlaut oder Sinn entsprechen, habe ich mit Quellenangaben kenntlich gemacht.

Jena, Februar 2013

_____
Daniela Hellwig

Danksagung

Zu Beginn möchte ich mich bei Professor Stephan Diekmann für die Vergabe des interessanten Themas sowie die Bereitstellung der notwendigen Mittel bedanken. Seine Tür stand mir immer offen; seine unkonventionelle und offene Art hat mir gezeigt, was wissenschaftliche Forschung bedeutet.

Allen derzeitigen und ehemaligen Mitgliedern der Arbeitsgruppe Molekularbiologie möchte ich für die hervorragende Zusammenarbeit und die außerordentlich gute Stimmung im Labor danken. Hierbei sind ganz besonders Dr. Christian Hoischen und Sylke Pfeifer zu nennen, welche mir immer mit Rat und Tat zur Seite standen.

Ich danke außerdem den Mitgliedern meines PhD-Committees Professor Stephan Diekmann, Professor Frank Große und Professor Matthias Görlach für anregende Diskussionen.

Professor Oliver Kurzai möchte ich für die Möglichkeit danken, in die universitäre Forschung zurückzukehren und mir somit meinen größten Wunsch zu erfüllen. Desweiteren danke ich der kompletten Arbeitsgruppe Fungal Septomics für das letzte tolle Jahr, besonders Cindy Büchner für die netten Gespräche bei unseren Freiluftpausen.

Es ist mir ein besonderes Anliegen, mich bei meinem ehemaligen Gymnasiallehrer für Biologie, Frank Kanzler, zu bedanken. Durch ihn wurde mein Interesse an der Biologie geweckt und somit den Grundstein für diese Arbeit und mein gesamtes berufliches Leben gelegt.

Danken möchte ich Rex Torka für den Halt, den er mir gegeben hat, die Akzeptanz und Unterstützung meiner Gartenleidenschaft und die Aussicht auf unglaublich viel mehr.

Ich danke Ronny Martin für die Freundschaft und Unterstützung sowie die fachlichen und privaten Gespräche, ausgenommen die politischen.

Ich möchte mich desweiteren bei Ilse Jakobsen bedanken. Trotz der erst kurzen andauernden Freundschaft hat sie eine Lücke in meinem Leben gefüllt, von der ich nicht einmal wusste, dass es sie gibt.

Im Besonderen danke ich meinen Eltern, für die liebevolle Unterstützung in allen Lebenslagen, die Geduld und die ersthafte Auseinandersetzung mit meinen teils abstrusen Ideen. Ohne sie wäre ich nie so weit gekommen.

Lebenslauf

Persönliche Daten

Name	Daniela Hellwig
Geburtstag:	15.02.1979
Geburtsort:	Leinefelde
Adresse:	Freiligrathstraße 72A, 07743 Jena
Email:	edoclebib@gmail.com

Ausbildung und beruflicher Werbegang

Dez. 2011 - Nov. 2012	wissenschaftlichen Mitarbeiter bei der Arbeitsgruppe Fungal Septomic an der Universität Jena
Aug. 2009 - Nov. 2011	wissenschaftlicher Mitarbeiter bei Eurobiosciences GmbH Jena
Juli 2005 - Juni 2009	Doktorand in der AG Molekularbiologie am Fritz-Lipmann-Institut für Altersforschung in Jena
Feb. 2005 - Juni 2005	wissenschaftlichen Hilfskraft mit Abschluss am IMB Jena
Okt. 1999 - Okt. 2004	Diplom-Studium der Biologie an der Friedrich-Schiller-Universität Jena

Publikationen

Use of the Porcine Intestinal Epithelium (PIE)-Assay to analyse early stages of colonization by the human fungal pathogen *Candida albicans*.
Wendland J, Hellwig D, Walther A, Sickinger S, Shadkchan Y, Martin R, Bauer J, Osherov N, Saluz HP.
J Basic Microbiol. 2006; (6):513-23

Functional analysis of *Candida albicans* genes whose *Saccharomyces cerevisiae* homologues are involved in endocytosis
Martin R, Hellwig D, Schaub Y, Bauer J, Walther A, Wendland J.
Yeast 2007 Jun; 24(6):511-22

Live-cell imaging reveals sustained centromere binding of CENP-T via CENP-A and CENP-B.
Hellwig D, Münch S, Orthaus S, Hoischen C, Hemmerich P, Diekmann S.
J Biophotonics. 2008 Aug;1(3):245-54.

Acceptor-photobleaching FRET analysis of core kinetochore and NAC proteins in living human cells.
Hellwig D, Hoischen C, Ulbricht T, Diekmann S.
Eur Biophys J. 2009 Jul;38(6):781-91.

Premitotic assembly of human CENPs -T and -W switches centromeric chromatin to a mitotic state.
Prendergast L, van Vuuren C, Kaczmarczyk A, Doering V, Hellwig D, Quinn N, Hoischen C, Diekmann S, Sullivan KF.
PLoS Biol. 2011 Jun;9(6):e1001082. doi: 10.1371/journal.pbio.1001082.

Dynamics of CENP-N kinetochore binding during the cell cycle
Hellwig D, Emmerth S, Ulbricht T, Döring V, Hoischen C, Martin R, Samora C, McAinsh A, Carroll C, Straight A, Meraldi P, Diekmann S
J Cell Sci. 2011 Nov 15;124(Pt 22):3871-83. doi: 10.1242/jcs.088625. Epub 2011 Nov 18

Step-wise assembly, maturation and dynamic behavior of the human CENP-P/O/R/Q/U kinetochore sub-complex.
Eskat A, Deng W, Hofmeister A, Rudolphi S, Emmerth S, Hellwig D, Ulbricht T, Döring V, Bancroft JM, McAinsh AD, Cardoso MC, Meraldi P, Hoischen C, Leonhardt H, Diekmann S.
PLoS One. 2012;7(9):e44717. doi: 10.1371/journal.pone.0044717. Epub 2012 Sep 18.

Wissenschaftliche Vorträge und Poster

Mai 2009	Beitrag zum Retreat des Fritz-Lipmann-Istituts für Altersforung in Form eines Posters über „Function of CENP-N at the human kinetochore”
Juni 2007	Beitrag zum 2nd Biannual Campus Workshop - Method and Concept Transfer in Form eines Vortrags über “Functional architecture of the human kinetochore”
Juni 2007	Beitrag zum Retreat des Fritz-Lipmann-Istituts für Altersforung in Form eines Posters über „Functional architecture of the human kinetochore“
Juni 2006	Beitrag zum Retreat des Fritz-Lipmann-Istituts für Altersforung in Form eines Posters über „Cloning and expression of human kinetochore proteins“